

# **Biotechnological production of natural products in entomopathogenic bacteria**

Dissertation

zur Erlangung des Doktorgrades

der Naturwissenschaften

vorgelegt beim Fachbereich Biowissenschaften (15)

der Johann Wolfgang Goethe-Universität

in Frankfurt am Main

von

Lukas Kreling

aus Frankfurt am Main

Frankfurt am Main 2022

D30



vom Fachbereich Biowissenschaften (15) der  
Johann Wolfgang Goethe-Universität als Dissertation angenommen.

Dekan: Prof. Dr. Sven Klimpel

Gutachter: Prof. Dr. Helge B. Bode

Zweitgutachter: Prof. Dr. Martin Grininger

Datum der Disputation:

# Table of Contents

1	List of abbreviations .....	6
2	Zusammenfassung .....	9
3	Summary.....	15
4	Introduction.....	19
4.1	<i>Photorhabdus</i> and its complex life cycle.....	20
4.2	Specialized NPs produced by <i>P. luminescens</i> .....	22
4.3	Thiotemplated assembly line in NRPS and PKS.....	24
4.4	Polyketide synthases .....	24
4.5	AQ biosynthesis and regulation in <i>Photorhabdus</i> .....	26
4.6	Biotechnological production of electrolytes for redox flow batteries.....	28
4.7	Electrolyte production from residual waste products .....	30
4.8	BGC elucidation and NP identification .....	31
4.9	NP identification using LC-MS-based strategies .....	32
4.10	Carotenoid-derived NPs .....	33
4.11	Oxidative tailoring of carotenoids.....	34
4.12	Function of apocarotenoids .....	37
4.13	Aim and motivation of this work.....	37
5	Material and Methods.....	39
5.1	General Methods .....	39
5.1.1	Plasmid isolation and purification .....	39
5.1.2	Purification of PCR products .....	40
5.1.3	Extraction of DNA from agarose gels.....	40
5.1.4	Isolation of genomic DNA .....	40
5.1.5	Measurement of DNA/protein concentration.....	40
5.1.6	Polymerase chain reaction (PCR).....	40
5.1.7	Colony PCR of <i>E. coli</i> and <i>Photorhabdus luminescens</i> strains.....	41
5.1.8	Hot Fusion assembly .....	42
5.1.9	Gel electrophoresis .....	42
5.2	Topic A.....	43
5.2.1	Cultivation .....	49
5.2.2	Preparation and Transformation of electrocompetent <i>E. coli</i> cells .....	52
5.2.3	Preparation and Transformation of electrocompetent <i>P. luminescens</i> cells.....	52

5.2.4	Construction of deletion mutants.....	52
5.2.5	Compound extraction from liquid cell culture .....	53
5.2.6	HPLC-MS analysis .....	53
5.2.7	Compound purification .....	54
5.2.8	Protein purification .....	55
5.2.9	Bioinformatic and phylogenetic analysis .....	55
5.2.10	In vitro characterization of MTs plu4890-4895 .....	55
5.2.11	NMR .....	56
5.3	Topic B.....	56
5.3.1	Cultivation .....	61
5.3.2	Preparation and Transformation of electrocompetent E. coli cells .....	64
5.3.3	Preparation and Transformation of electrocompetent P. luminescens cells....	64
5.3.4	Construction of deletion mutants.....	64
5.3.5	Compound extraction from liquid cell culture .....	65
5.3.6	HPLC-MS analysis .....	65
5.3.7	Compound purification .....	65
5.3.8	Absolute NP quantification .....	66
5.4	Topic C.....	66
5.4.1	Cultivation .....	78
5.4.2	Preparation and Transformation of electrocompetent E. coli cells .....	79
5.4.3	Preparation and Transformation of electrocompetent P. luminescens cells....	79
5.4.4	Construction of deletion mutants.....	79
5.4.5	Compound extraction from liquid cell culture .....	80
5.4.6	HPLC-MS analysis .....	80
5.4.7	Compound purification .....	80
5.4.8	Standards .....	81
5.4.9	Bioinformatic and phylogenetic analysis .....	81
5.4.10	Insect killing assay.....	81
6	Results.....	82
6.1	Topic A: Anthraquinone diversification in <i>Photorhabdus</i> .....	82
6.1.1	AQ production in P. luminescens.....	82
6.1.2	MTs involved in AQ derivative formation.....	83
6.1.3	In vivo production of methylated AQ derivatives in P. luminescens.....	83

6.1.4	Structure elucidation of AQ derivatives.....	85
6.1.5	In vitro production of methylated AQ derivatives.....	91
6.1.6	Combinatorial in vitro activity of plu4895-plu4890 on AQ-256 .....	92
6.1.7	In vitro AQ conversion assay with single purified MTs using mono-methylated derivatives as substrate.....	96
6.1.8	Summary of AQ diversification in <i>P. luminescens</i> subsp. TT01 .....	98
6.1.9	MT homologues in different <i>Photorhabdus</i> subspecies.....	98
6.1.10	AQ derivative formation in different <i>Photorhabdus</i> subspecies.....	100
6.1.11	AQ diversification in <i>Photorhabdus</i> .....	102
6.2	Topic B: AQ overproduction in <i>Photorhabdus</i> as electrolyte for redox flow batteries.....	103
6.2.1	Establishing an AQ production platform .....	103
6.2.2	AntJ as a regulator of AQ biosynthesis .....	105
6.2.3	Construction of an AQ production platform.....	107
6.2.4	Monooxygenase plu0947 supports AQ formation .....	111
6.2.5	Establishing a suitable NP production medium.....	114
6.2.6	Insect media screening .....	115
6.2.7	Absolute quantification of AQ production platform in novel XPP insect medium.....	116
6.3	Topic C: Elucidation of a putative terpenoid cluster in <i>Photorhabdus</i> .....	120
6.3.1	BGC putatively involved in terpenoid biosynthesis in different <i>Photorhabdus</i> species.....	120
6.3.2	Establishing a platform for carotenoid core production .....	122
6.3.3	Expression of terpenoid core genes and structure elucidation of the product.....	124
6.3.4	Carotenoid oxygenase activity on $\beta$ -carotene.....	126
6.3.5	Structure elucidation of 1 and 2 .....	128
6.3.6	Retinoid derivative formation in different <i>Photorhabdus</i> species.....	132
6.3.7	Carotenoid oxygenase from <i>P. luminescens</i> subs. PB45.5 and <i>Xenorhabdus</i> sp. KJ12.1 are active on $\beta$ -carotene .....	134
6.3.8	Carotenoid cluster exhibits in vivo effect in insect killing assays .....	136
6.3.9	Retinoid production in insect infection assays .....	137
6.3.10	Putative targets of retinoid derivatives produced by <i>P. luminescens</i> .....	143
6.3.11	Retinoid activity on channelrhodopsin ChR2 in <i>C. elegans</i> .....	145
7	Discussion .....	147

7.1	Topic A: Anthraquinone derivative formation in <i>Photorhabdus</i> .....	147
7.1.1	AQ diversification in <i>P. luminescens</i> .....	147
7.1.2	Monooxygenase plu0947 has an effect on AQ formation.....	150
7.1.3	Different <i>Photorhabdus</i> species show different AQ product spectra .....	151
7.1.4	Putative functions of AQs .....	153
7.1.5	Conclusion and Outlook.....	156
7.2	Topic B: AQ overproduction in <i>Photorhabdus</i> for redox flow batteries.....	156
7.2.1	Manipulation of AQ biosynthesis in <i>P. luminescens</i> .....	157
7.2.2	Utilizing the ecological background of <i>Photorhabdus</i> to develop a NP production medium from waste residues.....	159
7.2.3	Conclusion and Outlook.....	160
7.3	Topic C: Elucidation of a putative terpenoid cluster in <i>Photorhabdus</i> .....	161
7.3.1	$\beta$ -carotene as the product of core gene expression.....	162
7.3.2	Cleavage of $\beta$ -carotene through BGC-associated CCD .....	164
7.3.3	Carotenoid BGC is activated in insect environment .....	166
7.3.4	Chimeric role of carotenoid BGC in <i>Photorhabdus</i> species.....	166
7.3.5	Putative ecological role of $\beta$ -carotene in <i>Photorhabdus</i> species .....	167
7.3.6	Putative ecological role of 1 and 2.....	168
7.3.7	Conclusion and Outlook.....	170
8	References .....	171
9	Appendix.....	185
10	Record of Conferences.....	227
11	Acknowledgements.....	<b>Error! Bookmark not defined.</b>
12	Erklärung .....	228
13	Eidesstattliche Versicherung.....	229
14	Curriculum Vitae .....	<b>Error! Bookmark not defined.</b>

## 1 List of abbreviations

ACN	Acetonitrile
ACP	Acyl carrier protein
antiSMASH	Antibiotics and secondary metabolite analysis shell
AQ	Anthraquinone

ARO	Aromatase
BGC	Biosynthetic gene cluster
BlastP	Basic Local Alignment Search Tool (for Protein sequences)
bp	base pairs
CCD	carotenoid cleaving dioxygenase
CoA	Coenzyme A
CRISPR	Clustered regularly interspaced short palindromic repeats
CYC	Cyclase
DH	Dehydratase
DMSO	Dimethylsulfoxide
DNA	Deoxyribonucleic acid
D	doublet
EDTA	Ethylenediaminetetraacetic acid
EIC	Extracted Ion Chromatogram
ESI	Electrospray-ionisation
EtAC	Ethyl acetate
EtOH	Ethanol
FAR	Fatty acid- and retinoid-binding proteins
GXP	GameXPeptide
h	hour
Hfq	host factor bacteriophage q
HMM	Hidden Markov Model
HPLC	High performance liquid chromatography
HR	High resolution
IJ	infective juvenile
IT	ion trap
kDa	kilodalton
KR	Ketoreductase
KS	Ketosynthase
L	litre
LB	Lysogeny broth



LC	Liquid chromatography
MeOH	Methanol
MEP	2-C-methyl-D-erythritol 4-phosphate
MEV	mevalonate
MO	Monoxygenase
mRNA	messenger RNA
MS	Mass spectrometry
MT	Methyltransferase
NHR	Nuclear hormone receptor
NMR	Nuclear magnetic resonance
NP	Natural product
NRPS	Non-ribosomal peptide synthetase
OSMAC	One strain many compounds
PCP	Peptidyl carrier protein
PCR	Polymerase Chain Reaction
PFBHA	<i>O</i> -(2,3,4,5,6-Pentafluorobenzyl)hydroxylamine
PKS	Polyketide synthase
Ppm	Parts per million
PRISM	Prediction Informatics for Secondary Metabolomes
PPTase	Phosphopantetheinyltransferase
RNA	Ribonucleic acid
rpm	round per minute
SAM	S-Adenosylmethionine
S	Singlet
T	Triplet
UV	Ultraviolet
WT	Wild type
XPP	<i>Xenorhabdus-Photorhabdus</i> -Production

## 2 Zusammenfassung

*Photorhabdus* ist ein Gram-negativer, fakultativ anaerober Vertreter insektenpathogener (entomopathogener) Bakterien. Er besitzt einen komplexen Lebenszyklus in dem er zum einen in einer symbiotischen Phase mit Fadenwürmern (Nematoden) der Gattung *Heterorhabditis* assoziiert ist und zum anderen eine insektenpathogene Phase durchläuft. In der infektiösen Dauerform (infective juvenile) des Nematoden ist *Photorhabdus* in seinem Darm lokalisiert, wobei ihm die Cuticula Schutz vor äußeren Einflüssen bietet. Nachdem *Heterorhabditis* ein im Erdreich lebendes Insekt aufgespürt hat, dringt er in das Insekt durch natürliche Öffnungen oder Tracheen ein. Im nächsten Schritt werden die Bakterien in die Hämolymphe entlassen und beginnen sich schnell zu vermehren. Hierbei wird angenommen, dass der Wechsel von der symbiotischen M-Form zur insektenpathogenen P-Form von *Photorhabdus* durch insektenspezifische Signalmoleküle eingeleitet wird. Daraufhin produziert *Photorhabdus* eine Vielzahl von Naturstoffen, die unterschiedlichste Aufgaben erfüllen. Zu diesen Aufgaben zählen unter anderem die Überwindung des Immunsystems des Insekts und die anschließende Tötung. Durch die enzymatische Zersetzung der Beute werden Nährstoffe für die Nematoden und Bakterien bereitgestellt, welche mehrere Entwicklungszyklen durchlaufen. Andere produzierte Naturstoffe weisen biologische Aktivitäten gegenüber konkurrierenden Bodenorganismen wie Pilzen, Protozoen oder Insekten auf und dienen zur Verteidigung des Insektenkadavers und Sicherung der Nahrungsquelle. Schließlich sind einige der produzierten Naturstoffe für die Entwicklung der Nematoden notwendig. Sobald die Nährstoffquelle aufgebraucht ist, re-assoziiieren die Bakterien und die Nematoden und das symbiotische Paar bricht aus der Insektenhülle aus und ein neuer Lebenszyklus wird eingeleitet. Während diese mutualistische Beziehung hochspezifisch ist, können die Bakterien eine Vielzahl von verschiedenen Insekten töten, wovon einige Schädlinge der Landwirtschaft darstellen, was sie zu einer potenten Alternative zu Insektiziden macht.

Dieser ungewöhnliche Lebenszyklus qualifiziert *Photorhabdus* als Modellorganismus zur Untersuchung von Symbiose und Pathogenität speziell mit Fokus auf die produzierten Naturstoffe. Ein weiterer Vorteil hierbei ist die einfache Kultivierbarkeit bei 30°C in herkömmlichen Nährmedien, was die Untersuchung der Naturstoffe erleichtert. Zusätzlich

eignet sich die einfach kultivierbare Insektenlarve der Großen Wachsmotte *Galleria mellonella* als Modelorganismus, um die Insektenpathogenität von *Photorhabdus* zu studieren.

Häufig werden die zu untersuchenden Naturstoffe von Polyketid-Synthasen (PKS) produziert. Ähnlich zur Fettsäurebiosynthese erfolgt die Verknüpfung von Acetat- bzw. Malonat-Einheiten durch decarboxylierende Claisen-Kondensationen unter der Bildung von C-C-Bindungen. Die Biosynthese findet dabei kovalent an Proteine gebunden mit sogenannten Acyl-Carrier-Proteinen (ACPs) statt. In diesem Fall sorgt die posttranslationale Modifikation der ACPs mit dem hochflexiblen Phosphopantetheinyl-Arm (Ppant arm) dafür, dass Starter-, Verlängerungseinheiten und die entstehenden Intermediate, zur weiteren Prozessierung durch verschiedene Enzyme, kovalent gekoppelt werden können. In vielen Fällen werden die entstandenen Polyketide zusätzlichen Modifikationen unterzogen wie z. B. Zyklisierungen, Aromatisierungen, Methylierungen, Oxidationen und Glykosylierungen, was zu einer enormen strukturellen Vielfalt dieser Stoffe führt.

Oft sind die Gene, die für die Biosynthese der Naturstoffe verantwortlich sind, in sogenannten Biosynthesegenclustern (BCGs) organisiert. Die gezielte Manipulierung dieser BCGs z.B. durch Deletionen oder Austausch des nativen Promotors durch einen induzierbaren Promotor stellt ein potentes Werkzeug dar, um die produzierten Naturstoffe zu identifizieren und ihre Biosynthese aufzuklären. Hierbei werden oft massenspektrometrische Verfahren wie „high performance liquid chromatography-mass spectrometry“ (HPLC-MS) herangezogen, welche die Identifizierung ermöglichen.

Diese Arbeit beschäftigt sich mit der Biosynthese und Produktion von Pigmenten in *Photorhabdus laumondii*. Das erste Teilprojekt befasst sich mit der näheren Charakterisierung der Anthrachinon (AQ)-Biosynthese. *Photorhabdus laumondii* bildet orangene AQ-Derivate während der exponentiellen Wachstumsphase aus, wenn er unter Laborbedingungen kultiviert wird. Ungewöhnlich für Gram-negative Bakterien, wird der unmethylierte Vorläufer AQ-256 durch ein PKS II-System synthetisiert, welches neben der minimalen PKS (Ketosynthase, chain-length-factor, ACP) eine CoA-Ligase, eine Ketoreduktase (KR), eine Aromatase (ARO), eine Zyklase (CYC), eine Hydrolase und eine Sfp-Typ PPTase kodiert. Obwohl das BGC für die AQ Bildung bereits im Jahr 2007 beschrieben wurde und einige der Derivate strukturell aufgeklärt wurden, blieben die Methyltransferasen (MTs), welche AQ-256

in verschiedene methylierte Derivate umwandeln, unbekannt. Daher beschäftigt sich das erste Teilprojekt sich mit der Identifizierung und Charakterisierung der verschiedenen MTs vor allem mit Bezug auf die Bildung der unterschiedlichen Derivaten. In einem ersten Ansatz wurden durch bioinformatische Analyse potentielle Gen-Kandidaten im Genom von *P. luminescens* identifiziert (*plu4890-plu4895*), die vermeintlich für SAM-abhängige MTs kodieren könnten. Im nächsten Schritt wurde das gesamte MT-Gencluster deletiert wobei der resultierende *P. luminescens*  $\Delta$ MT keine methylierten AQ-Derivate mehr produzierte, sondern nur noch den unmethylierten Vorläufer AQ-256. Somit wurde die Beteiligung von *plu4890-plu4895* an der AQ-Biosynthese bestätigt. In den folgenden Schritten wurden verschiedene Deletionsstämme generiert, welche die Gene für eine oder mehrere MTs in ihrem Genom enthielten. Die Kultivierung dieser Stämme zeigte, dass die MTs *plu4890*, *plu4891* und *plu4895* spezifisch für die Bildung von jeweils einem einfach-methylierten AQ-Derivat verantwortlich sind. Zusätzlich konnte durch Aufreinigung der jeweiligen Derivate die Struktur per Kernspinresonanz (NMR) aufgeklärt werden. Somit konnte gezeigt werden, dass *plu4890* für die Generierung von AQ-270c, *plu4891* für die Generierung von AQ-270b und *plu4895* für die Generierung von AQ-270a verantwortlich sind. Gleichzeitig konnte in der *P. luminescens* Deletionsmutante, welche nur noch die Gene für *plu4890* und *plu4895* enthielt, gezeigt werden, dass diese beiden MTs verantwortlich sind für die Produktion von zweifach-methylierten-AQ-Derivaten (AQ-284 a/b). *In vitro* Experimente mit aufgereinigten MTs und aufgereinigten AQ-270-Derivaten lieferten schließlich die Erkenntnis, dass AQ-284a/b durch sequenzielle Aktivität von *plu4890* bzw. *plu4895* entstehen. Auch hier wurden alle Strukturen per NMR bestimmt. Somit konnte die Derivatisierung von AQ-256 in *P. luminescens* vollständig aufgeklärt werden. Der letzte Abschnitt dieses Teilprojekts befasst sich mit der AQ-Diversifizierung in verschiedenen *Photobacterium*-Spezies. Bioinformatische Analysen ergaben, dass das MT-Cluster ein hochkonserviertes Merkmal der meisten untersuchten Subspezies ist. Es konnte jedoch gezeigt werden, dass, trotz der hohen Homologien, verschiedene Stämme unterschiedliche Derivate produzieren.

Das im Rahmen dieser Arbeit zweite vorgestellte Teilprojekt befasst sich mit der Entwicklung eines *P. luminescens* AQ-Überproduktionsstammes, welcher AQ-256 als Elektrolyt für Redox-Flow-Batterien bereitstellen soll. Zusätzlich sollte im Rahmen dieses Projektes ein Medium entwickelt werden, welches maßgeblich aus Reststoffströmen besteht.

Treibhausgasneutralität stellt eine der großen Herausforderungen der Menschheit dar, um dem Menschen-gemachten Klimawandel entgegenzuwirken und ihn letztendlich zu stoppen. Einer der Hauptaspekte des Fünf-Punkte-Plans der Bundesregierung zur Bekämpfung des verursachten Klimawandels ist die Nutzbarmachung von industriellen Reststoffströmen zur Energiegewinnung und –Speicherung. Mit steigendem Energiebedarf einer immer größer werdenden Gesellschaft sind innovative Batteriesysteme essentiell, um die generierten Energiemengen effizient zu speichern. Einer dieser Batteriesysteme stellen Redox-Flow-Batterien dar, welche elektrische Energie in chemischen Verbindungen speichern, die in gelöster Form in einem Lösungsmittel vorliegen. Die zwei energiespeichernden Elektrolyte zirkulieren hierbei in getrennten Reaktionsräumen wobei der Ionenaustausch durch eine Membran erfolgt. Die Vorteile eines solchen Batteriesystems sind unter anderem lange Lebenszyklen und einfaches Scale-up. Im Jahr 2014 wurde bereits eine Chinon-basierte Redox-Flow-Batterie von Forschern aus Harvard entwickelt und in Betrieb genommen. Das in diesem Fall benutzte Chinon wurde aus Lignosulfat gewonnen, was die Notwendigkeit eines intensiven Aufreinigungs- und Gewinnungsprozesses mit sich bringt. In diesem Teilprojekt wurde *P. luminescens* genetisch manipuliert, um große Mengen AQ zu produzieren, welches als Chinon-basierter Elektrolyt im beschriebenen Batterie-System angewendet werden soll. Im ersten Schritt wurden die MTs deletiert, welche für die Derivatisierung von AQ-256 verantwortlich sind, um das produzierte AQ leichter quantifizierbar zu machen. Im nächsten Schritt wurde die Sfp-Typ PPTase NgrA deletiert, welche essentiell für die Produktion der meisten Naturstoffe in *Phototrhobdus* durch PKS oder nicht-ribosomale Peptidsynthetasen (NRPS) ist. Sie konvertiert die jeweilige *apo*-Form der ACPs (PKS) bzw. der „peptidyl-carrier-proteins“ (PCPs) (NRPS) in die *holo*-Form und katalysiert somit die Naturstoffproduktion. Während NgrA an der Produktion der meisten Naturstoffe in *Phototrhobdus* beteiligt ist, kodiert das AQ BGC eine hochspezifische eigene PPTase (AntB) und ist nicht abhängig von der Aktivität von NgrA. Die Idee für den AQ-Überproduktionsstamm war es, die intrazelluläre Konzentration von Malonat-Bausteinen, durch die Abschaltung der Produktion der meisten Naturstoffe, zu erhöhen. Zusätzlich wurde, basierend auf vorherigen Erkenntnissen, der AQ BGC-spezifische Aktivator AntJ überexprimiert, um so die Produktivität zu steigern. Schlussendlich führte die Kombination beider Ansätze zu einer 7.2-fachen Erhöhung der AQ-Produktion (von 35 mg/L auf 253 mg/L). Im zweiten Teil dieses Teilprojekts wurde ein Produktionsmedium entwickelt, welches zu großen Teilen aus Reststoffströmen besteht. In

Kooperation mit Jan Burkhardt, AG Czermak, THM wurde ein Aminosäure-Screening durchgeführt, welches die Aminosäuren in Xenorhabdus-Photorhabdus-Produktions-Medium (XPP-Medium) identifizierte, welche einen positiven Einfluss auf die AQ-Produktion hatten. Zusätzlich wurden mit der Soldatenfliege *Hermetia illucens* und dem Seidenspinner *Bombyx mori* zwei Kandidaten identifiziert, welche als potentielle Restströme nutzbar gemacht werden könnten. In Kombination mit einem verbesserten Extraktionsverfahren mit Amberlite XAD-16 konnte die AQ-Produktion vom *P. luminescens* Produktionsstamm in dem neuartigen Reststoffmedium schließlich auf über 1 g/L gesteigert werden.

Das dritte Teilprojekt dieser Arbeit befasst sich mit der Charakterisierung eines BGC, welches durch antiSMASH-Analyse in Genomdaten von *P. luminescens* entdeckt wurde und laut bioinformatischer Vorhersagen die Gene für die Biosynthese eines Terpens kodiert. Außerdem besitzt das BGC ein Gen, welches für eine Carotenoid-Oxygenase kodieren soll. Interessanterweise konnte das BGC nicht durch einen einfachen Promotoraustausch und anschließende Induktion aktiviert werden, was auf eine komplexe Regulation hindeutete, welche das BGC nur unter bestimmten Umständen aktiviert. Da die Aktivierung des BGC im natürlichen Produzenten nicht möglich war, sollten die Gene heterolog in *Escherichia coli* charakterisiert werden. Im ersten Schritt wurde die Gene, die für die Produktion des Terpen-Grundgerüst verantwortlich sein sollten, auf Expressionsvektoren in einem *E. coli* Stamm exprimiert, welcher Isoprenoid-Bausteine produziert, die für die Terpen-Biosynthese benötigt werden. Das Produkt wurde aufgereinigt und strukturell als  $\beta$ -Carotin per NMR bestimmt. Anschließend konnte gezeigt werden, dass die zusätzliche Expression der vorhergesagten Oxygenase zu einer asymmetrischen Spaltung des  $\beta$ -Carotins führt, wodurch eine Aldehyd- und ein Keton-Derivat entsteht ( $\beta$ -Apo-14'-carotenal und  $\beta$ -Apo-13-carotenone), welche große strukturelle Ähnlichkeit zu Retinol aufweisen. Hierfür wurde ein Mechanismus postuliert, in dem die Di-Oxygenase einen viergliedrigen Ring durch die Einführung von zwei Sauerstoffatomen an der 13',14'-Bindung des  $\beta$ -Carotin bildet, was schlussendlich in der Spaltung des Moleküls resultiert. Zusätzlich lieferte die Expression der Terpen-BCGs aus verschiedenen *Photorhabdus* Spezies die gleichen Ergebnisse, was darauf hindeutete, dass das Cluster eine wichtige ökologische Aufgabe im Lebenszyklus übernehmen könnte. Diese These wurde gestützt von dem Fakt, dass Retinol-Derivate in vielen Organismen zur Signaltransduktion bei wichtigen zellulären Prozessen verwendet wird. Um die potentielle

ökologische Funktion des BGC auch experimentell zu erforschen, wurden *P. luminescens*  $\Delta$ oxygenase und  $\Delta$ carotenoid Deletionsmutanten generiert und auf Toxizität gegen *G. mellonella* getestet. Es konnte gezeigt werden, dass *Photorhabdus* eine größere Zeitspanne benötigt, um *G. mellonella* erfolgreich zu töten, wenn das BGC deletiert ist. Hierbei wurde postuliert, dass die Expression des BGC durch die Infektion des Insekts induziert wird und das  $\beta$ -Carotin als Schutzmechanismus gegen die Immunantwort des Insekts fungiert. HPLC-MS Analysen von Extrakten infizierter *G. mellonella* Larven konnten die Produktion des Terpens bestätigen und ergaben zusätzlich, dass die Spaltung des  $\beta$ -Carotins durch die Oxygenase erst nach drei Tagen einsetzt, wodurch eine chimäre Funktion des BGCs abgeleitet wurde. Hierbei wird angenommen, dass die gebildeten Retinoid-Derivate vom Nematoden für die Signaltransduktion bei zellulären Prozessen verwendet wird. In bioinformatischen Analysen konnten zudem mögliche Bindungspartner in *Heterorhabditis* identifiziert werden. Zukünftige Untersuchungen könnten hierbei Aufschluss über weitere Details der Nematoden-Bakterien Interaktion ergeben.

Zusammenfassend beschreibt die Arbeit drei Teilprojekte. Im ersten Teilprojekt wurde die post-PKS Modifizierung von AQ-256 charakterisiert und aufgeklärt. Im zweiten Teilprojekt wurde *P. luminescens* genomisch manipuliert, um eine möglichst hohe AQ-256 Ausbeute zu erreichen. Zusätzlich wurde ein Reststoffstrom-Medium entwickelt, welches nicht nur die Produktivität steigert, sondern auch aus ökologischen Abfallprodukten besteht. Im dritten Teilprojekt konnte ein stilles Terpen BGC von *Photorhabdus* charakterisiert werden und seine ökologische Funktion in Ansätzen ergründet werden.

### 3 Summary

*Photorhabdus luminescens* is a Gram-negative, facultative anaerobic, motile bacterium, which lives in a mutualistic relationship with nematodes of the genus *Heterorhabditis*. During its complex life cycle, *Photorhabdus* is located in the gut of infective juvenile (IJ) stage nematodes in its mutualistic M-form while the nematode moves through the soil in order to search for insect prey. Upon entering the insect through natural opening or the cuticle, the bacteria are released into the hemocoel where they reproduce quickly and switch to the pathogenic P-form induced by unknown insect specific signals. During the process of infection, *P. luminescens* produces an array of natural products, which fulfill various different tasks such as suppression of the insect's immune system and killing the prey. The carcass provides nutrients for both the nematodes and the bacteria. Here, some of the produced natural products exhibit biological activity against food competitors such as fungi or other bacteria. Upon depletion of the food source IJ stage nematodes and bacteria re-associate and emerge from the dead insect larvae in order to seek a new insect host and the life cycle repeats.

This extraordinary life cycle qualifies *P. luminescens* as a model organism to study pathogenicity and symbiosis concerning the produced natural products. Additionally, the bacteria are easily cultivated at 30°C under laboratory conditions while larvae of *Galleria mellonella* can be utilized for insect pathogenicity assays.

Often, the natural products are produced by polyketide synthases (PKS). They condense acyl and malonyl moieties to yield polyketides using ketosynthase (KS) domains and the production is strongly dependent on activity of phosphopantetheinyltransferases (PPTase). The PPTase converts inactive *apo*-acyl-carrier-proteins (ACPs) (part of PKS) to the respective *holo* forms by posttranslational transfer of the 4'-phosphopantetheinyl (P-pant) moiety of coenzyme A to the side chain of a conserved serine residue in each carrier protein domain. Crucially, in many cases, the produced polyketides undergo certain modifications like cyclization, methylation, glycosylation or oxidation, which results in a high structural diversity.

Usually, the genes that are responsible for the biosynthesis of the respective NPs are organized in biosynthetic gene clusters (BGCs). Here, targeted manipulation through gene



deletions or exchange of native promoters for inducible ones represent potent tools for characterization of the respective BGCs and elucidation of the produced natural products (NPs). Additionally, high performance liquid chromatography-mass spectrometry (HPLC-MS) and nuclear magnetic resonance spectroscopy (NMR) are used to facilitate NP identification.

The first part of this work describes the closer characterization of the anthraquinone (AQ) BGC in *P. laumondii* with specific focus on late-stage modifications of the precursor AQ-256. *Photorhabdus* exhibits a characteristic orange-reddish color upon its exponential growth phase. This pigmentation is caused by the production of different AQ derivatives. While the BGC cluster was already described in 2007 and some of the AQ variants were structurally identified, the methyltransferases (MTs) which convert AQ-256 into methylated derivatives remained unknown. Bioinformatic analysis revealed a set of MT encoding genes (*plu4890-plu4895*) which were assumed to be involved in product formation. Consequently, multiple *P. luminescens* MT-deletion mutants were generated in order to investigate their involvement. It was shown, that deletion of the whole cluster in a *P. luminescens*  $\Delta$ MT strain terminated the production of all methylated derivatives, confirming their contribution. Additionally, single expressions of *plu4890*, *plu4891* and *plu4895* yielded one specific single-methylated derivative, respectively (AQ-270a/b/c), while *plu4892* and *plu4894* showed to be inactive. Finally, it was shown *in vivo* that the co-expression of *plu4890* and *plu4895* results in the formation of two double-methylated AQ variants (AQ-284a/b). Here, *in vitro* experiments with purified MTs confirmed a sequential activity of the respective MTs on the corresponding AQ-270 species. Thus, the derivatisation of AQ-256 in *P. luminescens* was fully elucidated. Finally, the AQ diversification in different *Photorhabdus* species was investigated as the MTs were shared among most strains. Interestingly, despite the high homologies, the product spectra differed among the investigated strains.

Greenhouse gas neutrality represents one of the key challenges that the modern world faces in order to combat human caused climate change. One of the keystones of the five-point plan of the German government to tackle this challenge is allegorized by the development of innovative energy storage systems like redox-flow batteries that utilize renewable energy sources. In the second part of this work, the development of an AQ-production platform is presented that can be utilized for electrolyte generation for redox-flow batteries. Additionally, the generation of a specialized AQ production medium is described that consists

of residual waste streams. Generally, a redox-flow battery is a type of electrochemical cell where chemical energy is provided by two chemical compounds that are dissolved in liquids and are pumped through the system on separate sides of a membrane. Here, flow of electric current occurs through the membrane while both liquids circulate in their respective cell spaces. Advantages of these energy storage systems are an easy scale-up and longevity. Already in 2014, a quinone-based battery cell was employed by researchers from Harvard that operated on lignosulfate, which unfortunately is connected to high operating expenses. Consequently, this work describes an alternative biotechnological approach to produce the quinone-derived AQ-256 that can be utilized as an electrolyte in redox-flow batteries. In the first step, the MTs were deleted that convert AQ-256 in different derivatives in *P. luminescens*, which allowed for only AQ-256 production. In the next step, the Sfp-type PPTase NgrA was deleted. It is essential for the production of most NP in *P. luminescens* as it converts inactive *apo*-acyl-carrier-proteins (ACPs) (part of PKS) or *apo*-peptidyl-carrier-proteins (PCPs) (part of NRPS) to their respective *holo* forms by posttranslational transfer of the 4'-phosphopantetheinyl (P-pant) moiety of coenzyme A to the side chain of a conserved serine residue in each carrier protein domain. While NgrA mediates the production of most NPs in *P. luminescens*, the AQ production is independent of the latter as the BGC harbors a highly cluster-specific PPTase (AntB). Here, the underlying idea was, to increase the pool of malonyl-CoA by shutting down production of most NPs other than AQ. Additionally, based on previous findings, the pathway-specific transcriptional activator AntJ was overexpressed to increase productivity. Ultimately, the combination of both approaches yielded an increase in AQ production of 7.2-fold (from 35 mg/L to 253 mg/L). In the second part of this project, in cooperation with Jan Burkhardt, AG Czermak, THM, an amino acid screening with generic XPP medium showed that some amino acid have beneficial effects on AQ production. On the same note, two insects (*Hermetia illucens* and *Bombyx mori*) were identified as potential residual waste streams for the generation of an AQ production medium. Ultimately, the AQ production rate of the manipulated *P. luminescens* strain could be increased to over 1 g/L in the new medium.

The third part of this work describes the characterization and elucidation of a silent BGC found in *P. luminescens* via antiSMASH analysis, which was predicted to result in the production of a terpenoid. As the cluster could not be activated through simple promoter exchange, the

expression was carried out in an engineered *E. coli* strain, which produces the isoprenoid building blocks necessary for terpenoid biosynthesis. Purification and subsequent elucidation of the product produced by the core genes of the cluster confirmed the structure as  $\beta$ -Carotene. Additionally, the cluster harbors a gene putatively encoding a carotenoid oxygenase. Subsequent experiments showed that the enzyme cleaved  $\beta$ -carotene asymmetrically into  $\beta$ -apo-14'-carotenal and  $\beta$ -apo-13-carotenone, which are structurally related to retinol that functions as a factor in signal transduction in many different organisms. As the expression of various carotenoid BGCs from different *Photorhabdus* species yielded the same results, it was postulated that the cluster is potentially involved in important ecological processes. Investigation of the ecological function in insect killing assays with *G. mellonella* showed that deletion of the cluster resulted in a decrease in lethality. Thus, it was assumed that the produced  $\beta$ -carotene exhibits a protective function against the insect's immune system. As the production of the cleavage products in HPLC-MS samples of infected *G. mellonella* was only observed after three days, it was assumed that the cluster exhibits a chimeric function where the retinoids are used by the nematode for signal transduction in late stages of the infection. This hypothesis was further substantiated by identification of putative retinoid binding partner in *H. bacteriophora* with bioinformatic tools. Here, future experiments are necessary to fully characterize the function of the retinoid cleavage products.

In summary, this work characterizes the post-PKS modifications of AQ-256. Additionally, the second part describes the establishment of an AQ production platform for electrolyte generation that can be utilized in redox-flow-batteries. Lastly, a silent BGC that encodes the genes for terpenoid biosynthesis was described and characterized with regards to product formation and putative ecological function.

## 4 Introduction

Over the course of millions of years, bacteria developed a tremendous diversity of different natural products (NPs). While they reveal a great range of useful bioactivities, often their physiological role remains unknown.<sup>1-4</sup> Ever since their discovery in the 17<sup>th</sup> century<sup>5</sup>, it has become more and more evident that bacteria produce NPs to facilitate a vast amount of mutualistic relationships to eukaryotes that result in alterations of many facets of their lives such as fitness, development, immune system and many others.<sup>6,7</sup> Additionally, bacteria can cohabit various hosts, amongst them parasites in synergistic relationships and are thus viewed as the driving force in host-parasite interactions. These interactions are relevant for evolutionary innovation as they contribute to an expansion of already existing ecological niches.<sup>8</sup> Sustaining a mutualistic interaction is often reliant on the formation of various NPs, which contribute to pathogenicity, development or suppression of food competitors.<sup>9,10</sup> Especially, the latter aspect is of major interest for pharmaceutical applications as those NPs can exhibit bioactivities against several groups of organisms such as fungi<sup>11</sup>, bacteria<sup>12-14</sup> and even higher eukaryotes.<sup>15-18</sup>

The main representatives of classes of NPs found in microorganisms include polyketides, non-ribosomal peptides, alkaloids and terpenes.<sup>19</sup> All of them can be assigned to different metabolic pathways, comprising a number of genes organized in an operon, so called biosynthetic gene cluster (BGC).<sup>20</sup> These BGCs consist of genes that encode for enzymes responsible for biosynthesis, modification, transport and regulation of the respective biosynthetic pathway. The discovery of the  $\beta$ -lactam antibiotic penicillin heralded the “golden era” of antibiotic and NP research.<sup>21,22</sup> Consequently, efficient treatment of infectious diseases became possible with the discovery of broad spectrum antibiotics like streptomycin, chloramphenicol, tetracycline and many others.<sup>23-25</sup> However, shortly after the introduction of the “wonder drugs”, some pathogenic bacteria developed resistances against certain antibiotics through mutations, horizontal gene transfer or over-and misuse.<sup>26,27</sup> At the present moment, the development of antibiotic resistances is without a doubt one of the most challenging health threats. According to the “Antibiotic Resistance Threats Report” from 2019, almost 3 million infections with antibiotic resistant bacteria and fungi are estimated every year in the US resulting in approximately 36.000 deaths.<sup>28</sup> Although new techniques for

culturing microorganisms and bioinformatic genome mining tools are developed with great effort, many NPs are still inaccessible as they are sometimes not produced under laboratory conditions.<sup>29,30</sup> Here, gaining knowledge about underlying regulatory mechanisms enables the possibility to manipulate production of unknown NPs to elucidate their ecological function.

#### **4.1 *Photorhabdus* and its complex life cycle**

*Photorhabdus luminescens* is a Gram-negative, facultative anaerobic, motile bacterium that was first described more than four decades ago and was originally isolated from its mutualistic partner *Heterorhabditis bacteriophora*.<sup>31–33</sup> Its name originates from the rod shape and its capability to produce bioluminescence.<sup>33</sup> The principle of the complex life cycle of *P. luminescens* has been known for some time and the nematode-bacteria interaction dependency has been investigated extensively (Fig. 1).<sup>34–36</sup>

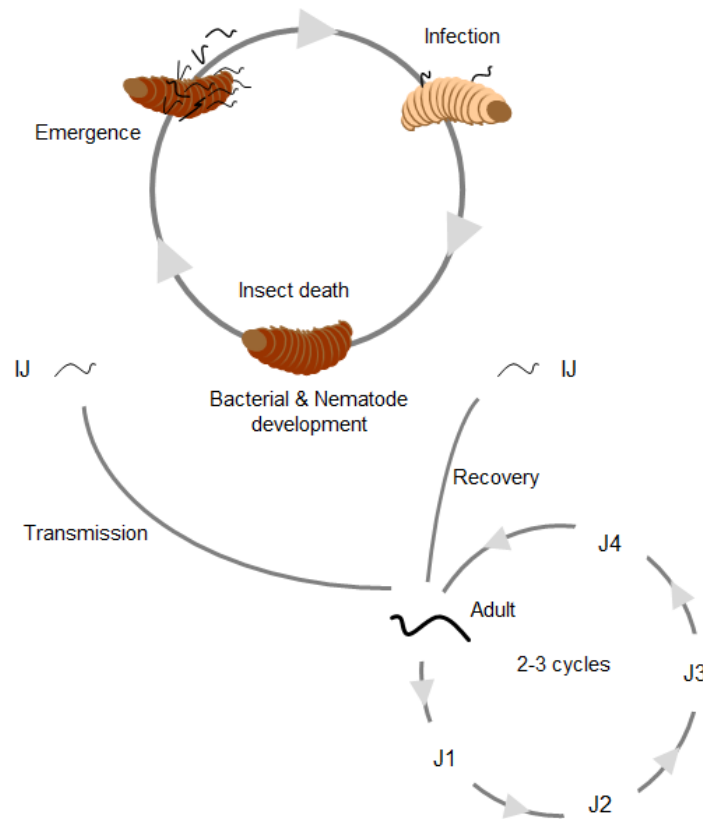


**Figure 1.** Life cycle of *Photorhabdus luminescens* in combination with its mutualistic nematode partner *Heterorhabditis bacteriophora*. *P. luminescens* is located in the gut of *H. bacteriophora* during its IJ stage. After infection of insect larvae by the nematode and the subsequent release of the bacteria into the hemocoel, the bacteria replicate and produce an array of NPs resulting in the death of the insect. The IJs recover into adults and cycle through different larval stages before a new generation of IJs develops after exhaustion of nutrients. Thereafter, the newly developed IJs receive their symbiont and the life cycle repeats. Parts of the figure were adapted<sup>37</sup>.

In the infective juvenile (IJ) stage *H. bacteriophora* carry the bacteria in their gut and cruise through the soil actively searching for insect prey.<sup>38</sup> Upon entering the insect larvae via natural openings or through the cuticle, the mutualistic bacteria are released into the hemocoel where they reproduce quickly.<sup>35,39</sup> Subsequently, a switch from the mutualistic form (M-form) of the bacteria to the pathogenic form (P-Form) is induced through unknown insect specific signals. In the process of infection, *Photorhabdus luminescens* produces an array of natural products (NPs) that contribute to the suppression of the insect's immune system and killing the prey.<sup>40,41</sup> The insect cadaver provides nutrient sources for both, bacteria and nematode, allowing for reproduction. Additionally, a wide range of different insect larvae can be killed by the entomopathogenic bacteria of which many represent agricultural pests.<sup>33,42</sup>

The mutualistic interaction between bacteria and nematodes is very specific whereas the nematode development highly depends on the presence of the cognate bacterial species.<sup>42,43</sup> After the carcass' depletion, IJ stage nematodes and bacteria re-associate and emerge from the dead insect larvae in order to seek a new insect host.<sup>44</sup> Finally, *Photorhabdus* can also kill insects when injected into its hemocoel in absence of its associated nematode under laboratory conditions, while naturally the bacteria benefit from the nematode as a vector transportation.<sup>45</sup>

## 4.2 Specialized NPs produced by *P. luminescens*

Although *Photorhabdus* have only been isolated from infected insect hosts or their associated mutualistic nematode host, the symbiosis is not obligate as they can be easily cultivated without their hosts in LB medium.<sup>46</sup> Thus, the bacteria are an excellent model organism for ecology and pathogenesis studies. When the genome of *P. luminescens* was first sequenced in 2003, it was confirmed that it encodes a high number of protein toxins in addition to biosynthetic gene clusters (BGCs) responsible for NP production.<sup>47</sup> By definition, a NP is a small molecule that is produced by a living organism, found in nature.<sup>48</sup> Consequently, this includes compounds produced in the primary as well as in the secondary metabolism. Primary NPs are central metabolites with assigned physiological functions in the respective organism that are crucial for its viability.<sup>49</sup> In contrast, secondary NPs are often highly diverse specialized compounds, which are not directly involved in development or growth of the respective organism but exhibit important ecological functions. Thus, absence of secondary NPs can reduce long-term survival, fitness or reproduction of the respective organism.<sup>50-52</sup> In *P. luminescens*, advanced molecular biological methods like heterologous expression and promoter exchange have been successfully applied in order to identify multiple NPs, still, there are cryptic BGCs that have not been elucidated yet as the compounds are not produced under laboratory conditions.<sup>53-56</sup> This suggests that NP production may be strictly controlled and the regulatory mechanisms and conditions to initiate production are not fully understood, yet.<sup>57</sup> The NPs identified in *P. luminescens* fulfill various tasks during its life cycle such as elimination of competitors<sup>40,58-60</sup>, host colonialization<sup>60,61</sup>, invasion and conversion of the insect cadaver<sup>47</sup> or cell-to-cell communication<sup>62,63</sup>. Selected NPs produced by *P.*

*luminescens* are depicted in Fig. 2. While kolossin, photobactin, GameXPeptide and indigoidine are produced by non-ribosomal peptide synthetases (NRPS), the synthesis of isopropylstilbene, photopyrone, dialkylresorcinols and anthraquinones (AQs) are carried out by polyketide synthases (PKS).<sup>64</sup>

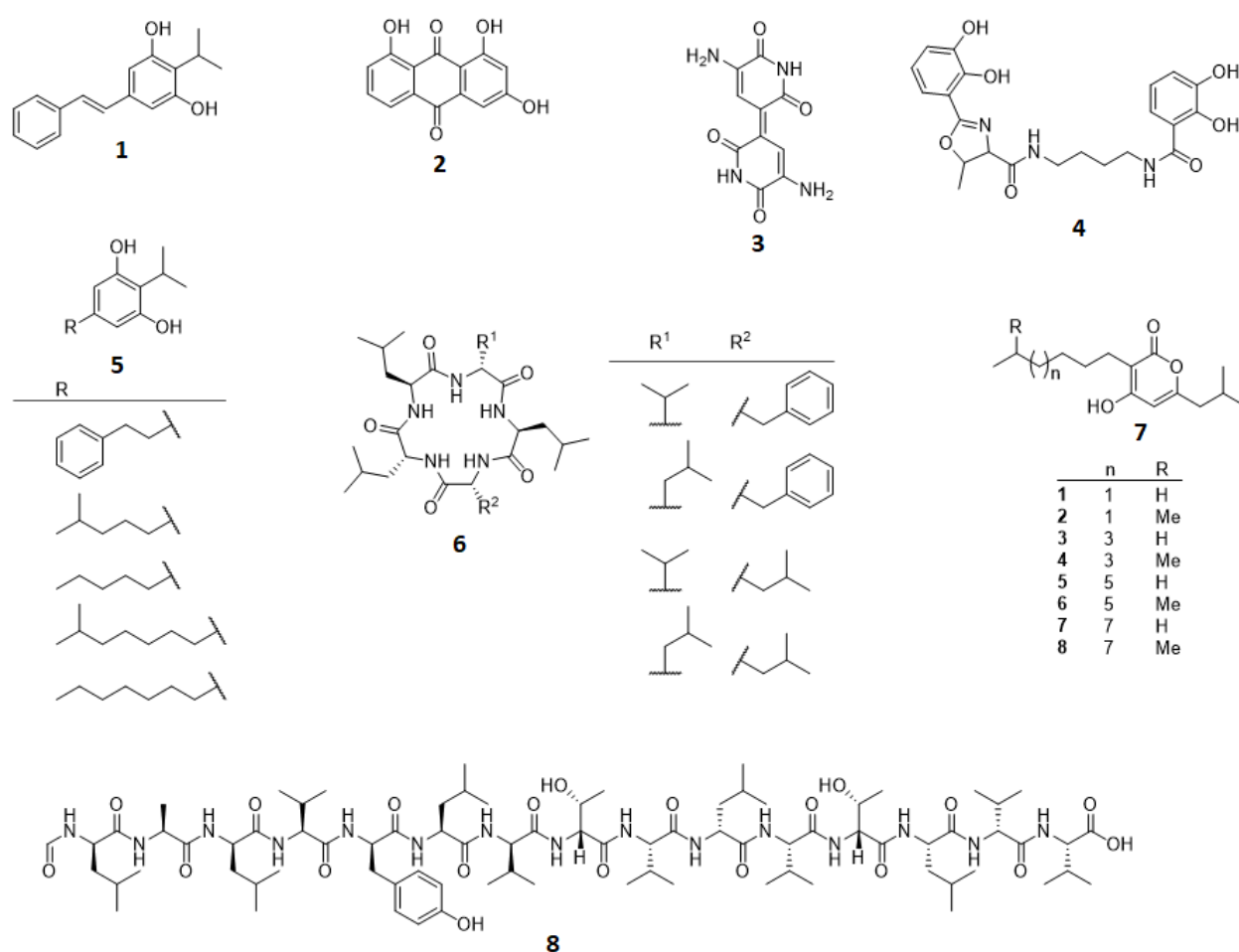


**Figure 2.** Selection of NPs produced by *P. luminescens*. Isopropylstilbene (1), AQ-256 (2), indigoidine (3), photobactin (4), dialkylresorcinols (5), GameXPeptides (6), photopyrones (7), kolossin (8).

Many of those bioactive molecules exist *in vivo* as small libraries composed of different derivatives that differ in methylation patterns, amino acid compositions or cyclic and linear variants. In a constant fluctuating environment with respects to different insect hosts and food competitors, these libraries are assumed to facilitate ecological adaptability. Here, a finely tuned regulatory system is required to overcome the described environmental challenges.



### 4.3 Thiotemplated assembly line in NRPS and PKS

NRPS and type I PKS enzymes belong to the family of megasynthases and show a modular organization.<sup>65</sup> Generally, one module is usually responsible for the incorporation of one building block during the biosynthesis whereas the number of modules is mostly congruent with the number of incorporated building blocks (type A NRPS, type I PKS).<sup>65</sup> While PKSs condense acyl and malonyl moieties to yield polyketides using ketosynthase (KS) domains, NRPSs link amino acid building blocks mediated by condensation domains.<sup>65</sup> For NRPS –and PKS-derived NPs, the production is strongly dependent phosphopantetheinyltransferases (PPTase).<sup>66</sup> The PPTase converts inactive *apo*-acyl-carrier-proteins (ACPs) (part of PKS) or *apo*-peptidyl-carrier-proteins (PCPs) (part of NRPS) to their respective *holo* forms by posttranslational transfer of the 4'-phosphopantetheinyl (P-pant) moiety of coenzyme A to the side chain of a conserved serine residue in each carrier protein domain. For PKSs, acetyl- and malonyl-building blocks are bound to *holo*-ACPs while for NRPSs, aminoacyl-moieties are bound to *holo*-PCPs. The genome of *P. luminescens* TT01 encodes two different types of PPTases. One being the AcpS-type PPTase plu3336 responsible for activation of fatty-acid ACPs and the other one being the Sfp-type PPTase NgrA, catalyzing secondary metabolite specific PCP/ACP-activation. Additionally, it encodes the pathway-specific PPTase AntB, which is embedded in the AQ BGC.

### 4.4 Polyketide synthases

Polyketide biosynthesis resembles fatty acid biosynthesis with respects to thiotemplate shuttling and includes activation of acyl and malonyl units by an acyltransferase followed by decarboxylative Claisen condensation reactions to yield linear or cyclic polyketides.<sup>67</sup> PKSs are divided in three different classes with Type I PKSs being multi-domain enzyme complexes and Type II PKSs being discrete enzymes that assemble to form megasynthases.<sup>67</sup> Finally, Type III PKSs act in an iterative manner and do not rely on ACPs as they extend the substrate while it is CoA bound.<sup>67,68</sup> This chapter mainly focuses on Type II PKS systems. As described, Type II PKS systems consist of freestanding monofunctional enzymes that act in an iterative manner. They are mainly found in Gram-positive bacteria, such as *Streptomyces*<sup>67</sup> and only a few examples exist in Gram-negative bacteria (described in chapter 4.3). The compounds

produced by Type II PKSs are mostly aromatic.<sup>69</sup> Typically, the starter unit consists of a malonyl-CoA-derived malonyl-ACP whereas the malonyl-CoA-acyl carrier protein transacylase (MCAT) is shared with fatty acid synthase type II systems (FAS II).<sup>70</sup> The transfer from the malonyl-CoA onto the *holo*-ACP creates the malonyl-ACP. As an extension unit, malonyl-CoA is used which is controlled by the stringent substrate specificity of the MCAT.<sup>71</sup> Furthermore, the malonate is transferred to the conserved cysteine of the elongation  $KS_{\alpha}$ .  $KS_{\alpha}$  forms a heterodimer with the chain-length factor (CLF) generating the acyl-starter unit.<sup>72</sup> Subsequently, the starter unit is elongated with a newly loaded malonyl-ACP resulting in the first  $\beta$ -ketoacyl product. Repeated elongation cycles are initiated by retransfer of the  $\beta$ -ketoacyl product onto  $KS_{\alpha}$ .<sup>72</sup> In the following steps, the polyketide is cyclized and reduced by a cyclase and a KR, respectively. Aromatization is facilitated by an aromatase. Finally, the polyketide is cleaved off and the aromatic structure is released.<sup>69</sup> Often, the released aromatic compound is further processed by tailoring enzymes such as methyltransferases (MTs), oxygenases or glycosyltransferases.<sup>73</sup> The basic mechanisms of aromatic polyketide biosynthesis are depicted in Fig. 3.

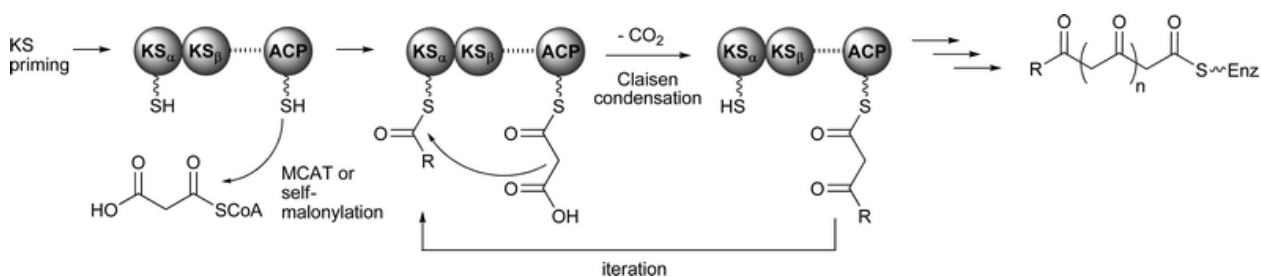


**Fig. 3.** The basic mechanisms of aromatic polyketide biosynthesis. Picture taken from Hertweck *et. al*<sup>69</sup>.

#### 4.5 AQ biosynthesis and regulation in *Photorhabdus*

*Photorhabdus* strains exhibit a characteristic orange-reddish color during its exponential growth phase. This pigmentation is caused by the production of different AQ derivatives. The corresponding gene cluster was already described in 2007<sup>74</sup> and displays one of the few examples of a type II PKS-derived product from Gram-negative bacteria.<sup>75</sup> In addition to the minimal PKS, the gene cluster encodes for a CoA-ligase, a ketoreductase (KR), an aromatase (ARO), a cyclase (CYC), a hydrolase and a Sfp-type PPTase which are responsible for the production of AQ-256 (Fig. 4, A). However, the MTs involved in converting AQ-256 into its methylated derivatives remained unknown until a gene cluster, encoding five highly homologous MTs (*plu4895-plu4890*), was recently discovered and partially described.<sup>76</sup> Furthermore, the work identified AntJ as a novel pathway-specific transcriptional regulator that specifically activates the expression of the AQ BGC in *P. luminescens*. Transcriptome analysis revealed a significant downregulation of *antA-I* in the absence of the activator whereas it had no effect on the expression of other NP-BGCs. AntJ is predicted to comprise a N-terminal DNA-binding domain and a C-terminal putative ligand binding domain and binds specifically upstream of *antA*<sup>77</sup>. In addition, AntJ regulation itself is governed by a global regulatory mechanism, which affects general NP production in *P. luminescens*. The RNA chaperone Hfq appeared to be indispensable for general NP production, as its deletion led to abolishment thereof.<sup>78</sup> In this work, the derivative formation during late steps of the AQ biosynthesis were investigated extensively.

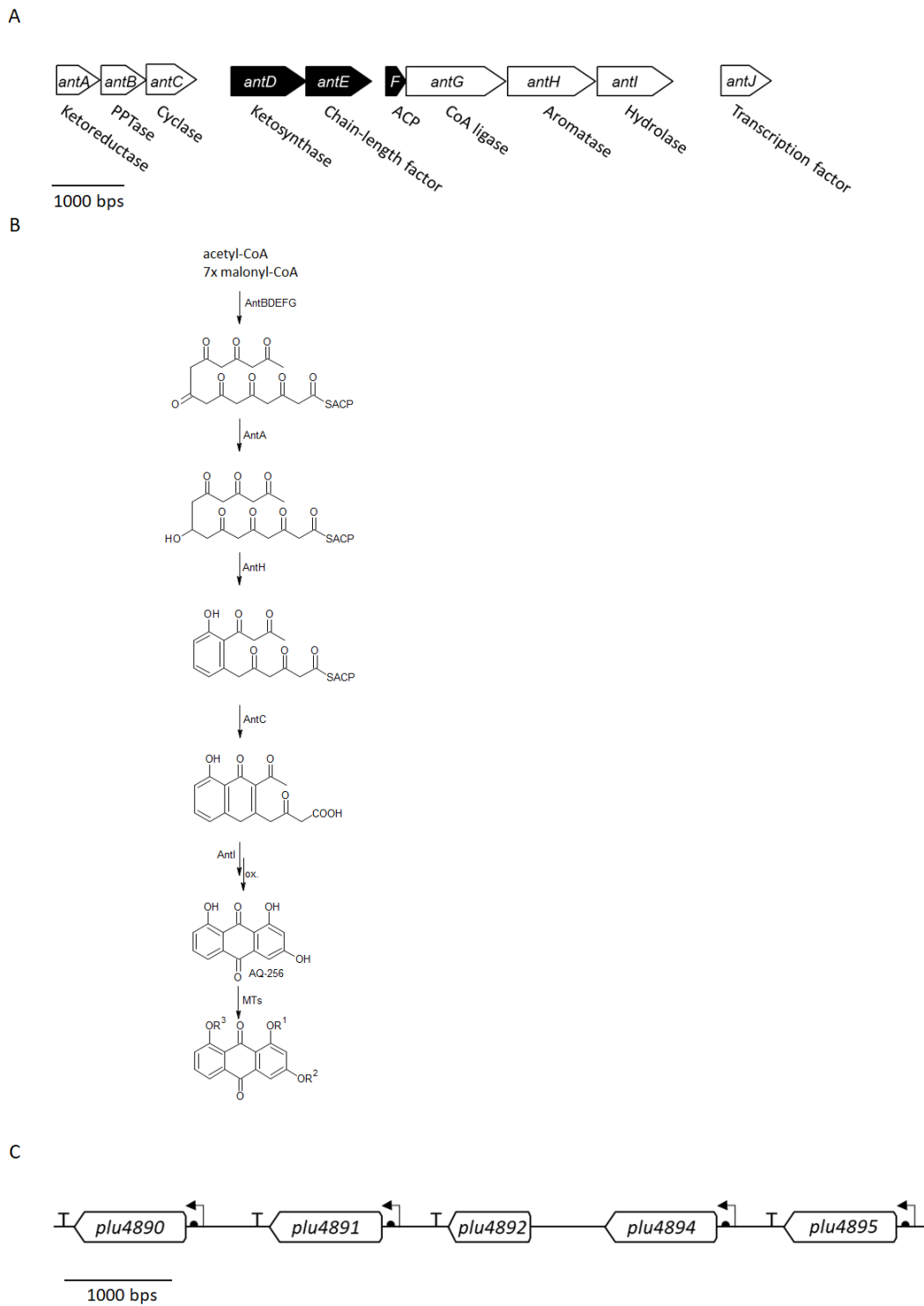


**Figure 4.** AQ biosynthesis and AQ-derivatives in *P. luminescens*. (A) *antA-J* gene cluster identified in *P. luminescens*. (B) AQ biosynthesis and AQ-derivatives in *P. luminescens* (C) The gene cluster *plu4895-4890* encodes five homologous MTs, which are involved in methylation of AQ-256 in its derivatives. Genes in black depict transposase remnants. Promoters are depicted as arrows, ribosome binding sites as semicircles and terminators are indicated as T.

#### 4.6 Biotechnological production of electrolytes for redox flow batteries

Greenhouse gas neutrality represents one of the key challenges that the modern world faces in order to stop human caused climate change and is concomitant with the invocation for innovative technologies regarding a turnaround in energy policy.<sup>79</sup> The German government developed a five-point approach in order to establish greenhouse gas neutrality until 2050.<sup>79</sup> Here, one of the key aspects is represented by the utilization of residual waste streams for energy generation and storage. Consequently, with increasing demand for energy from renewables, reliability of power supply is crucial and requires expansion of the power grid and establishment of decentral energy storage.<sup>80</sup> Currently, while the power generation in Germany lies within the range of TWh, the energy storage capacity of battery-based systems is limited to kWh.<sup>81</sup> Thus, in order to overcome this gap in storage demand and supply, researchers heavily focus on advancement of lithium-ion batteries and development of novel redox-flow batteries. A Redox-flow battery is a type of electrochemical cell where chemical energy is provided by two chemical compounds that are dissolved in liquids and are pumped through the system on separate sides of a membrane. Here, flow of electric current occurs through the membrane while both liquids circulate in their respective cell spaces.<sup>82,83</sup> The principle is depicted in Fig. 5. The main advantages of these batteries are easy scale-ups that are only limited by the deployed electrolyte, flexible layouts, long cycle lives and no harmful emissions.<sup>84</sup> Congruent with guidelines of environmental compatibility, research currently focuses on utilization of common renewable electrolyte sources. Accordingly, in 2014 a quinone-based redox-flow battery was developed by scientists in Harvard.<sup>85</sup> A nearly unlimited supply of quinone is harbored in lignosulfate as a waste product of paper industry. Unfortunately, the harvest of the respective electrolytes is connected to high operating expenses.<sup>86</sup> Consequently, this work describes an alternative biotechnological approach to produce the quinone-derived AQ-256 that can be utilized as an electrolyte in redox-flow batteries. In here, the establishment of a *P. luminescens* AQ-256 high producer is shown that is based on overexpression of the pathway-specific transcriptional regulator AntJ in addition to elevation of malonate building block levels.

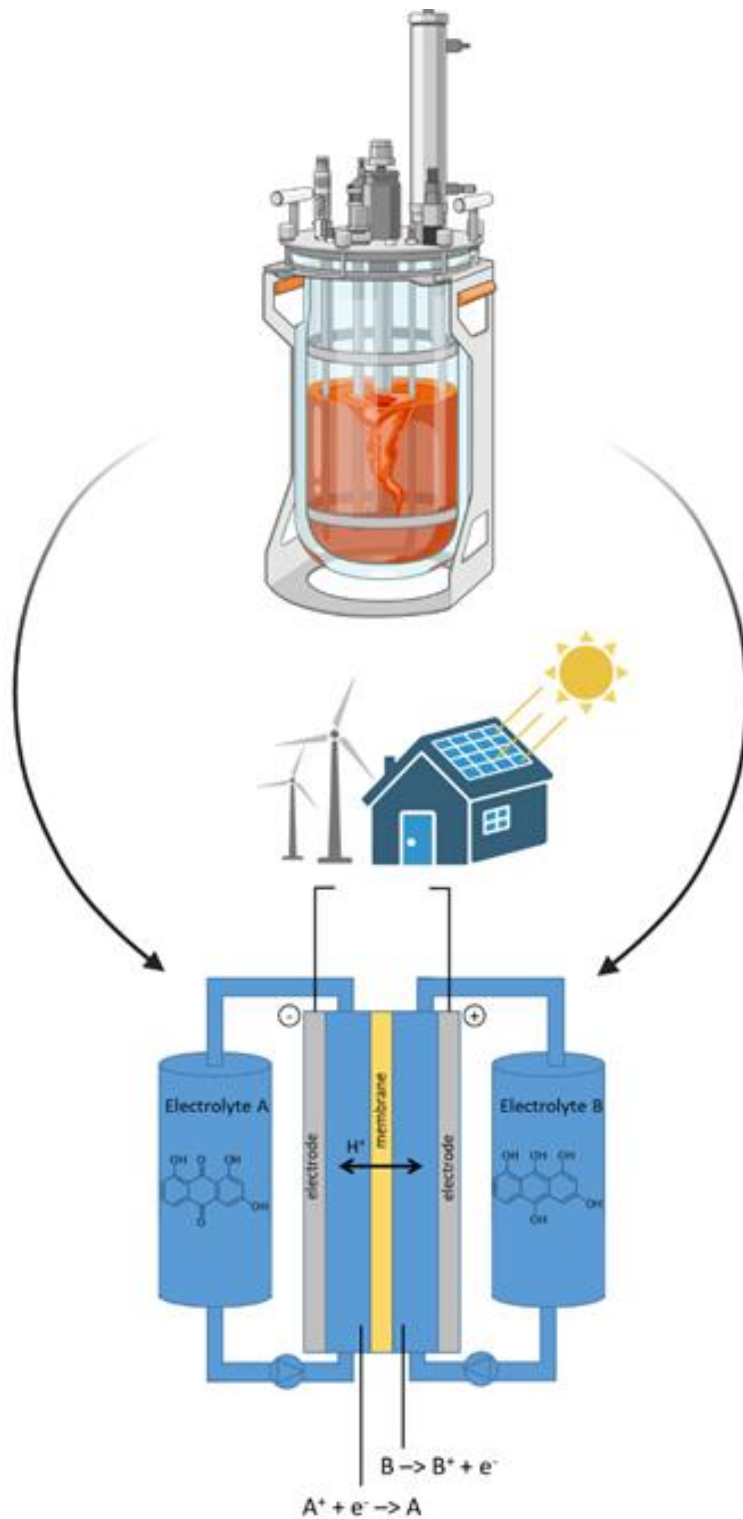


**Fig. 5.** Schematic illustration of a redox flow battery that facilitates quinone-derived electrolytes to store energy produced by renewable energy sources. In the depicted approach, the electrolytes are produced by fermentation in *P. luminescens*, harvested and subsequently induced into the reactor. Figure 5 was partially generated with biorender.com.

#### 4.7 Electrolyte production from residual waste products

In accordance with guidelines of environmental compatibility, a specialized *Photobacterium* NP production medium was established that is based on residual waste products. In preliminary work, the influence of simulating the insect host environment was studied for alterations on NP production.<sup>87</sup> It was shown that supplementing insect homogenate from *Galleria mellonella* larvae to LB cultures altered the NP profile of *P. luminescens*. Crucially, production of AOs and IPS was increased. Unfortunately, *Galleria mellonella* larvae are not recyclable waste products, costly and thus not suited for generating an inexpensive NP production medium. In an extensive literature research, two insect candidates were identified that are cost efficient to obtain and part of industrially recyclable waste products. Firstly, the black soldier fly (*Hermetia illucens*) is an insect that can be grown and harvested without dedicated facilities and is not pestiferous.<sup>88</sup> Importantly, their biggest advantage over other insects is their ability to convert waste into food, generating value and closing nutrient loops as they reduce pollution and costs.<sup>88</sup> Secondly, the silkworm (*Bombyx mori*) is industrially used for silk production. However, after entering pupal phase, the silk cocoons are harvested while the silkworms remain as leftovers.<sup>89</sup> In this work, NP production was carried out in an improved version of XPP medium described in chapter 6.2 in addition to insect powder obtained from *Bombyx mori* and *Hermetia illucens* insects, respectively. In the screening, *P. luminescens* was used and the NP profile of selected NPs was analyzed. A schematic overview of the medium generation is depicted in Fig. 6.

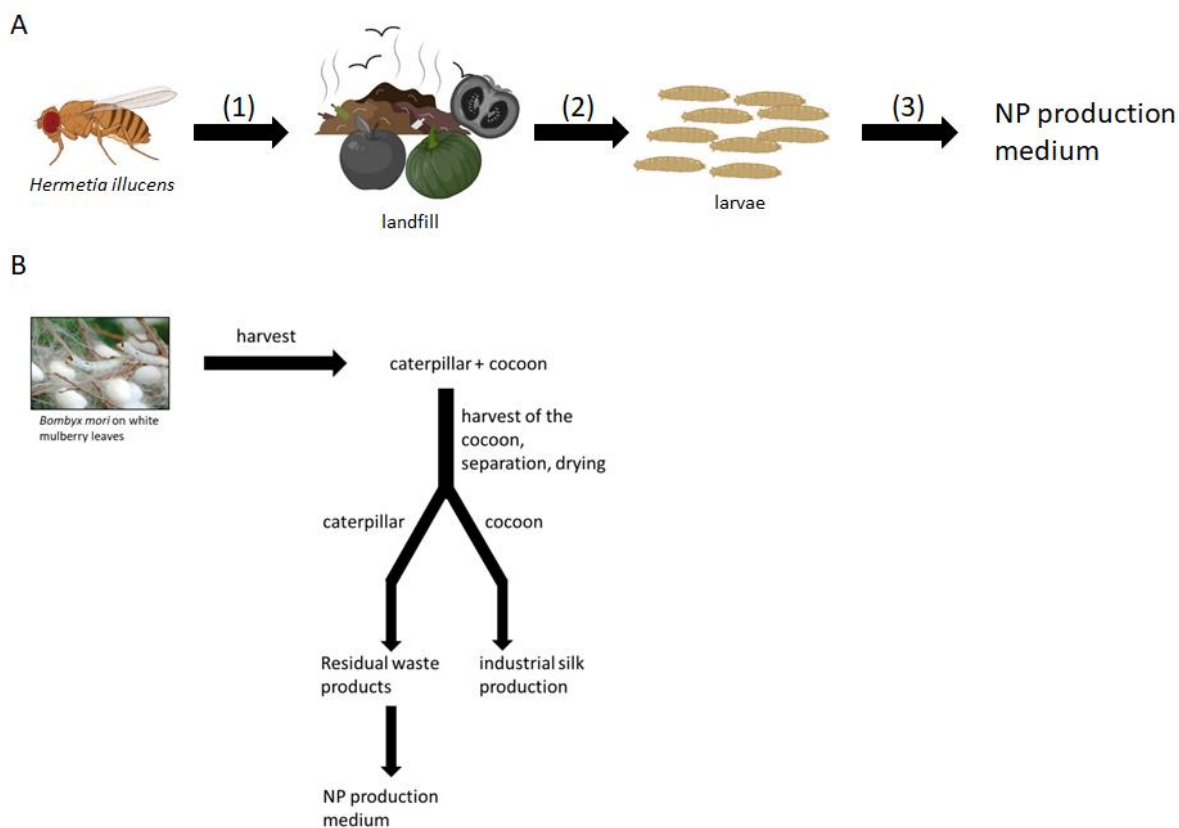


**Fig. 6.** Schematic overview of the insect powder contents utilized for NP production media. (A) *Hermetia illucens* are cultivated on landfill sites (1) and the subsequently emerging larvae (2) are harvested and utilized for the development of NP production media (3). (B) *Bombyx mori* are cultivated on white mulberry leaves. In the subsequent harvest, the worm and the cocoon are separated while the cocoon is used for industrial silk production whereas the caterpillar remains as residual waste that can be utilized in NP production media. Parts of the figure were generated with biorender.com.

#### 4.8 BGC elucidation and NP identification

Traditional approaches for NP identification are based on strain cultivation, followed by compound purification and subsequent screening for biological activity.<sup>90</sup> In such cases, altering cultivation parameters such as medium ingredients, fermentative scale, oxygen flow or the supplementation of additives such as enzyme inhibitors can yield additional compounds or result in derivative formation and is often referred to as the “One strain many compounds” (OSMAC) approach.<sup>91,92</sup> Compound production is assumed to only be carried out upon demand and might be influenced by environmental conditions such as cell-cell communication, competition against other organisms or stress factors e.g. nutrient depletion or temperature.<sup>93</sup> Additionally, co-cultivation of different strains can trigger the production



of novel NPs.<sup>94</sup> Generally, the above described approaches for NP identification mostly do not require genomic information and are often bioactivity guided. The identification of the first BGC as origin of NP production including non-ribosomal peptides and polyketides and the conclusion that the respective genes are arranged in clusters were seen as remarkable milestones of NP research.<sup>20</sup> Per definition, a BGC consists of at least two genes, which are located in close proximity in the same genome and encode enzymes that are responsible for the biosynthesis of a specialized NP.<sup>95</sup> Here, BGCs that are not expressed under laboratory conditions are referred to as “silent” but can be predicted by bioinformatics tools and specifically activated for compound elucidation.<sup>96</sup> Consequently, bioinformatics tools like ANTIbiotics and Secondary Metabolite Analysis Shell (antiSMASH), Prediction Informatics for Secondary Metabolomes (PRISM) and Secondary Metabolite Unknown Regions Finder (SMURF) are powerful instruments to predict and elucidate BCGs based on sequence information.<sup>97</sup> Generally, BGCs are identified based on similarity to conserved domains of core biosynthetic enzyme domains by Hidden Markov Model (HMM) profiles.<sup>97</sup> Upon identification of a BGC candidate, various methods can be employed for elucidation. In untargeted approaches, global transcription factors can be utilized as it was shown in *Xenorhabdus szentirmaii* where the expression of the global transcriptional regulator LeuO from *X. nematophila* led to the identification of two new compounds.<sup>98</sup> Additionally, they include deletion or overexpression of specific transcriptional regulators.<sup>96</sup> A powerful and highly efficient tool for BGC elucidation includes heterologous expression of the respective BGC in model organisms like *Escherichia coli*.<sup>99</sup> Here, the BGCs are cloned on specific expression vectors and subsequently compound production is conducted.

#### **4.9 NP identification using LC-MS-based strategies**

Nuclear magnetic resonance (NMR) techniques are applied for structural elucidation of a NP subsequent to compound isolation and purification.<sup>100</sup> Often, the bottleneck for NMR-based elucidation approaches are low production titers or impurities. In order to overcome these limitations, various LC-MS-based methods have been developed to gain structural information without the necessity of purification. First, high resolution (HR) MS experiments allow sum formula predictions of investigated compounds.<sup>101</sup> Additionally, cultivation of the

respective NP producer strain in  $^{13}\text{C}$  and  $^{15}\text{N}$  labelled medium results in the production of compounds with increased molecular weight, which can be utilized to confirm the predicted sum formula via HR-MS.<sup>102</sup> Furthermore, comparison of retention time and MS<sup>2</sup>-spectra between the respective NP and a synthetic standard in LC-MS experiments can be used for structure confirmation.<sup>103</sup> Finally, LC-MS analysis is also suitable to investigate production characteristics such as derivative formation and production titers of the respective BCGs. For this, tools like heterologous expression, specific gene deletions or precursor complementation are often facilitated.<sup>104,105</sup>

#### **4.10 Carotenoid-derived NPs**

Carotenoids are one of the most widely spread and ubiquitous compounds, which are found in plants, algae, bacteria and fungi.<sup>106</sup> In terms of application, carotenoids play a versatile biological role that crucially contribute to therapeutic effects, including anti-cancer, anti-inflammatory, antibacterial, cardiovascular diseases, anti-oxidants, anti-tuberculosis, anti-diabetic and neuroprotective.<sup>107–117</sup> Thus, carotenoid-derived compounds represent an attractive research field for pharmaceutical applications. Furthermore, these phytochemical compounds belong to the isoprenoids and their core structure comprises eight isoprene units resulting in a C<sub>40</sub> backbone.<sup>118</sup> Generally, carotenoids are subdivided in two different classes. While carotenes consist of pure hydrocarbons, xanthophylls contain one or more oxygen functions.<sup>118</sup> Their biosynthesis has been investigated in various plants and microorganisms and is known as carotenogenesis (Fig. 7). In general, the active isoprene are formed through isoprenoid building blocks. Subsequently, condensation of isoprene units results in phytoene formation. While lycopene is formed through extension by four desaturation steps and isomerization, cyclization of lycopene ends to generate carotenes. Finally, involvement of oxygen results in various xanthophylls.

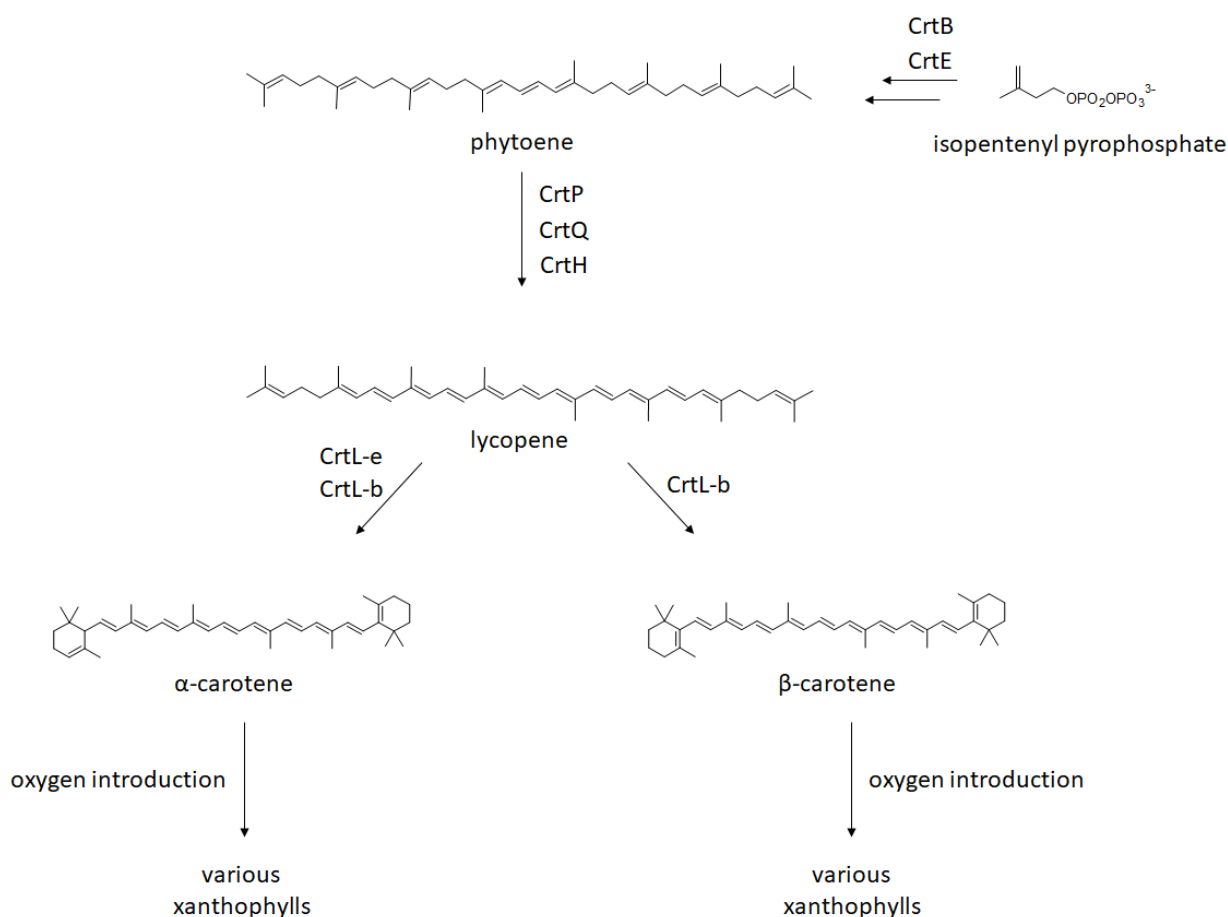


**Fig.7.** Carotenogenesis pathways and enzymes, whose functions are confirmed in oxygenic phototrophs. Condensation of isopentenyl pyrophosphate through the phytoene synthase (CrtB) and geranylgeranyl pyrophosphate synthase (CrtE) leads to biosynthesis of phytoene. Lycopene is formed in multiple steps through activity of the phytoene desaturase (CrtP), carotene desaturase (CrtQ) and carotene isomerase (CrtH). Generation of α-carotene and β-carotene, respectively, is mediated by variants of the lycopene cyclase (CrtL-e, CrtL-b). Ultimately, introduction of oxygen results in various xanthophylls.

#### 4.11 Oxidative tailoring of carotenoids

Not only do carotenoids play a crucial role in their intact form in various organisms but they also act as important reservoirs for lipid-derived bioactive mediators.<sup>119</sup> This process is initiated by specific tailoring enzymes that cleave the respective carotenoids into apocarotenoids.<sup>120,121</sup> Majorly, the extended polyene chromophore of carotenoids make them susceptible to cleavage at almost every position. Various apocarotenoids and their designated cleavage sites are displayed in Fig. 8. Generally, these compounds are widespread in most taxonomic groups and play important roles in different physiological processes (see

4.12).<sup>122</sup> Additionally, apocarotenoids include compounds that account for high economical value in industrial applications.<sup>122</sup>

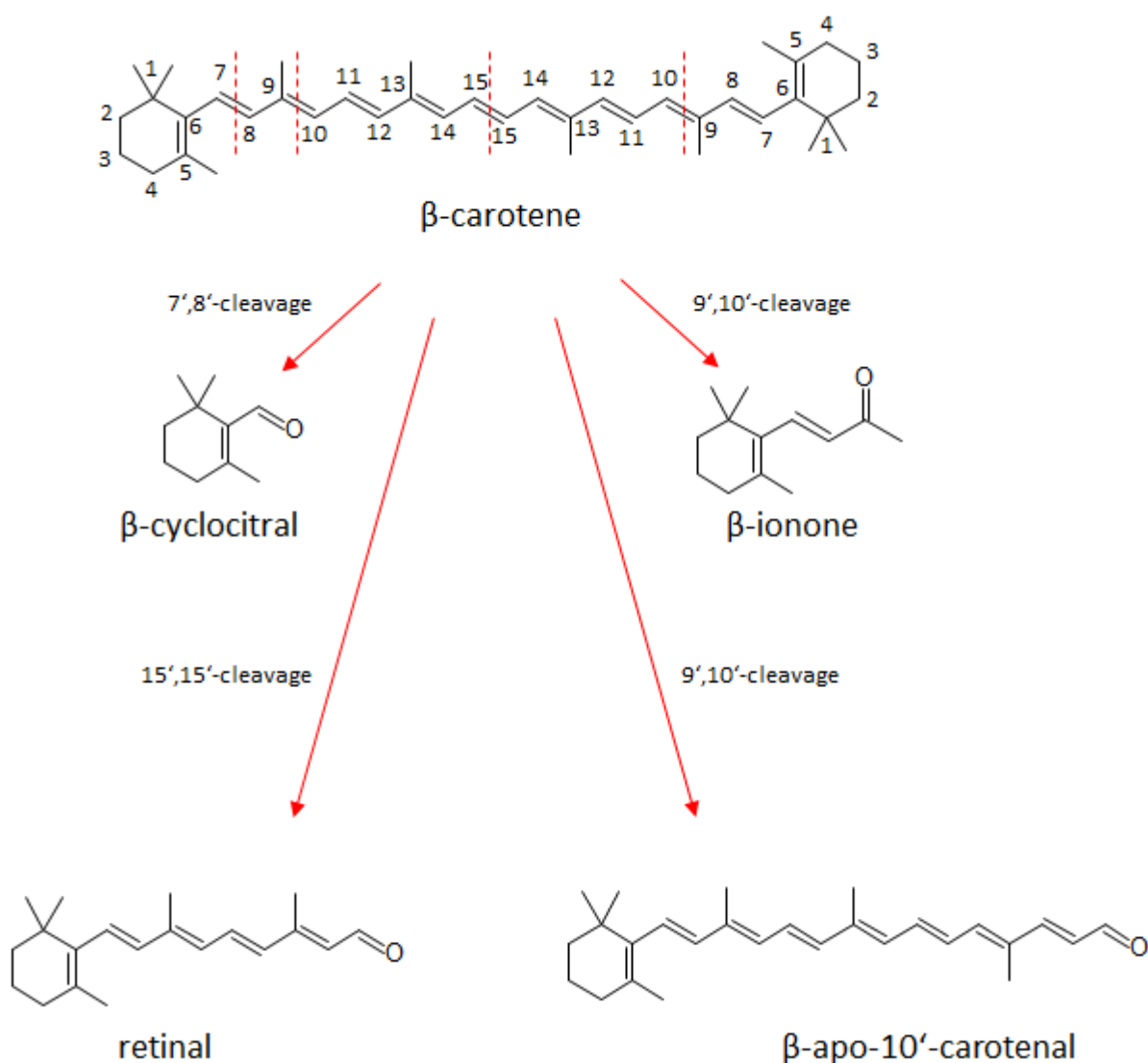


**Fig. 8.** Diversity of apocarotenoids cleavage products.  $\beta$ -carotene acts as a precursor and gets subsequently cleaved by specific oxygenases resulting in several cyclic and linear derivatives. The respective cleavage sites are indicated with red dotted lines.

Several carotenoid cleavage enzymes have been identified in plants, animals and microorganisms and grouped into different classes based on their substrate specificity.<sup>123–125</sup> In general, carotenoid cleaving dioxygenases (CCDs) group by their ability to cleave carotenoids either symmetrically or asymmetrically.<sup>126</sup> However, the biological roles of CCDs in bacteria are not well established. In cyanobacteria, apocarotenoids act as photo-protective compounds in thylakoid membranes<sup>127</sup> and are responsible for flavors and odors<sup>122</sup>. Crucially,

in some archaea and eubacteria, CCDs play an essential role in retinal biosynthesis, the chromophore for rhodopsin or similar pumps<sup>128-130</sup>. On the same note, retinal derivatives are a major part of signaling pathways as they exhibit ligand functions of retinoic acid receptors<sup>131</sup>. Structurally, bacterial CCDs resemble 7-bladed propellers whereas the active center is located on top of the enzyme<sup>132</sup>. As a cofactor,  $\text{Fe}^{2+}$  is coordinated by four histidine residues and is indispensable for the cleavage activity<sup>132</sup>. Characteristically, CCDs contain a tunnel perpendicular to the “propeller axis” that is important for the entrance of the substrate and is located in a large hydrophobic patch that allows for membrane localization (Fig. 9).<sup>132</sup>

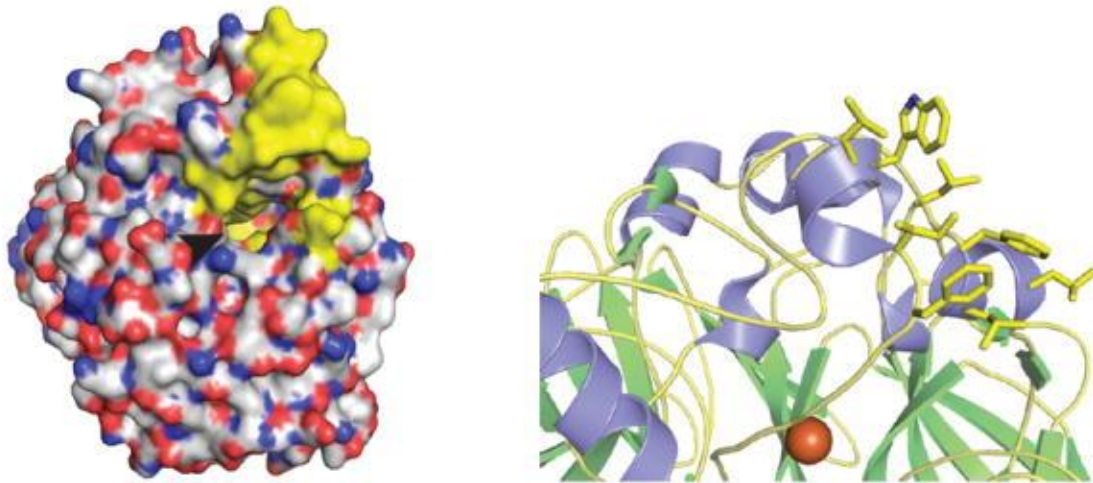


**Fig. 9.** Surface view of crystal structure of CCD ACO from cyanobacterium *Synechocystis sp.* Hydrophobic surface portions are colored in yellow. Right, hydrophobic residues colored in yellow for membrane penetration are shown. The arrowhead indicates the opening of cavities that lead to the active site iron. Figure taken from Sui et. al.<sup>132</sup>

#### 4.12 Function of apocarotenoids

In a vast amount of organisms from several taxonomic groups, retinal-derived apocarotenoids play a crucial role in signal transduction.<sup>133,134</sup> In higher animals, carotenoids commonly are scavenged from their surrounding and furthermore processed by certain CCDs. As an example, the  $\beta$ -carotene 15,15-oxygenase BCO1 found in rats cleaves  $\beta$ -carotene symmetrically resulting in two retinal molecules which bind to retinoid receptors (RXRs) to modulate signaling pathways that are involved cognitive stimulation.<sup>135,136</sup> In plants, carotenoids are often synthesized by the organism itself and subsequently cleaved by a number of CCDs into different products. The group of plant apocarotenoids comprises important phytohormones, such as abscisic acid and strigolactones, and signaling molecules, such as  $\beta$ -cyclocitral. Abscisic acid is one of the key regulators of plant's response to abiotic stress and is involved in different developmental processes, such as seed dormancy<sup>137,138</sup>. Strigolactone acts a main regulator of plant architecture and an important signaling molecule in the plant-rhizosphere communication<sup>139</sup>.  $\beta$ -Cyclocitral, a volatile derived from  $\beta$ -carotene oxidation, mediates the response of cells to singlet oxygen stress.<sup>140,141</sup> However, the role of apocarotenoids in bacteria is not well established yet. In cyanobacteria, apocarotenoids act as photo-protective compounds in thylakoid membranes<sup>127</sup> and are responsible for flavors and odors.<sup>122</sup> This work describes the identification and elucidation of a carotenoid BGC in *P. luminescens*. Furthermore, the CCD putatively associated with the BGC is characterized concerning product formation and putative ecological functions. Here, the focus lied especially on the mutualistic bacteria-nematode interaction.

#### 4.13 Aim and motivation of this work

The overarching goal of this work is to expand the knowledge about function, regulation and utilization of pigment production in *P. luminescens*. Recent research highlighted value of the two pigment classes (AQ and carotenoids) that are encoded in the genome of *P. luminescens*. This work focuses on three different topics described below.

### *Topic A*

The first chapter of this work focuses on the identification and elucidation of the MTs that are involved in AQ derivative formation. As mentioned above, *Photorhabdus* strains exhibit a characteristic orange-reddish color upon their exponential growth phase. This pigmentation is caused by the production of different AQ derivatives. However, the MTs involved in converting AQ-256 into its methylated derivatives remained unknown until a gene cluster, encoding five highly homologous MTs (*plu4895-plu4890*), was recently discovered and partially described. The experiments described in this thesis elucidate the MT production formation patterns *in vivo* and *in vitro*. Additionally, the generated products were elucidated with detailed HPLC-MS, 1D and 2D NMR experiments.

### *Topic B*

As already mentioned, in the quest for greenhouse gas neutrality one of the key aspects is represented by the utilization of residual waste streams for energy generation and storage. Furthermore, researchers heavily focus on advancement of lithium-ion batteries and development of novel redox-flow batteries to overcome storage capacity limitations. Previous work already showed that quinone-based batteries are easy to scale-up and capable of storing high amounts of energy. However, one of the main bottlenecks represents the difficult and inefficient isolation and preparation of these compounds. Consequently, this work focused on an alternative biotechnological approach to produce the quinone-derived AQ-256 in industrial scales that can be utilized as an electrolyte in redox-flow batteries. Additionally, in accordance with guidelines of environmental compatibility, a specialized *Photorhabdus* NP production medium was established that is based on residual waste products.

## Topic C

The third part of this work focused on the elucidation and characterization of a hitherto unknown BGC in *P. luminescens* that was predicted to encode genes associated with carotenoid biosynthesis. Carotenoids are one of the most widespread and ubiquitous compounds, which are found in plants, algae, bacteria and fungi. In terms of application, carotenoids play a versatile biological role that crucially contribute to therapeutic effects, thus representing an attractive research field for pharmaceutical applications. Additionally, through usage of bioinformatic tools like antiSMASH and Blastp, a predicted CCD was identified putatively involved in carotenoid tailoring. Consequently, this work aimed for cluster characterization, product elucidation, and their putative ecological function.

# 5 Material and Methods

## 5.1 General Methods

General methods which include cloning associated steps that apply to all projects are described in chapter 5.1. Material and methods for specific experiments conducted for the respective projects are presented in sections 5.2-5.4.

### 5.1.1 Plasmid isolation and purification

4 ml of *E. coli* LB overnight culture was centrifuged at 13300 rpm for 1 min. After discarding the supernatant, the pellet was resuspended in 250 µl Buffer 1 (50 mM Tris-HCl pH 8, 10 mM EDTA pH 8, 100 µg/ml RNase A). Subsequently, 250 µl Buffer 2 (200 mM NaOH, 1% SDS) was added and the reaction tube was inverted a couple of times. In the next step, 250 µl Buffer 3 (3 M NaAc pH 5.4) was added to the mix and after inverting the sample was centrifuged for 5 min at 13300 rpm. DNA was precipitated by adding 600 µl isopropanol to the sample followed by centrifugation. The remaining supernatant was discarded and the DNA-plasmid pellet was washed with 400 µl 70% EtOH and after drying resuspended in 20 µl ddH<sub>2</sub>O. The samples were stored at -20°C.



### **5.1.2 Purification of PCR products**

PCR product purification was done by using Monarch PCR&DNA Cleanup Kit (New England Biolabs, Frankfurt).

### **5.1.3 Extraction of DNA from agarose gels**

DNA extraction from agarose gels was performed by using the Invisorb® Spin DNA Extraction Kit (Stratec Molecular GmbH) according to the manufacturer's instructions.

### **5.1.4 Isolation of genomic DNA**

Isolation of genomic DNA was performed by using the Gentra Puregene Yeast/Bact. Kit (QIAGEN GmbH) according to the manufacturer's instructions.

### **5.1.5 Measurement of DNA/protein concentration**

Determination of DNA/protein concentration was performed by using a NanoDrop spectrophotometer (Thermo Scientific).

### **5.1.6 Polymerase chain reaction (PCR)**

Polymerase chain reaction (PCR) was used to amplify DNA fragments by using oligonucleotides as primers. For standard 2-step PCR reactions Phusion High Fidelity Polymerase (Thermo Scientific) was used. All reactions were performed according to the following protocol (Table 1):

**Table 1:** PCR standard protocol.

Reagent	Amount [ $\mu$ l]	Reaction step	Temperature[ $^{\circ}$ C]	Time [s]	Cycles
5x Buffer	4	Denaturation	98	30	1
dNTPs 10mM	0.4	Denaturation	98	10	25
MgCl <sub>2</sub> 50mM	0.4	Annealing	55-65	15	25
DMSO	0.4	Elongation	72	30/kb	25
Phusion	0.1				
Primer fw 0.2 $\mu$ M	4				
Primer rv 0.2 $\mu$ M	4				
Template DNA	variable				
H <sub>2</sub> O	ad. 20 $\mu$ l				

### 5.1.7 Colony PCR of *E. coli* and *Photothabdus luminescens* strains

Colony PCR was used to verify plasmid cloning. Additionally, it was employed to confirm genomic integration and deletion events during conjugation in *Photothabdus luminescens*. In the case of *E. coli*, cell material of a single colony was resuspended in 50  $\mu$ l ddH<sub>2</sub>O and 1  $\mu$ l of the suspension was used as template for PCR. For colony PCR with *Photothabdus luminescens* cell material of a single colony was resuspended in 50  $\mu$ l 10x Thermo Pol<sup>®</sup> Buffer and subsequently incubated in a thermocycler at 95 $^{\circ}$ C for 15 min while shaking. Here, 1  $\mu$ l of the suspension was used as template for PCR (Table 2).

**Table 2:** Standard colony PCR protocol.

Reagent	Amount [ $\mu$ l]	Reaction step	Temperature[ $^{\circ}$ C]	Time [s]	Cycles
10x Thermo Pol <sup>®</sup> Buffer	2.5	Denaturation	95	150	1
dNTPs 10mM	0.5				
Taq Polymerase	0.1	Annealing	68	15	25
Primer fw 10 $\mu$ M	0.5	Elongation	68	30/1 kb	25
Primer rv 10 $\mu$ M	0.5	Final Extension	68	300	1
Cell suspension	1				
H <sub>2</sub> O	ad. 25 $\mu$ l				

### 5.1.8 Hot Fusion assembly

Hot Fusion assembly was performed for DNA fragment assembly accordingly<sup>142</sup>. Subsequently, the reaction mix was transformed into electrocompetent *E. coli* cells or stored at -20 $^{\circ}$ C.

### 5.1.9 Gel electrophoresis

For separation of DNA fragments, gel electrophoresis was performed. Standard protocols were derived<sup>143</sup>. In short, gels were prepared with 1% agarose (w/v) and 3  $\mu$ l ethidium bromide per gel in 1xTAE buffer. 10x loading dye was added to DNA samples. Gels were subsequently run at 120-140 V and 160-210 mA for 25-40 min. For band visualization and analysis, a Gelstick imager (INTAS Science imaging) with a UV lamp was used.

## 5.2 Topic A

The following part contains all materials and methods used for the experiments covered in topic A. Oligonucleotides and gene fragments were purchased from Eurofins Genomics and are listed in table 3 and 4, respectively. Used plasmids are listed in table 5. Strains used in this work are listed in table 6.

**Table 3:** Overview of oligonucleotides used in this work.

Oligonucleotides	Sequence (5'->3')
plu4895_fw	CCTCTAGAGTCGACCTGCAGCGCCCAGATAAAAAGTGC
plu4895_rv	AGTTCCTACAATTGAATTACCCTTTCTGTATTTTTAAATG
plu4890_fw	AAGGGTAATTCAATTGTAGGAACTACAGATTATTCCC
plu4890_rv	TCCCGGGAGAGCTCAGATCTCTGGCTGATGAATATCTTCG
veri_Δplu4895- plu4890_fw	CAAAACTGACGATGTTCAACC
veri_Δplu4895- plu4890_rev	TTCTTTACCGCCATTAGTGG
Veri_Δplu4890_fw	GATAATTAAAGTGAGTTAGCTGGTTG
Veri_pAR20_fw	TGAATCCCATAGGGCAGG
Veri_pAR20_rv	GATCTATCAACAGGAGTCCAAG

**Table 4:** Overview of gene fragments purchased for this work.

<p><math>\Delta</math>plu4895_upstream</p>	<p>ACTATATATGGTTATTTATAGTGTTACTATCTATGTATTATATAATA  ACCTCATTTAAAAATACAGAAAGGGTAATTCAATGCTAATCGATC  TCATTACGTCATATAGAAAAACCGCTGCAATCTATACTTTTGTGGA  TGCGGGTTTATCTATTCACTTTAAAAATGGAGACTATGTAGATATT  AACAACTTGCCAGTCAATATGGTATTGATTATTCGAGACTTAATC  GACTATGTGATTTCTTAATTGAAATAGGCGTATTGGTTAGCAGTG  ACCACGGAGTTGCACTTTCTGAGGAATGCAGTGCCTTGTCTGATC  CTAATAGCGTAGAATTCTAACAGTAAAATATGAAATCAATTCAG  AACATTGGGATTCTTGGTTAATGTATCCAAAATCCTTATTGGAAAA  CAATGGCAAATCGGCATTTGAAATGGTGCATGGAAAATCATTTTT  TGAGCATTTGGATAGTAATAAGGGATTAATAATCAGATTTTGATG</p>
<p><math>\Delta</math>plu4895_downstream</p>	<p>AAAGTGAATAGATAAACCGGTATCAACAAAAGCGTAGATTGCGG  CTGATTTTCTATATGATGTAATAAGTTCGGCTAGCATTGAGTTATC  CTTTATACCCGTTATCCTTCAAGTTGCCTCTTTGTTGGCTGCGCTCA  CTCACCCCGTACATCGTTATCTATGCTCCCGGGGATTGCTCCC  TTGCCGTCGTGACGCATCTTGAATCCATTGGGTATATGTCTTTGT  CTAAAGTATATGAAATACCATAATGCATAATTGGGTATTTGATCA  CTAATATGTAATTATTAGCTTTGTTACCTTTTCTTAGTGAGATAATA  AAAATTCCATTCTCCTATTTTCCCATTGTTCAACTTACTTTAATAA  CGCATTTTTAGGAACAAAATTGTTAACTATCAGACTATATTAATT  CGACAAAATAAATGACAAAGATCACAATTAECTTCCCATAAA  TTTTCCAAAATAAATAGAAATTTTTTAATATAGTTATTAAT</p>
<p><math>\Delta</math>plu4894-4891_upstream</p>	<p>ATTAATAACTATATTAATAAATTCTATTTTATTTTGGAAATTTATGG  GAAGAGTTAATTGTGATCTTTGTCATTTATTTTTGTGCAATTTAAT  ATAGTCTGATAGTTAACAATTTTGTTCCTAAAAATGCGTTATTA  GTAAGTTGAACAATGGGAAAATAAGGAGAATGGAATTTTTATTAT  CTCACTAAGAAAAGGTAACAAAGCTAATAATTACATATTAGTGAT  CGAAATACCCAATTATGCATTATGGTATTTTCATATACTTTAGACAA  AGACATATACCCAATGGATTTCAAGATGCGTCACGACGGCAAGG  GAGCGAATCCCCGGGAGCATAGATAACGATGTGACCGGGGTGA  GTGAGCGCAGCCAACAAGAGGCAACTTGAAGGATAACGGGTAT  AAAGGATAACTCAATGCTAGCCGAECTTATTACATCATATAGAAA  ATCAGCCGCAATCTACGCTTTTGTGATACCGGTTTATCTATTCAC  TTT</p>
<p><math>\Delta</math>plu4894-4891_downstream</p>	<p>GTCATTTACATTCATTTATTAATAAATGATAATTATAAAACCTGAG  AAATTACAGGTATTTTTGAATGTGTTATTTAGGCAATAGGAAAA  AAAACATCAATGATGTTACTCCCTAAAGATCATCAATGAAGGGTA  GTGATATTCTACCTACTAATTAATTTCAATATTAATAAATATGG  CATCAAATATTTTGTGATGCCATCTTGTATATCTATTTTAAAGATAC  AATATCCATATAATTATCTTTTTCGAACTCCATAATTATCTATAATT  TATTTTACCCCAGCTCTATAATTGCATATTTCTCGTTTATATCTTT  GATACGTTTAAACAACAATCCTGCCTGGTTGGCTAAATCTTCTAAT  TCATTCAAATAACGCTCTTTTCTAATAACAGTACATCCATTAATAT  ATCCGTAGAATCAATTATTTCTAATCGTAATTTTTTACCCTGCTTA  TCAACAAAACAGTTGCATTATCATCCATAGC</p>

<p>Δplu4894-4892_upstream</p>	<p>ATTAATAACTATATTAAAAAATTCTATTTTATTTTGGAAATTTATGG  GAAGAGTTAATTGTGATCTTTGTCATTTATTTTGTGCAATTTAAT  ATAGTCTGATAGTTAACAAATTTGTTCTAAAAATGCGTTATTA  GTAAGTTGAACAATGGGAAAATAAGGAGAATGGAATTTTATTAT  CTCACTAAGAAAAGGTAACAAAGCTAATAATTACATATTAGTGAT  CGAAATACCCAATTATGCATTATGGTATTTTCATATACTTTAGACAA  AGACATATACCCAATGGATTTCAAGATGCGTCACGACGGCAAGG  GAGCGAATCCCCGGGAGCATAGATAACGATGTGACCGGGGTGA  GTGAGCGCAGCCAACAAAGAGGCAACTTGAAGGATAACGGGTAT  AAAGGATAACTCAATGCTAGCCGAACTTATTACATCATATAGAAA  ATCAGCCGCAATCTACGCTTTTGTGATACCGGTTTATCTATTCAC  TTT</p>
<p>Δplu4894-4892_downstream</p>	<p>TTATTATAAAATTTAAATCCACATTCTATTTAAACATTTTATTGATA  TAAAGTGAAAATATGGCATCAAATATCTCGATGCCATATTTTCCAT  ATATTTATCAAAAATACAATATCCATATCATTATATTTAATTAAGAT  TCCTATTATCTATAATTTATTTTACGCCTAGTTGAATAATTGAATAT  GATTCATCGATATCTTTAACATCTTGAATGATCAACCCTGCTCGTT  TAGCCAAACATTCAAATTCCGTTAAGTTACGCTCTTGCCTAAAGA  TGTCATATCCATCAATATATCTAAATATTTAACAAATTTAGATTGT  GGTTTTTTCATTAAGTTATTAATAAAATAGTTGCATTCTTATGCAT  TGCCTTACGGCAATTTTCTAAATGAGTATTTATTATTATCAGAC  CAATCATGAATAATATTCTTTAAGATATATAAATCGTAACCTGATG  GAATTGATTTGAAAAATCTCCATCTATAAAATCTA</p>
<p>Δplu4895-4891_upstream</p>	<p>ACTATATATGGTTATTTATAGTGTTACTATCTATGTATTATATAATA  ACCTCATTTAAAAATACAGAAAGGGTAATTCAATGCTAATCGATC  TCATTACGTCATATAGAAAAACCGCTGCAATCTATACTTTTGTGGA  TGCGGGTTTATCTATTTACTTTAAAAATGGAGACTATGTAGATATT  AACAACTTGCCAGTCAATATGGTATTGATTATTCGAGACTTAATC  GACTATGTGATTTCTTAATTGAAATAGGCGTATTGGTTAGCAGTG  ACCACGGAGTTGCACTTTCTGAGGAATGCAGTGCCTTGTGATC  CTAATAGCGTAGAATTCTTAACAGTAAAATATGAAATCAATTCAG  AACATTGGGATTCTTGGTTAATGTATCCAAAATCCTTATTGGAAAA  CAATGGCAAATCGGCATTTGAAATGGTGCATGGAAAATCATTTTT  TGAGCATTGGATAGTAATAAGGGATTAATAATCAGATTTTGATG</p>
<p>Δplu4895-4891_downstream</p>	<p>GTATAACTTAGGTCAAAAAGGGGTTTATTGGTCTATCACTATTTTC  CTGATATTACTCGCTGTGAGTGGTATTATTTGGCGCCCCTATT  TTGCTGATCTCTCTATTCCAATAATTCGAATTGCGCTTCTAATC  CATTCAATGTCAGCTATTGGTTAATCTTGACGATTATGGTTCACG  CTTATGCGGCATTCTGGGTGAAAGGAATCTTCGAGCAATGGTTG  AAGGTTGGGTAACCCGTGGATGGGCGAAGAAACATCACCCACGT  TGGTATCGTGAAATAATGAAACAGGAGCAGCAAGAAGAGAAAC  GTTAATACGTTTATACCCTATGGATTTCAAGATGGATCGCGGCGG  CAAGGGAGCGAATCCCCGGGAGCATAGCAAACGATGTGACCGG  GGTGAGCGAGCGCAGCCAACAAAGAAGCAACTTGAAGGATAAC  GGGTATATTCTTATTAAGCACGAATAATGCAAGGAATGATTA  TATT</p>

<p><math>\Delta</math>plu4895-4892_upstream</p>	<p>ACTATATATGGTTATTTATAGTGTTACTATCTATGTATTATATAATA  ACCTCATTTAAAAATACAGAAAGGGTAATTCAATGCTAATCGATC  TCATTACGTCATATAGAAAAACCGCTGCAATCTATACTTTTGGTGA  TGCGGGTTTATCTATTCACTTTAAAAATGGAGACTATGTAGATATT  AACAACTTGCCAGTCAATATGGTATTGATTATTCGAGACTTAATC  GACTATGTGATTTCTTAATTGAAATAGGCGTATTGGTTAGCAGTG  ACCACGGAGTTGCACTTTCTGAGGAATGCAGTGCCTTGCTGATC  CTAATAGCGTAGAATTCTTAACAGTAAAATATGAAATCAATTCAG  AACATTGGGATTCTTGGTTAATGTATCCAAAATCCTTATTGGAAAA  CAATGGCAAATCGGCATTTGAAATGGTGCATGGAAAATCATTTTT  TGAGCATTGGATAGTAATAAGGGATTAATAATCAGATTTTGATG</p>
<p><math>\Delta</math>plu4895-4892_downstream</p>	<p>TTATTATAAAATTTAAATCCACATTCTATTTAAACATTTTATTGATA  TAAAGTGAAAATATGGCATCAAATATCTCGATGCCATATTTTCCAT  ATATTTATCAAAAATACAATATCCATATCATTATATTTAATTAAGAT  TCCTATTATCTATAATTTATTTTACGCCTAGTTGAATAATTGAATAT  GATTCATCGATATCTTTAACATCTTGAATGATCAACCCTGCTCGTT  TAGCCAAACATTCAAATTCCGTTAAGTTACGCTCTTGCCCTAAAGA  TGTCATATCCATCAATATATCTAAATATTTAACAAATTTAGATTGT  GGTTTTTTCATTAAGTTATTAATAAAATAGTTGCATTCTTATGCAT  TGCCTTACGGCAATTTTCTAAAATGAGTATTTATTCATTATCAGAC  CAATCATGAATAATATTCTTTAAGATATATAAATCGTAACCTGATG  GAATTGATTTGAAAAATCTCCATCTATAAAATCTA</p>

**Table 5:** Plasmids used for this work.

Plasmid	Comment	Reference
pAR20	pSEVA631 origin, p15A <i>ori</i> ; <i>kanR</i> ; <i>oriT</i> ; <i>sacB</i> ; relaxase <i>tral</i> ; <i>P<sub>Bad</sub></i> ; <i>P<sub>Tet</sub></i>	Alexander Rill, unpublished
pΔ <i>plu4895-4890</i>	Deletion plasmid based on pAR20 with inserted fusion of <i>plu4895</i> up- and <i>plu4890</i> downstream region	This work
pΔ <i>plu4895-4891</i>	Deletion plasmid based on pAR20 with inserted fusion of <i>plu4895</i> up- and <i>plu4891</i> downstream region	This work
pΔ <i>plu4895-4892</i>	Deletion plasmid based on pAR20 with inserted fusion of <i>plu4895</i> up- and <i>plu4892</i> downstream region	This work
pΔ <i>plu4894-4890</i>	Deletion plasmid based on pAR20 with inserted fusion of <i>plu4894</i> up- and <i>plu4890</i> downstream region	This work
pΔ <i>plu4894-4891</i>	Deletion plasmid based on pAR20 with inserted fusion of <i>plu4894</i> up- and <i>plu4891</i> downstream region	This work
pΔ <i>plu4890</i>	Deletion plasmid based on pAR20 with inserted fusion of <i>plu4890</i> up- and <i>plu4890</i> downstream region	This work
pΔ <i>plu4895</i>	Deletion plasmid based on pAR20 with inserted fusion of <i>plu4895</i> up- and <i>plu4895</i> downstream region	This work



**Table 6:** Overview of bacterial strains used in this work.

Strain	Genotype	Reference
<i>Escherichia coli</i> DH10B	F- <i>araDJ39</i> $\Delta$ ( <i>ara</i> , <i>leu</i> )7697 $\Delta$ <i>lacX74 galU galK rpsL deoR</i> $\phi$ 8OdlacZ $\Delta$ M15 <i>endAI nupG recAI mcrA</i> $\Delta$ ( <i>mrr hsdRMS mcrBC</i> )	144,145
<i>Escherichia coli</i> ST18	<i>E. coli</i> S17-1 $\lambda$ <i>pir</i> $\Delta$ <i>hemaA</i>	146
<i>Escherichia coli</i> ST18 + p $\Delta$ <i>plu4895-4890</i>	<i>Escherichia coli</i> ST18 + p $\Delta$ <i>plu4895-4890</i>	This work
<i>Escherichia coli</i> ST18 + p $\Delta$ <i>plu4895-4891</i>	<i>Escherichia coli</i> ST18 + p $\Delta$ <i>plu4895-4891</i>	This work
<i>Escherichia coli</i> ST18 + p $\Delta$ <i>plu4895-4892</i>	<i>Escherichia coli</i> ST18 + p $\Delta$ <i>plu4895-4892</i>	This work
<i>Escherichia coli</i> ST18 + p $\Delta$ <i>plu4894-4890</i>	<i>Escherichia coli</i> ST18 + p $\Delta$ <i>plu4894-4890</i>	This work
<i>Escherichia coli</i> ST18 + p $\Delta$ <i>plu4894-4891</i>	<i>Escherichia coli</i> ST18 + p $\Delta$ <i>plu4894-4891</i>	This work
<i>Escherichia coli</i> ST18 + p $\Delta$ <i>plu4890</i>	<i>Escherichia coli</i> ST18 + p $\Delta$ <i>plu4890</i>	This work
<i>Escherichia coli</i> ST18 + p $\Delta$ <i>plu4895</i>	<i>Escherichia coli</i> ST18 + p $\Delta$ <i>plu4895</i>	This work
<i>Photobacterium luminescens</i> TT01	Wildtype, rif <sup>R</sup> (spontaneous)	147
<i>Photobacterium luminescens</i> TT01 $\Delta$ <i>plu4895-4890</i>	Deletion of <i>plu4895-4890</i>	This work
<i>Photobacterium luminescens</i> TT01 $\Delta$ <i>plu4895-4891</i>	Deletion of <i>plu4895-4891</i>	This work
<i>Photobacterium luminescens</i> TT01 $\Delta$ <i>plu4895-4892</i>	Deletion of <i>plu4895-4892</i>	This work
<i>Photobacterium luminescens</i> TT01 $\Delta$ <i>plu4894-4890</i>	Deletion of <i>plu4894-4890</i>	This work
<i>Photobacterium luminescens</i> TT01 $\Delta$ <i>plu4894-4891</i>	Deletion of <i>plu4894-4891</i>	This work
<i>Photobacterium luminescens</i> TT01 $\Delta$ <i>plu4890</i>	Deletion of <i>plu4890</i>	This work
<i>Photobacterium luminescens</i> TT01 $\Delta$ <i>plu4895</i>	Deletion of <i>plu4895</i>	This work
<i>Photobacterium temperata</i>	Wildtype	147
<i>Photobacterium bodei</i>	Wildtype	147

<i>Photorhabdus luminescens</i> subs. <i>hainanensis</i>	Wildtype	147
<i>Photorhabdus luminescens</i> subs. PB45.5	Wildtype	147
<i>Photorhabdus luminescens</i> subs. <i>akhurstii</i>	Wildtype	147
<i>E. coli</i> BL21 (DE3) Gold	<i>Tpr Smr recA, thi, pro, hsdR-M+RP4: 2-Tc:Mu:Km Tn7 λpir</i>	Invitrogen
<i>E. coli</i> BL21 (DE3) Gold + p4890_His	<i>E. coli</i> BL21 (DE3) Gold + p4890_His	Eva Huber
<i>E. coli</i> BL21 (DE3) Gold + p4891_His	<i>E. coli</i> BL21 (DE3) Gold + p4891_His	Eva Huber
<i>E. coli</i> BL21 (DE3) Gold + p4892_His	<i>E. coli</i> BL21 (DE3) Gold + p4892_His	Eva Huber
<i>E. coli</i> BL21 (DE3) Gold + p4894_His	<i>E. coli</i> BL21 (DE3) Gold + p4894_His	Eva Huber
<i>E. coli</i> BL21 (DE3) Gold + p4895_His	<i>E. coli</i> BL21 (DE3) Gold + p4895_His	Eva Huber

### 5.2.1 Cultivation

*Photorhabdus* strains were cultivated in either LB broth (10 g/l tryptone, 5 g/l yeast extract, 5 g/l NaCl) or XPP medium (Table 7) while shaking at 30°C. All *E. coli* strains were cultivated in LB broth while shaking at 37°C. Strains carrying plasmids were cultivated by adding the corresponding antibiotics to the media (chloramphenicol (34 µg/µl), ampicillin (100 µg/µl), spectinomycin (50 µg/µl), kanamycin (50 µg/µl)). When transferring a plasmid via conjugation in *Photorhabdus luminescens* utilizing *E. coli* S17  $\lambda$ pir, rifampicin (50 µg/µl) was used as selection marker against *E. coli* after conjugation. For long-term storage, 500 µl of glycerol (50% (v/v)) was added to 1 ml liquid culture of the respective strains and stored at -80°C. All used strains are listed in Tab. 6.

**Table 7:** XPP medium preparation.

XPP medium (1L)	<p>10 g glycerol</p> <p>20 mL salt A (M9) 20 mL salt B (M9)</p> <p>2g L-amino acid mix</p> <p>1g sodium pyruvate</p> <p>add H<sub>2</sub>O, after autoclaving</p> <p>2 mL vitamin solution</p> <p>1 mL trace element solution</p>
Salt A (M9) (1L)	<p>350 g K<sub>2</sub>HPO<sub>4</sub></p> <p>100 g KH<sub>2</sub>PO<sub>4</sub></p>
Salt B (M9) (1L)	<p>29.4 g sodium citrate</p> <p>50 g (NH<sub>4</sub>)<sub>2</sub>SO<sub>4</sub></p> <p>5 g MgSO<sub>4</sub></p>
Trace element solution (1L)	<p>40 mg ZnCl<sub>2</sub></p> <p>200 mg FeCl<sub>3</sub> x 6 H<sub>2</sub>O</p> <p>10 mg CuCl<sub>2</sub> x 2 H<sub>2</sub>O</p> <p>10 mg MnCl<sub>2</sub> x 4 H<sub>2</sub>O</p> <p>10 mg Na<sub>2</sub>B<sub>4</sub>O<sub>7</sub> x 10 H<sub>2</sub>O</p> <p>10 mg (NH<sub>4</sub>)<sub>6</sub>Mo<sub>7</sub>O<sub>24</sub> x 4 H<sub>2</sub>O</p>
Vitamin solution (1L)	<p>10 mg folic acid</p> <p>6 mg Biotin</p> <p>200 mg p-aminobenzoic acid</p> <p>1 g thiamin hydrochloride</p> <p>1.2 g pantothenic acid</p> <p>2.3 g nicotinic acid</p> <p>12 g pyridoxin hydrochloride</p> <p>20 mg vitamin B12</p> <p>Add H<sub>2</sub>O</p>
L-amino acid mix	<p>2g L-alanine</p> <p>2 g L-arginine</p>

	2 g L-aspartate
	2 g L-asparagine
	2g L-cysteine
	2 g L-glutamate
	2 g L-glutamine
	2 g L-glycine
	2 g L-histidine
	2 g L-isoleucine
	2g L-leucine
	2 g L-lysine
	2 g L-methionine
	2 g L-phenylalanine
	2 g L-proline
	2 g L-serine
	2 g L-threonine
	2 g L-tyrosine

### 5.2.2 Preparation and Transformation of electrocompetent *E. coli* cells

For preparation of electrocompetent *E. coli* cells, an LB culture was inoculated 1:100 from an overnight culture and was grown at 37°C while shaking until an OD<sub>600</sub>=0.6-0.9 was reached. Subsequently, the cells were incubated on ice for 10-15 min and afterwards centrifuged for 2 min at 10000 rpm and the supernatant discarded. In the following step, the cells were washed three times with 1/2 volume of ice-cold water. After incubating the cells on ice for 20 min, the pellet was resuspended in 10% glycerol (v/v) and stored at -80°C.

### 5.2.3 Preparation and Transformation of electrocompetent *P. luminescens* cells

For preparation of electrocompetent *Photobacterium luminescens*, an LB culture was inoculated 1:25 from an overnight culture and was grown 30°C while shaking until an OD<sub>600</sub>=0.8-1.0 was reached. Subsequently, the cells were incubated on ice for 10 min and afterwards centrifuged for 15 min, 4°C at 4000 rpm. After discarding the supernatant, the pellet was resuspended in 1 volume 10% glycerol (v/v) and centrifuged for 15 min, 4°C at 4000 rpm. The washing step was repeated three times with the volumes of glycerol being reduced to 1/2, 1/20, 1/100 of the original volume. In a final step, the pellet was resuspended in 1/3000 volume 10% glycerol and 120 µl aliquots were directly used for transformation.

### 5.2.4 Construction of deletion mutants

Construction of markerless deletion mutants was carried out according to Alexander Rill (unpublished results, patent pending). In the first step, 500 bp fragments upstream and downstream of the respective gene of interest were bought from Eurofins Genomics with overhangs to each other and the vector pAR20. Subsequently, the gene fragments were fused and integrated into the pAR20 backbone via GoldenGate assembly. *E. coli* ST18 cells were transformed with the assembled plasmid and used for conjugation. As for conjugation, 10 ml LB cultures were inoculated 1:25 (*Photobacterium luminescens*) and 1:100 (*E. coli* ST18) from overnight cultures and incubated at 30°C and 37°C, respectively, until an OD<sub>600</sub> 0.6-0.8 was reached. 1 ml of the respective cultures were pelleted, washed with 1 ml LB broth and subsequently resuspended in 400 µl LB broth. In the following step, cultures were mixed in a ratio 3:1 *E. coli* ST18 donor and *Photobacterium luminescens* recipient on LB agar plates without

antibiotics. After incubation overnight at 30°C, the cell pellet was subsequently scrapped off the plate with an inoculation loop and resuspended in 2 ml LB broth. The cell suspension was then diluted 1:2, 1:5 and 1:10, plated on LB agar plates containing rifampicin and kanamycin as selection markers and incubated for 72 h at 30°C. Subsequently, single clones were inoculated in 5 ml LB broth containing kanamycin overnight at 30°C while shaking. For selection of double-crossover mutants, 1:25 of the respective culture was inoculated at 30°C for 2 h while shaking. The CRISPR/Cas9 system was induced with 200 ng/l anhydrotetracycline (AHT) and 0.4 % (w/v) arabinose. After 5h of incubation at 30°C, 50 µl cell suspension was plated out on LB plates containing kanamycin. Markerless deletion mutants were confirmed by performing colony PCR.

### **5.2.5 Compound extraction from liquid cell culture**

For comparison of NP production, 10 ml LB cultures of the respective strains were inoculated with a starting OD<sub>600</sub>=0.1 from an overnight culture for 72 h while shaking at 30°C. When required, NP production was induced with 0.1 mM IPTG at OD<sub>600</sub>=0.6-0.8. After 72 h, 1 ml of liquid LB culture was mixed with ethylacetate (EtAc) in a ratio of 1:1 and incubated for 1 h on a wheel mixer. Subsequently, the EtAc phase was separated, dried under nitrogen flow and dissolved in 250 µl methanol (MeOH). Dilutions of 1:10 in MeOH were subjected to HPLC-MS analysis.

### **5.2.6 HPLC-MS analysis**

Prior to HPLC-MS analysis, extracts were centrifuged for 30 min at 13300 rpm. The samples were analyzed via AmaZon X HPLC-MS (ESI-IT-MS) using a 5-95% H<sub>2</sub>O-acetonitrile (ACN) gradient over 16 min with a flowrate of 0.4 ml/min. Both solvents were supplemented with 0.1% formic acid (FA). The applied scan range was *m/z* 100-1200 in alternating positive/negative mode. Separation of compounds was achieved by using a C18-column. HR-MS measurements were conducted in a Dionex Ultimate 3000 system equipped with Acquity UPLC BEH C18 column (Waters, Eschborn, Germany) and Bruker Impact II (ESI-Q- OTOF). A linear 5-95% H<sub>2</sub>O-ACN gradient, supplemented with 0.1% FA, for 16 min at a flowrate of 0.4 ml/min and a scan range from *m/z* 100-1200 in positive mode was used. Relative

quantification of NPs was performed as described in (Heinrich et al., 2016) using the software Bruker Compass Analysis 4.3. The  $m/z$  ratios which were used for generation of extracted ion chromatograms (EICs) are listed in table 8.

**Table 8:** MS data ( $m/z$   $[M+H]^+$  ratios) used for generation of EICs.

Compound	$m/z$ $[M+H]^+$
Anthraquinone 256	257.04
Anthraquinone 270a/b/c	271.06
Anthraquinone 284a/b	285.07
Anthraquinone 300	301.07
Anthraquinone 314	315.08

### 5.2.7 Compound purification

For compound purification, 1 l LB cultures of the respective strains were inoculated with a starting  $OD_{600} = 0.1$  from an overnight culture and supplemented chloramphenicol. NP production was induced with 0.1 mM IPTG at  $OD_{600} = 0.6-0.8$ . Cells were harvested after 72 h. Subsequently, compounds were extracted by adding EtAc in a ratio of 3:1 and separating the EtAc phase with a separatory funnel. The extraction was repeated three times. After solvent evaporation, the compounds were dissolved in 20 ml MeOH and subjected to Sephadex LH-20 (MeOH, 25-100  $\mu$ m, Pharmacia Fine Chemical Co. Ltd.) size-exclusion chromatography. The collected fractions were subjected to HPLC-MS analysis. In an additional chromatographic step, compounds were purified using a 1260 Semiprep LC system coupled to a G6125B LC/MSD ESI-MS (Agilent). A 75% isocratic ACN-H<sub>2</sub>O gradient was applied over 16 min on a Cholesterol column (1.0 mm ID x 250mm, COSMOSIL) with a flowrate of 3 ml/min. Finally, the structures of all purified compounds were elucidated by detailed 1D and 2D NMR experiments.

### 5.2.8 Protein purification

For protein purification of the respective methyltransferases, the cell pellets were resuspended in binding buffer (500 mM NaCl, 20 mM imidazol, 50 mM HEPES, 10 % (w/v) glycerol, pH 7.5). For cell lysis benzonase (500 U, Fermentas), protease inhibitor (Complete EDTA-free, Roche), 0.1 % Triton-X and lysozym (0.5 mg/mL, ~20,000 U/mg, Roth) were added and the cells were incubated rotating for 30 min at 4 °C. Afterwards, the cells were placed on ice and lysed by ultra-sonication. Subsequently, the lysed cells were centrifuged (25,000 rpm, 30 min, 4 °C).

The yielded supernatant was passed through a 0.2 µm filter and loaded with a flow rate of 0.5 ml/min on a 5 ml HisTrap HP column (GE Healthcare) equilibrated with 12 CV binding buffer. Unbound protein was washed off with 8 CV with 4 % and 8 CV with 8 % elution buffer (500 mM NaCl, 500 mM imidazol, 50 mM HEPES, 10 % (w/v) glycerol, pH 7.5). The purified protein of interest was eluted with 35 % elution buffer. Following, the purified protein containing fraction was concentrated (Centriprep® Centrifugal Filters Ultacel® YM - 50, Merck Millipore).

### 5.2.9 Bioinformatic and phylogenetic analysis

For bioinformatic analysis, BlastP was used to identify MTs in different *Photorhabdus* strains. For further characterization of hits from BlastP, antiSMASH analysis was used. Sequence alignments and tree models were generated in Geneious 6.1.8.

### 5.2.10 *In vitro* characterization of MTs plu4890-4895

Purified versions of the respective MTs were used *in vitro* in order to characterize their involvement in methylation of AQ-256. Here, the 50 µl reaction volume included 20 mM Tris/HCl pH 7.5, 100 mM NaCl, 1 mM DTT, 1 mM AQ-derivative, 1 mM SAM and 1 µM purified protein. The assays were carried out at 25°C for 24h. Subsequently, reactions were stopped by diluting in 10-fold MeOH. Samples were centrifuged and subjected to HPLC-MS analysis. All measurements were performed by using an Ultimate 3000 RSLC (Dionex) with an ACQUITY UPLC BEH Amide Column, 130 Å, 1.7 µm, 2.1 mm x 50 mm, 1/pkg coupled to an Impact II qTOF (Bruker) equipped with an ESI Source set to positive ionization mode. The software DataAnalysis 4.3 (Bruker) was used to evaluate the measurements.



### 5.2.11 NMR

Isolated compounds were elucidated by detailed 1D and 2D NMR experiments.  $^1\text{H}$ ,  $^{13}\text{C}$ , HSQC, HMBC,  $^1\text{H}$ - $^1\text{H}$  COSY and  $^1\text{H}$ - $^1\text{H}$  ROESY spectra were measured on Bruker AV500 and AV600 spectrometers, using  $\text{D}_6$ -DMSO or  $\text{CD}_3\text{Cl}$  as solvent. Coupling constants are expressed in Hz and chemical shifts are given on a ppm scale.

## 5.3 Topic B

The following part contains all materials and methods used for the experiments covered in topic B. Oligonucleotides and gene fragments were purchased from Eurofins Genomics and are listed in table 9 and 10, respectively. Used plasmids are listed in table 11. Strains used in this work are listed in table 12.

**Table 9:** Overview of oligonucleotides used in this work.

Oligonucleotides	Sequence (5'->3')
pCOLA/ACYC_fw	CTGCAGGAGCTGTTGACAATTA
pCOLA/ACYC_rv	GGAATTCCTCCTGTTAGCCCAA
pCOLA/ACYC_fw_V	GCTATGCCATAGCATTTTTATCCATAAG
pCOLA/ACYC_rv_V	GCTAGTTATTGCTCAGCGG
plu0947_fw	CCGTTTTTTTTGGGCTAACAGGAGGAATTCCATGGTCAAGCTAGAAGAAATGGAC
plu0947_rv	CCGATGATTAATTGTCAACAGCTCCTGCAGTTATGCCACGCAAATTCCA
plu0948_fw	CCGTTTTTTTTGGGCTAACAGGAGGAATTCCGTGTCAACCGAGAAACTTC
plu0948_rv	CCGATGATTAATTGTCAACAGCTCCTGCAGTTATATAGTGCTATTTGGTACTGGTG
$\Delta$ plu0947_fw	CATAGCGCTACATAACATAGTGC
$\Delta$ plu0947_rv	GCCGTCTACTGATGCTTTTG
$\Delta$ plu0948_fw	GATTATCTCCTTATCACAACCG
$\Delta$ plu0948_rv	TATGCTTGATTGCTATCCTGC
Veri_pAR20_fw	TGAATCCCATAGGGCAGG
Veri_pAR20_rv	GATCTATCAACAGGAGTCCAAG

**Table 10:** Overview of gene fragments purchased for this work.

<p>Δplu0947_upstream</p>	<p>GGCTACGGTCTCCAGATTATTAGGGTGTGAGCCATTGAGGGATCAAC  AGTCTAAGAACTTTAAATAATTTCTACTGTTGTAGATGAGAAGTCATT  TAATAAGGCCACTGGCTCACCTTCGGGTGGGCCTTTCTGCGCAATTGT  TAGGCCAATTACCAACTTGGTGAGTGGGTCCGATCACTGGTGCAATC  CACGGATCCTAACGAGCTAAAAGTGACATTAACACCTTGATAAGCCT  GGAGACGAAGCTGGAAGAGTCACCAAGTACCAAATAGCACTATATAAA  AATAGCACTATAAAAATAGCACTACATAACATAGCGCTACATAACATA  GTGCTACGGATTCTTCGTTAATAACGACAAAGAGCTACCAAACAGTT  AAACGAAATACAACGTGGAAACAGCATGAATTAGTGGAACACATTTG  TCTCTACGTTGACACATTGTTGCCGTTAAAAGCCACGTAATCACGCG  ACTCGCCTCGGCAGGATAGCAATACAAGCATATACCTTATAGATTTCA  AGATGCATCGCGACGGCAAGGGAGTGAATCCCCGGGAGCATAGAGA  ACTATGTGACCAGGGTGAGCGAGCGCAGCCAACAAAGAGGCAACTT  GAAAGATGACGGGTATAAATATAAACACATAATTTTCAGGAGATAGA  AGCCAAGGAAAATCGTCACAGGAGACCGTAGCC</p>
<p>Δplu0947_downstream</p>	<p>GGCTACGGTCTCCACAATCCATCGTCAATAACGATATCGTGAGAAA  AAGAGCGCACCCGCTCAATGTTTACCTCAGGTGCGCTCATTGATGAAT  TACTGATTATTTAGCAAAGCTTTAGCCTTAGCGACCACATTCTCTAC  AGTGAAACCAAACGTTTTAAACAACCTGATCAGCAGGTGCTGACTCACC  AAATGTATCCATACCAACGATAGCGCCATTCATACCGACATATTTAAA  CCAGTAATCGGCGATACCCGCTTCGACTGCAACACGTGCAGAAACCG  CAGCAGGCAGAACCGCTTCTCGGTATGCAGCATCTTGCTTATCAAAAG  CATCAGTAGACGGCATTGAGACTACGCGCACCTGACGACCTTCCTCAG  TCAATTGGTGGTAAGCACTACCGCCAATTCAATTTCTGAACCCGTTG  CGATCAAAATCAGTTCTGGTTGCCCTGACAATCTTTCAGGATGTAAG  CCCCTTCTCGATATTAGGGATCCCACACCGCATATGCTGGATCCTTG  ACAGCTAGCTCAGTCTAGGTATAATACTAGTTGAGATTTTCAGGAG  CTAAGGAAGCTAAAGTCTAAGAACTTTAAATAATTTCTACTGTTGTAG  ATCGCGCCGCTTCACGGACCCTGAATTCAAGGGTCTTGAGACCGTA  GCC</p>
<p>Δplu0948_upstream</p>	<p>GGCTACGGTCTCGAGATGAGAGCAGTAGGGCGTTGAGCCGAAATAC  CGGTCTAAGAACTTTAAATAATTTCTACTGTTGTAGATGAGAAGTCAT  TTAATAAGGCCACTGGCTCACCTTCGGGTGGGCCTTTCTGCGCAATTG  TTAGGCCAATTACCAACTTGGTCCAAAACCCTAGATATGATCCGTGTT  CGCCTGGAGCAAGGAATCACCGACGGTGATCTCCACCCAATACAAA  CGTGGATGTGTTGGCGTCGATTTTCCTTGTTTGACCCAAACTATTTCA  TTCCAAGCTCGTGACGGCGTACCTCGTGAACGACTTAGGCGCTTGATT  GAACCCGCAATGGCAGCTATTCCAGGCAACTGATTCCAATAACGATT  ATCTCCTTATACAACCGTGGCTATAGAACTCAGCATATTAAGATG  CCTGTAAGCAACTACAGCCACCTTCACCGTCAGCTACCAACAGTCCAC  CCGCTCAATGACCGCCTTGCTACAAATAAAGGCTAAAGCTCGTCTTCA  TCAGTAAGGCAAAATCTGTCACAAATCACATGTGACACATTAATTTCC  CTACATCACTTGTGAAATATTGACATTTAACCCGAAAAGTGGAAC  TGGTTGTCGTTTTTTGATGTACTTAAGGAAAAGGTGAGACCGTAGCC</p>

<p>Δplu0948_downstream</p>	<p>GGCTACGGTCTCAAAGGAAGTAAATCAAATAGCACTATAAAAATAGC  ACTACATAACATAGCGCTACATAACATAGTGCTACGGATTCGTTGTT  AATAACGACAAAGAGCTACCAAACAGTTAAACGAAATACAACGTGGA  AACAGCATGAATTAGTGGAACACATTTGTCTCTACGTTGACACATTGT  TGCCGTTAAAAGCCACGTAAATCACGCGACTCGCCTCGGCAGGATAG  CAATACAAGCATATACCTTATAGATTTCAAGATGCATCGCGACGGCAA  GGGAGTGAATCCCCGGGAGCATAGAGAACTATGTGACCAGGGTGAG  CGAGCGCAGCCAACAAAGAGGCAACTTGAAAGATGACGGGTATAAA  TATAAACACATAATTTTCAGGAGATAGAAATGGTCAAGCTAGAAGAA  ATGGACACCCACGTAACCCTGCGGGAACAGTTATTTTCGAACACCGAT  GGCTCCATCGTGCTGGTGAACATATTCCATGTTGATCCCTCAATGGCT  GACACCGGATCCCACACCGCATATGCTGGATCCTTGACAGCTAGCTCA  GTCCTAGGTATAACTAGTTCGAGATTTTCAGGAGCTAAGGAAGCT  AAAGTCTAAGAACTTTAAATAATTTCTACTGTTGTAGATATGCGGCGA  TATCGCTGGAAGCTGAGTGGGTGTCTTGAGACCGTAGCC</p>
<p>Δplu0947-0948_upstream</p>	<p>GGCTACGGTCTCGAGATGAGAGCAGTAGGGCGTTGAGCCGAAATAC  CGGTCTAAGAACTTTAAATAATTTCTACTGTTGTAGATGAGAAGTCAT  TTAATAAGGCCACTGGCTCACCTTCGGGTGGGCCTTTCTGCGCAATTG  TTAGGCCAATTACCAACTTGGTCCAAAACCCTAGATATGATCCGTGTT  CGCCTGGAGCAAGGAATCACCGACGGTGATCTCCACCCAATACAAA  CGTGGATGTGTTGGCGTCGTATTTCTTGGTTTGACCCAAACTATTTCA  TTCCAAGCTCGTGACGGCGTACCTCGTGAACGACTTAGGGCGTTGATT  GAACCCGCAATGGCAGCTATTCCAGGCAACTGATTCGAATAACGATT  ATCTCCTTATCACAACCGTGGCTATAGAACTCAGCATATTAAGATG  CCTGTAAGCAACTACAGCCACCTTCACCGTCAGCTACCAACAGTCCAC  CCGCTCAATGACCGCCTTGCTACAAATAAAGGCTAAAGCTCGTCTTCA  TCAGTAAGGCAAATCTGTCAAAATCACATGTGACACATTAATTTCC  CTACATCACTTGTGAAATATTGACATTTAACCCCGAAAAGTGGA AAC  TGTTGTGTTTTTTGATGTACTTAAGGAAAAGGAAGTAAATCGCCAA  GGAAAATCGTCACATGAGACCGTAGCC</p>
<p>Δplu0947-0948_downstream</p>	<p>GGCTACGGTCTCACACAATCCATCGTCAATAACGATATCGTGCGAGAA  AAGAGCGCACCCGCTCAATGTTTACCTCAGGTGCGCTCATTATGAAT  TACTGATTATTTAGCAAAGCTTTAGCCTTAGCGACCACATTCTCTAC  AGTGAAACCAAACGTTTTAAACA ACTGATCAGCAGGTGCTGACTCACC  AAATGTATCCATACCAACGATAGCGCCATTCATACCGACATATTTAAA  CCAGTAATCGGCGATACCCGCTTCGACTGCAACACGTGCAGAAACCG  CAGCAGGCAGAACCGCTTCTCGGTATGCAGCATCTTGCTTATCAAAAG  CATCAGTAGACGGCATTGAGACTACGCGCACCTGACGACCTTCCTCAG  TCAATTGGTGGTAAGCACTACCGCCAATTCAATTTCTGAACCCGTTG  CGATCAAAATCAGTTCTGGTTGCCCTGACAATCTTTAGGATGTAAG  CCCCTTCTCGATATTAGGGATCCCACACCGCATATGCTGGATCCTTG  ACAGCTAGCTCAGTCTAGGTATAACTAGTTCGAGATTTTCAGGAG  CTAAGGAAGCTAAAGTCTAAGAACTTTAAATAATTTCTACTGTTGTAG  ATCGCGCCGCTTCACGGACCCTGAATTCAAGGGTCTTGAGACCGTA  GCC</p>

**Table 11:** Plasmids used for this work.

Plasmid	Comment	Reference
pCOLA_tacl/I (pEV <sup>kan</sup> )	expression vector, ColA ori, kan <sup>R</sup> , 2 MCSs under control of P <sub>tacl</sub>	<sup>148</sup>
pACYC_tacl/I (pEV <sup>kan</sup> )	expression vector, p15A ori, cm <sup>R</sup> , 2 MCSs under control of P <sub>tacl</sub>	<sup>148</sup>
pAntJ	pACYC_tacl/I with <i>plu4185</i> insert	This work
pΔNgrA	Deletion plasmid based on pCK_cipB with inserted fusion of <i>plu0992</i> up- (1037 bp) and downstream (949 bp) region	Alexander Brachmann
pCOLA_ <i>plu0947</i> _tacl/I	pCOLA_tacl/I with <i>plu0947</i> insert	This work
pCOLA_ <i>plu0948</i> _tacl/I	pCOLA_tacl/I with <i>plu0948</i> insert	This work
pCOLA_ <i>plu0947-plu0948</i> _tacl/I	pCOLA_tacl/I with <i>plu0947-plu0948</i> insert	This work
pAR20	pSEVA631 origin, p15A <i>ori</i> ; <i>kanR</i> ; <i>oriT</i> ; <i>sacB</i> ; relaxase <i>traI</i> ; P <sub>Bad</sub> ; P <sub>Tet</sub>	Alexander Rill, unpublished
pΔ <i>plu0947</i>	Deletion plasmid based on pAR20 with inserted fusion of <i>plu0947</i> downstream region	This work
pΔ <i>plu0948</i>	Deletion plasmid based on pAR20 with inserted fusion of <i>plu0948</i> downstream region	This work
pΔ <i>plu0947-plu0948</i>	Deletion plasmid based on pAR20 with inserted fusion of <i>plu0947</i> up- and <i>plu0948</i> downstream region	This work

**Table 12:** Overview of used bacterial strains in this work.

Strain	Genotype	Reference
<i>Escherichia coli</i> DH10B	F- <i>araDJ39</i> $\Delta$ ( <i>ara</i> , <i>leu</i> )7697 $\Delta$ <i>lacX74</i> <i>galU galK rpsL deoR</i> $\phi$ 8O <i>dlacZ</i> $\Delta$ M15 <i>endAI nupG recAI mcrA</i> $\Delta$ ( <i>mrr hsdRMS mcrBC</i> )	Invitrogen
<i>Escherichia coli</i> DH10B + pCOLA_tacl/I (pEV <sup>kan</sup> )	DH10B + pCOLA_tacl/I (pEV <sup>kan</sup> )	This work
<i>Escherichia coli</i> DH10B + pACYC_tacl/I (pEV <sup>kan</sup> )	DH10B + pACYC_tacl/I (pEV <sup>cm</sup> )	This work
<i>Escherichia coli</i> DH10B + pCOLA_ <i>plu0947</i> _tacl/I	DH10B + pCOLA_ <i>plu0947</i> _tacl/I	This work
<i>Escherichia coli</i> DH10B + pCOLA_ <i>plu0948</i> _tacl/I	DH10B + pCOLA_ <i>plu0948</i> _tacl/I	This work
<i>Escherichia coli</i> DH10B + pCOLA_ <i>plu0947-plu0948</i> _tacl/I	DH10B + pCOLA_ <i>plu0947-plu0948</i> _tacl/I	This work
<i>Escherichia coli</i> S17 $\lambda$ pir	Tp Smr <i>recA thi hsdRM+</i> RP4::2-Tc::Mu::Km Tn7, $\lambda$ pir phage lysogen	<sup>146</sup>
<i>Escherichia coli</i> S17 $\lambda$ pir + p $\Delta$ <i>plu0992</i>	S17 $\lambda$ pir + p $\Delta$ <i>plu0992</i>	This work
<i>Escherichia coli</i> ST18	<i>E. coli</i> S17-1 $\lambda$ pir $\Delta$ <i>hema</i>	<sup>146</sup>
<i>Escherichia coli</i> ST18 + p $\Delta$ <i>plu0947</i>	ST18 + p $\Delta$ <i>plu0947</i>	This work
<i>Escherichia coli</i> ST18 + p $\Delta$ <i>plu0948</i>	ST18 + p $\Delta$ <i>plu0948</i>	This work
<i>Escherichia coli</i> ST18 + p $\Delta$ <i>plu0947-plu0948</i>	ST18 + p $\Delta$ <i>plu0947-plu0948</i>	This work
<i>P. luminescens</i> TT01	Wildtype, rif <sup>R</sup> (spontaneous)	<sup>147</sup>
<i>P. luminescens</i> TT01 $\Delta$ <i>hfq</i>	$\Delta$ <i>hfq</i>	Nick Neubacher
<i>P. luminescens</i> TT01 $\Delta$ <i>plu4895-4890</i>	$\Delta$ <i>plu4895-4890</i>	This work
<i>P. luminescens</i> TT01 $\Delta$ <i>plu4895-4890</i> + pEV <sup>kan</sup>	$\Delta$ <i>plu4895-4890</i> + pCOLA_tacl/I	This work
<i>P. luminescens</i> TT01 $\Delta$ <i>plu4895-4890</i> + pAntJ	$\Delta$ <i>plu4895-4890</i> + pAntJ	This work

<i>P. luminescens</i> TT01 $\Delta$ NgrA	$\Delta$ plu0992	This work
<i>P. luminescens</i> TT01 $\Delta$ NgrA + pAntJ	$\Delta$ plu0992 + pAntJ	This work
<i>P. luminescens</i> TT01 $\Delta$ NgrA + pEV <sup>cm</sup>	$\Delta$ plu0992 + pACYC tacl/l	This work
<i>P. luminescens</i> TT01 $\Delta$ plu4895-4890 $\Delta$ NgrA	$\Delta$ plu4890-4895 and $\Delta$ plu0992	This work
<i>P. luminescens</i> TT01 $\Delta$ plu4895-4890 + pAntJ	$\Delta$ plu4890-4895 $\Delta$ NgrA + pAntJ	This work
<i>P. luminescens</i> TT01 $\Delta$ plu4895-4890 + pEV <sup>cm</sup>	$\Delta$ plu4890-4895 $\Delta$ NgrA + pACYC tacl/l	This work
<i>P. luminescens</i> TT01 $\Delta$ plu0947	$\Delta$ plu0947	This work
<i>P. luminescens</i> TT01 $\Delta$ plu0948	$\Delta$ plu0948	This work
<i>P. luminescens</i> TT01 $\Delta$ plu0947-plu0948	$\Delta$ plu0947-plu0948	This work
<i>P. luminescens</i> TT01 + pCOLA_ plu0947_tacl/l	<i>P. luminescens</i> + pCOLA_ plu0947_tacl/l	This work
<i>P. luminescens</i> TT01 + pCOLA_ plu0948_tacl/l	<i>P. luminescens</i> + pCOLA_ plu0948_tacl/l	This work
<i>P. luminescens</i> TT01 + pCOLA_ plu0947-plu0948_tacl/l	<i>P. luminescens</i> + pCOLA_ plu0947-plu0948_tacl/l	This work

### 5.3.1 Cultivation

*Photobacterium luminescens* strains were cultivated in either LB broth (10 g/l tryptone, 5 g/l yeast extract, 5 g/l NaCl), XPP (Table 7) medium, improved XPP medium (Table 13) or XPP-insect media (Table 14) while shaking at 30°C. For medium containing insect powder, dead *Bombyx mori* and *Hermetia illucens* were purchased commercially and subsequently shredded to powderous consistency with a grinder. All *E. coli* strains were cultivated in LB broth while shaking at 37°C. Strains carrying plasmids were cultivated by adding the corresponding antibiotics to the media (chloramphenicol (34 µg/µl), ampicillin (100 µg/µl), spectinomycin (50 µg/µl), kanamycin (50 µg/µl)). When transferring a plasmid via conjugation in *Photobacterium luminescens* utilizing *E. coli* S17  $\lambda$ pir, rifampicin (50 µg/µl) was used as selection marker against *E. coli* after conjugation. For long-term storage, 500 µl of glycerol

(50% (v/v)) was added to 1 ml liquid culture of the respective strains and stored at -80°C. All used strains are listed in Tab. 12.

**Table 13:** Improved XPP medium for AQ production

XPP medium (1L)	10 g glycerol 20 mL salt A (M9) 20 mL salt B (M9) 2 g L-amino acid mix add dd H <sub>2</sub> O, after autoclaving 2 mL vitamin solution
Salt A (M9) (1L)	350 g K <sub>2</sub> HPO <sub>4</sub> 100 g KH <sub>2</sub> PO <sub>4</sub>
Salt B (M9) (1L)	29.4 g sodium citrate 50 g (NH <sub>4</sub> ) <sub>2</sub> SO <sub>4</sub> 5 g MgSO <sub>4</sub>
Vitamin solution (1L)	1 g thiamin hydrochloride 1.2 g pantothenic acid  Add dd H <sub>2</sub> O
L-amino acid mix	2g L-alanine 2 g L-arginine 2 g L-aspartate 2 g L-asparagine 2g L-cysteine 2 g L-glutamate 2 g L-histidine 2 g L-isoleucine 2 g L-lysine 2 g L-methionine 2 g L-phenylalanine 2 g L-proline

	2 g L-serine
--	--------------

**Table 14:** XPP-insect media preparation.

XPP medium (1L)	10 g insect powder 20 mL salt A (M9) 20 mL salt B (M9) 2 g L-amino acid mix add dd H <sub>2</sub> O, after autoclaving 2 mL vitamin solution
Salt A (M9) (1L)	350 g K <sub>2</sub> HPO <sub>4</sub> 100 g KH <sub>2</sub> PO <sub>4</sub>
Salt B (M9) (1L)	29.4 g sodium citrate 50 g (NH <sub>4</sub> ) <sub>2</sub> SO <sub>4</sub> 5 g MgSO <sub>4</sub>
Vitamin solution (1L)	1 g thiamin hydrochloride 1.2 g pantothenic acid  Add dd H <sub>2</sub> O
L-amino acid mix	2g L-alanine 2 g L-arginine 2 g L-aspartate 2 g L-asparagine 2g L-cysteine 2 g L-glutamate 2 g L-histidine 2 g L-isoleucine 2 g L-lysine 2 g L-methionine 2 g L-phenylalanine 2 g L-proline 2 g L-serine



### **5.3.2 Preparation and Transformation of electrocompetent *E. coli* cells**

Preparation and transformation of electrocompetent *E. coli* cells was carried out as described in section 5.2.

### **5.3.3 Preparation and Transformation of electrocompetent *P. luminescens* cells**

Preparation and transformation of electrocompetent *Photobacterium luminescens* cells was carried out as described in section 5.2.

### **5.3.4 Construction of deletion mutants**

Construction of markerless deletion mutants was carried out as described before<sup>63</sup>. In the first step, 1 kb fragments upstream and downstream of the respective gene of interest were either bought from Eurofins Genomics or amplified using oligonucleotides resulting in two PCR products with overhangs to each other and the vector pCK\_cipB. Subsequently, the gene fragments were fused and integrated into the linearized pCK\_cipB plasmid via Hot Fusion assembly. *E. coli* S17  $\lambda$ pir cells were transformed with the assembled plasmid and used for conjugation. As for conjugation, 10 ml LB cultures were inoculated 1:25 (*Photobacterium luminescens*) and 1:100 (*E. coli* S17  $\lambda$ pir) from overnight cultures and incubated at 30°C and 37°C, respectively, until an OD600 0.6-0.8 was reached. 1 ml of the respective cultures were pelleted, washed with 1 ml LB broth and subsequently resuspended in 400  $\mu$ l LB broth. In the following step, cultures were mixed in a ratio 3:1 *E. coli* S17  $\lambda$ pir donor and *Photobacterium luminescens* recipient on LB agar plates without antibiotics. After incubation overnight at 30°C, the cell pellet was subsequently scrapped off the plate with an inoculation loop and resuspended in 2 ml LB broth. The cell suspension was then diluted 1:2, 1:5 and 1:10, plated on LB agar plates containing rifampicin and chloramphenicol as selection markers and incubated for 72 h at 30°C. Subsequently, single clones were inoculated in 5 ml LB broth containing chloramphenicol overnight at 30°C while shaking. For selection of double-crossover mutants, 15  $\mu$ l of the respective culture was plated out on LB agar plates containing chloramphenicol and 6% sucrose. Markerless deletion mutants were confirmed by performing colony PCR. In case of markerless deletions conducted with CRISPR/Cas9, the workflow was performed as described in topic A.

### 5.3.5 Compound extraction from liquid cell culture

For comparison of NP production, 10 ml LB cultures of the respective strains were inoculated with a starting  $OD_{600}=0.1$  from an overnight culture for 72 h while shaking at 30°C. When required, NP production was induced with 0.1 mM IPTG at  $OD_{600}=0.6-0.8$ . After 72 h, 1 ml of liquid LB culture was mixed with EtAc in a ratio of 1:1 and incubated for 1 h on a wheel mixer. Subsequently, the EtAc phase was separated, dried under nitrogen flow and dissolved in 250  $\mu$ l methanol (MeOH). Dilutions of 1:10 in MeOH were subjected to HPLC-MS analysis. When using insect media, the cultures were supplemented with 4% XAD-16. Subsequently, NPs were eluted using a mixture of MeOH/EtAc (70%/30%). Afterwards, the solvents were evaporated and the samples were dissolved in MeOH and subjected to HPLC-MS analysis.

### 5.3.6 HPLC-MS analysis

Prior to HPLC-MS analysis, extracts were centrifuged for 30 min at 13300 rpm. The samples were analyzed via AmaZon X HPLC-MS (ESI-IT-MS) using a 5-95%  $H_2O$ -acetonitrile (ACN) gradient over 16 min with a flowrate of 0.4 ml/min. Both solvents were supplemented with 0.1% formic acid (FA). The applied scan range was  $m/z$  100-1200 in alternating positive/negative mode. Separation of compounds was achieved by using a C18-column. HR-MS measurements were conducted in a Dionex Ultimate 3000 system equipped with Acquity UPLC BEH C18 column (Waters, Eschborn, Germany) and Bruker Impact II (ESI-Q- OTOF). A linear 5-95%  $H_2O$ -ACN gradient, supplemented with 0.1% FA, for 16 min at a flowrate of 0.4 ml/min and a scan range from  $m/z$  100-1200 in positive mode was used. Relative quantification of NPs was performed as described in (Heinrich et al., 2016) using the software Bruker Compass Analysis 4.3.

### 5.3.7 Compound purification

Compound purification was carried out as described in 5.2.

### 5.3.8 Absolute NP quantification

Absolute quantification of NP production in the respective strains was conducted by using a calibration curve and HPLC-MS measurements. As standards, exact amounts of the purified compound were used. 10 ml LB cultures of the respective strains were inoculated with a starting OD<sub>600</sub>=0.1 from an overnight culture for 72 h while shaking at 30°C. NP production was induced with 0.1 mM IPTG at OD<sub>600</sub>=0.6-0.8. Compound extraction was performed as described above.

## 5.4 Topic C

The following part contains all materials and methods used for the experiments covered in topic B. Oligonucleotides and gene fragments were purchased from Eurofins Genomics and are listed in table 15 and 16, respectively. Used plasmids are listed in table 17. Strains used in this section are listed in table 18.

**Tab. 15:** Overview of oligonucleotides used in this work.

Oligonucleotides	Sequence (5'->3')
pEB17_fw	CTCATTTCACATAAATAATAGTGAACGG
pEB17_rv	ACATGTGGAATTGTGAGCGG
<i>Δoxygenase_up_fw</i>	CCTCTAGAGTCGACCTGCAGTAGACGACTTACTTATTTGAATAG
<i>Δoxygenase_up_rv</i>	CTTTAGGGTATATATCCGTCATCTTGCCTTACCTCTATATTTCC
<i>Δoxygenase_down_F</i>	AAGATGACGGATATATACCCTAAAGATTTCC
<i>Δoxygenase_down_R</i>	TCCCGGGAGAGCTCAGATCTGAAACTGCCCTTGGACAAGAC
<i>Δoxygenase_V_fw</i>	CATCACATCAAAGGTGTGTTACTG
<i>Δoxygenase_V_rv</i>	GTGCATTCACAGCAATTGC
pCOLA/ACYC_fw	CTGCAGGAGCTGTTGACAATTA
pCOLA/ACYC_rv	GGAATTCCTCCTGTTAGCCCAA

pCOLA/ACYC_fw_V	GCTATGCCATAGCATTTTTATCCATAAG
pCOLA/ACYC_rv_V	GCTAGTTATTGCTCAGCGG
Core_TT01_fw	CCGTTTTTTTTGGGCTAACAGGAGGAATTCATGATGTACGACTGGGATCTG
Core_TT01_rv	CCGATGATTAATTGTCAACAGCTCCTGCAGTTAATGAGGTCGCTGCCACA
crtE_TT01_fw	CCGTTTTTTTTGGGCTAACAGGAGGAATTCATGAACGTCAGTACTGCACGAG
fni_TT01_rv	CCGATGATTAATTGTCAACAGCTCCTGCAGTCATGTTGGTAGCAAAACAGC
Oxygenase_TT01_fw	CCGTTTTTTTTGGGCTAACAGGAGGAATTCCTTGAGCGACGTTGTATTATCGA
Oxygenase_TT01_rv	CCGATGATTAATTGTCAACAGCTCCTGCAGTCAAGTTGCTTCTTTGCCGT
Oxygenase_PB45.5_F	CCGTTTTTTTTGGGCTAACAGGAGGAATTCCTTGAGCGATTTTGTATTCTCG
Oxygenase_PB45.5_R	CCGATGATTAATTGTCAACAGCTCCTGCAGTTATAGCATAACTTCATTTATCCAGCAG
Oxygenase_bodei_fw	CCGTTTTTTTTGGGCTAACAGGAGGAATTCCTTGAGCGATTTTGTATTCTCG
Oxygenase_bodei_rv	CCGATGATTAATTGTCAACAGCTCCTGCAGTTAGTCTTCCAGCATAACTTCATTTATC
Oxygenase_KJ12.1_F	CCGTTTTTTTTGGGCTAACAGGAGGAATTCCTTGAGAGATTTTATTTTATCAAAGATG
Oxygenase_KJ12.1_rv	CCGATGATTAATTGTCAACAGCTCCTGCAGTCACAGCATTACTTCGTCAATC
Oxygenase_haina_F	CAATTTACACAGGAGGCTAGCATTGAGCGATTTTGTAGTCTCG
Oxygenase_haina_rv	CTCAGCGGTGGCAGCAGCTTATAGCATAACTTCATTTATCCAGC
Core_KJ12.1_fw	CCGTTTTTTTTGGGCTAACAGGAGGAATTCATGGAAGTACTTAGACTTCGACAAATAC
Core_KJ12.1_rv	CCGATGATTAATTGTCAACAGCTCCTGCAGTCACTTAGGTCTTTGCCATAAG

pSeva_fw	GTCGTGACTGGGAAAACCTG
pSeva_rv	TCCTGTGTGAAATTGTTATCCGC

**Table 16:** Overview of gene fragments purchased for this work.

<i>Oxygenase_crtE</i>	<p>GAGCTCTTAATTAAGCGGATAACAATTCACACAGGAGCTTAACGATCGTT  GGCTGAACAAACAGACAATCTGGTCTGTTTGTATTATGGAAAATTTTCTGTA  TAATAGATTCAACAAACAGACAATCTGGTCTGTTTGTATTATAGCTGTCACCG  GATGTGCTTTCCGGTCTGATGAGTCCGTGAGGACGAAACAGCCTCTACAAAT  AATTTTGTTAATGTCCGGAAGGGCACCGTATTTTATTAACATAAGGAGGTT  TTTTTTGAGCGACGTTGTATTATCGAAAACCATATTAATCCCTTTCAATCTC  AGCTGGAGGAACTTGATTCAAATAGTTCCTATTGAGGGAGAGGCTCCTTC  AGAGTTAAAAGGTACTTTCTTTAGAATTGGTCCCGGTCGCCTGCATAGGGGA  GACGAATATTATAATCATCCATTTGATGGGGATGGAATGATATTTAAAGTAA  CGTTCAGTGATAATGGGATATTCTATAGAAACAGACATGTGTTAACAAAGGA  ATACTTAAAAGAGGAAGAAGCTCAAAGGTTACTGTATCGCTCGGTTGGAAC  CGTCCCCAAAAACTAAAACCTCAGGATGAGATTTTTTATTATTAATAATCCG  GCAAATACAAATATTGTATATCATTCTCATAAGCTTCTGGCGTTGTGGGAAG  GAGGGATGCCACATTTAATTAATCCGGTAACTCTTGAGACAATTTCAAATA  TGACTTTTCTGGAAAGCTAAAAGCACGATTTTCTTCCCTCCCAAACCTAACCT  TCGTGAAGTACCATTTACAGCACATCCTAAAAAATACCAAATGATGATAAT  TTATATGGATTTGGTGTGACATATGGTATTGGATCTAAGTTAACGCTATACA  AAATAGACAGTGCCGGCGATATGATGGTTATACGCAAATTTGCTTAAGAA  AAGGTATTTAATTCACGATTTCATAGTGACAAAAAATTACTTTTTATTTTTTT  AGGTGGGCCGCATATAAATCTTAAGTTGAGCAATGTAATTGGCAATGAAAG  CATCATTGCATCCATGAATTCACGTGAAAGTGAAGATGGCCGGGTTCTTTTA  GTTTCAAGAAAATGCCATGATGTGAAATTCTATGATGCAGTTCCTGGATTTAT  TTTTCATTTTGCAAATGGTTATGAAGATGCCGATGGGAATGTGATTTTCGAC  GCCTCATTTTGGCGGTCATTCCCAGTATTTACACAGAATATATTTAAAATAA  TAGTTCAGAACTTTGTCGTTTTACTTTATGCACAGCATCCGGGAATGTTGATA  AAGAAATTTTATTCAGGGGGAATACTGATTTCCAGCCATAAACCTACAGT  CTGTGGTAGACAGCACAGATATGCCTGGTTCGTTTGCTGGGAGGATTCTGAC  AGTGAAGGGAGATCAATAATTAATTTGATTGTTTTGATAAGAGTGTATTAA  GCCACAGTTTTGATAATGATTTGCCGGAAGAACCTGTTTTTGTAGCCAAACC  GGGTGCTGTAAAGAAGATGATGGTTGGCTTATTTTAAGGTTTATGTCGAA</p>
-----------------------	----------------------------------------------------------------------------------------------------------------------------------------------------------------------------------------------------------------------------------------------------------------------------------------------------------------------------------------------------------------------------------------------------------------------------------------------------------------------------------------------------------------------------------------------------------------------------------------------------------------------------------------------------------------------------------------------------------------------------------------------------------------------------------------------------------------------------------------------------------------------------------------------------------------------------------------------------------------------------------------------------------------------------------------------------------------------------------------------------------------------------------------------------------------------------------------------------------------------------------------------------------------------------------------------------------------------------------------------------------------------------------------------------------------------------------------------------------------------------------------------------------------------------------------------------------------------------------------------------------------------------------------------------------------------------------------------------------------------------------------------------------------------------------------------------

AAATTGCACTGTACAGATATCGTAGTTTTAAATGCTGATGATCTCTCAATGGT  
GTGCAGATTACGTTTGCCGCACCATATTCCAATGGGAATGCATCACTGCTGG  
ATAAATGAAGTTATGCTATACCCTATGGATTTCAAGATGCATCGCGACGGCA  
AAGAAGCAACTTGACTCGGTACCAAATTCCAGAAAAGAGGCCTCCCGAAAG  
GGGGGCCTTTTTTCGTTTTGGTCCAATGGCGGCGCGCCATCGAATGAGGTTT  
TGTTTCGATTATCGAACAAATTATTGAAATATCGAACAAAACCTCTAAACTACT  
GTGGCACTGAATCAAAAAATTATAAACCTGATCAGAAGCTGTCACCGGATG  
TGCTTCCGGTCTGATGAGTCCGTGAGGACGAAACAGCCTCTACAAATAATT  
TTGTTTAAGTCATAATAGACGATAAGGAGGGGTTTTAATGAACGTCAGTACT  
GCACGAGCTATGAATTACGAAGAGACATTACTGGAGCTACAGAGTGCCTA  
CAACAACACCTAGAACTGGTACTTCCTTCAGGAGCCCCAGATGATAAAGTCT  
GCGCAGCCATGCGAGAAAGTACACTGGTGTCTGGAAAACGTATCCGCCCCC  
TCTTATTGCTACTCATAGTCTGGATCTTGGAGAAAACCCCTGGAAGACTGA  
CTTTCTACAGCTGGCATCTGCAATTGAAATAGTGCATGCCGCCTCATTAAATTT  
TAGACGATCTTCCCTGTATGGATAATGCGGAGTATCGGCGCGGACGCCCGG  
CTATTCATCGGCAGTATGGTGAAAGTGTAGCGATCCTAGCGGCTGTAGCCTT  
GCTGAGCCGGGCTTTTTGCCTCATTGTAGAAACAAACCTTTCTGAATACGAT  
AAATCTGCTGCTGTCGCCATACTTTCCCATACAGTGGGTTTAAACGGTCTTGT  
CCAAGGGCAGTTTCGCGATCTGAACAATACATTATGTGCTGGTAATTATCAT  
GCCATTGCTACCACCAACGATTTAAAAACGGGTTTGCTTTTCGACACAACATT  
TCAGTTAGCGGCAATTGCTGTGAATGCACCTGATATAATTCGCCAGGCATTG  
CGTCATGTATCACAACATCTGGGGCAAGCGTTTCAATACTGGATGACTTGA  
GCGATGACCTGAATAATACAGGGAAAGATATGTATCAGGATAAGGAAAAGT  
TAACAATGGTTACGCTGCTCGGAAAATCTAAAGTGCATAAACAATTACGCAG  
GCACATCAGATACATTGATAAATATTTGGCAATAGTGTATCGCAGAAATTTA  
GCTTCACGATATTTTATACGACACTGGTTTGATAAAAATATTGCGATGTTTAA  
TTAACCAATTATTGAAGGCCTCCCTAACGGGGGGCCTTTTTTTGTTTCTGGTC  
TCCCGATATCCTGGGCCGAGCTC

<p><i>fni_lycopene cyclase</i></p>	<p>GAGCTCCTGGTCTCCCGATATCCTGGGCCTCATGGGCAGAATATGTGATACA  GGAAATGGCGGCGCGCCATCGAATGAGGTGTTGACAATTAATCATCGGCTC  GTATAATGTGTGGAATTGTGAGCGCTACAATTAGTAGTCACCGGCTGTGCT  TGCCGGTCTGATGAGCCTGTGAAGGCGAAACTACCTCTACAAATAATTTTGT  TTAAAGGGCGAGAGATCGCCGACAACGAATATTTAAGAGAGGTTTTTTATG  AAAAAGATCGATCACACTCAGCGCAAGAATGAGCATCTGGATATTATATTCC  GTCCTCCTCAAACGGAGTCCCAAGTAAGTACGGGGTTTGCTGAGTGGCGAT  TTCAGCATTGTGCTCTGCCAGAATTGGATCTAGACAGTATAGATCTTAAGTG  TTCCCTCTTTGGAAAAATTTGCAGGCACCACTGCTCATAAGCTCTATGACTG  GAGGGGTTTCATCGTGCTCATGCGATTAATCATCATCTTGCAGAGGCAGCTCA  AGTACTGGGCATTTCAATGGGAGTCGGGTCGCAACGTGTTGCTCTTGAAAAT  GAAGCAAACGATGGGCTTAGTCGCTCACTACGCCAGATAGCTCCTGATATTC  TCCTTTTCGCTAATCTCGGGGCAGCCCAAATTCGTGGCGAGCGCGGGTTTAA  TTATGCTCTGCGAGCAGTACAGATGATTGAAGCCGATGCTCTAATTATCCAT  CTGAATCCGCTACAGGAGGCGCTGCAACAGGGAGGAGACCGTAACTGGTG  CCATATTCTATATGCTATTGAACAACCTCGTAACAAAACCTGGGGTTCCTATAA  TTGTTAAAGAAGTAGGTTCAAGGCTTATCGCTTCTGTGCGACGCCAATTGGC  AGAAGCTGGCGTCAGTATGCTGGATATAGCCGGGGCTGGGGGAACCAAGTT  GGGCAGCGATTGAAGCAGAACGAGCATCCACACCGTATCACCGCGCATTGG  CCATGGCATTGCTGACTGGGGAATTCCGACCGCGACAGCACTGCGTGAAA  TACGCGAGGCACTTCAAATATGCCACTGATCGCCTCTGGCGGTATCAGAAA  TGGTGTTGATGCCGCCAAAGCTTATTGCATGGGGGCACAATTGGTCGGCCA  AGCCGCTGCCGTCATACATAGTGCAGCCCTCTCCACAGATGCAGTTATAGAA  CATTTCCAATTAATTATTGAGCAGATAAAAGTCGCCTGCTTTTGCACAGGGA  GCGCCGATATTGCTGCGCTGCGTACAGCTGTTTTGCTACCAACATGAAAAAA  AAAAAACACCCTAACGGGTGTTTTTTTTTTTTTTGGTCTCCCAATGGCGGCGC  GCCATCGAATGAGGTTTTTCAGCAGGACGCACTGACCTCCCTATCAGTGATAG  AGATTGACATCCCTATCAGTGATAGAGATACTGAGCACAGCGGTCAACGCAT  GTGCTTTGCGTTCTGATGAGACAGTGATGTCGAAACCGCCTCTACAAATAAT  TTTGTTTAAAATAGTAAACGAAGACATAAGAGGTAGAGGATGATGTACGAC  TGGGATCTGATTCTGGTGGGAGGAGGATTGGCCAACGGACTGATCGCAATG</p>
------------------------------------	----------------------------------------------------------------------------------------------------------------------------------------------------------------------------------------------------------------------------------------------------------------------------------------------------------------------------------------------------------------------------------------------------------------------------------------------------------------------------------------------------------------------------------------------------------------------------------------------------------------------------------------------------------------------------------------------------------------------------------------------------------------------------------------------------------------------------------------------------------------------------------------------------------------------------------------------------------------------------------------------------------------------------------------------------------------------------------------------------------------------------------------------------------------------------------------------------------------------------------------------------------------------------------------------------------------------------------------------------------------------------------------------------------------------------------------------------------------------------------------------------------------------------------------------------------------------------------------------------------------------------------------------------------------------------------------------------------------------------------------------------------------------------------------------------------------------------------------------------------------



	<p>CGTTTCCAGCAGTGTAACCACATCTGCGAGTGTTGCTTATTGAAAACACAG  AAACAATAGGAGGCAATCACACGTGGTCATTTTCATCAACATGATCTTACTGA  GGCGGAACATGAGTGGATAGCACCGCTGATTACCTATCGCTGGTCAGGTTA  CGACGTCATTTTTCCAGCATTTC AACGCACATTGCCACATTCATATTTAGTAT  CACATCCCAACACTTTGCAAGCATACTCCATGCATATTTGGGCGAACGTATAC  AGACTCGTTTATTGGTACAGGAGCTGACTCCACAGAAAGTTTACTTACAGGA  CGGCTCGTCTAAGTGCTGGCGCAGTCATTGATGGGAGAGGCTGGCGACC  AGGACCATTTATAGGGAGTGGCACCCAGGCATTTTTTGGTCAGGAATGGGA  GCTGGAAGAGTCGCACTCTTTAACCCACCCGATTTTAATGGATACTAGTGTG  GGACAGGATACAGGTTATCGATTTATCTATGTCCTGCCGTTCTCCTCAACTCG  TCTGCTGATAGAGGACACTCATTACGTTGATCGGGGGCCACCTGATAAGGCT  TTGTCGCAGGCTACTATCGCAGAGTACGCGAAGAAACATGGATGGAAACTG  GGTAAACTCATTGAGAAGAGAGCGGTTGTCTTCCAATTACACTTACGGGAG  ATTTTACCTCTTTCTGGGCACAGCTAGCAGGACAGCCCACCTGTGGGTTACG  TGCAGCTTTGTTTCACCCACAACAGGCTACTCTCTGCCACACGCTATTCGGT  TGGCAGATCGTATTGTTGCTCTGCCGGAGCTTACCGATACCTCCTTATTCATT  ACCCTCAGGGATTACGCACGACAACAGTGGCAACACCAGCGCTTTTTCCGTC  TTCTAAATCGCATGCTCTTCCTCGCTGGGGATCCACAACAACGTTGGCAGGT  AATGCAACGTTTCTATCAACTTTCCCAAATCTGATTGCACGTTTTTATGCGG  AGCAACTTAATTCCGTGACAAGGCCCGGATTCTCATAGGTAAACCACCAGT  GCCGATAAAGGGTGCTCTAAAGGCAATGTTTAAACAACACAAGAAGCTTCA  GGGTTTTTATTATGATTA ACTCGGTACCAAAAAAAAAAAAAAAAAAGACGCTGAA  AAGCGTCTTTTTTTTTTTTTGGTCCGTGACAAGGCCGTCAAGGCCGAGCTC</p>
<p><i>Phytoene  desaturase_phy  toene synthase</i></p>	<p>GAGCTCGTCGACAAGGCCGTCAAGGCCGCATGTCGACGGCGCGCCATCGAA  TGAGGCACCCAGCAGTATTTACAAACAACCATGAATGTAAGTATATTCCTTA  GCAAAGCTGTCACCGGATGTGCTTTCCGGTCTGATGAGTCCGTGAGGACGA  AACAGCCTCTACAAATAATTTTGTTTAAGTCACAAAGGGAAATGTCCCGTAA  ATATCGAGGAGGCGTTGTATGATTAAGCGCTGGTAATTGGTGCTGGTTTTG  GTGGGCTGGCACTGGCAATAAGGCTCCAGTCTGCGGGGATTCCGACATGTA  TTTTGGAGCAACGGGATAAACCAGGTGGACGCGCTTATGTTTATAAGGAAC  AGGGATTACCTTTGATGCCGGCCCCACCGTAATCACCGCTCCTAATGTCATT</p>

GAAGAATTGTTTACCCAGGCTGGTAAACGTATGGCTGATTACGTCGATTTAC  
TTCCCGTACACCCTTTTTATCGGCTCTGTTGGGAGTCGGGTAAGATGTTTGAT  
TACGACAATGATCAGCAACATCTGGAAGCACAAATCCATACGTTCAATCCAA  
GAGATGTTAACGGGTATCGACGCTTTCTAGACTATTCCCGGGAAGCCTTTAA  
TGAAGGCTACCTGAAACTTGAACGGTGCCCTTCCTCTCTTTTCGCGACATGT  
TGAGTGCGGCTCCACAGTTGATACGTCTACACGCATGGCGTAGTGTTTATAG  
TCAGGTGGCAGCCTTTATCAAGGATGAGAGCCTGCGCCAGGCATTTTCATTT  
CACTCGCTATTGATAGGAGGTAACCCCTTTGCTGCATCTTCTATCTATACTTT  
GATCCACGCACTGGAACGAGAATGGGGAGTCTGGTTTCCGCGAGGAGGAA  
CCAGCGCTCTGGTTGAGGCAATGGTGA AATTGTTACTGACATTGGTGGAG  
AAATTGAGCTTAATGCAAAGGTAAAACGCTTCACCACCCATGGCAATCGGGT  
CACAGGTGTCCAATTAGCTGATGGACGAAATATGACATGTGACGTTGTGGC  
CTCAAATGCCGATGTTATTCATACCTATAAGCACCTGTTAGGTCAGCATCCGG  
TCGGAATAGCCCGCTCGAACACTGGTGCGTAAACGAATGAGCAACTCAC  
TGTTTCGTGCTTTATTTTCGGTCTGAACCATCACCATACGCAATTAGCCCATCAT  
ACAGTTTGCTTTGGTCCACGCTATAAGGAACTCATCGAAGATATTTTTTATCA  
TGACCGACTGTCAGAGGATTTTTCACTCTATCTCCATGCCCCCTCTGTTACTG  
ACCCATCCCTTGCTCCCCGAGGATGCGCAAGTTACTACGTTCTGGCCCTGTA  
CCACATTTGGGGACAGCTAATTTAACTGGGATATAGAGGGGCCACGCTTA  
CGTGACCGTATTTTCGCGTATCTGGA AAAAGTACTATATGCCCGGTCTGCTCA  
AGCAGTTAGTCGTTTCATCGTATTTTTACCCATTTGATTTTCGTGACCAACTCA  
ATGCCCATCTCGTTTCGGCCTTCTCCTTTGAACCGTTGCTGACACAAAGCGCT  
TGGTCCGACCACACAATCGGGACAACCGCATTGATAATCTGTATCTCGTCG  
GCGCAGGCACGCATCCTGGAGCAGGTATTCCCGGCGTGATTGGATCAGCAA  
AAGCCACCGCCACATTGATGTTAGAGGATATCGCTAAATGACTCGGTACCAA  
ATTCCAGAAAAGAGGCCTCCCGAAAAGGGGGCCTTTTTTCGTTTTGGTCCAA  
TGGCGGCGCGCCATCGAATGAGGAGAAACCAATTGTCCATATTGCATCAGA  
CATTGCCGTCACTGCGTCTTTTACTGGCTCTTCTCGCTAACCAAACCGGTAAC  
CCCGCTTATTA AAAGCATTCTGTAACAAAGCGGGACCAAAGCCATGACAAAA  
ACGCGTAACAAAAGTGTCTATAATCACGGCAGAAAAGTCCACATTGATTATT  
TGCACGGCGTCACACTTTGCTATGCCATAGCATTTTTATCCATAAGATTAGCG

GATCCTACCTGACGCTTTTTATCGCAACTCTCTACTGTTTCTCCATACCCGAGC  
CCCATAGGGTGGTGTGTACCACCCCTGATGAGTCCAAAAGGACGAAATGGG  
GCCTCTACAAATAATTTTGTTTAATACGAAGGTTTTGGAGGTAGCCATGAAT  
CCTGCGCTACTTAAACACGTTACTCAGATAATGGAGCAAGGCTCAAAAAGTT  
TTGCCAGTGTACCCGACTTTTCGATACAGCAACACGACACAGCACAATGAT  
GCTGTACGCCTGGTGCCGTTATTGTGATGATATAATAGACGGGCAAGAGCT  
GGGGAGACAAATAAGCAGTGTGATAAGTATAGCGCCCGGAGAACTTCA  
AATGCTGCAATACCTGACAAAGCAGGCTTACGACGGTTTTGCCGATGACCGA  
ACCTGCTTTTGCAGCCTTTCAGACAGTAGCTCTGAGTAATGAAATCCCTCAGC  
AACAGGCCTTCGAACATCTGGAAGGATTCGCAATGGATGTACTCTGTGAGCC  
TTACAGAACGTTGGATGATACTCTGAGATATTGCTACCATGTCGCGGGAGTA  
GTTGGGCTGATGATGGCAAGGGTTATGGGGGTTTCGCGAGGCGAGTGTGCT  
GGATCGGGCCTGCGATCTAGGAATTGCTTTTCAGTAACTAACATTGCTCGG  
GATATTATTGAGGATGCGAAGGCCGGCGTTGCTATCTTCCGCTAGAATGG  
CTTACCAAGAAGGGCTAATGCCAGACACACTTATTTATACCGAAAACCGTC  
CTGCGCTAGCTCGGGTGGCATCCCGATTGATTGTGGAAGCGGAATCTTATTA  
TACCTCCGCTCTGACAGGGCTTGTGGTTTACCTTTGCGTTCAGCCTGGGTCA  
TCGTTCTGCTCATGGTATCTATCGTGAAATCGGCATTAAAGTGCAACAAGC  
AGGAGTACGGGCCTGGGAATGCAGACAAAGAACTAATCGTGGAGAGAAGG  
TTACCTTATTAATGGCTGGCGCAATGAAGGCGCTTATATCTCGGGTGGCGAT  
AACACGCCTCGCGATCCCAAATTGTGGCAGCGACCTCATTAACCTCGGTACC  
AAAGACGAACAATAAGACGCTGAAAAGCGTCTTTTTTCGTTTTGGTCCACTA  
GTCTGGGCCTCATGGTCGTGACTGGGAAAACCCTGGCGAGCTC

**Table 17:** Plasmids used for this work.

Plasmid	Comment	Reference
pCOLA_ara/tacl/I (pEV <sup>kan</sup> )	expression vector, ColA ori, kan <sup>R</sup> , 2 MCSs under control of P <sub>Bad</sub> or P <sub>tac</sub>	148
pACYC_ara/tacl/I (pEV <sup>kan</sup> )	expression vector, p15A ori, cm <sup>R</sup> , 2 MCSs under control of P <sub>Bad</sub> or P <sub>tac</sub>	148
pCDF_ara/tacl/I (pEV <sup>spec</sup> )	expression vector, CloDF13 ori, spec <sup>R</sup> , 2 MCSs under control of P <sub>Bad</sub> or P <sub>tac</sub>	Carsten Kegler, unpublished
pACYC_ara_TT01_core	pACYC expression vector with TT01 carotenoid core genes under the control of P <sub>Bad</sub>	This work
pCOLA_ara_TT01_crtE_fni	pCOLA expression vector with <i>crtE_fni</i> under the control of P <sub>Bad</sub>	This work
pCDF_ara_TT01_oxygenase	pCDF expression vector with TT01 <i>oxygenase</i> gene under the control of P <sub>Bad</sub>	This work
pCK_cipB	pDS132 with an additional <i>Bgl</i> II restriction site, R6K ori; cmR; oriT; <i>sacB</i> ; relaxase <i>traI</i>	53
pΔ <i>oxygenase</i>	Deletion plasmid based on pCK_cipB with inserted fusion of 1 kb up- and downstream fragments of <i>plu4336</i>	This work
pCDF_ara_PB45.5_oxygenase	pCDF expression vector with PB45.5 <i>oxygenase</i> gene under the control of P <sub>Bad</sub>	This work
pCDF_ara_KJ12.1_oxygenase	pCDF expression vector with KJ12.1 <i>oxygenase</i> gene under the control of P <sub>Bad</sub>	This work
pCDF_ara_bodei_oxygenase	pCDF expression vector with <i>bodei oxygenase</i> gene under the control of P <sub>Bad</sub>	This work
pCDF_ara_haina_oxygenase	pCDF expression vector with <i>hainanensis oxygenase</i> gene under the control of P <sub>Bad</sub>	This work
pSeva231	Empty expression vector, oriT, pBBR1 ori, kan <sup>R</sup>	Zeocin®
pSeva_Carotenoid_TT01	Expression vector based on pSEVA231 harbouring the <i>P. lum</i> TT01 carotenoid cluster	This work
pSeva_Carotenoid_bodei	Expression vector based on pSEVA231 harbouring the <i>P. bodei</i> carotenoid cluster	This work

pSeva_Carotenoid_hainanensis	Expression vector based on pSEVA231 harbouring the <i>P. lum subs. hainanensis</i> carotenoid cluster	This work
pSeva_Carotenoid_temperata	Expression vector based on pSEVA231 harbouring the <i>P. temperata</i> carotenoid cluster	This work
pSeva_Carotenoid_akhurstii	Expression vector based on pSEVA231 harbouring the <i>P. lum subs akhurstii</i> carotenoid cluster	This work
pSeva_Carotenoid_PB45.5	Expression vector based on pSEVA231 harbouring the <i>P. lum subs. PB45.5</i> carotenoid cluster	This work
pSeva_Carotenoid_core_KJ12.1	Expression vector based on pSEVA231 harbouring the <i>Xenorhabdus sp. KJ12.1</i> carotenoid cluster	This work

**Table 18:** Overview of used bacterial strains in this work.

Strain	Genotype	Reference
<i>Escherichia coli</i> DH10B	F- <i>araDJ39</i> $\Delta$ ( <i>ara, leu</i> )7697 $\Delta$ <i>lacX74 galU galK rpsL deoR</i> $\phi$ 8 <i>OdlacZ</i> $\Delta$ M15 <i>endAI nupG recAI mcrA</i> $\Delta$ ( <i>mrr hsdRMS mcrBC</i> )	Invitrogen
<i>Escherichia coli</i> DH10B + pCOLA_ara (pEV <sup>kan</sup> )	DH10B + pCOLA_ara (pEV <sup>kan</sup> )	This work
<i>Escherichia coli</i> DH10B + pACYC_ara (pEV <sup>kan</sup> )	DH10B + pACYC_ara (pEV <sup>cm</sup> )	This work
<i>Escherichia coli</i> DH10B + pCDF_ara (pEV <sup>kan</sup> )	DH10B + pACYC_ara (pEV <sup>spec</sup> )	This work
<i>Escherichia coli</i> DH10B + pACYC_ara_TT01_core	DH10B + pACYC_ara_TT01_core	This work
<i>Escherichia coli</i> DH10B + pCOLA_ara_TT01_crtE_fni	DH10B + pCOLA_ara_TT01_crtE_fni	This work
<i>Escherichia coli</i> DH10B + pCDF_ara_TT01_oxygenase	pCDF_ara_TT01_oxygenase	This work
<i>Escherichia coli</i> S17 $\lambda$ pir	Tp Smr <i>recA thi hsdRM+</i> RP4::2-Tc::Mu::Km Tn7, $\lambda$ pir phage lysogen	<sup>146</sup>
<i>Escherichia coli</i> S17 $\lambda$ pir + p $\Delta$ oxygenase	S17 $\lambda$ pir + p $\Delta$ oxygenase	This work
<i>P. luminescens</i> TT01 $\Delta$ oxygenase	$\Delta$ <i>plu4336</i>	This work
<i>P. luminescens</i> TT01 $\Delta$ carotenoid	$\Delta$ <i>plu4336</i> $\Delta$ <i>crtE_crtB</i>	Alexander Rill

<i>Escherichia coli</i> BL21 (DE3)-Marionette-diterpene	<i>Marionette cassette; MEV, ggps; redox Tpr Smr recA, thi, pro, hsdR-M+RP4; 2- Tc:Mu:Km Tn7 λpir</i>	149
<i>Escherichia coli</i> BL21 (DE3)-Marionette-diterpene + pCOLA_ara (pEV <sup>kan</sup> ) + pACYC_ara (pEV <sup>kan</sup> )	BL21 (DE3)-Marionette-diterpene + pCOLA_ara (pEV <sup>kan</sup> ) + pACYC_ara (pEV <sup>kan</sup> )	This work
<i>Escherichia coli</i> BL21 (DE3)-Marionette-diterpene + pCOLA_ara (pEV <sup>kan</sup> ) + pACYC_ara (pEV <sup>kan</sup> ) + pCDF_ara (pEV <sup>kan</sup> )	BL21 (DE3)-Marionette-diterpene + pCOLA_ara (pEV <sup>kan</sup> ) + pACYC_ara (pEV <sup>kan</sup> ) + pCDF_ara (pEV <sup>kan</sup> )	This work
<i>Escherichia coli</i> BL21 (DE3)-Marionette-diterpene + pACYC_ara_TT01_core + pCOLA_ara_TT01_crtE_fni	BL21 (DE3)-Marionette-diterpene + pACYC_ara_TT01_core + pCOLA_ara_TT01_crtE_fni	This work
<i>Escherichia coli</i> BL21 (DE3)-Marionette-diterpene + pACYC_ara_TT01_core + pCOLA_ara_TT01_crtE_fni + pCDF_ara_TT01_oxygenase	BL21 (DE3)-Marionette-diterpene + pACYC_ara_TT01_core + pCOLA_ara_TT01_crtE_fni + pCDF_ara_TT01_oxygenase	This work
<i>Escherichia coli</i> BL21 (DE3)-Marionette-diterpene + pSeva_Carotenoid_TT01	BL21 (DE3)-Marionette-diterpene + pSeva_Carotenoid_TT01	This work
<i>Escherichia coli</i> BL21 (DE3)-Marionette-diterpene + pSeva_Carotenoid_bodei	BL21 (DE3)-Marionette-diterpene + pSeva_Carotenoid_bodei	This work
<i>Escherichia coli</i> BL21 (DE3)-Marionette-diterpene + pSeva_Carotenoid_hainanensis	BL21 (DE3)-Marionette-diterpene + pSeva_Carotenoid_hainanensis	This work
<i>Escherichia coli</i> BL21 (DE3)-Marionette-diterpene + pSeva_Carotenoid_akhurstii	BL21 (DE3)-Marionette-diterpene + pSeva_Carotenoid_akhurstii	This work
<i>Escherichia coli</i> BL21 (DE3)-Marionette-diterpene + pSeva_Carotenoid_temperata	BL21 (DE3)-Marionette-diterpene + pSeva_Carotenoid_temperata	This work
<i>Escherichia coli</i> BL21 (DE3)-Marionette-diterpene + pSeva_Carotenoid_PB45.4	BL21 (DE3)-Marionette-diterpene + pSeva_Carotenoid_PB45.4	This work
<i>Escherichia coli</i> BL21 (DE3)-Marionette-diterpene + pSeva_Carotenoid_core_KJ12.1	BL21 (DE3)-Marionette-diterpene + pSeva_Carotenoid_core_KJ12.1	This work
<i>Escherichia coli</i> DH10B + pCDF_ara_PB45.5_oxygenase	DH10B + pCDF_ara_PB45.5_oxygenase	This work

<i>Escherichia coli</i> DH10B + pCDF_ara_KJ12.1_oxygenase	DH10B + pCDF_ara_KJ12.1_oxygenase	This work
<i>Escherichia coli</i> DH10B + pCDF_ara_bodei_oxygenase	DH10B + pCDF_ara_bodei_oxygenase	This work
<i>Escherichia coli</i> DH10B + pCDF_ara_haina_oxygenase	DH10B + pCDF_ara_haina_oxygenase	This work
<i>Escherichia coli</i> BL21 (DE3)-Marionette-diterpene + pSeva_Carotenoid_TT01 + pCDF_ara_PB45.5_oxygenase	BL21 (DE3)-Marionette-diterpene + pSeva_Carotenoid_TT01 + pCDF_ara_PB45.5_oxygenase	This work
<i>Escherichia coli</i> BL21 (DE3)-Marionette-diterpene + pSeva_Carotenoid_TT01 + pCDF_ara_KJ12.1_oxygenase	BL21 (DE3)-Marionette-diterpene + pSeva_Carotenoid_TT01 + pCDF_ara_KJ12.1_oxygenase	This work
<i>Escherichia coli</i> BL21 (DE3)-Marionette-diterpene + pSeva_Carotenoid_TT01 + pCDF_ara_bodei_oxygenase	BL21 (DE3)-Marionette-diterpene + pSeva_Carotenoid_TT01 + pCDF_ara_bodei_oxygenase	This work
<i>Escherichia coli</i> BL21 (DE3)-Marionette-diterpene + pSeva_Carotenoid_TT01 + pCDF_ara_haina_oxygenase	BL21 (DE3)-Marionette-diterpene + pSeva_Carotenoid_TT01 + pCDF_ara_haina_oxygenase	This work

#### 5.4.1 Cultivation

*Photorhabdus luminescens* strains and *E. coli* strains were cultivated in LB broth (10 g/l tryptone, 5 g/l yeast extract, 5 g/l NaCl) while shaking at 30°C. Strains carrying plasmids were cultivated by adding the corresponding antibiotics to the media (chloramphenicol (34 µg/µl), ampicillin (100 µg/µl), spectinomycin (50 µg/µl), kanamycin (50 µg/µl)). Gene expression of the pCOLA/pACYC/pCDF-derived constructs was induced with 0.2% (w/v) arabinose. In case of pSeva-Marionette-constructs the respective promoters were induced with 50 µM cuminic acid (*CymR*), 200 nM AHT (*TetR*), 250 µM dihydroxybenzoic acid (*3B5C*), 0.1 mM IPTG (*lac*), 250 µM naringenin (*Ttg*), 0.2% (w/v) arabinose. Additionally, when necessary, 0.5 mM O-(2,3,4,5,6-pentafluorobenzyl)hydroxylamine (PFBHA) was supplemented to the culture for

aldehyde catching. For long-term storage, 500 µl of glycerol (50% (v/v)) was added to 1 ml liquid culture of the respective strains and stored at -80°C. All used strains are listed in Tab. 17.

#### **5.4.2 Preparation and Transformation of electrocompetent *E. coli* cells**

Preparation and transformation of electrocompetent *E. coli* cells was carried out as described in section 5.2.

#### **5.4.3 Preparation and Transformation of electrocompetent *P. luminescens* cells**

Preparation and transformation of electrocompetent *Photobacterium luminescens* cells was carried out as described in section 5.2.

#### **5.4.4 Construction of deletion mutants**

Construction of markerless deletion mutants was carried out as described before<sup>63</sup>. In the first step, 1 kb fragments upstream and downstream of the respective gene of interest were either bought from Eurofins Genomics or amplified using oligonucleotides resulting in two PCR products with overhangs to each other and the vector pCK\_cipB. Subsequently, the gene fragments were fused and integrated into the linearized pCK\_cipB plasmid via Hot Fusion assembly. *E. coli* S17 λpir cells were transformed with the assembled plasmid and used for conjugation. As for conjugation, 10 ml LB cultures were inoculated 1:25 (*Photobacterium luminescens*) and 1:100 (*E. coli* S17 λpir) from overnight cultures and incubated at 30°C and 37°C, respectively, until an OD<sub>600</sub> 0.6-0.8 was reached. 1 ml of the respective cultures were pelleted, washed with 1 ml LB broth and subsequently resuspended in 400 µl LB broth. In the following step, cultures were mixed in a ratio 3:1 *E. coli* S17 λpir donor and *Photobacterium luminescens* recipient on LB agar plates without antibiotics. After incubation overnight at 30°C, the cell pellet was subsequently scrapped off the plate with an inoculation loop and resuspended in 2 ml LB broth. The cell suspension was then diluted 1:2, 1:5 and 1:10, plated on LB agar plates containing rifampicin and chloramphenicol as selection markers and incubated for 72 h at 30°C. Subsequently, single clones were inoculated in 5 ml LB broth



containing chloramphenicol overnight at 30°C while shaking. For selection of double-crossover mutants, 15 µl of the respective culture was plated out on LB agar plates containing chloramphenicol and 6% sucrose. Markerless deletion mutants were confirmed by performing colony PCR.

#### **5.4.5 Compound extraction from liquid cell culture**

For comparison of NP production, 10 ml LB cultures of the respective strains were inoculated with a starting OD<sub>600</sub>=0.1 from an overnight culture for 72 h while shaking at 30°C. NP production was induced according 5.1. After 72h, 1 ml of liquid culture was centrifuged and the supernatant was discarded. Subsequently, the pellet was dissolved in 250 µl acetone. Next, the solvent was evaporated under nitrogen flow and the dried pellet was dissolved in 100 µl of a mixture of MeOH and chloroform (70%/30%). In the following step, the samples were subjected to HPLC-MS analysis.

#### **5.4.6 HPLC-MS analysis**

Prior to HPLC-MS analysis, extracts were centrifuged for 30 min at 13300 rpm. The samples were analyzed via Impact II qTOF (Bruker) equipped with an ESI source set to positive ionization mode using a 5-95% H<sub>2</sub>O-acetonitrile (ACN) gradient over 12 min followed by 95% ACN 5% water for 4 min with a flowrate of 0.4 ml/min. Both solvents were supplemented with 0.1 % formic acid (FA). The applied scan range was *m/z* 100-1200. Separation of compounds was achieved by using a C18-column. Generated data was analyzed using the software Bruker Compass Analysis 4.3.

#### **5.4.7 Compound purification**

For compound purification, 2 l LB cultures of the strain *Escherichia coli* BL21 (DE3)-Marionette-diterpene + pACYC\_ara\_TT01\_core + pCOLA\_ara\_TT01\_crtE\_fni were inoculated with a starting OD<sub>600</sub>=0.1 from an overnight culture and supplemented with kanamycin, chloramphenicol and spectinomycin. Gene expression was induced with 0.2% arabinose. After 72 h of incubation, cells were harvested, pelleted and subsequently dissolved in

MeOH/chloroform (90%/10%). Compounds were purified using a 1260 Semiprep LC system coupled to a G6125B LC/MSD ESI-MS (Agilent). A 5-95% H<sub>2</sub>O-acetonitrile (ACN) gradient over 16 min followed by 95% ACN 5% water for 4 min was applied over 20 min on a Cholesterol column (10 ID x 250mm, COSMOSIL) with a flowrate of 3 ml/min. Finally, the structures of  $\beta$ -Carotene and  $\beta$ -apo-13-carotenone were confirmed with standards.

#### **5.4.8 Standards**

$\beta$ -apo-13-carotenone standard was purchased from ChemScience (New Jersey, USA).  $\beta$ -Carotene standard was purchased from Sigma-Aldrich Chemie GmbH (Taufkirchen, Germany).

#### **5.4.9 Bioinformatic and phylogenetic analysis**

For bioinformatic analysis, BlastP was used to identify carotenoid clusters in different *Photorhabdus* strains and other organisms. For further characterization of hits from BlastP, antiSMASH analysis was used. Sequence alignments and tree models were generated in Geneious 6.1.8 and ClustalW. Big scale analysis of nuclear hormone receptors (NHRs) and fatty acid- and retinoid-binding proteins (FARs) was done in cooperation with Prof. Dr. Ingo Ebersberger (Goethe University Frankfurt).

#### **5.4.10 Insect killing assay**

*Galleria mellonella* were grown in maggot feeding medium (500 g honey, 500 g wheat bran, 30 g yeast, 300 g flour, 200 g cream of wheat, 100 g milk powder, 400 g 100% glycerol) for three weeks. Subsequently, the larvae were harvested at an appropriate size and sedated on ice for 20 min while being sprayed with 70% EtOH once. A sterile Hamilton glass syringe was used to inject the bacteria. Injection volume was set to 10  $\mu$ l. In the following step, the larvae were stored in empty petri dishes to confirm the successful injection. Lastly, insect death was determined in a Tecan-reader by missing movement of the larvae. Generated data was analyzed in Rstudio (Rstudio PBC). HR-MS data for galleria infection assays was kindly provided by Dr. Yi-Ming Shi.

## 6 Results

### 6.1 Topic A: Anthraquinone diversification in *Photorhabdus*

#### 6.1.1 AQ production in *P. luminescens*

*Photorhabdus* strains exhibit a characteristic orange-reddish color upon their exponential growth phase. This pigmentation is caused by the production of different AQ derivatives. The BGC responsible for the AQ biosynthesis was described earlier<sup>74</sup>. However, the methyltransferases (MTs) involved in AQ derivative formation have not been characterized yet. Thus, the following topic describes the characterization and elucidation thereof. First, the AQ production of the *P. luminescens* WT was analyzed after a production period of 72 h (Fig. 9).

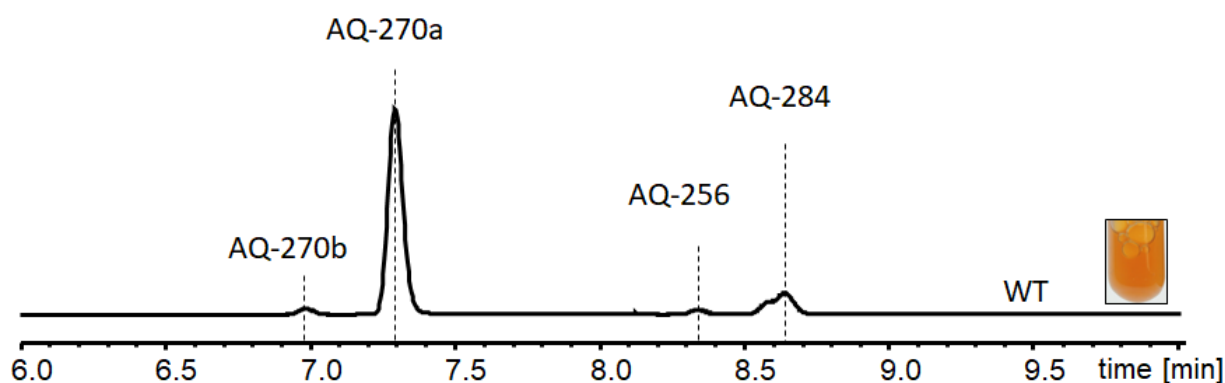


**Figure 9.** AQ production in *P. luminescens* wildtype. Shown is a HPLC-UV-chromatograms at 430 nm of EtAc extracts. The culture was cultivated for 72 h in LB broth at 30°C. The color of the culture is depicted on the right. Dashed lines indicate the retention times of the respective AQ derivatives.

While the non-methylated precursor AQ-256 produced by the BGC *AntA-I* was only detectable in minor amounts after 72 h of cultivation, two mono-methylated derivatives AQ-270a and AQ-270b and multiple di-methylated AQ-284 derivatives were detected. Interestingly, the UV-signal intensity of AQ-270a was significantly higher than the intensity of all other remaining AQ derivatives.

### 6.1.2 MTs involved in AQ derivative formation

Bioinformatic analysis of the *P. luminescens* genome identified a set of SAM-dependent methyltransferases (MTs) (*plu4895-plu4890*) that are putatively involved in AQ derivative formation. Interestingly, the locus of the core BGC *AntA-I* is situated approximately 1 mbp apart from *plu4890-plu4895* (Fig. 10).

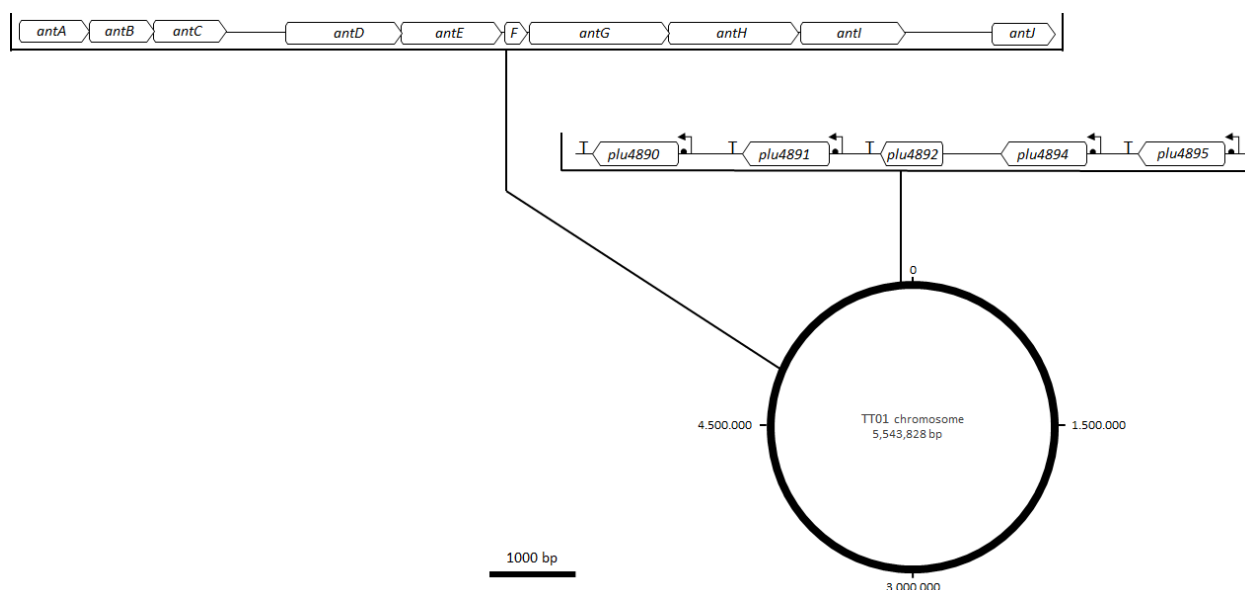


**Fig. 10.** Localization of the AQ-biosynthesis (*AntA-I*)- and MT-encoding (*plu4895-4890*) regions in the genome of *P. luminescens* TT01. *antA*: Ketoreductase, *antB*: PPTase, *antC*: Cyclase, *antD*: Ketosynthase, *antE*: chain-length factor, *antF*: ACP, *antG*: CoA ligase, *antH*: Aromatase, *antI*: Hydrolase, *antJ*: transcription factor. *Plu4895-plu4890*: SAM-dependent MTs. While *plu4890*, *plu4891* and *plu4895* are separate transcription units, *plu4892* and *plu4894* are organized in an operon. Promoters are displayed as arrows, terminators are displayed as T, ribosome binding sites are displayed as semicircles.

### 6.1.3 *In vivo* production of methylated AQ derivatives in *P. luminescens*

Consequently, in order to investigate the putative involvement of *plu4895-plu4890* several *P. luminescens* deletion mutants were generated using the protocol described earlier in the section Material and Methods (5.2) (Fig.11). For structural elucidation of the respective produced AQ derivatives, detailed NMR experiments were performed (described in a later section).

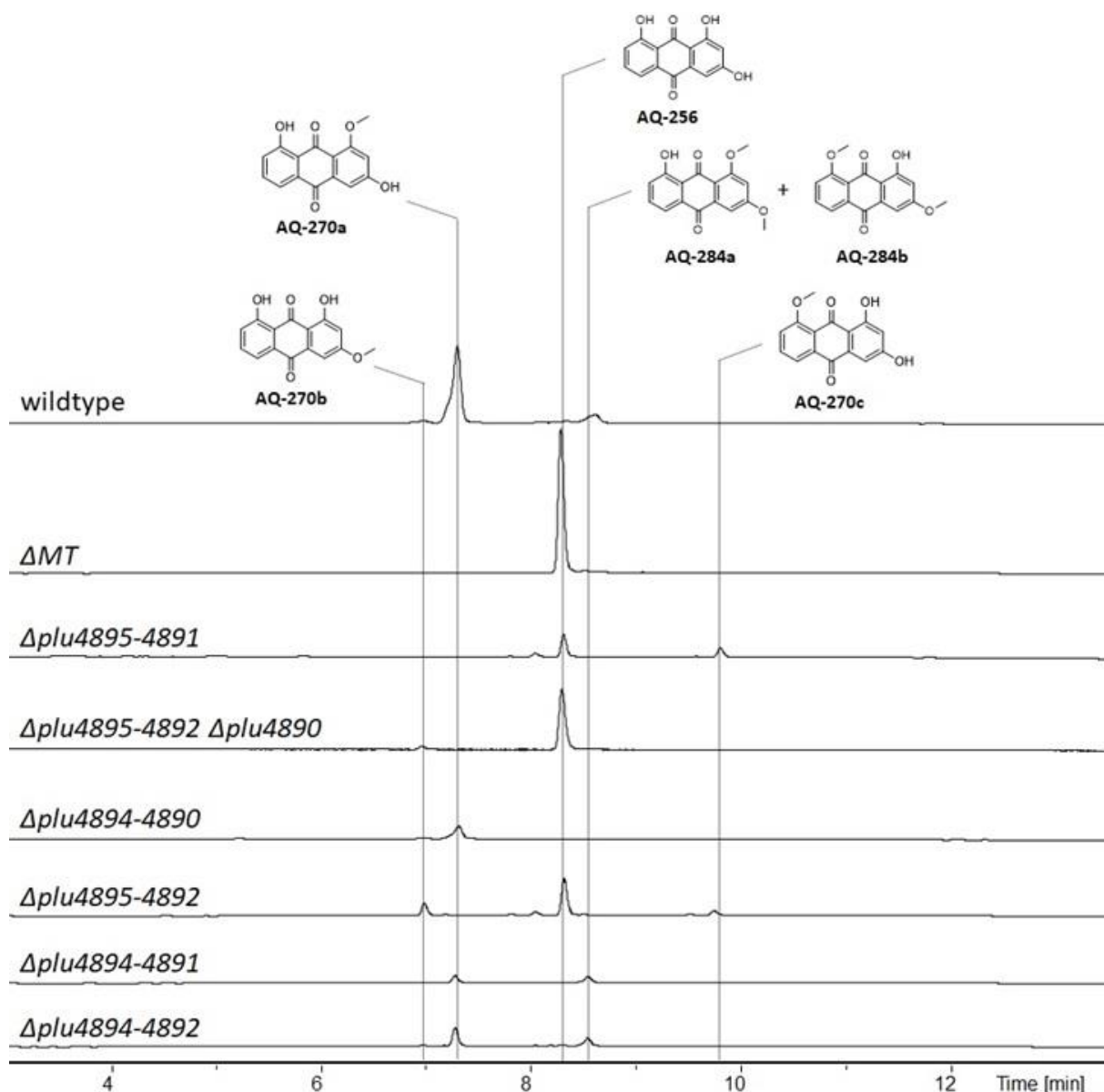


**Fig. 11.** *In vivo* production of methylated AQ derivatives in different *P. luminescens* methyltransferase deletion mutants. Shown are HPLC-UV-chromatograms at 430 nm of EtAc extracts. All chromatograms are scaled equally. Cultures were cultivated for 72 h in LB broth at 30°C. Dashed lines indicate the retention times of the respective AQ derivatives.

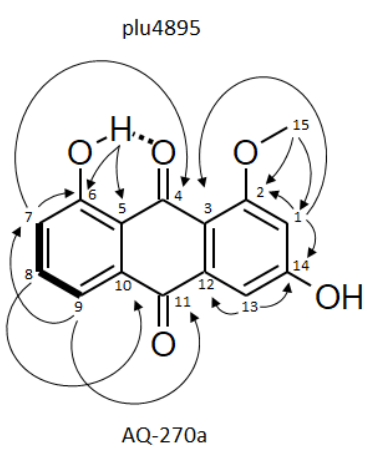
Upon deletion of the whole MT cluster, all production of methylated AQ derivatives was terminated confirming the involvement of *plu4895-4890* in AQ derivative formation. The respective strains expressing the genes encoding for a single MT (*plu4890*, *plu4891* and *plu4895*) produced single mono-methylated derivatives, while the strains expressing the corresponding genes for *plu4892* and *plu4892* did not yield any methylated AQ species. In case of *plu4895* ( $\Delta$ *plu4894-4890*), AQ-270a was produced which is the most abundant AQ in the wildtype strain after 72 h of cultivation. Additionally, a small signal for AQ-270b was

detectable. The strain expressing *plu4891* ( $\Delta plu4895-4892 \Delta 4890$ ) was only capable of producing AQ-270b. Interestingly, in contrast to  $\Delta plu4894-4890$ , the strain did not fully convert AQ-256 in a methylated derivative as AQ-256 was still detectable as the main product after 72 h of cultivation. Additionally, the relative amounts of generated AQ-270b of  $\Delta plu4895-4892 \Delta 4890$  were significantly lower than the relative amounts of AQ-270a produced by  $\Delta plu4894-4890$ . Crucially, the deletion of *plu4895-4891* (single expression of *plu4890*) led to the production of a single methylated AQ derivative AQ-270c that has not been observed to be produced in the WT. Exactly like for  $\Delta plu4895-4892 \Delta 4890$ , the strain was not able to fully convert AQ-256 into the single-methylated derivative after 72 h. The deletion of all MT-encoding genes except of *plu4894* and *plu4892* did not result in the production of AQ derivatives other than AQ-256 (data not shown). In addition, deletion mutants were generated that harbor deletions of two and three of the five MT-encoding genes, respectively. In accordance with the mutants expressing only one of the MT-encoding genes,  $\Delta plu4895-4892$  resulted in the production of both single methylated derivatives AQ-270b and AQ-270c. For  $\Delta plu4894-4891$ , AQ-270a produced by *plu4895* was detectable in addition to two double-methylated AQ-284. Notably, AQ-270c produced by *plu4890* was not detectable after 72 h of cultivation. Lastly, expression of *plu4890*, *plu4891* and *plu4895* ( $\Delta plu4894-4892$ ), respectively, mimicked the product spectrum of the WT, confirming that *plu4894* and *plu4892* are not involved in AQ derivative formation.

#### 6.1.4 Structure elucidation of AQ derivatives

Since the structures of both, the three AQ-270 derivatives and the two AQ-284 derivatives, were based on postulations regarding the exact position of the methoxy-group(s), an attempt was made to elucidate their structure via NMR experiments (Fig. 12-16). For this, 1 l production cultures of the strains described in section 5.2 were grown for 72 h at 30°C. Compound extraction was performed as described in Material and Methods section 5.2. The crude extract was subsequently separated on a Sephadex LH-20 (MeOH, 25-100  $\mu$ m, Pharmacia Fine Chemical Co. Ltd.) size-exclusion chromatography. After HPLC-MS analysis of the collected fractions, derivatives were purified in an additional chromatographic step using a 1260 Semiprep LC system coupled to a G6125B LC/MSD ESI-MS (Agilent). A 75% isocratic ACN-H<sub>2</sub>O gradient was applied over 16 min on a C18 column (1.0 mm ID x 250 mm, COSMOSIL)

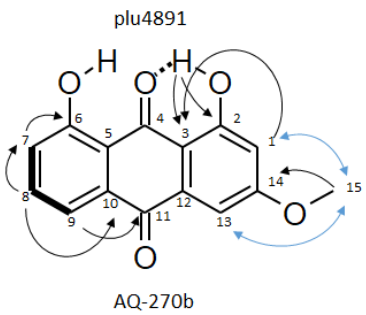
with a flowrate of 3 ml/min. First, the structure of AQ-270a was elucidated. Here, purification of the culture crude extract yielded 5.2 mg AQ-270a. The  $^1\text{H}$ -NMR spectrum showed signals for 10 protons, three of which point towards a methyl-group as singlet ( $\delta_{\text{H}} = 3.9$ ). In addition, the  $^{13}\text{C}$ -NMR spectrum shows signals for 15 carbons. Proton and carbon signal assignments resulted from a  $^1\text{H}$ - $^{13}\text{C}$  correlation spectrum. Proton connectivities arose from a  $^1\text{H}$ - $^1\text{H}$  COSY experiment (displayed in bold). As the core structure of AQ-256 was already described elsewhere<sup>74</sup> with 14 carbons, the position of the methyl-group had to be assigned. Here, HSQC (coupling of  $\delta_{\text{C}} = 105.55$  with  $\delta_{\text{H}} = 6.79$ ,  $\delta_{\text{C}} = 56.68$  with  $\delta_{\text{H}} = 3.9$ ) and HMBC (coupling of  $\delta_{\text{C}} = 105.55$  with  $\delta_{\text{H}} = 3.9$ ,  $\delta_{\text{C}} = 164.17$  with  $\delta_{\text{H}} = 6.79$ ,  $\delta_{\text{C}} = 164.17$  with  $\delta_{\text{H}} = 3.9$ ) spectra provided the necessary correlations to confirm the location of the methoxy group of AQ-270a produced by plu4895 at position C2. The nomenclature of carbons was set according to the biosynthesis.



	Position	$\delta_{\text{C}}$	$\delta_{\text{H}}$ (HSQC)	$\delta_{\text{H}}$ (HMBC)	mult (J in Hz)	$^1\text{H}$
	1	105.55	6.79	7.17, 3.90	d (2.4)	
	2	164.17		6.79, 3.90		
	3	112.20		7.17, 6.79		
	4	183.63		7.60, 7.29, 6.79		
	5	124.81		13.23, 7.67, 7.60		
	6	162.02		13.23, 7.67, 7.60, 7.29		
	7	118.44	7.29	7.67, 7.29	dd (8.3, 1.2)	
	8	132.83	7.67		t (8.1)	
	9	117.10	7.60	7.67, 7.60, 7.29	dd (7.5, 1.2)	
	10	135.79		7.67, 7.60, 7.29		
	11	182.94		7.67, 7.60, 7.17		
	12	137.19				
	13	108.32	7.17	7.29, 6.79	d (2.3)	
	14	166.72		7.17, 6.79		
	15	56.68	3.90	3.90	s	
	6-OH					13.23

**Figure 12.** Structure of AQ-270a produced by plu4895. NMR spectroscopic data ( $^1\text{H}$  (500 MHz),  $^{13}\text{C}$  (125 MHz)) in  $\text{DMSO-}d_6$ ,  $\delta$  in ppm. HSQC and HMBC correlations are listed and indicated by black arrows, COSY correlations shown in bold, phenol-OH correlations are indicated by dotted lines. S: singlet; d: doublet; t: triplet. For NMR spectra, see Fig. S1 – Fig. S5.

Next, the structure of AQ-270b, produced by plu4891, was elucidated. Purification of the culture crude extract yielded 4.1 mg AQ-270b. NMR analysis was performed as for AQ-270a.  $^1\text{H}$ -NMR spectrum showed signals for 10 protons, three of which point towards a methyl-group ( $\delta_{\text{H}} = 3.93$ ). In addition, the  $^{13}\text{C}$ -NMR spectrum shows signals for 15 carbons. Proton and carbon signal assignments resulted from a  $^1\text{H}$ - $^{13}\text{C}$  correlation spectrum. Proton connectivities arose from a  $^1\text{H}$ - $^1\text{H}$  COSY experiment. In analogy to the structure elucidation of AQ-270a, as the core structure of AQ-256 was already described elsewhere<sup>74</sup> with 14 carbons, the position of the methyl-group had to be assigned. Here, HSQC (coupling of  $\delta_{\text{C}} = 56.61$  with  $\delta_{\text{H}} = 3.93$ ) and HMBC (coupling of  $\delta_{\text{C}} = 164.56$  with  $\delta_{\text{H}} = 13.2$ ,  $\delta_{\text{C}} = 110.58$  with  $\delta_{\text{H}} = 13.2$ ,  $\delta_{\text{C}} = 166.54$  with  $\delta_{\text{H}} = 3.93$ ) spectra provided the necessary correlations to predict the location of the methoxy group of AQ-270b produced by plu4891 at position C14. Finally, a  $^1\text{H}$ - $^1\text{H}$ -ROESY spectrum showed the necessary correlations ( $\delta_{\text{H}} = 6.89$  with  $\delta_{\text{H}} = 3.93$ ,  $\delta_{\text{H}} = 7.21$  with  $\delta_{\text{H}} = 3.93$ ) to confirm the location of the methoxy group of AQ-270b at C14. The nomenclature of carbons was set according to the biosynthesis.



Position	$\delta_{\text{C}}$	$\delta_{\text{H}}$ (HSQC)	$\delta_{\text{H}}$ (HMBC)	ROESY	mult (J in Hz)	$^1\text{H}$
1	107.32	6.89			d (2.3)	
2	164.56		13.20			
3	110.58		13.20, 6.89			
4	186.66					
5						
6	163.81		7.37			
7	125.01	7.37	7.71		dd (8.3, 1.1)	
8	137.78	7.77			t (7.0)	
9	119.77	7.71	7.71, 7.37		dd (7.8, 1.2)	
10	133.42		7.77			
11	181.68		7.71			
12						
13	107.24	7.21			d (2.3)	
14	166.54		3.93			
15	56.61	3.93		1, 13	s	
2-OH						13.20

**Figure 13.** Structure of AQ-270b produced by plu4891. NMR spectroscopic data ( $^1\text{H}$  (500 MHz),  $^{13}\text{C}$  (125 MHz)) in  $\text{DMSO}-d_6$ ,  $\delta$  in ppm. HSQC and HMBC correlations are listed and indicated by black arrows, COSY correlations shown in bold, ROESY correlations are indicated by blue arrows, phenol-OH correlations are indicated by dotted lines. S: singlet; d: doublet; t: triplet. For NMR spectra, see Fig. S6 – Fig. S11.



Furthermore, the structure of AQ-270c was elucidated which has not been observed *in vivo* yet. Purification of the culture crude extract yielded 3.2 mg AQ-270c. NMR analysis was performed as for AQ-270a.  $^1\text{H}$ -NMR spectrum showed signals for 10 protons, three of which point towards a methyl-group singlet ( $\delta_{\text{H}} = 3.95$ ). In addition, the  $^{13}\text{C}$ -NMR spectrum shows signals for 15 carbons. Proton and carbon signal assignments resulted from a  $^1\text{H}$ - $^{13}\text{C}$  correlation spectrum. Proton connectivities arose from a  $^1\text{H}$ - $^1\text{H}$  COSY experiment. In analogy to the already confirmed AQ species and as the core structure of AQ-256 was already described elsewhere<sup>74</sup> with 14 carbons, the position of the methyl-group had to be assigned. Here, HSQC (coupling of  $\delta_{\text{C}} = 56.95$  with  $\delta_{\text{H}} = 3.95$ ) and HMBC (coupling of  $\delta_{\text{C}} = 160.86$  with  $\delta_{\text{H}} = 3.95$ ,  $\delta_{\text{C}} = 119.87$  with  $\delta_{\text{H}} = 3.95$ ,  $\delta_{\text{C}} = 119.96$  with  $\delta_{\text{H}} = 3.95$ ) spectra provided the necessary correlations to confirm the location of the methoxy group of AQ-270c produced by plu4890 at position C6. The nomenclature of carbons was set according to the biosynthesis.

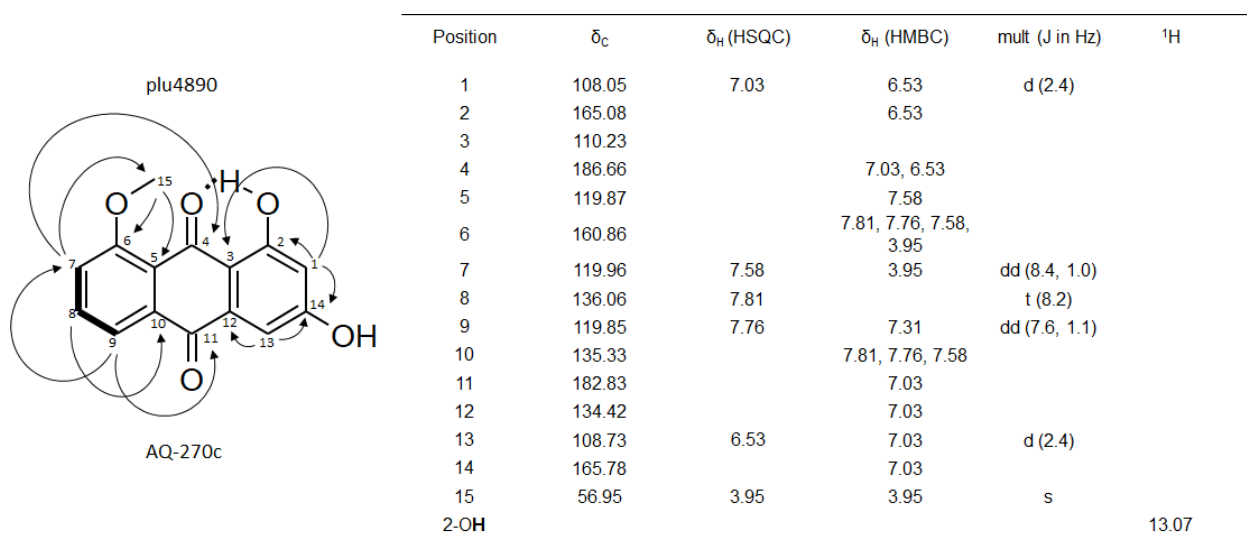
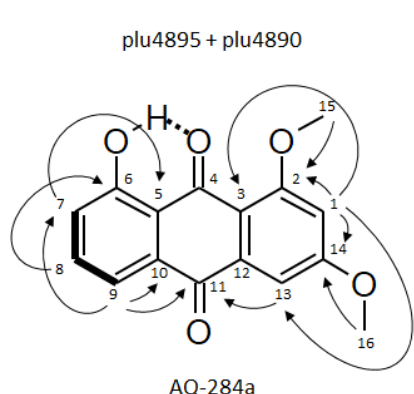


**Figure 14.** Structure of AQ-270c produced by plu4890. NMR spectroscopic data ( $^1\text{H}$  (500 MHz),  $^{13}\text{C}$  (125 MHz)) in  $\text{DMSO}-d_6$ ,  $\delta$  in ppm. HSQC and HMBC correlations are listed and indicated by black arrows, COSY correlations shown in bold, phenol-OH correlations are indicated by dotted lines. S: singlet; d: doublet; t: triplet. For NMR spectra, see Fig. S12 – Fig. S17.

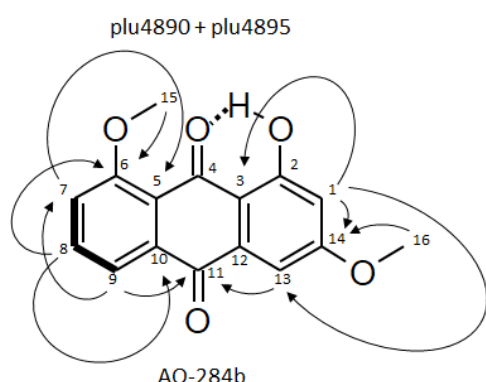
Next, the structure of AQ-284a was elucidated. Purification of the culture crude extract yielded 3.1 mg AQ-284a. NMR analysis was performed as for AQ-270a.  $^1\text{H}$ -NMR spectrum showed signals for 12 protons, 6 of which point towards methyl-groups ( $\delta_{\text{H}} = 4.01$ ,  $\delta_{\text{H}} = 4.06$ ). In addition, the  $^{13}\text{C}$ -NMR spectrum shows signals for 16 carbons. Proton and carbon signal assignments resulted from a  $^1\text{H}$ - $^{13}\text{C}$  correlation spectrum. Proton connectivities arose from a  $^1\text{H}$ - $^1\text{H}$  COSY experiment. In analogy to the already confirmed AQ species and as the core structure of AQ-256 was already described elsewhere<sup>74</sup> with 14 carbons, the position of the methyl-group had to be assigned. Here, HSQC (coupling of  $\delta_{\text{C}} = 56.65$  with  $\delta_{\text{H}} = 4.06$ ,  $\delta_{\text{C}} = 56.08$  with  $\delta_{\text{H}} = 4.01$ ,  $\delta_{\text{C}} = 104.75$  with  $\delta_{\text{H}} = 6.83$ ,  $\delta_{\text{C}} = 104.01$  with  $\delta_{\text{H}} = 7.51$ ) and HMBC (coupling of  $\delta_{\text{C}} = 163.09$  with  $\delta_{\text{H}} = 4.06$ ,  $\delta_{\text{C}} = 165.46$  with  $\delta_{\text{H}} = 4.01$ ) spectra provided the necessary correlations to confirm the location of the two methoxy-groups of AQ-284a produced by plu4895 + plu4890 at position C2 and C14, respectively. The nomenclature of carbons was set according to the biosynthesis.



Position	$\delta_{\text{C}}$	$\delta_{\text{H}}$ (HSQC)	$\delta_{\text{H}}$ (HMBC)	mult (J in Hz)	$^1\text{H}$
1	104.75	6.83	7.51	d (2.7)	
2	163.09		6.83, 4.06		
3	115.23		7.51, 6.83		
4	182.76				
5	116.89		7.31		
6	162.47		7.61		
7	124.96	7.31	7.78	dd (8.4, 1.6)	
8	135.34	7.61		t (7.7)	
9	118.85	7.78	7.31	dd (7.4, 1.3)	
10	132.62		7.78		
11	187.79		7.78, 7.51		
12	137.68				
13	104.01	7.51	6.83	d (2.9)	
14	165.46		6.83, 4.06		
15	56.65	4.06		s	
16	56.08	4.01		s	
6-OH					13.25

**Figure 15.** Structure of AQ-284a produced by plu4890 and plu4895. NMR spectroscopic data ( $^1\text{H}$  (500 MHz),  $^{13}\text{C}$  (125 MHz)) in DMSO- $d_6$ ,  $\delta$  in ppm. HSQC and HMBC correlations are listed and indicated by black arrows, phenol-OH correlations are indicated by dotted lines. S: singlet; d: doublet; t: triplet. For NMR spectra, see Fig. S18 – Fig. S22.

Finally, the structure of the remaining AQ-284b derivative was confirmed. Purification of the culture crude extract yielded 3.9 mg AQ-284b. NMR analysis was performed as for AQ-270a.  $^1\text{H}$ -NMR spectrum showed signals for 12 protons, 6 of which point towards methyl-groups as singlets ( $\delta_{\text{H}} = 4.1$ ,  $\delta_{\text{H}} = 3.95$ ). In addition, the  $^{13}\text{C}$ -NMR spectrum shows signals for 16 carbons. Proton and carbon signal assignments resulted from a  $^1\text{H}$ - $^{13}\text{C}$  correlation spectrum. Proton connectivities arose from a  $^1\text{H}$ - $^1\text{H}$  COSY experiment. In analogy to the already confirmed AQ species and as the core structure of AQ-256 was already described elsewhere<sup>74</sup> with 14 carbons, the position of the methyl-group had to be assigned. Here, HSQC (coupling of  $\delta_{\text{C}} = 51.94$  with  $\delta_{\text{H}} = 4.1$ ,  $\delta_{\text{C}} = 51.2$  with  $\delta_{\text{H}} = 3.95$ ,  $\delta_{\text{C}} = 102.62$  with  $\delta_{\text{H}} = 6.74$ ,  $\delta_{\text{C}} = 113.01$  with  $\delta_{\text{H}} = 7.38$ ,  $\delta_{\text{C}} = 130.58$  with  $\delta_{\text{H}} = 7.75$ ) and HMBC (coupling of  $\delta_{\text{C}} = 156.05$  with  $\delta_{\text{H}} = 7.75$ ,  $4.1$ ,  $\delta_{\text{C}} = 160.54$  with  $\delta_{\text{H}} = 3.95$ ,  $\delta_{\text{C}} = 160.54$  with  $\delta_{\text{H}} = 6.74$ ) spectra provided the necessary correlations to confirm the location of the two methoxy-groups of AQ-284b produced by plu4890 + plu4895 at position C6 and C14, respectively. The nomenclature of carbons was set according to the biosynthesis.



Position	$\delta_{\text{C}}$	$\delta_{\text{H}}$ (HSQC)	$\delta_{\text{H}}$ (HMBC)	mult (J in Hz)	$^1\text{H}$
1	102.62	6.74	7.35	d (2.8)	
2	160.77				
3	106.94		7.35, 6.74		
4	182.78				
5	116.13		7.38		
6	156.05		7.75, 4.1		
7	113.61	7.38	7.98	dd (8.5, 0.9)	
8	130.58	7.75		t (7.9)	
9	115.52	7.98	7.98, 7.38	dd (7.6, 1.1)	
10	130.96		7.75		
11	178		7.98, 7.35		
12	129.47				
13	101.79	7.35	6.74	d (2.7)	
14	160.54		6.74, 3.95		
15	51.94	4.1		s	
16	51.2	3.95		s	
2-OH					13.16

**Figure 16.** Structure of AQ-284b produced by plu4890 and plu4895. NMR spectroscopic data ( $^1\text{H}$  (500 MHz),  $^{13}\text{C}$  (125 MHz)) in DMSO- $d_6$ ,  $\delta$  in ppm. HSQC and HMBC correlations are listed and indicated by black arrows, COSY correlations shown in bold, phenol-OH correlations are indicated by dotted lines. S: singlet; d: doublet; t: triplet. For NMR spectra, see Fig. S23 – Fig. S27.

### 6.1.5 *In vitro* production of methylated AQ derivatives

In order to consolidate the findings described above, single MT-encoding genes were cloned into expression vectors. For protein purification, the plasmids were transformed into *E. coli* BL21 Gold and the *in vitro* assays were carried out as described in Material and Methods section (5.2). The purification of the respective MTs was conducted by Dr. Eva Huber, TU Munich. First, single MTs activity on AQ-256 was investigated (Fig.17).

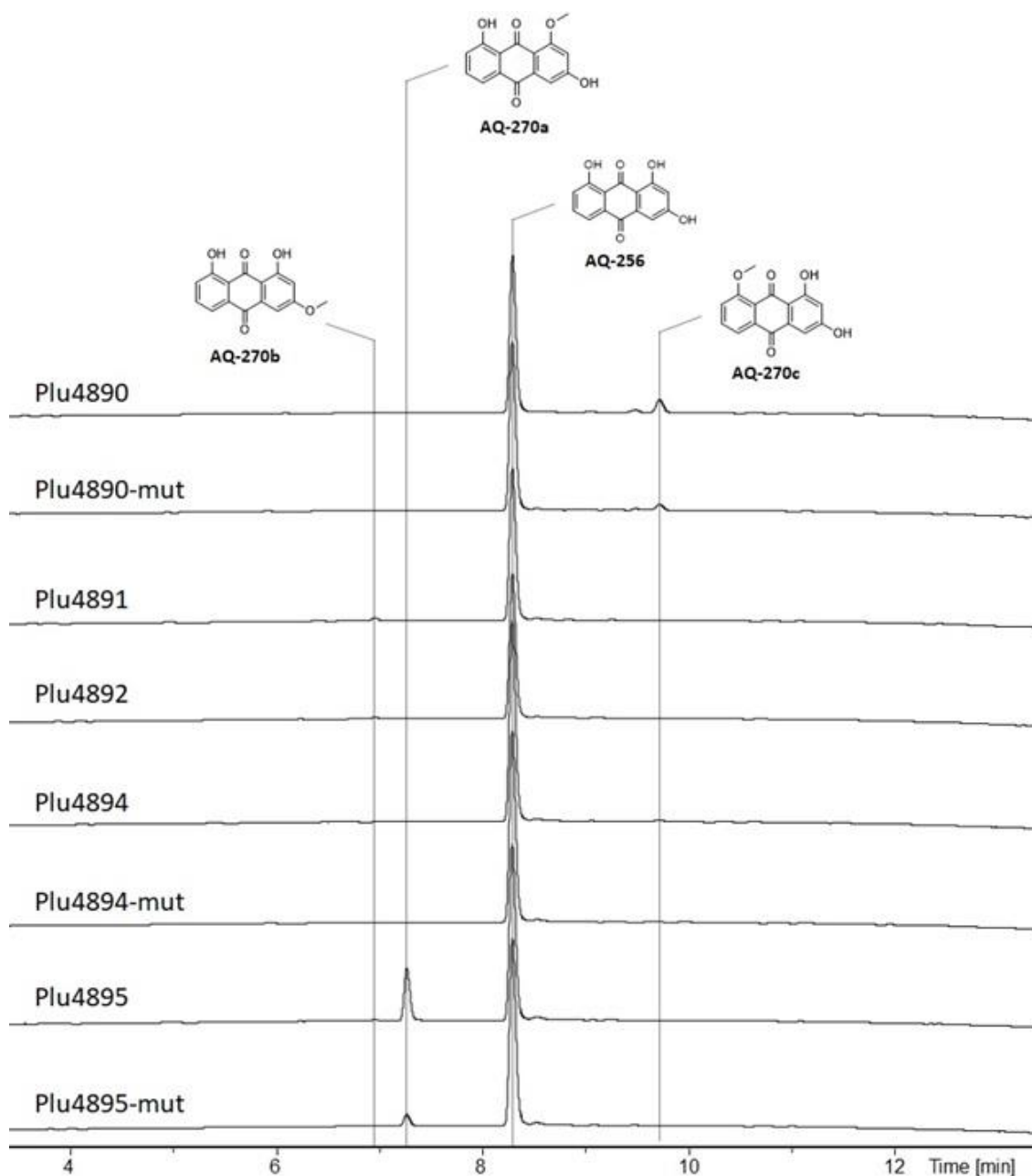


**Fig. 17.** *In vitro* AQ conversion assay with single purified methyltransferases. Active site H229N and N229H mutants are indicated. Shown are HPLC-UV-chromatograms at 430 nm. All chromatograms are scaled equally. Assays were conducted using 1  $\mu$ M purified protein, 1 mM AQ-256 as substrate, 1 mM SAM as co-factor at 20°C overnight. Dashed lines indicate the retention times of the respective AQ derivatives.

Essentially, the findings *in vivo* are further substantiated by the observations made *in vitro*. Both plu4894 and plu4892 exhibit no detectable activity on AQ-256. In case of plu4890, AQ-256 is converted in the single-methylated AQ-270c. While for plu4891, AQ-270b is formed, the activity of plu4895 results in the formation of AQ-270a as the major compound and minor amounts of AQ-270b. Interestingly, the relative activity of the respective MTs also differs *in vitro* which stands in agreement with the observations *in vivo*. Whereas plu4895 was able to convert 22.7% of AQ-256 into AQ-270a overnight (24 h), the conversion rate of AQ-256 into AQ-270b and AQ-270c by plu4891 and plu4890 was 1.9% and 8.7%, respectively. Additionally, an attempt was made to generate an active form of the inactive plu4894 and plu4892 variants. Here, active site mutations were introduced into the respective MTs based on alpha-fold predictions (performed by Dr. Eva Huber, TU Munich). Specifically, both plu4894 and plu4892 harbor a histidine in their active site at position 229. In contrast, plu4895, plu4891 and plu4890, position 229 shows a conserved asparagine. Consequently, plu4894-H229N and plu4892-H229N mutants were generated. Additionally, in case of plu4895, plu4891 and plu4890, N229H substitutions were conducted. As expected, the N229H mutation constructs exhibited a decreased activity in comparison to their wildtype versions. Here, plu4895-mut was only able to convert 5.9% of the AQ-256 substrate, plu4891-mut did not produce any detectable amount of AQ-270b and plu4890 activity was reduced to 3.8% conversion rate. Unfortunately, for plu4894 and plu4892, the H229N substitution did not result in any kind of activity on AQ-256.

#### **6.1.6 Combinatorial *in vitro* activity of plu4895-plu4890 on AQ-256**

In the following step, different combinations of MTs were tested *in vitro* in order to unravel the involvements of the respective MTs in the formation of multi-methylated derivatives (Fig.18).

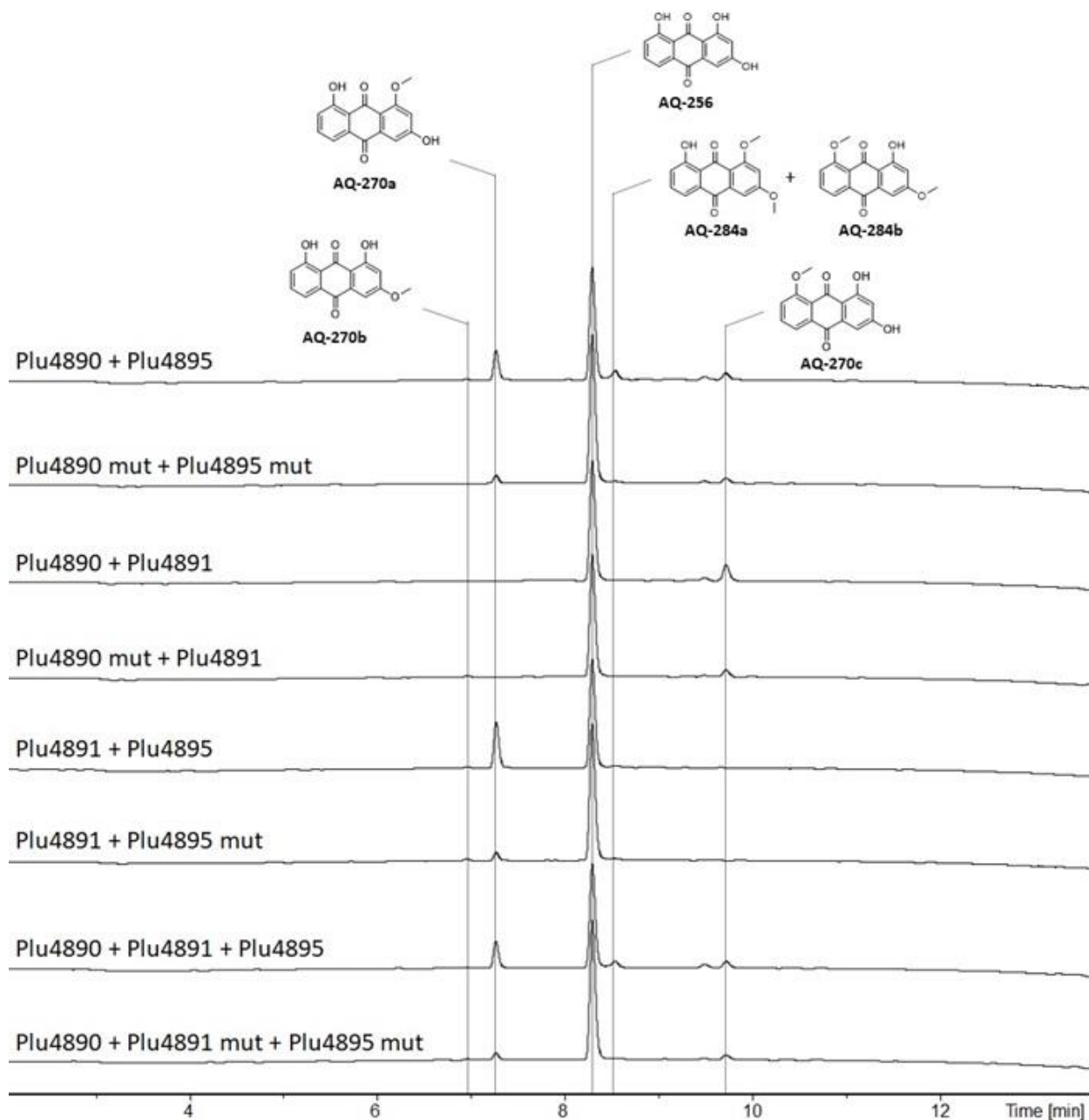


**Fig. 18.** *In vitro* AQ conversion assay combining different purified methyltransferases. H229N and N229H mutants are indicated. Shown are HPLC-UV-chromatograms at 430 nm. All chromatograms are scaled equally. Assays were conducted using 1  $\mu$ M purified protein, 1 mM AQ-256 as substrate, 1 mM SAM at 20°C overnight. Dashed lines indicate the retention times of the respective AQ derivatives.

Interestingly, the combination of plu4895 and plu4890 proved to be the only combination of two different MTs that resulted in the generation of double-methylated AQ-284 derivatives apart from the already known single-methylated AQ-270 derivatives. Here, a mixture of two AQ-284 derivatives was observed (284a/284b). Both combinations of plu4895 and plu4890 with plu4891 did not result in any new detectable di-methylated derivatives. Additionally, the combination of all three active MTs plu4895, plu4891 and plu4890 in one assay mimicked the AQ product spectrum of the *P. luminescens* wildtype *in vivo*. As expected, all mutated versions of the different MTs exhibited less activity than their respective wildtype counterparts when being combined in one assay. Conversion rates of the different assays are displayed in Table 19.

**Table 19:** AQ-256 conversion rates combining different purified MTs.

Proteins	Product	Conversion Rate
plu4890 + plu4895	AQ-270a	17.70%
	AQ-270b	0.80%
	AQ-270c	5.80%
	AQ-284a/b	5.10%
plu4890-mut + plu4895	AQ-270a	4.80%
	AQ-270b	below detection level
	AQ-270c	4.60%
	AQ-284a/b	1.00%
plu4890 + plu4891	AQ-270a	-
	AQ-270b	1.20%
	AQ-270c	12.50%
	AQ-284a/b	-
plu4890-mut + plu4891	AQ-270a	-
	AQ-270b	1.50%
	AQ-270c	6.30%
	AQ-284a/b	-
plu4891 + plu4895	AQ-270a	27.70%
	AQ-270b	0.80%
	AQ-270c	-
	AQ-284a/b	1.50%
plu4891 + plu4895-mut	AQ-270a	5.30%
	AQ-270b	1.20%
	AQ-270c	-
	AQ-284a/b	1.60%
plu4890 + plu4891 + plu4895	AQ-270a	16.70%
	AQ-270b	0.40%
	AQ-270c	4.00%
	AQ-284a/b	4.10%
plu4890-mut+ plu4891-mut + plu4895-mut	AQ-270a	4.30%
	AQ-270b	0.70%
	AQ-270c	4.40%
	AQ-284a/b	0.30%



Generally, according to the AQ-256 conversion rates shown in table 19, plu4895 shows to exhibit the highest activity in comparison to plu4890 and plu4891, while plu4891 showed the least activity on the substrate. These findings were congruent with the observations made *in vivo*.

### 6.1.7 *In vitro* AQ conversion assay with single purified MTs using mono-methylated derivatives as substrate

Even with the findings above, the exact position of methylation by plu4895 and plu4890 regarding double-methylated AQ derivatives remained vague. Therefore, the purified mono-methylated derivatives (see 6.1.4) (Fig. 19) were used for *in vitro* assay with the respective MTs (Fig. 20).

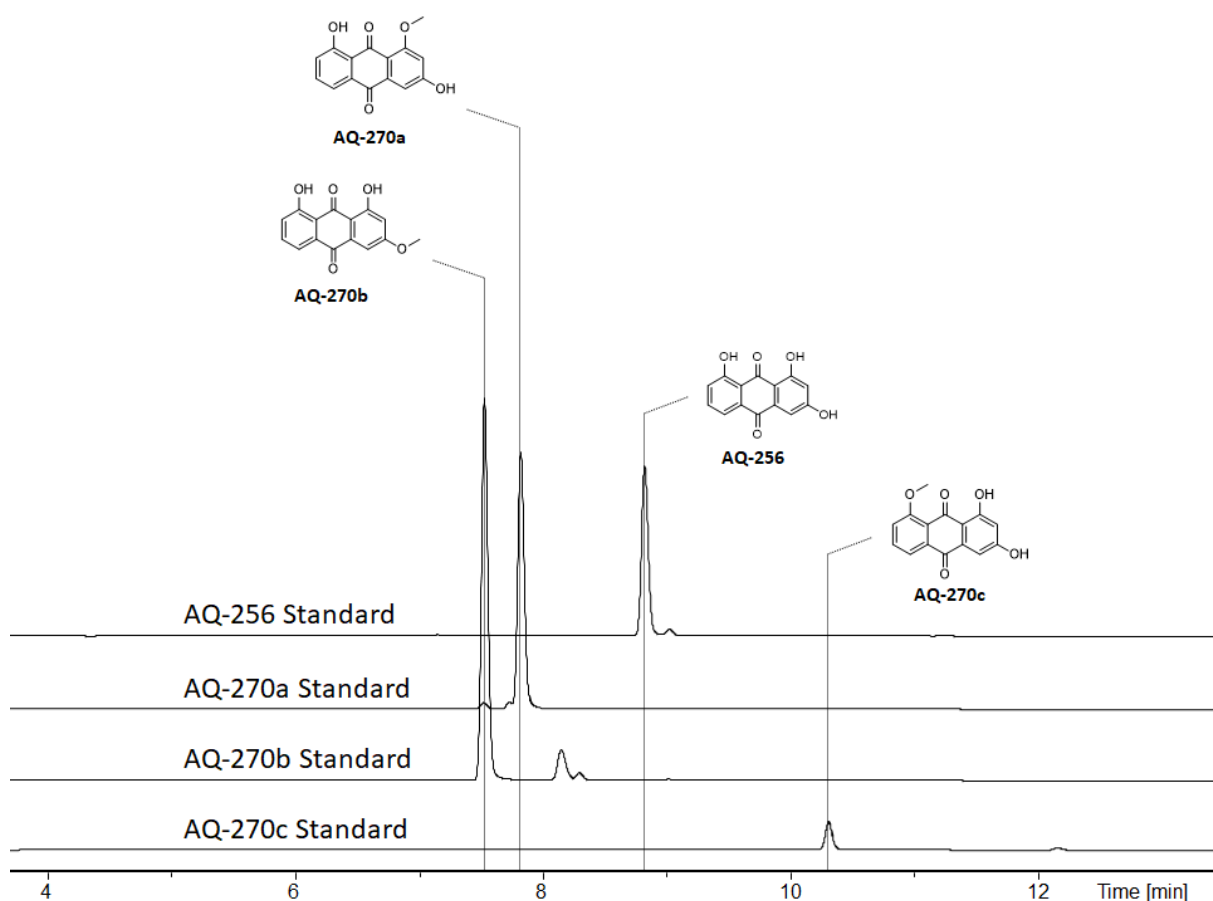


**Fig. 19.** Purification of AQ-270a/b/c. Shown are HPLC-UV-chromatograms at 430 nm. Purification was carried out using a 1260 Semiprep LC system coupled to a G6125B LC/MSD ESI-MS (Agilent). A 75% isocratic ACN-H<sub>2</sub>O gradient was applied over 16 min on a Cholesterol column (1.0 mm ID x 250 mm, COSMOSIL) with a flowrate of 3 ml/min. All chromatograms are scaled equally. Dashed lines indicate the retention times of the respective AQ derivatives.

All AQ derivatives apart from AQ-270c showed minor impurities after purification but were used for the following *in vitro* assays (Fig.20) without further purification.

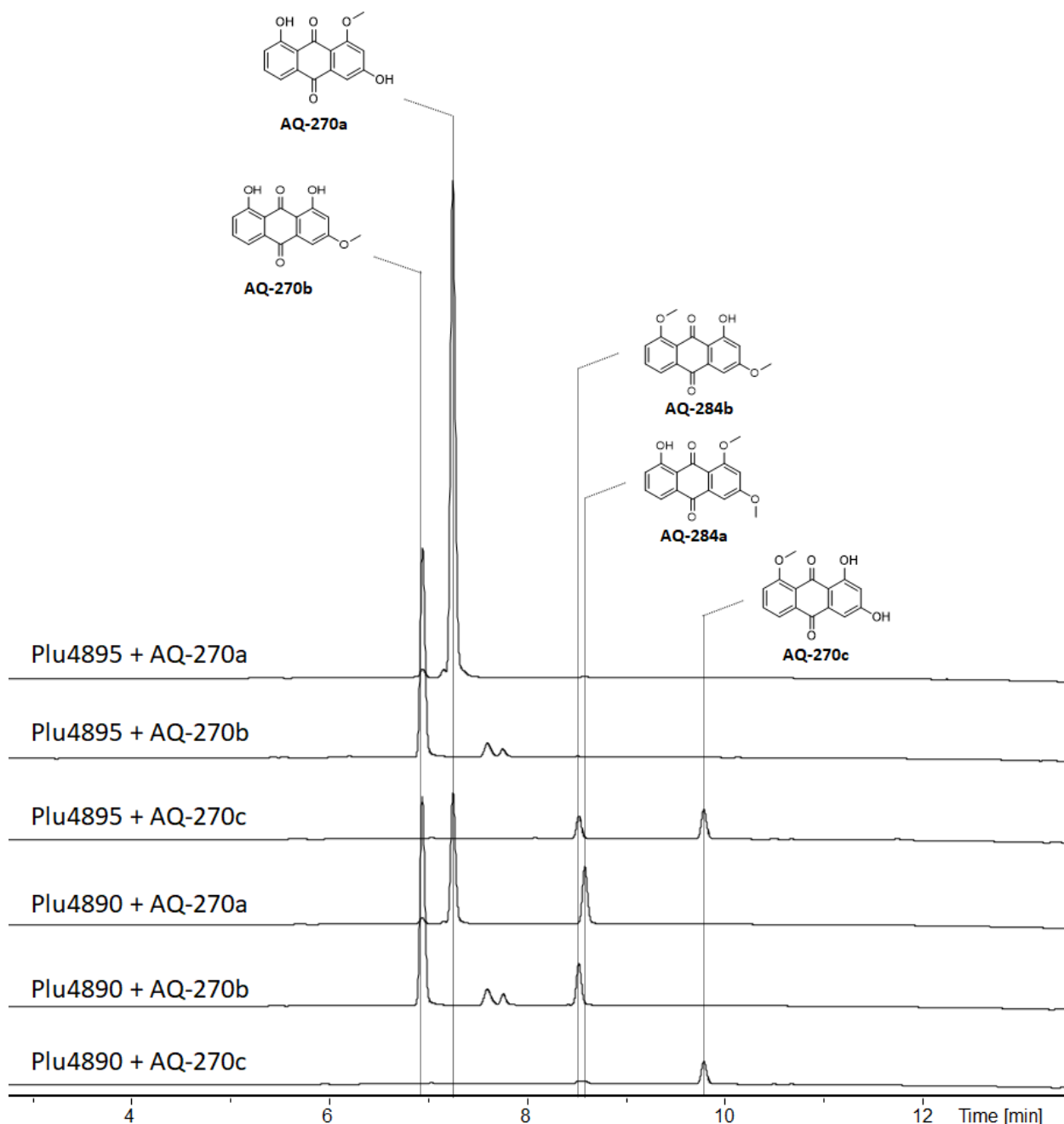


**Figure 20.** *In vitro* AQ conversion assay with single purified MTs using mono-methylated derivatives as substrate. Shown are HPLC-UV-chromatograms at 430 nm. All chromatograms are scaled equally. Assays were conducted using 1  $\mu$ M purified protein, 1 mM AQ-270a/b/c as substrate, 1 mM SAM as co-factor at 20°C overnight. Dashed lines indicate the retention times of the respective AQ derivatives.

As expected, plu4895 was active on the purified AQ-270c (produced by plu4890) derivative resulting in AQ-284b which also showed to be the main AQ-284 derivative produced *in vivo*.

In addition, plu4890 converted AQ-270a (produced by plu4895) into AQ-284a as second AQ-284 derivative observed *in vivo*. Interestingly, plu4890 was also active on AQ-270b (produced by plu4891) which stands in contrast to the findings made in section 6.1.3. Additionally, when using AQ-270c as a substrate for its own responsible MT plu4890, a small UV-signal corresponding to the mixture of AQ-284a/b was observed. Finally, when combining plu4895 with AQ-270b a small UV-signal corresponding to AQ-284b was detectable.

#### **6.1.8 Summary of AQ diversification in *P. luminescens* subsp. TT01**

In summary, the three active MTs plu4890, plu4891 and plu4895 showed to be responsible for the conversion of AQ-256 into AQ-270a (plu4895), AQ-270b (plu4891) and AQ-270c (plu4890), respectively. Sequential action of plu4890 and plu4895 resulted in the formation of AQ-284a and AQ-284b, respectively. Generally, plu4895 exhibited the highest activity on AQ-256 in comparison to plu4890 and plu4891 *in vivo* and *in vitro*, whereas plu4891 showed the lowest activity on the substrate.

#### **6.1.9 MT homologues in different *Photorhabdus* subspecies**

Bioinformatic tools described in Material and Methods chapter 5.2 were used to identify MTs in *P. luminescens* subs. *namnaonensis* PB45.5, *P. luminescens* subs. *hainanensis*, *P. luminescens* subs. *akhurstii*, *P. bodei* and *P. temperata* closely homologous to the ones identified in *P. luminescens* TT01 (Fig.21). The focus in this section was to get a deeper insight into the methylation patterns of MTs in several different *Photorhabdus* species.

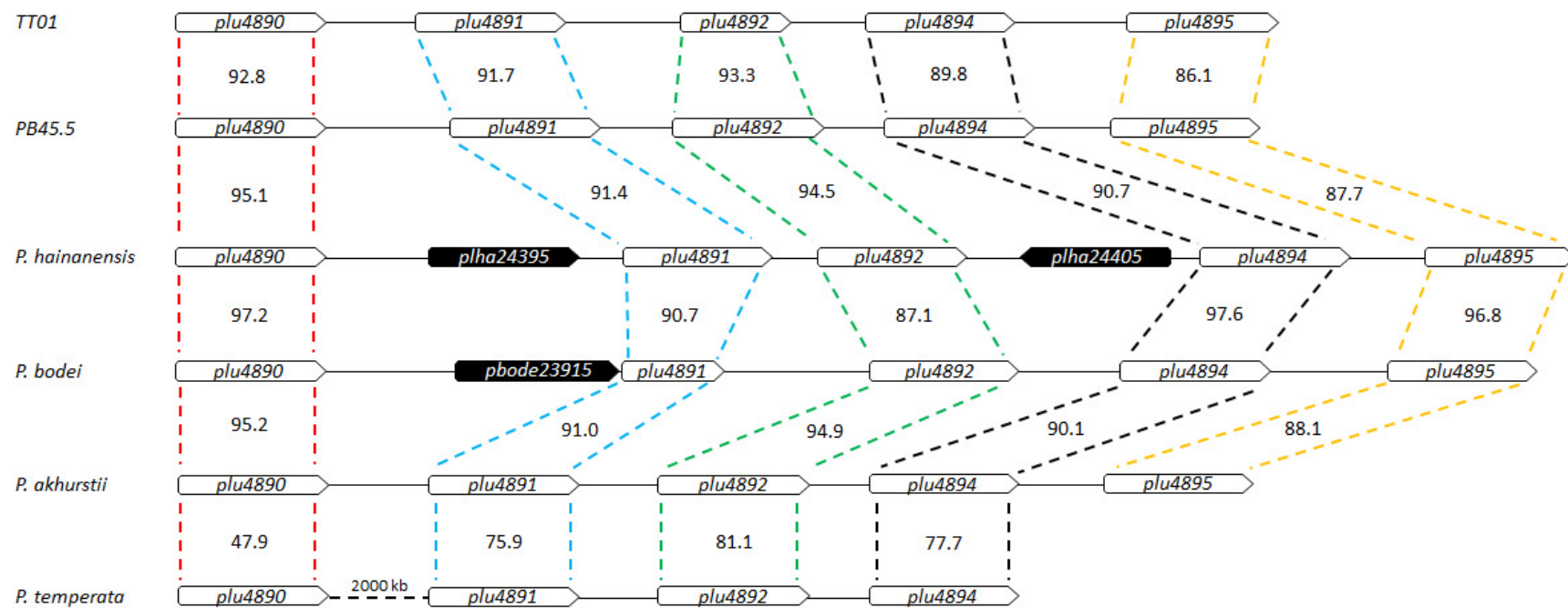


**Fig. 21** Alignment of MT clusters in different *Photorhabdus* strains. Homologous MTs are connected with dashed lines. Amino acid sequence similarities (%) in comparison to *P. luminescens* TT01 are depicted inside the respective boxes. Black genes display transposases.

Generally, all depicted *Photorhabdus* strains carry the genes encoding for plu4895-plu4890 in their genomes with the only exception being *P. temperata* that is missing *plu4895*. Interestingly, the respective MTs thoroughly show a high amino acid sequence similarity to the ones identified in *P. luminescens* TT01 (>90%). Again, the exception being *P. temperata* where plu4891 and plu4894 only show amino acid sequence similarity <80%, while plu4892 is 81.1% similar. Additionally, *plu4890* is located 2000 kb apart from the other MTs (for full sequence alignments, see Figure S33 – S37).

#### **6.1.10 AQ derivative formation in different *Photorhabdus* subspecies**

Finally, the AQ derivative formation in the aligned *Photorhabdus* strains was investigated. For this, the respective strains were grown for 72 h at 30°C in LB media. Subsequently, the compounds were extracted as described in Material and Methods chapter 5.2 and subjected to HPLC-MS analysis. The results are displayed in Fig. 22.

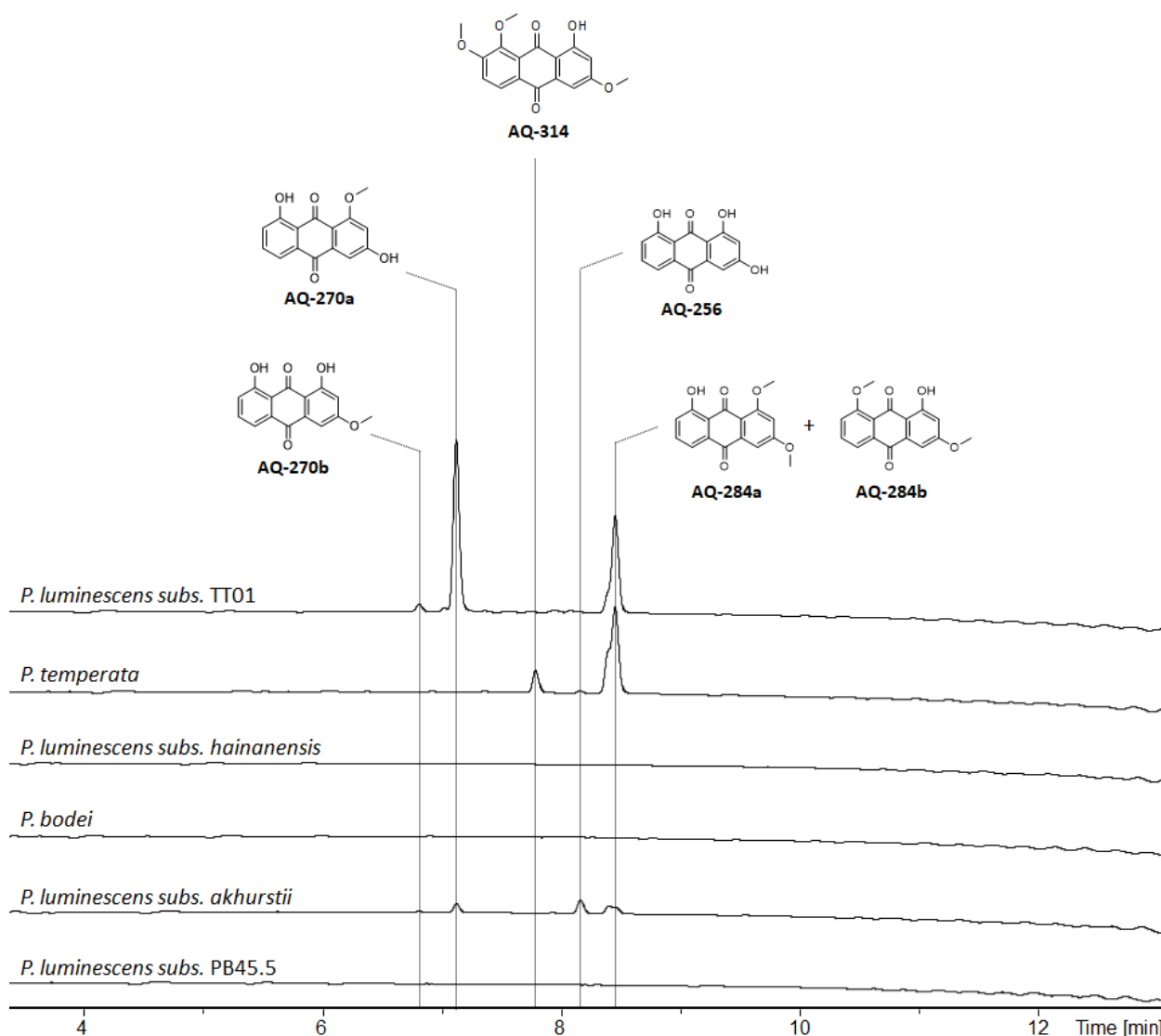


**Fig. 22.** *In vivo* production of methylated AQ derivatives in different *Photorhabdus* strains. Shown are HPLC-UV-chromatograms at 430 nm of EtAc extracts. All chromatograms are scaled equally. Cultures were cultivated for 72 h in LB broth at 30°C. Dashed lines indicate the retention times of the respective AQ derivatives.

*P. luminescens subs. akhurstii* features the highest similarity among all MTs in comparison to the other *Photorhabdus* strains to *P. luminescens subs. TT01*. Similarly, the strain shares the AQ product spectrum with *P. luminescens subs. TT01*. Interestingly, the overall amounts of produced AQ in *P. luminescens subs. akhurstii* are significantly reduced in comparison to *P. luminescens subs. TT01*, especially regarding AQ-270a, which is the main compound produced by *P. luminescens subs. TT01*. Additionally, unlike *P. luminescens subs. TT01*, *P. luminescens subs. akhurstii* does not fully convert the entire precursor AQ-256 into methylated derivatives. Furthermore, *P. temperata* shows a different AQ product spectrum. In this case, no single-

methylated AQ derivative is produced, while both double-methylated AQ-284a/b are still present. Crucially, the strain is the only investigated *Photorhabdus* species that is capable of producing a triple methylated AQ-314 derivative requiring an additional hydroxylation first. In contrast, *P. luminescens subs. namnaonensis* PB45.5, *P. luminescens subs. hainanensis* and *P. bodei* do not exhibit any AQ production at all under laboratory conditions.

#### **6.1.11 AQ diversification in *Photorhabdus***

In summary, it was observed that the three MTs plu4890, plu4891 and plu4895 are responsible for converting the unmethylated AQ-256 into three mono-methylated derivatives AQ-270a/b/c in *P. luminescens subs. TT01*. Furthermore, the combination plu4890 and plu4895 leads to the generation of two double-methylated derivatives AQ-284a/b. These observations were confirmed in both, *in vitro* and *in vivo* experiments. Additionally, as the respective MTs thoroughly show a high amino acid sequence similarity in different *Photorhabdus subspecies* to the ones identified in *P. luminescens TT01*, the AQ derivative formation in the respective strains was investigated. Here, it was observed that not only the methylation patterns highly differs between the respective strains but also the overall production levels of certain AQs vary.

## 6.2 Topic B: AQ overproduction in *Photorhabdus* as electrolyte for redox flow batteries

The technical and economic potential for energy storage in novel redox battery systems is generally very large regarding the aspired greenhouse gas neutrality of countries like Germany<sup>150</sup>. Therefore, it is necessary to establish new and innovative energy storage systems that can keep up with the immense demand for energy in the modern world. In this topic, the generation of a *P. luminescens* TT01 strain is described which strongly overproduces AQ-256 as the sole AQ derivative which can be utilized in redox flow batteries for electron transport. Additionally, a cheap NP production medium was established which is based on recyclable waste products.

### 6.2.1 Establishing an AQ production platform

Redox flow batteries that function on electrolytes generally increase in efficiency with increasing polarity of their respective electrolyte<sup>151</sup>. In this chapter, the AQ production in different *P. luminescens* strains that carried deletions generally known to alter NP production was investigated (Fig. 23). Some of the mutants were already generated previously<sup>152</sup>.



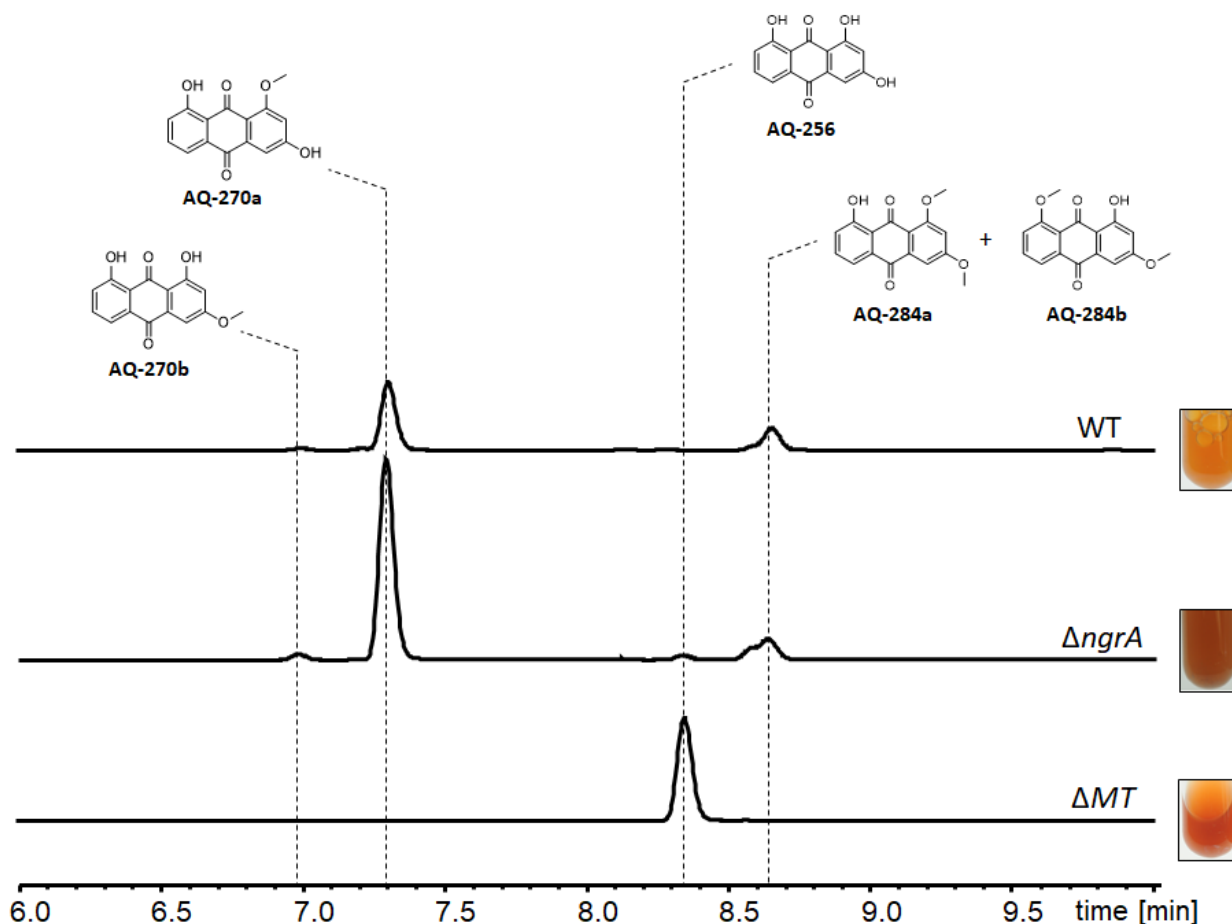


**Fig 23.** Comparison of AQ production in different *P. luminescens* strains. Shown are HPLC-UV-chromatograms at 430 nm of EtAc extracts. All chromatograms are scaled equally. Cultures were cultivated for 72 h in LB broth at 30°C. The color of the respective cultures is depicted on the right. Dashed lines indicate the retention times of the respective AQ derivatives. Parts of the extracts were already generated and used elsewhere<sup>152</sup>.

In the wildtype, the precursor AQ-256 is converted into different methylated derivatives mediated by a set of homologous MTs as described in Topic A. As the phenol groups Aqs are generally preferred over methoxy groups for electron storage in batteries, deletion of the respective MTs was carried out as described in Material and Methods chapter 5.3. Consequently, the  $\Delta MT$  was only capable of producing the non-methylated AQ-256. Preliminary work already described the AQ BGC responsible for AQ-256 biosynthesis<sup>74</sup>. Crucially, the BGC encodes a PPTase (*antB*), which was investigated to be highly specific for phosphopantetheinylation of the apo-ACP AntF (Qiuqin Zhou, unpublished results). Therefore, we tried to increase AQ production by preventing the production of other NPs. In order to abolish the production of NPs other than Aqs, a deletion of the gene encoding the globally active Sfp-type PPTase NgrA was introduced. Impairment of production of several

non-AQ-NPs was assumed to result in increased AQ production levels through higher availability of building blocks. In line with expectations, marker-less deletion of *ngrA* led to a significantly increased AQ-production of all derivatives, also indicated by the deeper red color of the culture. Furthermore, the ratio of UV-signal intensities between the methylated derivatives did not shift drastically. Interestingly, in contrast to the WT, the non-methylated AQ-256 was detectable after 72 h cultivation.

### **6.2.2 AntJ as a regulator of AQ biosynthesis**

Preliminary results revealed that AntJ acts as a pathway-specific transcriptional factor that activates the expression of the *antA-I* operon, while AQ production is terminated when *antJ* is deleted<sup>37,152</sup>. In order to investigate the effects of *antJ* overexpression on AQ production, *antJ* was cloned into an expression vector under the control of an IPTG inducible *tac*-promoter. The plasmid construction was based on the pACYC-version already used before<sup>152</sup> with an additional introduction of an engineered  $P_{tac}$  described elsewhere<sup>149</sup>. Subsequently, the plasmid was transformed into *P. luminescens* strains (Fig. 24).

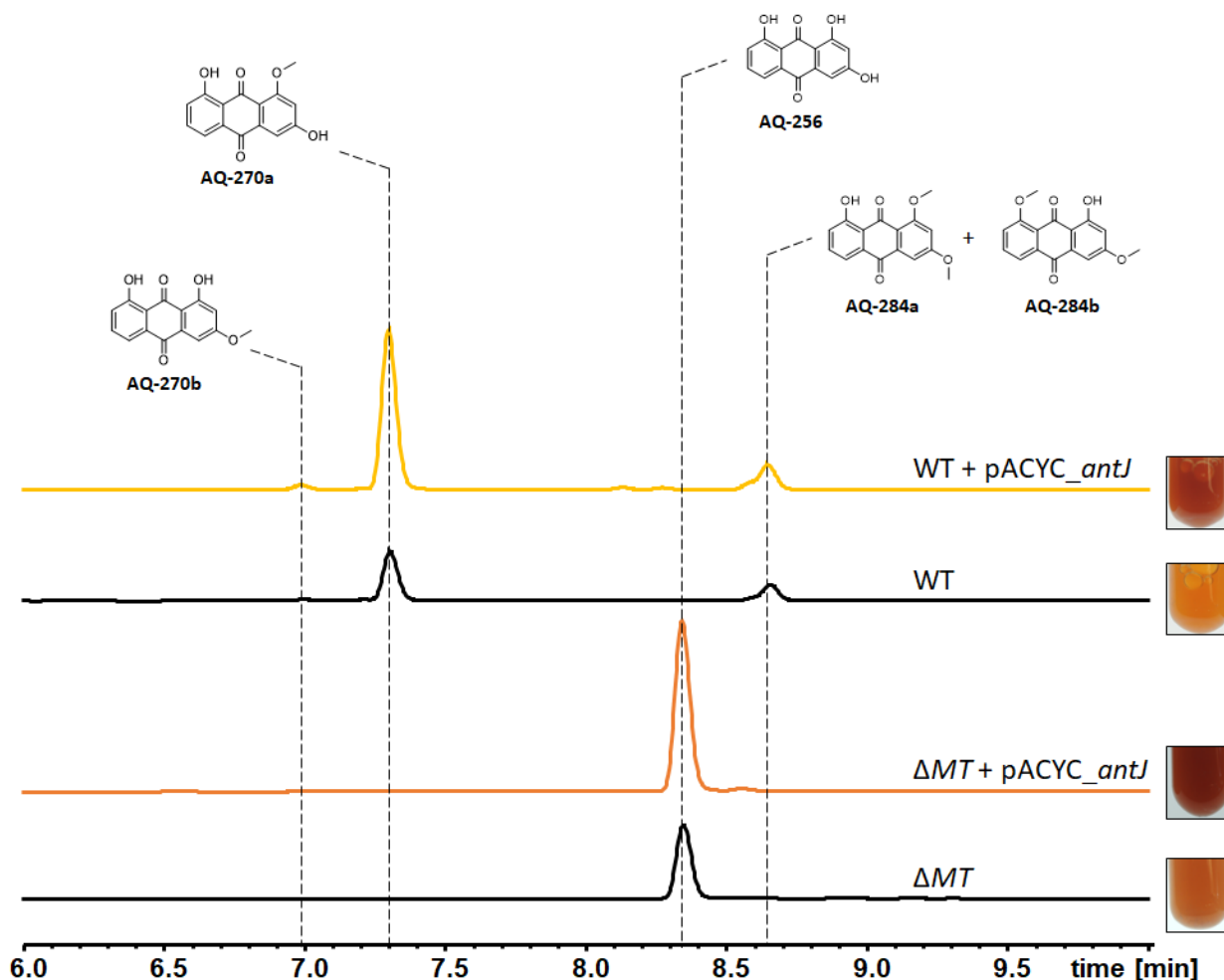


**Figure 24.** AQ production in *P. luminescens*. WT,  $\Delta$ MT strains in comparison to the respective strains overproducing the pathway-specific transcriptional regulator AntJ. Shown are HPLC-UV-chromatograms at 430 nm of EtAc extracts. All chromatograms are scaled equally. Cultures were cultivated for 72 h in LB broth at 30°C while being supplemented with the respective antibiotics and plasmid-based *antJ* overexpression was induced with 0.1 mM IPTG. Culture extracts of *P. luminescens* WT and  $\Delta$ MT in presence of the respective empty vector were analyzed as control (data not shown). The color of the respective cultures is depicted on the right. Dashed lines indicate the retention times of the respective AQ derivatives.

Clearly, the *antJ* overexpression resulted in a phenotypic change in both WT and  $\Delta$ MT as both strains displayed a more intense reddish color in comparison to their counterparts not overexpressing *antJ* indicating an increase in AQ production. As expected, the observation was confirmed by HPLC-UV analysis. In case of the WT overexpressing *antJ*, the relative amounts of AQ-270a were significantly increased in comparison to the control. Interestingly, relative AQ-270b and AQ-284a/b production was not elevated as drastically. Congruent with the WT,  $\Delta$ MT also showed a significant increase in AQ-256 production.

### 6.2.3 Construction of an AQ production platform

In the next step, the set of findings on AQ production increase, see above, were combined. Here, a deletion of *ngrA* was introduced in *P. luminescens*  $\Delta MT$  in combination with plasmid based *antJ* overexpression. Importantly, the Sfp-type PPTase NgrA, catalyzes secondary metabolite specific PCP/ACP-activation whereas its deletion leads to a loss of production of most PKS –and NRPS–derived NPs in *P. luminescens* resulting in higher malonate building block availability for AQ biosynthesis. Additionally, the *antJ* overexpression results in higher AQ productions levels (see chapter 6.2.2). Cultures were grown for 72 h at 30°C and expression was induced with 0.1 mM IPTG as described earlier. Results are shown in Fig. 25.

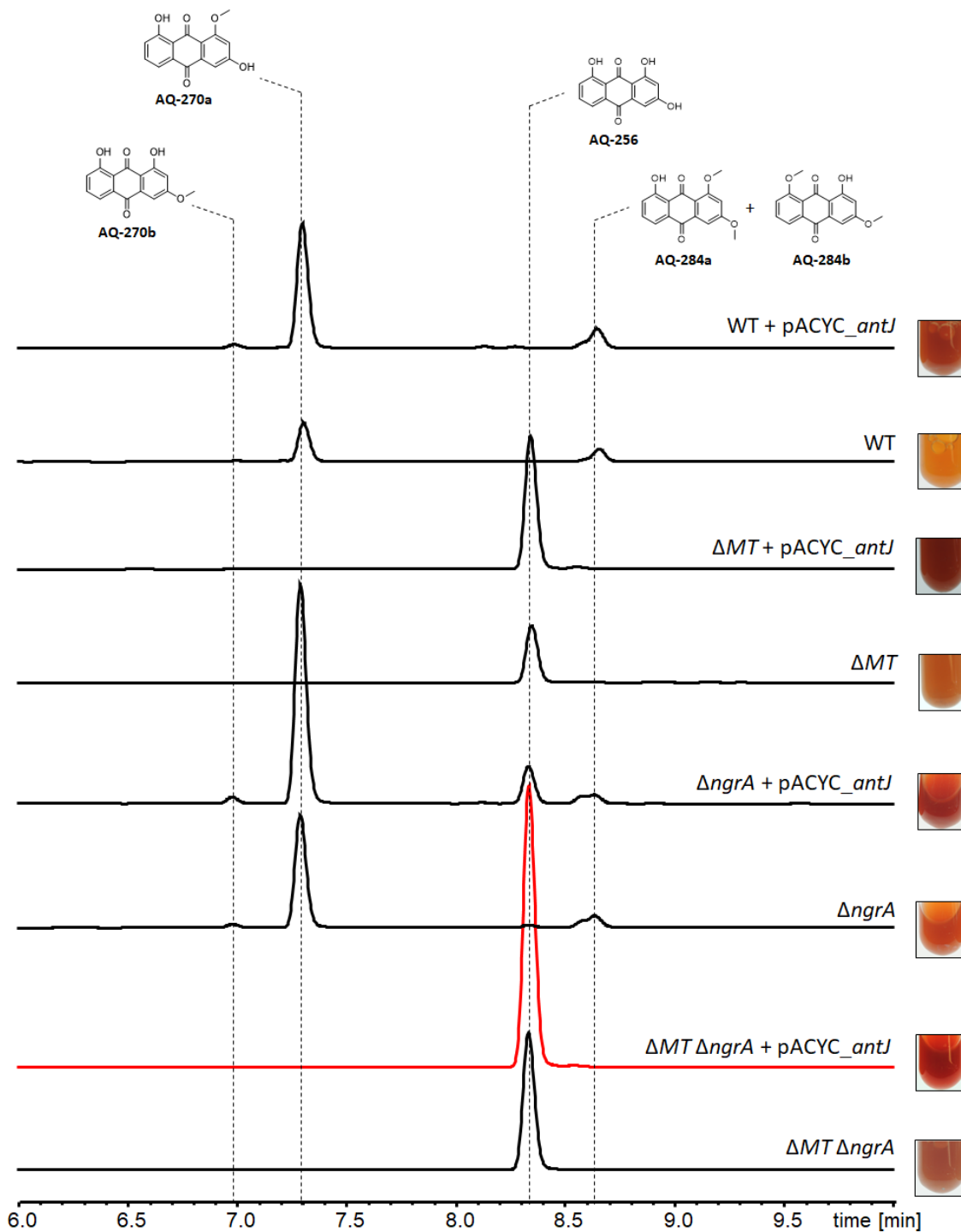


**Figure 25.** The combination of *ngrA* deletion and *antJ* overexpression impact on AQ production. Shown are HPLC-UV-chromatograms at 430 nm of EtAc extracts. All chromatograms are scaled equally. Cultures were cultivated for 72 h in LB broth at 30°C while being supplemented with the respective antibiotics and plasmid-based *antJ* overexpression was induced with 0.1 mM IPTG. Culture extracts of *P. luminescens* strains in presence of the empty vector were analyzed as control (data not shown). The color of the respective cultures is depicted on the right. Dashed lines indicate the retention times of the respective AQ derivatives.

Congruent to the findings in chapter 6.2.1, the  $\Delta MT \Delta ngrA$  strain showed a significant increase in AQ production in comparison to  $\Delta MT$ . Furthermore, plasmid based overexpression of *antJ*

in  $\Delta ngrA$  led to elevated AQ production as well. Finally, the combination of both approaches resulted in a significant increase in AQ levels in  $\Delta MT \Delta ngrA$  overexpressing *antJ* in comparison to all other AQ producing *Photobacterium* strains. In the next step, AQ-256 production in all strains was quantified relatively (Fig. 26).

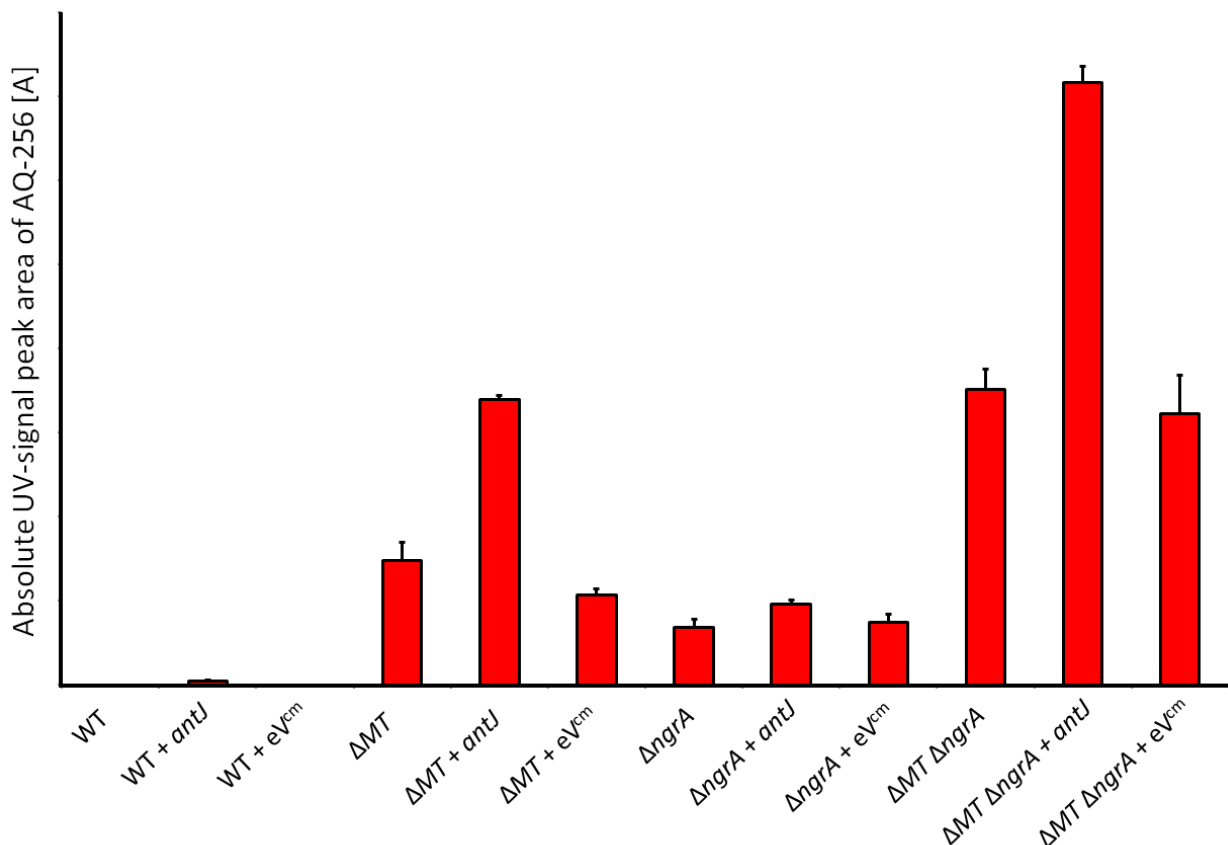


**Figure 26.** Relative quantification of AQ-256 in *P. luminescens* WT,  $\Delta MT$ ,  $\Delta ngrA$ ,  $\Delta MT \Delta ngrA$  and the respective strains additionally overproducing AntJ. Cultures were cultivated for 72 h in LB broth at 30°C while being supplemented with the respective antibiotics and plasmid-based *antJ* overexpression was induced with 0.1 mM IPTG. Culture extracts of *P. luminescens* strains in presence of the empty vector (eV) were analyzed as control. Error bars represent SD of three independent biological replicates.

When comparing relative AQ-256 production in  $\Delta MT$  background, overexpression of *antJ* led to UV-signal peak area increase of 3.2-fold. Similarly, the deletion of *ngrA* in  $\Delta MT$  resulted in an increase of 2.5-fold. Finally, plasmid based overexpression of *antJ* in *P. luminescens*  $\Delta MT \Delta ngrA$  led to an elevation of AQ-256 production by 6.6-fold in comparison to  $\Delta MT$ . Finally, especially for industrial applications, it is of major importance to quantify production titers. For this purpose, a calibration curve was generated for AQ-256 (Fig. 27).

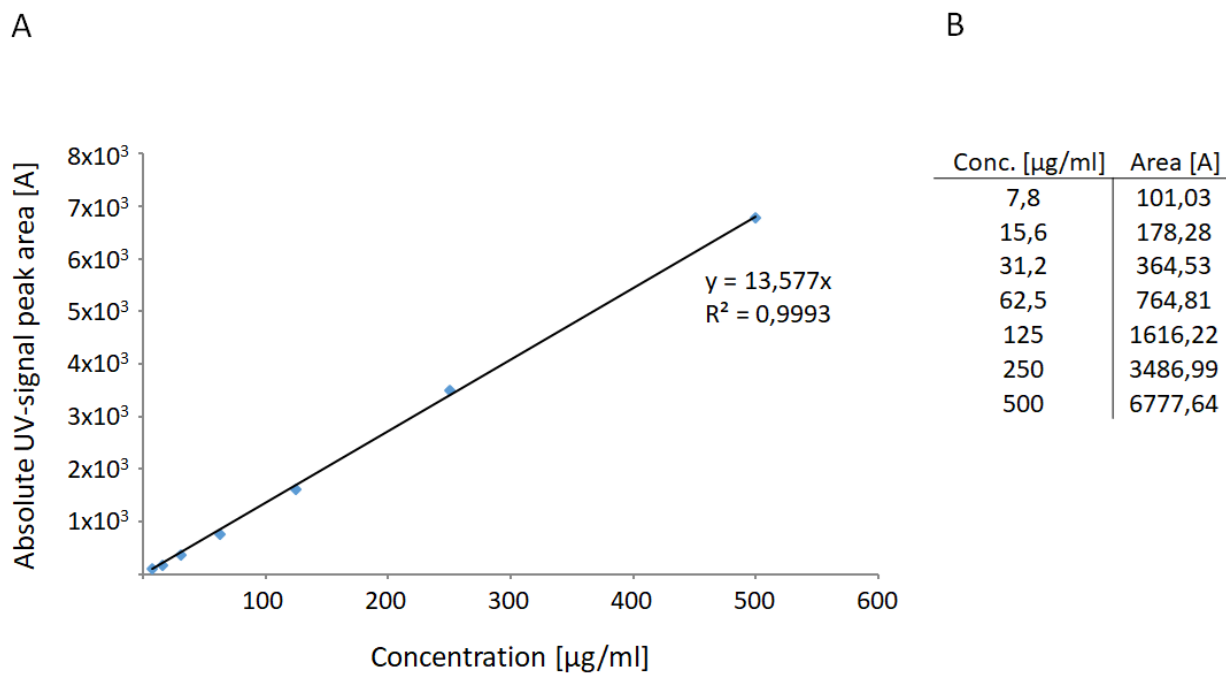


**Figure 27.** Calibration curve for absolute AQ-256 quantification (A). Exact data is depicted in (B). AQ-256 standards were generated from isolated and purified AQ-256 which was subjected to HPLC-MS analysis.

Here, 3 l of *P. luminescens*  $\Delta MT \Delta ngrA + pACYC\_antJ$  was cultivated for 72 h at 30°C. Compound extraction was performed as described earlier. Purification was conducted using a Sephadex LH-20 (MeOH, 25-100 µm, Pharmacia Fine Chemical Co. Ltd.) size-exclusion chromatography. After HPLC-MS analysis of the collected fractions, AQ-256 was purified in an additional chromatographic step using an Agilent 1260 Semiprep LC system coupled to a G6125B LC/MSD ESI-MS (Agilent). A 75% isocratic ACN-H<sub>2</sub>O gradient was applied over 16 min on a Cholesterol column (1.0 mm ID x 250 mm, COSMOSIL) with a flowrate of 3 ml/min with a final yield of 350 mg. Finally, the purity was confirmed by HPLC-UV (data not shown). Subsequently, the absolute AQ-256 production was quantified (Fig. 28).

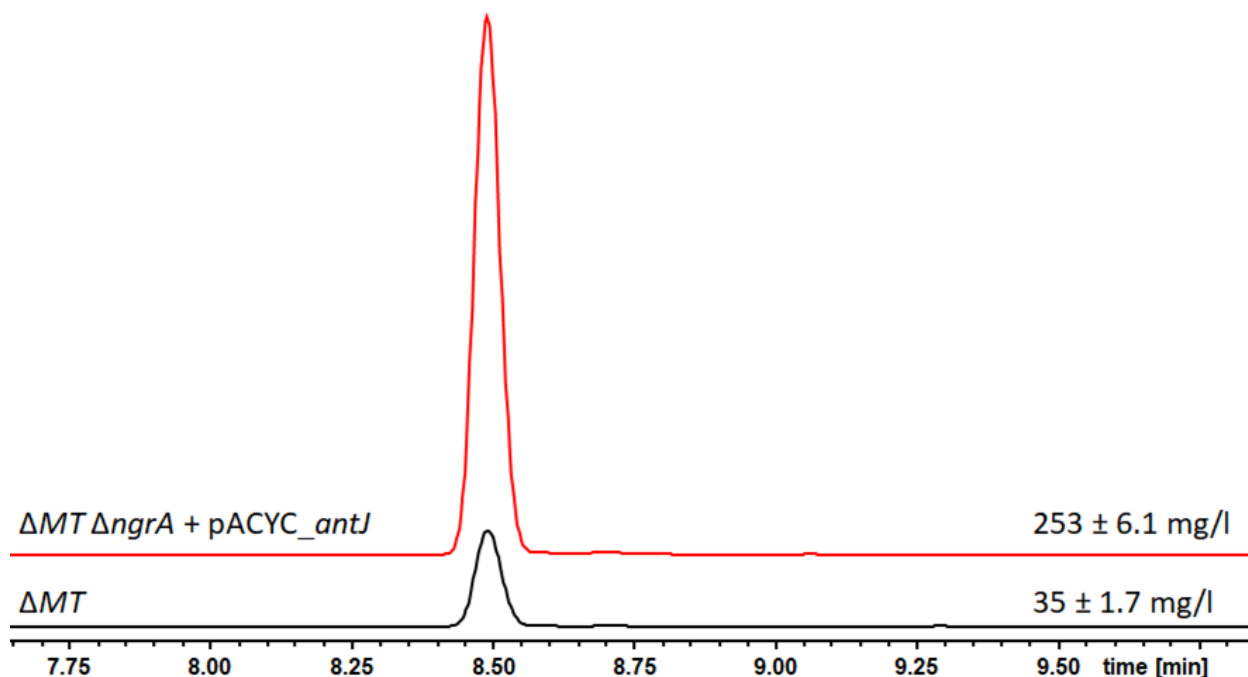


**Fig. 28.** Absolute quantification of AQ-256 amounts in *P. luminescens*  $\Delta MT$  strain and  $\Delta MT \Delta ngrA$  strain overexpressing *antJ*. Shown are HPLC-UV-chromatograms at 430 nm of EtAc extracts. All chromatograms are scaled equally. Cultures were cultivated in LB broth for 72 h at 30°C while being supplemented with the respective antibiotics. Plasmid-based overexpression of *antJ* was induced with 0.1 mM IPTG. Culture extracts of *P. luminescens* strains in presence of the empty vector were analyzed as control (not shown). For absolute quantification of AQ-256 levels, the calibration curve (Fig. 27) was used.  $\pm$  SD of three independent biological replicates was calculated.

As depicted,  $\Delta MT \Delta ngrA$  overexpressing *antJ* was able to produce 253 mg/l AQ-256 which accounts for an increase by 7.2 fold.

#### 6.2.4 Monooxygenase plu0947 supports AQ formation

Transcriptome analysis revealed that the monooxygenase (MO) plu0947 is significantly downregulated in *P. luminescens*  $\Delta antJ^{37}$ . These findings suggested that the MO might be involved in AQ biosynthesis, specifically, the introduction of the quinone oxygen. Additionally, the upstream region of *plu0947* encodes a putative MarR-family transcriptional factor plu0948 with a wHTH-DNA-binding domain that was also downregulated in absence of AntJ. Interestingly, neither upstream region of *plu0947* or *plu0948* encodes the specific AntJ-binding site that was identified in previous work.<sup>77</sup> Consequently, the effect of the MO on AQ production levels was investigated (Fig. 29). Deletions were conducted in frame.



A



B

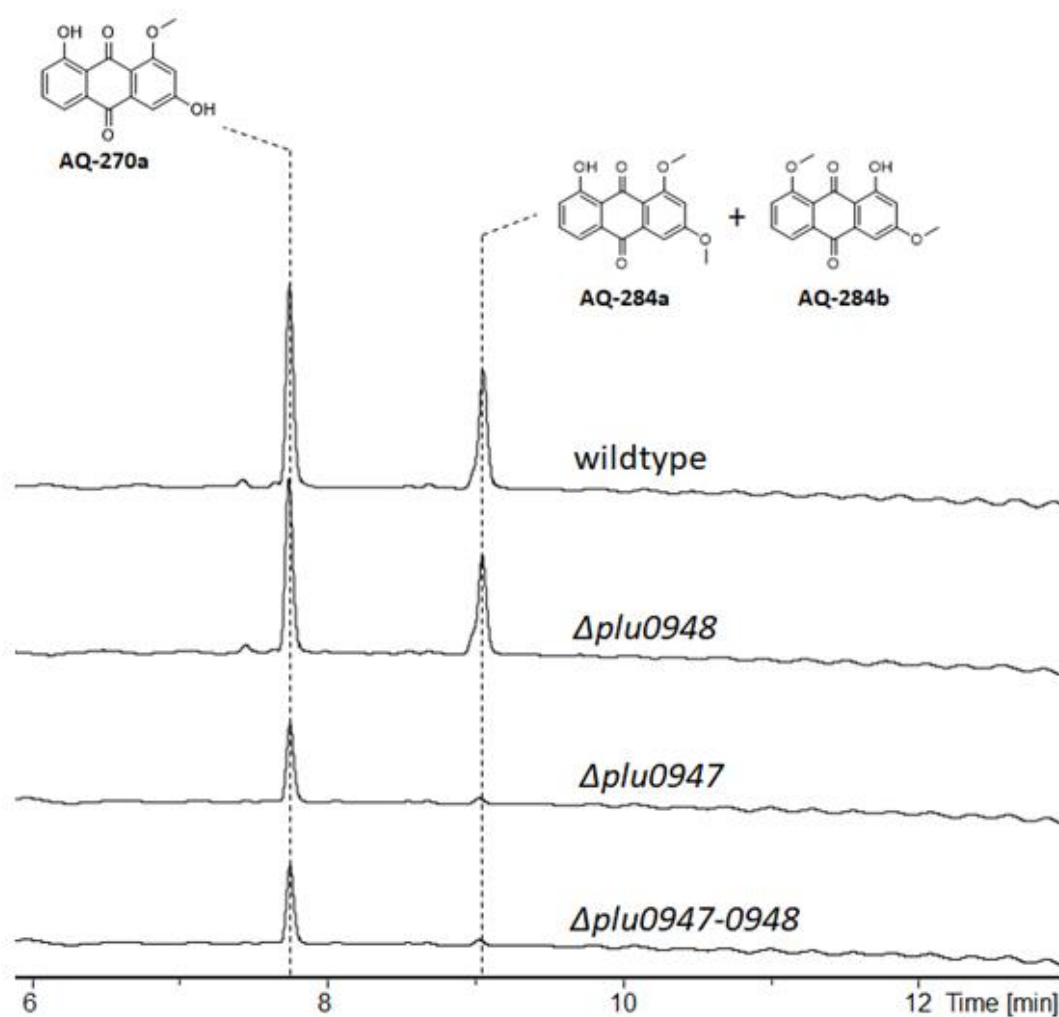


**Fig. 29.** (A) Gene locus of *plu0948-0947*. Promoters are indicated as arrows while ribosome binding sites are displayed as semicircles. (B) Impact of the monooxygenase *plu0947* and the putative transcriptional factor *plu0948* on AQ product formation. Shown are HPLC-UV-chromatograms at 430 nm of EtAc extracts. All chromatograms are scaled equally. Cultures were cultivated for 72 h in LB broth at 30°C. Dashed lines indicate the retention times of the respective AQ derivatives.

While the deletion of the putative transcription factor *plu0948* had no effect on AQ levels in *P. luminescens*  $\Delta$ *plu0948*, the deletion of *plu0947* resulted in a significant decrease of AQ levels. Interestingly, the production of AQ-284 derivatives was stronger downregulated than the production of AQ-270a. Additionally, plasmid complementation of *plu0947* with pACYC\_ *plu0947* was able to restore AQ production in the  $\Delta$ *plu0947* strain (data not shown). As these findings suggested that *plu0947* is indeed involved in AQ biosynthesis, an attempt was made to increase AQ production by overexpression of *plu0947*. For this purpose, *plu0947* was cloned on a pACYC expression vector under the control of an IPTG inducible  $P_{tac}$  (Fig. 30).

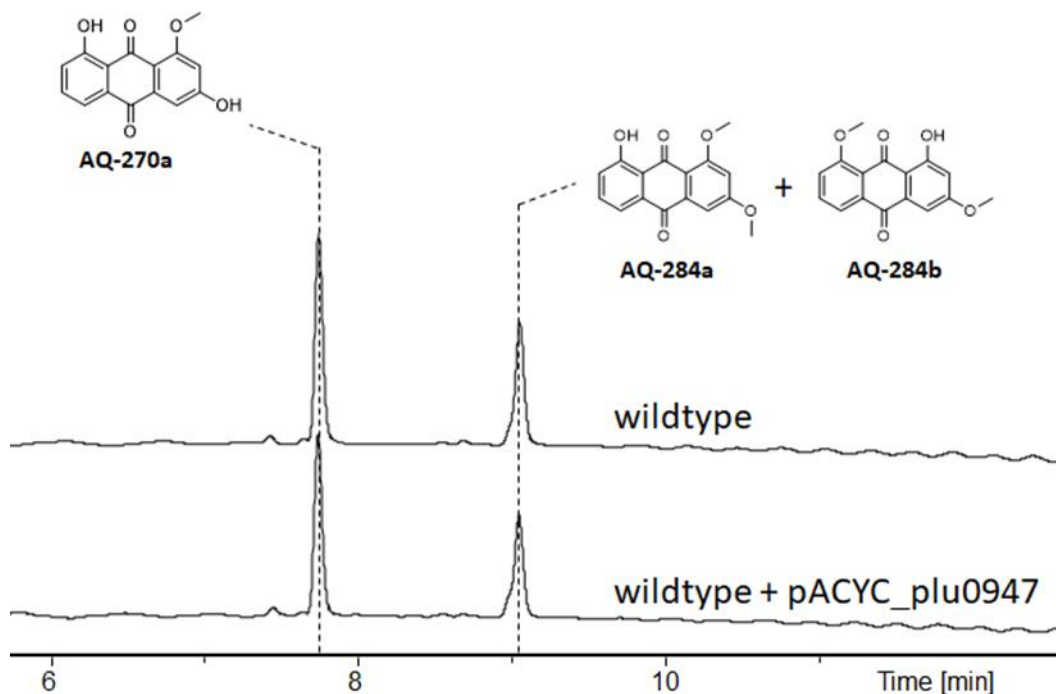


**Fig. 30.** Impact of MO *plu0947* overexpression on AQ product formation. Shown are HPLC-UV-chromatograms at 430 nm of EtAc extracts. All chromatograms are scaled equally. Cultures were cultivated for 72 h in LB broth at 30°C. Dashed lines indicate the retention times of the respective AQ derivatives.

Unfortunately, while *plu0947* seems to be involved in AQ product formation, its overexpression did not increase AQ production in the wildtype.

### 6.2.5 Establishing a suitable NP production medium

In this chapter, the development of a NP production medium suitable for *Photorhabdus* is described. Crucially, we wanted to establish a cost-efficient production medium and moreover being compatible and consistent with environment conservation guidelines. For this reason, major parts of the media contents were taken from recyclable waste products. Media screenings were conducted in cooperation with Jan Burkhardt, AG Czermak, THM. Preliminary data<sup>153</sup> suggested that XPP medium allows compound extraction with considerably low background in comparison to LB and additionally, production titers of certain NPs are increased. Thus, XPP medium was used as the basis for media generation. In a first step, the amino acid contents of XPP medium were investigated on their positive and negative effects on AQ production in *P. luminescens*. Here, a two-staged factorial design was chosen whereas the lower stage is represented by the absence of the respective amino acid. As the upper stage, 0.1 g/l of the respective amino acid was supplemented. A significance model ( $p < 0.05$ ) was chosen. Two different t-limits were plotted. The highest limit was based on the Bonferroni limit. The lower limit was based on standard t-critical for individual effects tests. The screening identified arginine, histidine, cysteine, isoleucine, phenylalanine, methionine and valine as significant positive effects. Additionally, glutamine was identified as a negative effect on AQ production. In the following step, the two-staged factorial design was applied to screen the vitamins and trace elements used in XPP medium. The screening showed that only thiamine and pantothenic acid had a positive effect on AQ-256 production. Consequently, in subsequent experiments, the contents of XPP medium were reduced to the respective amino acids, vitamins and trace elements (described in section 5.3.1). The plots were generated and analyzed with Design-Expert 12 (Stat-Ease, Minneapolis, USA) by Jan Burkhardt and are shown in supplementary information. In the following, the productivity of *P. luminescens*  $\Delta MT \Delta ngrA$  overexpressing *antJ* was compared in LB, generic XPP medium and improved XPP medium (shown in Table 20).

**Table 20:** AQ production of *P. luminescens*  $\Delta MT \Delta ngrA$  + pACYC\_ *antJ* in different media.

Medium	OD <sub>600</sub>	AQ-256 [mg/l]
LB	12.8 ± 1.7	253 ± 6.1
XPP medium	12.2 ± 3.2	195 ± 10.5
Improved XPP medium	13.5 ± 1.4	244 ± 4.9

Ultimately, the AQ-256 production in the improved version of XPP medium was increased by 25% over the generic version, reaching LB-level titers.

### 6.2.6 Insect media screening

In preliminary work, the influence of simulating the insect host environment was assayed for alterations on NP production<sup>154</sup>. It was shown, that supplementing insect homogenate from *Galleria mellonella* larvae to LB cultures altered the NP profile of *P. luminescens*. Crucially, NPs like AQs and isopropylstilbene (IPS) were overproduced. Unfortunately, *Galleria mellonella* larvae do not live on waste products, they are costly and thus not suited for generating an inexpensive NP production medium. In an extensive literature research, two insect candidates were identified that are cost efficient to obtain and part of industrially recyclable waste products. Firstly, the black soldier fly (*Hermetia illucens*) is an insect that can be grown and harvested without dedicated facilities and is not pestiferous<sup>88</sup>. Importantly, their biggest advantage over other insects is their ability to convert organic waste into food, generating value and closing nutrient loops as they reduce pollution and costs. Secondly, the silkworm (*Bombyx mori*) is industrially used for silk production. However, after entering pupal phase, the silk cocoons are harvested while the silkworms remain as leftovers. In the following step, NP production was carried out in XPP insect media that contain the improved version of XPP medium described in chapter 5.3 supplemented with 1% (w/v) insect powder obtained from *Bombyx mori* or *Hermetia illucens* insects (Fig. 34). In the screening, *P. luminescens* was used and the NP profile of selected NPs was analyzed.

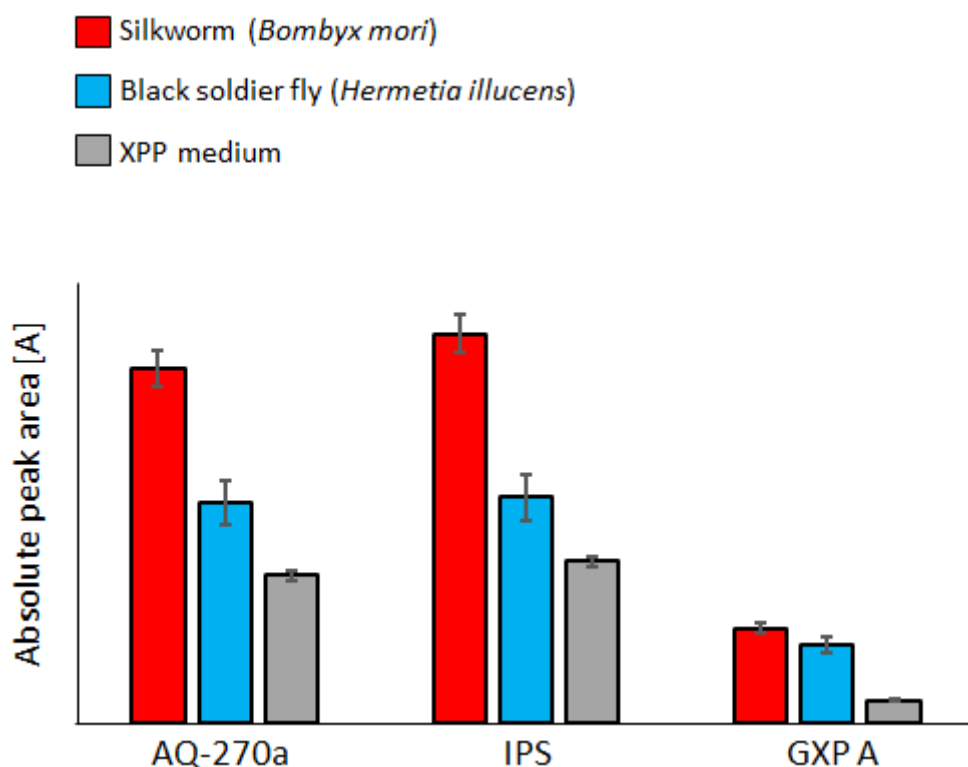


**Fig. 34.** Screening of different XPP-insect media. Improved XPP medium was used as basis whereas glycerol was substituted for 1% (w/v) insect powder (red= *Bombyx mori*, blue= *Hermetia illucens*) as described earlier. *Photorhabdus luminescens* TT01 cultures were grown for 72h at 30°C and supplemented with 2% XAD-16. Relative NP production was compared by absolute peak area [A] comparison of the respective compounds. Cultures grown in LB were used as a control. Error bars represent SD of three independent biological replicates.

Both XPP insect media resulted in a higher production of the selected NPs in comparison to generic XPP medium with glycerol. In case of the XPP medium supplemented with powder from *Hermetia illucens*, the production of GameXPeptide A (GXP A) was increased by 3.4-fold. Additionally, the IPS production and AQ-270a production was increased by 1.4-fold and 1.5-fold, respectively. Furthermore, insect powder from *Bombyx mori* resulted in an increase in production by GXP A by 4.1-fold whereas AQ-270a and IPS production titers were elevated 2.4-fold and 2.5-fold, respectively. Consequently, insect powder obtained from *Bombyx mori* was used for subsequent experiments.

### 6.2.7 Absolute quantification of AQ production platform in novel XPP insect medium

In the next step, the AQ-256 production of *P. luminescens*  $\Delta MT \Delta ngrA + pACYC\_antJ$  was tested in the improved version of XPP medium containing the necessary amino acids, vitamins

and trace elements described in chapter 5.3.1 in addition to insect powder obtained from *Bombyx mori* (Fig. 35). Additionally, the cultures were supplemented with 4% XAD-16 to bind secreted AQ-256 from the medium. Beads were continuously harvested with a sterile filter and added freshly to the medium over 72 h every 24 h.

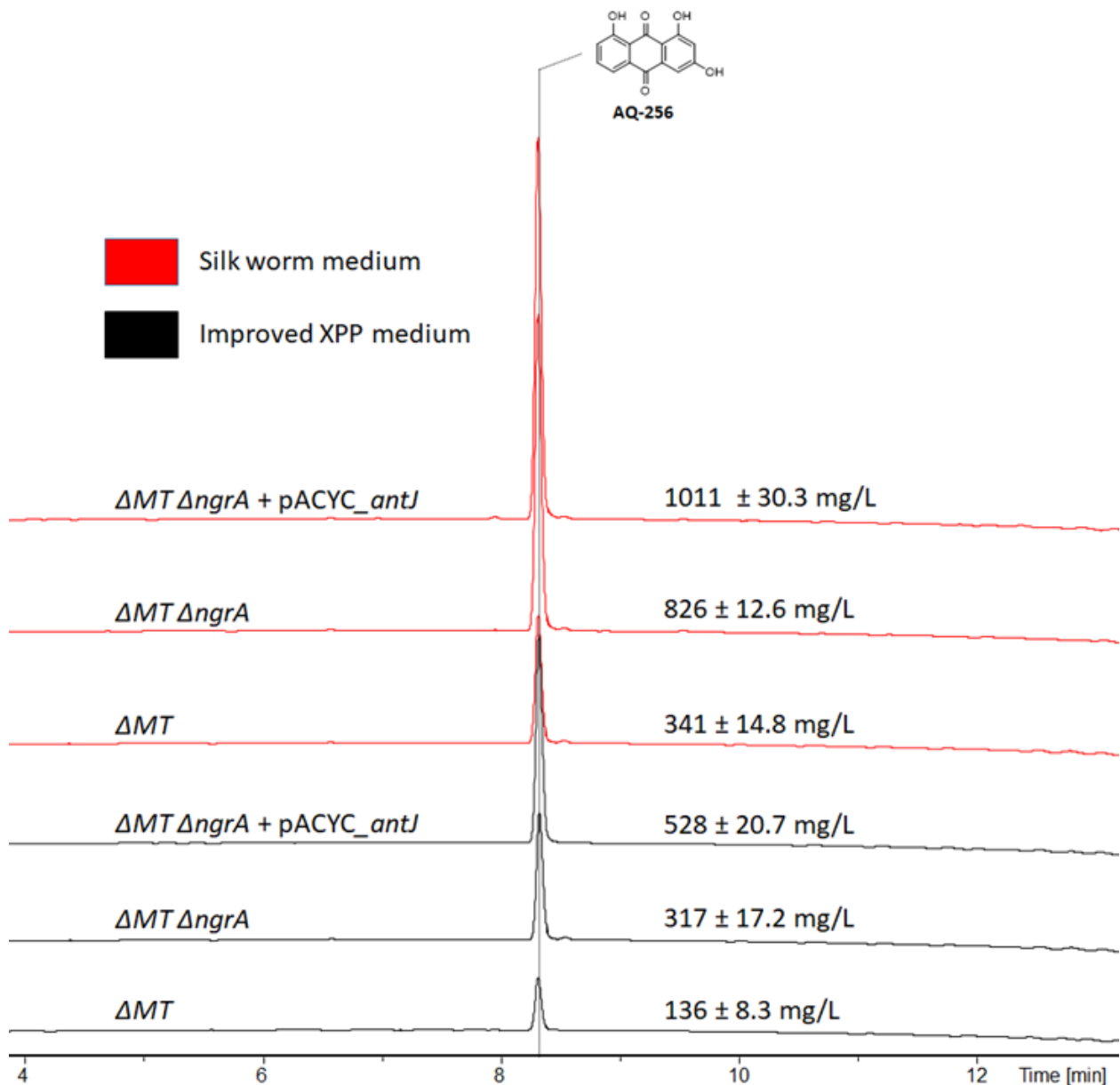


**Fig. 35.** Absolute quantification of AQ-256 amounts in *P. luminescens*  $\Delta MT$ ,  $\Delta MT \Delta ngrA$  and  $\Delta MT \Delta ngrA$  strain overexpressing *antJ*. Shown are HPLC-UV-chromatograms at 430 nm of EtAc extracts. All chromatograms are scaled equally. Cultures were either cultivated in improved XPP medium or XPP-insect medium for 72 h at 30°C while being supplemented with the respective antibiotics. Cultures were supplemented with 4% XAD-16 and extraction of AQ-256 was carried out as described earlier. Plasmid-based overexpression of *antJ* was induced with 0.1 mM IPTG. Culture extracts of *P. luminescens* strains in presence of the empty vector were analyzed as control (not shown). For absolute quantification of AQ-256 levels, the calibration curve (Fig. 27) was used.

In improved XPP medium, the extraction method already increased the AQ-256 yield by 2.34-fold to a total production titer of 528 ± 20.7 mg/l. Ultimately, when using the XPP silkworm medium, a AQ-256 production of 1011 ± 30.3 mg/l was achieved in  $\Delta MT \Delta ngrA + pACYC\_antJ$  reaching industrial scale production titers. A final comparison of the used media is displayed

in Table 21. The final OD<sub>600</sub> in Silkworm XPP medium could not be measured because of the high turbidity of the medium.

**Table 21:** AQ production of *P. luminescens*  $\Delta MT \Delta ngrA$  + pACYC\_ *antJ* in different media.

Medium	OD <sub>600</sub>	AQ-256 [mg/l]
LB	12.8 ± 1.7	253 ± 6.1
XPP medium	12.2 ± 3.2	195 ± 10.5
Improved XPP medium	13.5 ± 1.4	244 ± 4.9
Improved XPP medium (4% XAD-16)	12.9 ± 0.6	528 ± 20.7
Silkworm XPP medium	-----	1011 ± 30.3



### **6.3 Topic C: Elucidation of a putative terpenoid cluster in *Photorhabdus***

Within its complex life cycle, *Photorhabdus* produces an array of NPs, which exhibit various functions such as nematode development, protection against the prey's defensive immune response or mediate cell-cell communication<sup>9</sup>. These NPs are produced via activation of certain BGCs in distinct stages of their life cycle. Often, the induction of these BGCs is mediated by external environmental factors while they remain silent under laboratory conditions<sup>96</sup>. Here, I describe the elucidation of a silent BGC that was assumed to be putatively involved in terpenoid biosynthesis in *Photorhabdus*.

#### **6.3.1 BGC putatively involved in terpenoid biosynthesis in different *Photorhabdus* species**

A combination of antiSMASH and blastP analysis revealed the presence of a highly conserved BGC in several *Photorhabdus* species predicted to be responsible for terpenoid biosynthesis. Interestingly, upstream of the BGC, a gene putatively encoding a carotenoid oxygenase protein is located (Fig. 36). Transcriptome analysis revealed that the BGC remains silent under laboratory conditions (unpublished data).

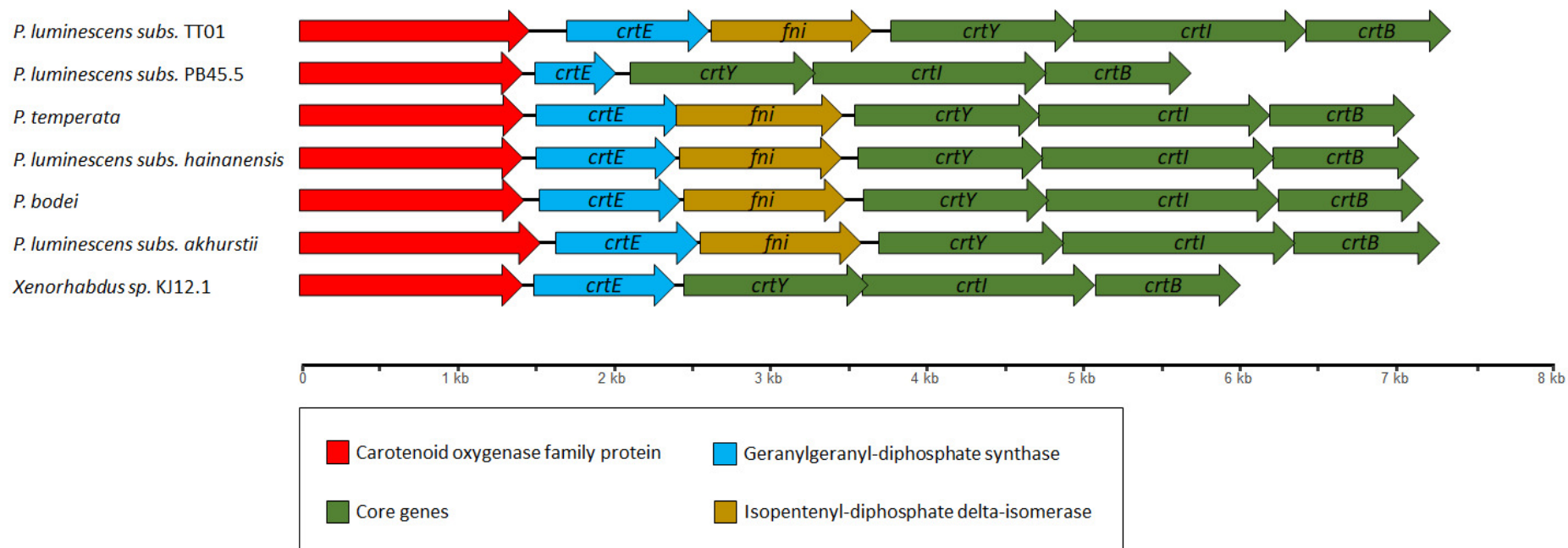


**Fig. 36.** Overview of the biosynthetic gene clusters that are assumed to be involved in terpenoid biosynthesis in different *Photorhabdus* and *Xenorhabdus* strains. Genes required for terpenoid core production *crtY*, *crtI*, *crtB* are displayed in green, genes encoding a geranylgeranyl-diphosphate synthase *crtE* and an isopentenyl-diphosphate-isomerase *fni* are depicted in blue and yellow, respectively. Additionally, an expected carotenoid oxygenase family protein is displayed in red.

The highly conserved BGC consists of six genes. Three genes, *crtY*, *crtI* and *crtB*, are predicted to compose the terpenoid core genes assumed to be responsible for production of a terpenoid core structure (displayed in green, Fig. 36). Additionally, *crtE* and *fni* putatively encode a geranylgeranyl-diphosphate synthase and an isopentenyl-diphosphate delta-isomerase, respectively, which are both involved in late steps of the 2-C-methyl-D-erythritol 4-phosphate (MEP) pathway for terpenoid building block generation<sup>155</sup>. Finally, upstream of all depicted BGCs, a gene predicted to encode a carotenoid oxygenase family protein is located. Interestingly, *P. luminescens subsp.* PB45.5 is missing *fni* encoding the isopentenyl-diphosphate delta-isomerase. Additionally, *crtE* is truncated.

### 6.3.2 Establishing a platform for carotenoid core production

As transcriptome analysis revealed that the carotenoid cluster is not expressed under laboratory conditions, an attempt was made in order to activate the cluster *in vivo*. For this purpose, an arabinose-inducible *P<sub>Bad</sub>* promoter was inserted in front of the gene cluster upstream of the putative carotenoid oxygenase in *P. luminescens* TT01. Unfortunately, no compound was produced upon cultivation (data not shown). In a recent publication<sup>149</sup>, it was shown that an engineered *E. coli* BL21 strain is able to produce lycopene through a combination of plasmid-based and genomic expression of different pathways. Firstly, the strain harbors the genes encoding the mevalonate pathway (MEV pathway) for overproduction of isoprenoid building blocks on its genome. Secondly, the genes for lycopene biosynthesis were introduced in a plasmid-based approach. As this strain presented a promising platform to elucidate the NPs produced by the putative terpenoid cluster from *Photorhabdus*, it was kindly obtained from the authors. The genomic integration of the MEV pathway is displayed in Fig. 37.

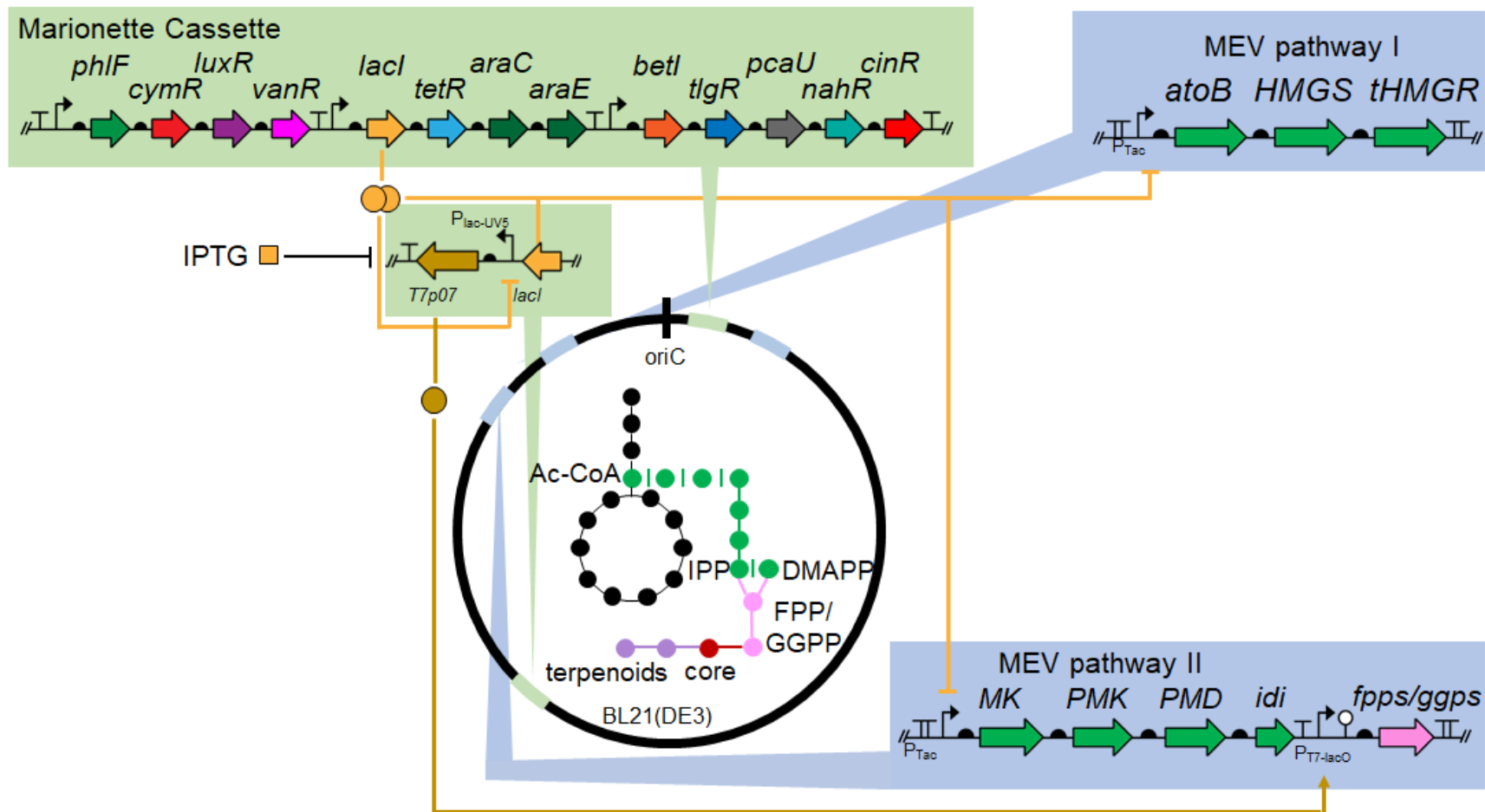


**Fig. 37** Introduction of the MEV pathway into the genome of *E. coli* BL21. In addition to the pathway specific genes, the strain was engineered with the Marionette cassette<sup>149</sup> which allows improved promoter control. The strain was obtained from the authors<sup>149</sup>. Figure adapted from Prof. Dr. Eric Helfrich, Goethe University, Frankfurt.

The MEV pathway encoding genes are split into two separate parts and under the control of IPTG inducible  $P_{tac}$  promoters. Additionally, the genome harbors the marionette cassette, which consists a set of regulator genes for tight control of several different types of promoters allowing well-directed genetic control<sup>149</sup>.

### **6.3.3 Expression of terpenoid core genes and structure elucidation of the product**

In the first step, the product of the carotenoid core genes was investigated. For this purpose, the three predicted core genes were cloned on a pACYC expression vector under the control of an arabinose inducible  $P_{Bad}$  promoter. In addition, *crtE* and *fni* putatively encoding a geranylgeranyl-diphosphate synthase and an isopentenyl-diphosphate delta-isomerase were cloned on a pCOLA expression vector under the control of an arabinose inducible  $P_{Bad}$  promoter. Subsequently, the plasmids were transformed into *E. coli* BL21 (DE3) Marionette. Cultivation was carried out for 72 h in LB at 30°C. Results of the HPLC-UV analysis are depicted in Fig. 38.

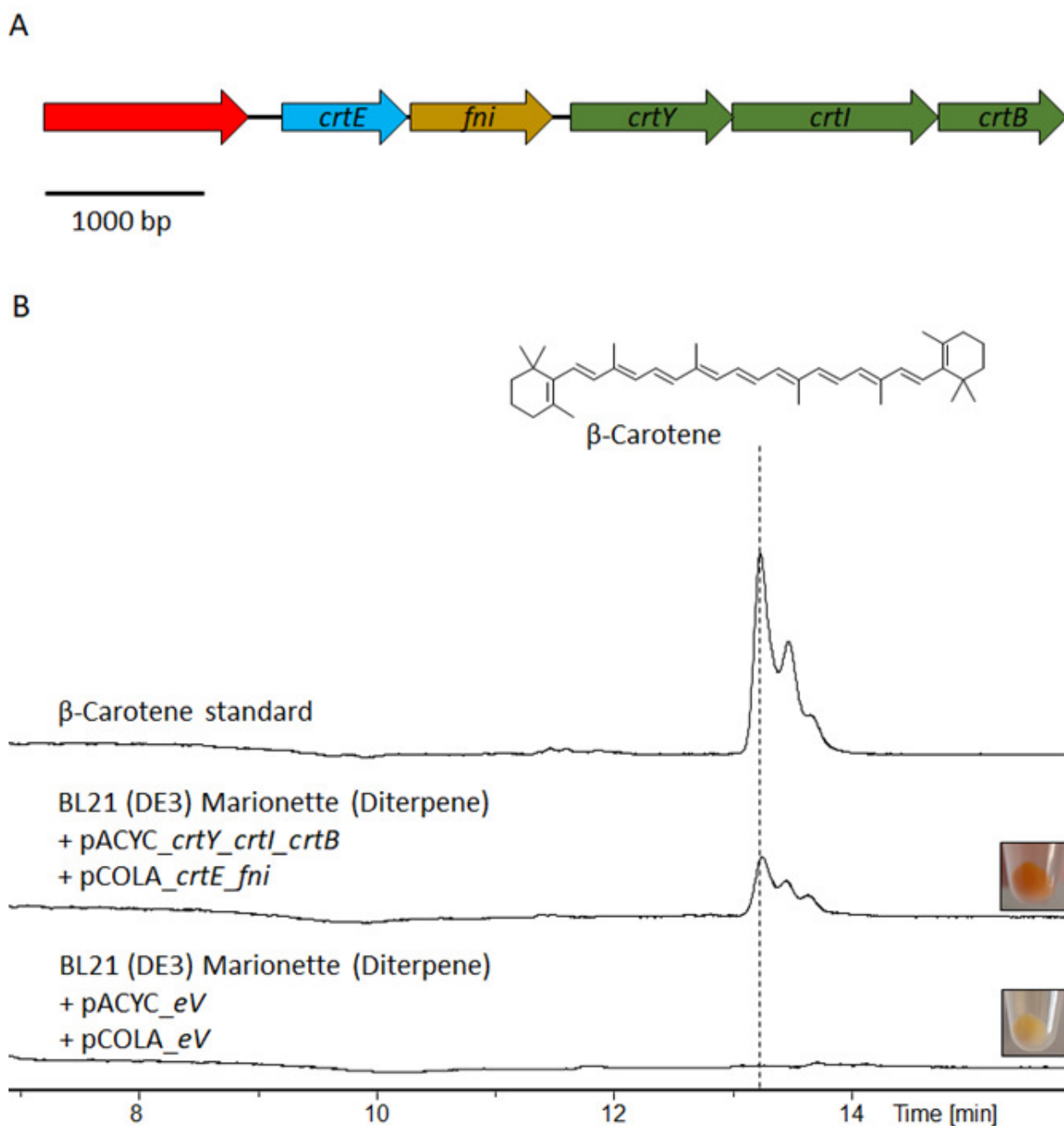


**Fig. 38.** (A) Terpenoid cluster from *P. luminescens* subs. TT01. (B) Production of  $\beta$ -carotene from core gene expression in *Escherichia coli* BL21 (DE3)-Marionette-diterpene. Shown are HPLC-UV-basepeak-chromatograms ranging from 100-800 nm of MeOH/ $\text{CHCl}_3$  extracts. All chromatograms are scaled equally. Cultures were cultivated for 72 h in LB broth at 30°C while being supplemented with the respective antibiotics and gene expression was induced with 0.2% arabinose and 0.1 mM IPTG, respectively. Empty vector cultures were analyzed as control. The color of the respective cell pellet is depicted on the right. Dashed lines indicate the retention times of the respective carotenoid.

Upon expression of the carotenoid core, a UV signal at 13.2 min appeared with a maximum absorbance at 452 nm. In addition, the strain exhibited a phenotypic shift with compound production as the color of the cells changed from yellow to deep orange. Subsequently, the

compound was isolated, purified and finally elucidated in detailed 1D –and 2D NMR experiments as described in Material and Methods, section 5.4. Additionally, as the NMR experiments revealed the compound as  $\beta$ -carotene, a commercially available standard was purchased, confirming the elucidated structure. Signal tailoring occurred due to UV-light induced *cis/trans* isomeric shifts.

### 6.3.4 Carotenoid oxygenase activity on $\beta$ -carotene

In the next step, the role of the predicted carotenoid oxygenase was investigated. Here, similarly, the oxygenase-encoding gene was cloned on a pCDF expression vector under the control of an arabinose inducible  $P_{Bad}$  promoter. Subsequently, the plasmid was transformed into the *E. coli* BL21 (DE3) Marionette  $\beta$ -carotene production strain containing pACYC\_ *crtY\_crtI\_crtB* and pCOLA\_ *crtE\_fni* (Fig. 39).

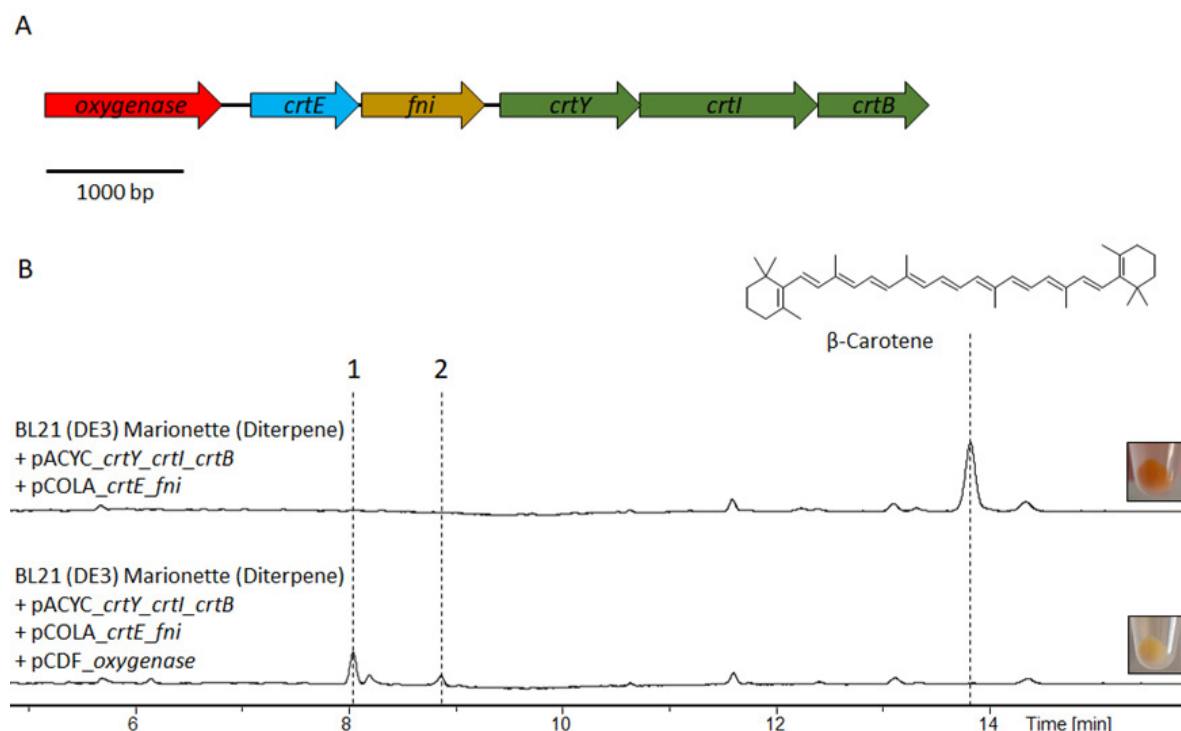


**Figure 39.** (A) Terpenoid cluster from *P. luminescens* subs. TT01. (B) Production of two new compounds through oxygenase activity in *Escherichia coli* BL21 (DE3) Marionette (Diterpene) producing  $\beta$ -carotene. Shown are HPLC-UV-basepeak-chromatograms ranging from 100-800 nm of MeOH/ $\text{CHCl}_3$  extracts. All chromatograms are scaled equally. Cultures were cultivated for 72 h in LB broth at 30°C while being supplemented with the respective antibiotics and gene expression was induced with 0.2% arabinose and 0.1 mM IPTG, respectively. Culture extracts in presence of the empty vectors were analyzed as control (data not shown). The color of the respective cultures is depicted on the right. Dashed lines indicate the retention times of the respective compounds.

The expression of the oxygenase led to two new UV signals (1 and 2) at 8.1 with  $m/z$  259.205  $[M+H]^+$  and 8.9 min with  $m/z$  311.236  $[M+H]^+$ , respectively. Furthermore, the signal corresponding to  $\beta$ -carotene was only detectable in very low amounts, indicating its further modification. Congruently, a phenotypical shift was observed as the deep orange color exhibited by  $\beta$ -carotene changed back to the original yellow color.

Additionally, the oxygenase activity on  $\beta$ -carotene was visualized by electron microscopy (Fig. 40). Pictures were taken in cooperation with Dr. Christoph Spahn, AK Bode, Goethe University, Frankfurt.

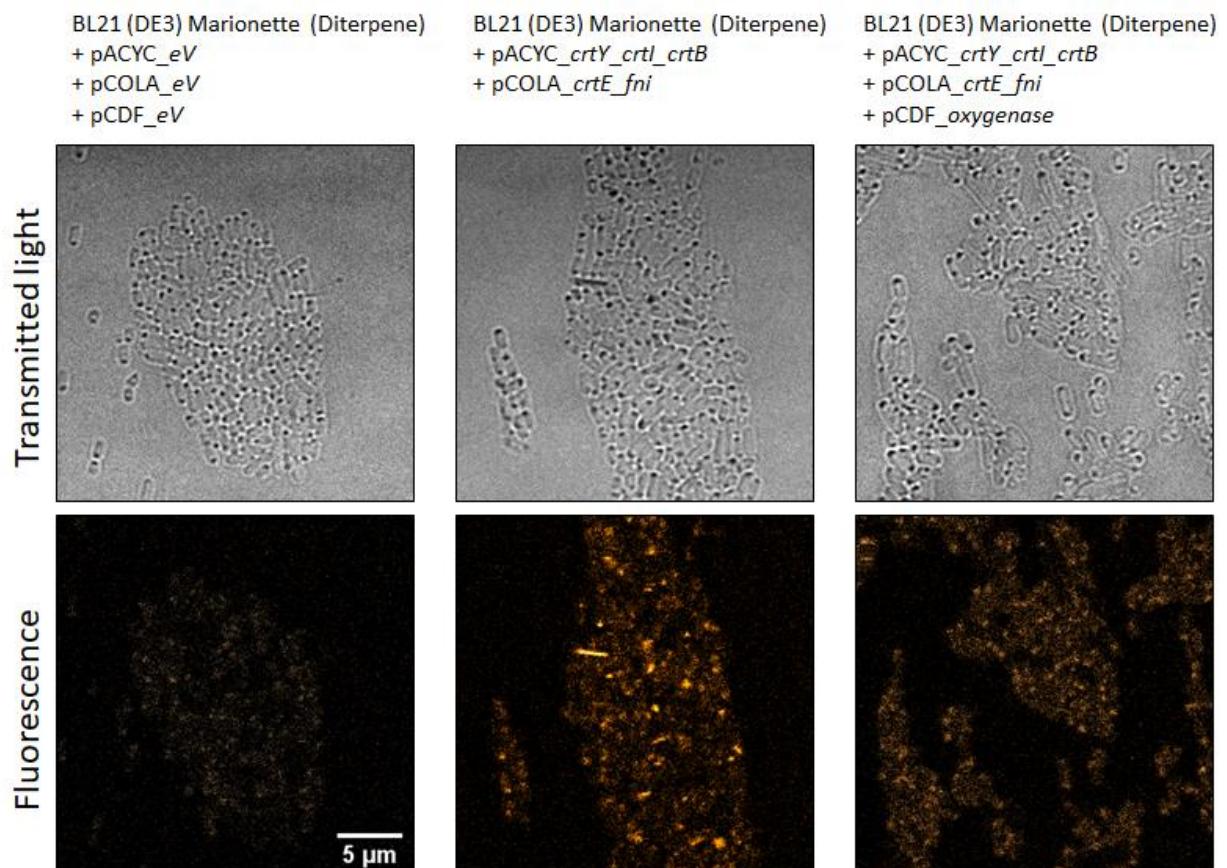


**Figure 40.** Visualization of oxygenase activity in *Escherichia coli* BL21 (DE3) Marionette (Diterpene). Imaging was performed with 10% 514 nm laser and 520 – 650 nm emission window. Notch filter was crucial to reduce background by reflected laser light.

As expected, the  $\beta$ -carotene produced through core gene expression is visible at 514 nm excitation. Interestingly, the signals for  $\beta$ -carotene were mostly detectable in polar cell bodies as no clear membrane localization was observed. In accordance with the HPLC-UV findings, the fluorescence at 514 nm was reduced drastically in cells expressing the carotenoid



oxygenase. Finally, *E. coli* (DE3) BL21 carrying the empty vector controls did not show any fluorescence.

### 6.3.5 Structure elucidation of **1** and **2**

It has been reported before that carotenoid dioxygenases cleave their respective carotenoid substrate into retinoid derivatives<sup>120,121</sup>. In fact, retinol, which is one of the commonly used factors for signal transduction in several organisms<sup>156–158</sup>, is generated through symmetric cleavage of  $\beta$ -carotene into two retinal molecules<sup>159</sup>. As the putative cleavage products of the oxygenase remained unknown, an attempt was made to elucidate their structure by conducting high-resolution MS analysis of **1** and **2** (Fig. 41).

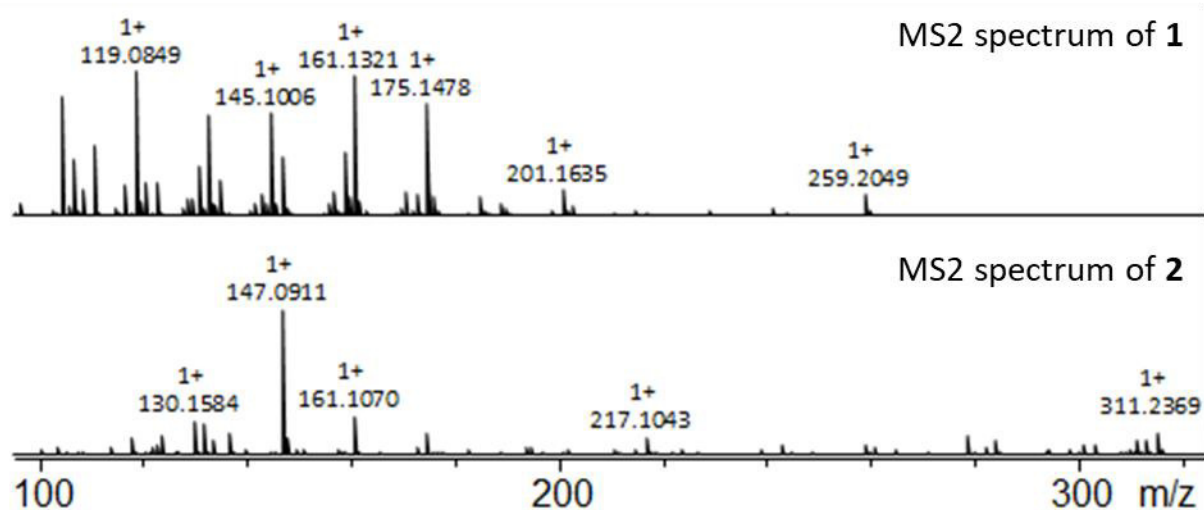


**Fig. 41.** MS2 spectra of compounds **1** and **2** observed in *Escherichia coli* BL21 (DE3)-Marionette-Diterpene expressing the biosynthetic carotenoid core genes in addition to the oxygenase encoding gene in LB.

The designated masses of  $m/z$  259.205  $[M+H]^+$  for **1** and  $m/z$  311.236  $[M+H]^+$  for **2** indicated a cleavage of  $\beta$ -carotene which originally possesses the mass of  $m/z$  537.445  $[M+H]^+$ . Typically, carotenoid dioxygenases introduce two oxygen molecules into the carotenoid core to form a four-membered ring that subsequently cleaves the molecule into two aldehyde retinoid derivatives in a symmetrical cleavage whereas an asymmetrical cleavage results in one aldehyde and one ketone retinoid derivative, respectively<sup>120</sup>. As the masses of **1** and **2**

were different from each other, an asymmetrical cleavage was postulated. In order to elucidate the structure of **1**, a commercially available  $\beta$ -apo-13-carotenone standard was purchased. Subsequently, the standard was compared to the isolated extract of **1** (Fig. 42).

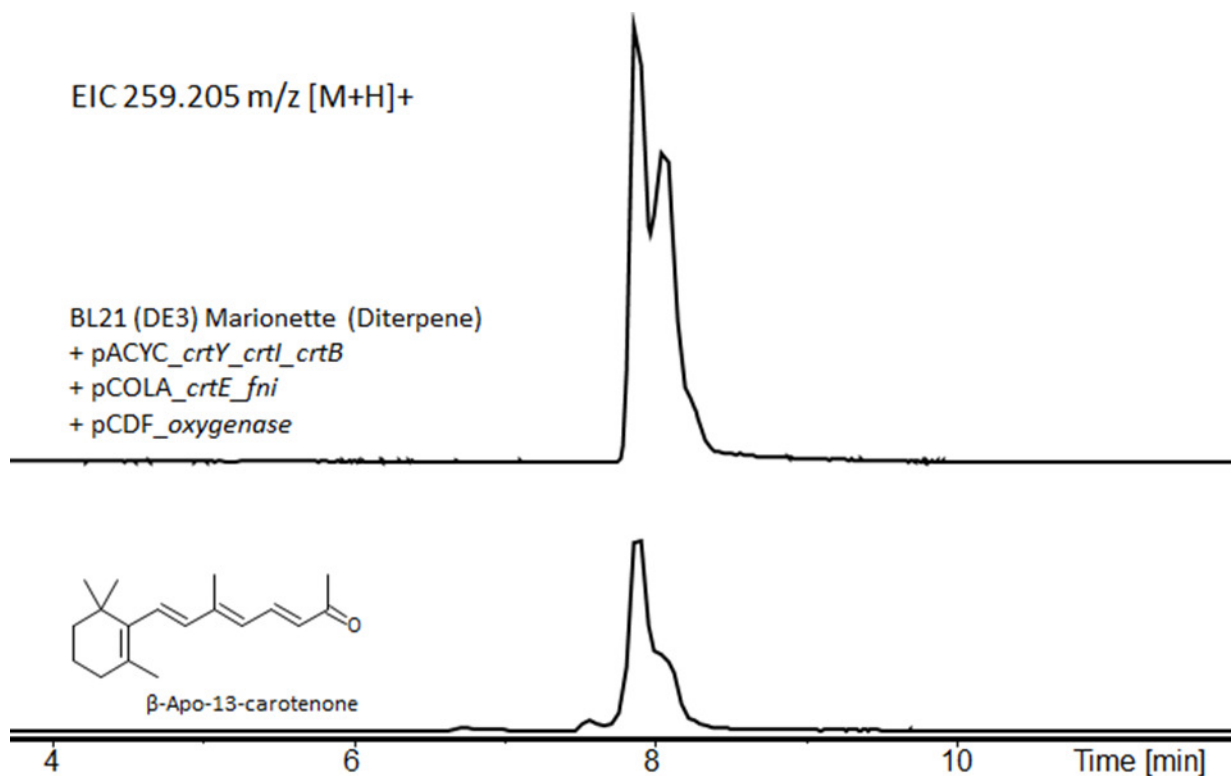
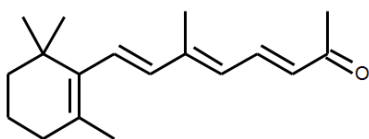
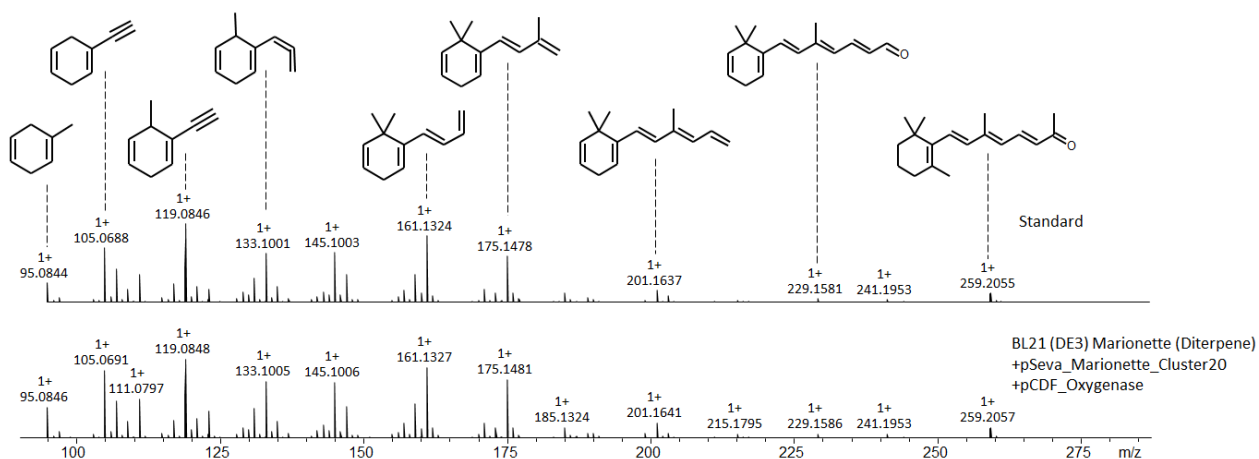


**Figure 42.** Comparison of the retention times of **1** and a commercially purchased  $\beta$ -Apo-13-carotenone standard. The retention time of the standard exactly matched the retention time of **1** confirming its structure. Furthermore, to finally elucidate the structure of **1**,  $MS^2$  spectra of both compounds were compared and a fragmentation tree was generated (Fig. 43).

A



B



C

m/z [M+H] <sup>+</sup>	Fragment	Error [ppm]
259.205	C <sub>18</sub> H <sub>27</sub> O	3.0
229.158	C <sub>16</sub> H <sub>21</sub> O	1.3
201.164	C <sub>15</sub> H <sub>21</sub>	1.7
175.148	C <sub>13</sub> H <sub>19</sub>	2.0
161.132	C <sub>12</sub> H <sub>17</sub>	1.4
145.100	C <sub>11</sub> H <sub>13</sub>	4.6
133.100	C <sub>10</sub> H <sub>13</sub>	4.4
119.084	C <sub>9</sub> H <sub>11</sub>	4.5
105.069	C <sub>8</sub> H <sub>9</sub>	6.0
95.084	C <sub>7</sub> H <sub>11</sub>	5.7

**Figure 43.** Structure confirmation of **1**. (A) Proposed structure of **1** based on  $\beta$ -apo-13-carotenone standard. (B) Comparison of fragmentation pattern of **1** and  $\beta$ -apo-13-carotenone standard. Dashed lines indicate the structure of the respective fragments. (C) Table of MS fragments with their respective error values in ppm.

As shown in Fig.43, B the fragmentation pattern of **1** was identical to the  $\beta$ -Apo-13-carotenone standard, thus confirming the structure. Next, the structure of **2** was elucidated. Here, structure confirmation showed to be more difficult as the MS<sup>2</sup> spectrum of expected aldehyde retinoid derivative did not result in a sufficient fragmentation pattern. Additionally, purification of **2** was not possible despite multiple attempts. Consequently, 10-(2,3,4,5,6-Pentafluorobenzyl)-hydroxylamin-hydrochlorid (PFBHA) was used as an aldehyde-catching reagent in order to stabilize **2** for structure elucidation (Fig. 44).

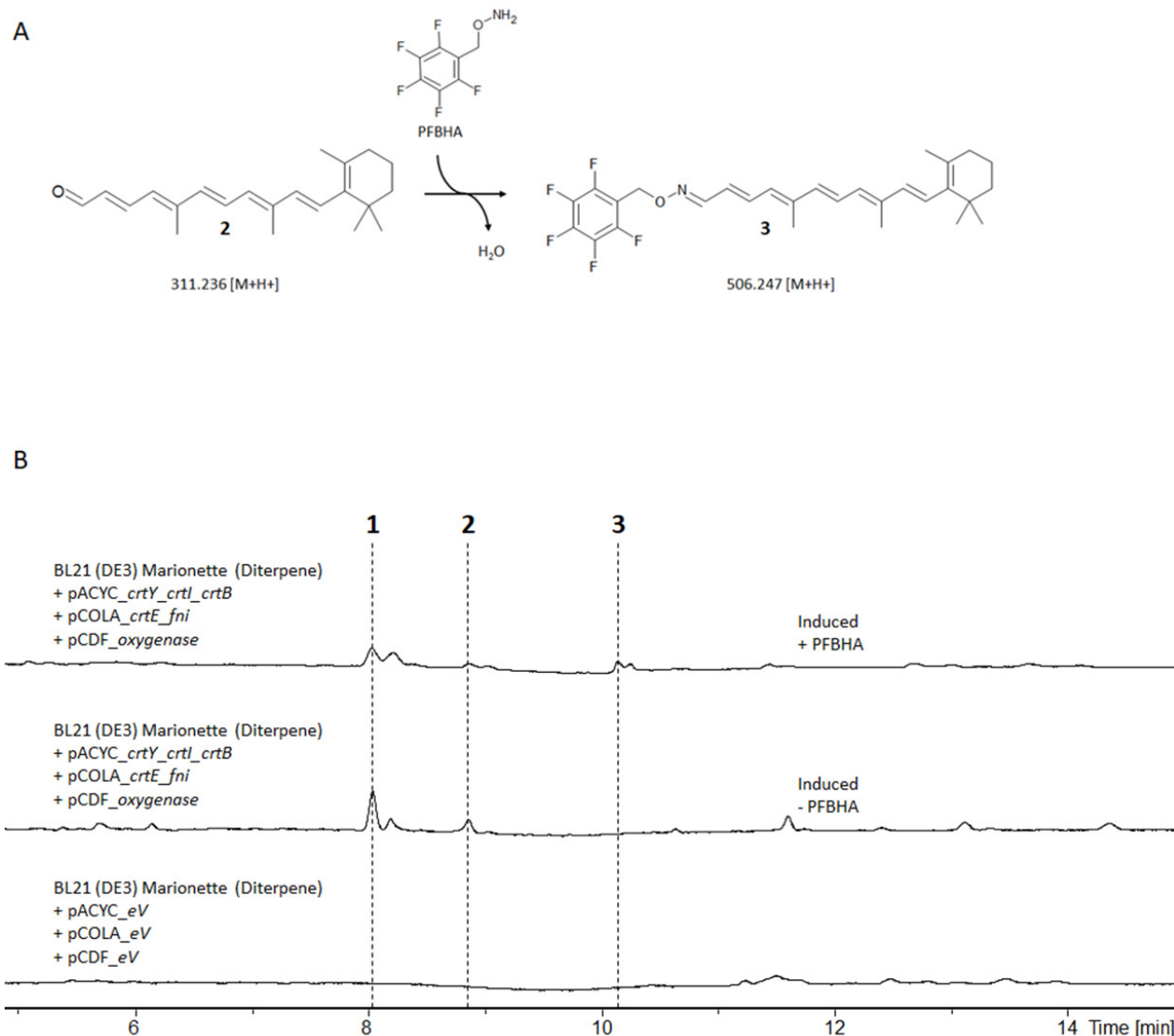


**Fig. 44.** Aldehyde derivatisation of **2**. (A) Proposed structure of cleavage product **2** based on structure of **1**. PFBHA was used as an aldehyde catcher. (B) Production of **1**, **2** and **3** in *Escherichia coli* BL21 (DE3) Marionette (Diterpene) producing  $\beta$ -carotene. Shown are HPLC-UV-basepeak-chromatograms ranging from 100-800 nm of MeOH/CHCl<sub>3</sub> extracts. All chromatograms are scaled equally. Cultures were cultivated for 72 h in LB broth at 30°C while being supplemented with the respective antibiotics and gene expression was induced with 0.2% arabinose and 0.1 mM IPTG, respectively. Culture extracts in presence of the empty vectors were analyzed as control. Dashed lines indicate the retention times of the respective compounds.

Upon supplementation of PFBHA to the production strain of **1** and **2**, a new UV-signal **3** at 10.2 min with the mass  $m/z$  506.247 [M+H]<sup>+</sup> was detectable whereas the amount of **2** decreased. As the mass matched the calculated mass of **3** depicted in Fig. 44, A, a fragmentation tree of **3** was generated in order to fully confirm the postulated structure of **2** (Fig. 45).

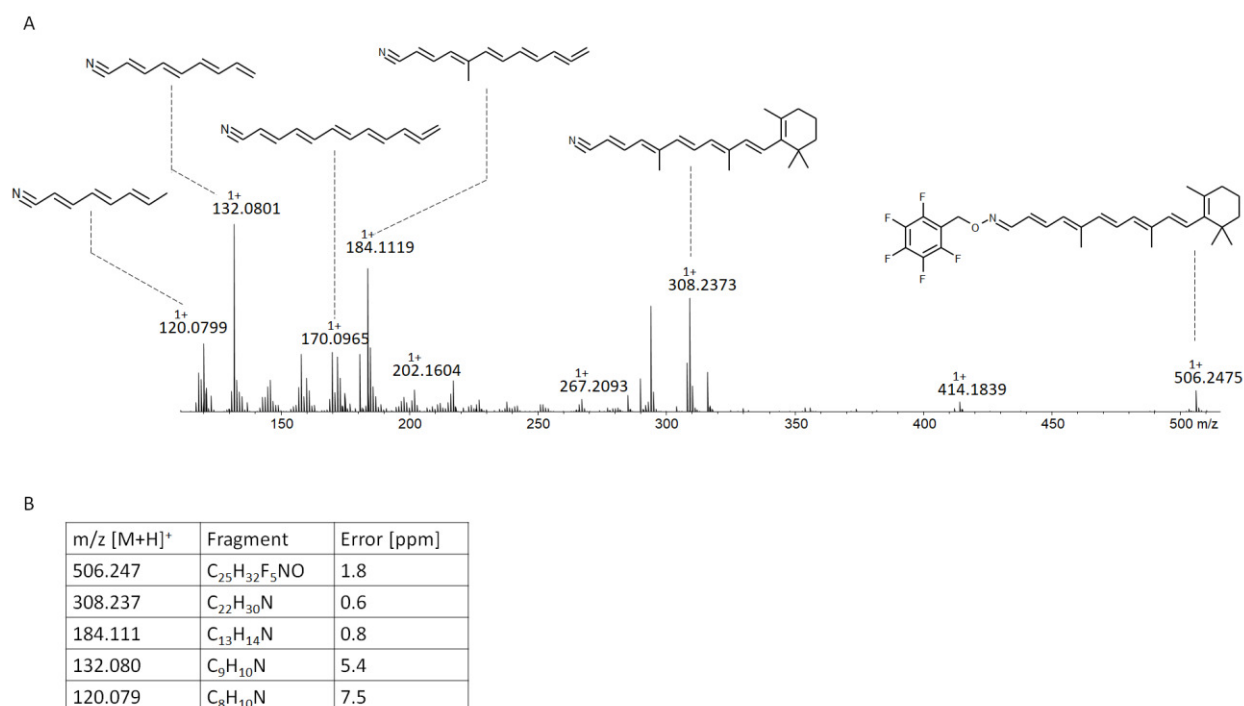


**Fig. 45.** Structure verification of **2**. (A) Proposed structure of cleavage product **2** based on structure of **1**. PFBHA was used as an aldehyde catcher with fragmentation pattern of **2**. Dashed lines indicate the structure of the respective fragments. (B) Table of MS fragments with their respective error values in ppm.

Finally, the fragmentation tree confirmed the structure of **2** as  $\beta$ -apo-14'-carotenal based on the low error values of the fragments displayed in Fig. 45, B.

### 6.3.6 Retinoid derivative formation in different *Photorhabdus* species

As it was shown in section 6.3.1, the carotenoid cluster is conserved in several *Photorhabdus* species. Consequently, it was investigated whether the production of **1** and **2** is universally featured in all of the analyzed strains (Fig. 46). Here, each of the genes of the respective clusters were cloned in a pSEVA expression vector each under the control of a different promoter as described earlier<sup>149</sup>. Subsequently, the plasmids were transformed into *E. coli* BL21 (DE3)-Marionette. Cultivation, gene expression, compound extraction and HPLC-MS analysis was carried out as described in Material and Methods chapter 5.4.

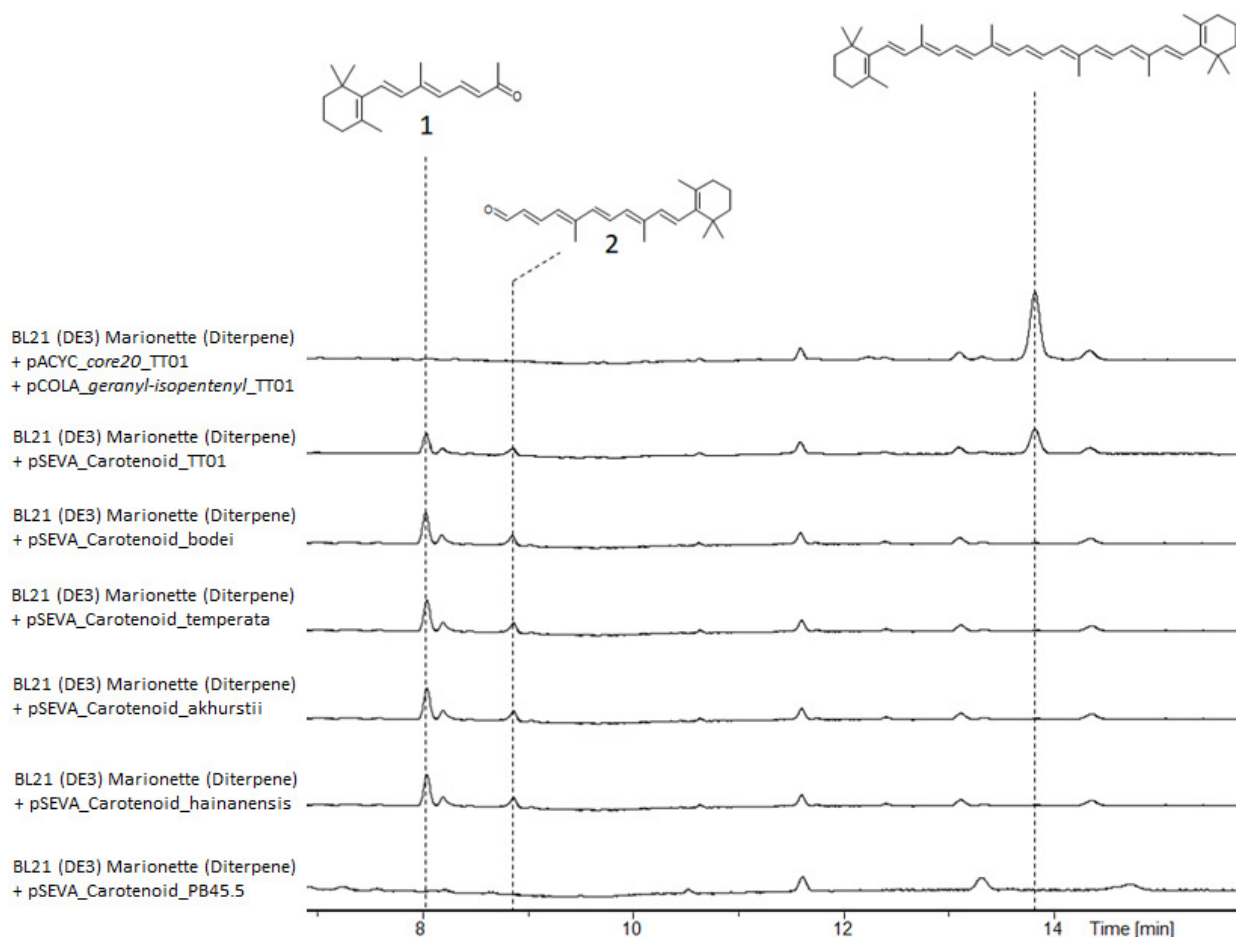


**Fig. 46.** Comparison of product formation expressing carotenoid clusters from different *Photorhabdus* strains in *Escherichia coli* BL21 (DE3) Marionette (Diterpene). Shown are HPLC-UV-basepeak-chromatograms ranging from 100-800 nm of MeOH/CHCl<sub>3</sub> extracts. All chromatograms are scaled equally. Cultures were cultivated for 72 h in LB broth at 30°C while being supplemented with the respective antibiotics and gene expression was induced as described earlier. Culture extracts in presence of the empty vectors were analyzed as control (data not shown). Dashed lines indicate the retention times of the respective compounds.

Expression of constructs harboring the carotenoid clusters of the respective *Photorhabdus* strains resulted in the UV-signals corresponding to **1** and **2**. Subsequent comparison of MS<sup>2</sup>-spectra confirmed the observation (data not shown). Interestingly, the expression of the carotenoid cluster from *P. luminescens subsp. PB45.5* did not result in any retinoid or carotenoid production possibly due to the absence of *fni* and truncation of *crtE* (see Fig. 36).

### 6.3.7 Carotenoid oxygenase from *P. luminescens subs. PB45.5* and *Xenorhabdus sp. KJ12.1* are active on $\beta$ -carotene

Often, organisms that utilize retinoid derivatives in specific pathways only possess the respective oxygenase to cleave the carotenoid into the desired product while they scavenge the substrate from their environment<sup>160</sup>. As *Photorhabdus* and *Xenorhabdus* share a similar ecological niche with a similar life cycle in mutualistic associations with nematodes, which infect different kinds of prey, it is possible that some species receive the carotenoid substrate from external sources. Interestingly, *Xenorhabdus sp. KJ12.1* is the only *Xenorhabdus* species that encodes a carotenoid BGC and a corresponding oxygenase in its genome. In the following work, it came under scrutiny whether the carotenoid oxygenases found in *P. luminescens subs. PB45.5* and *Xenorhabdus sp. KJ12.1* were active on  $\beta$ -carotene. Firstly, production was investigated using their respective BGCs. Secondly, the carotenoid core genes from *P. luminescens* TT01 were used for  $\beta$ -carotene production while the cleavage reactions were conducted with oxygenases from *P. luminescens subs. PB45.5* and *Xenorhabdus sp. KJ12.1*. To this end, the respective oxygenase-encoding genes were cloned separately on a pCDF expression vectors. Subsequently, plasmids were co-transformed into *E. coli* BL21 (DE3)-Marionette and cultivation, gene expression, compound extraction and HPLC-MS analysis was carried out as described earlier. Results are displayed in Fig. 47.

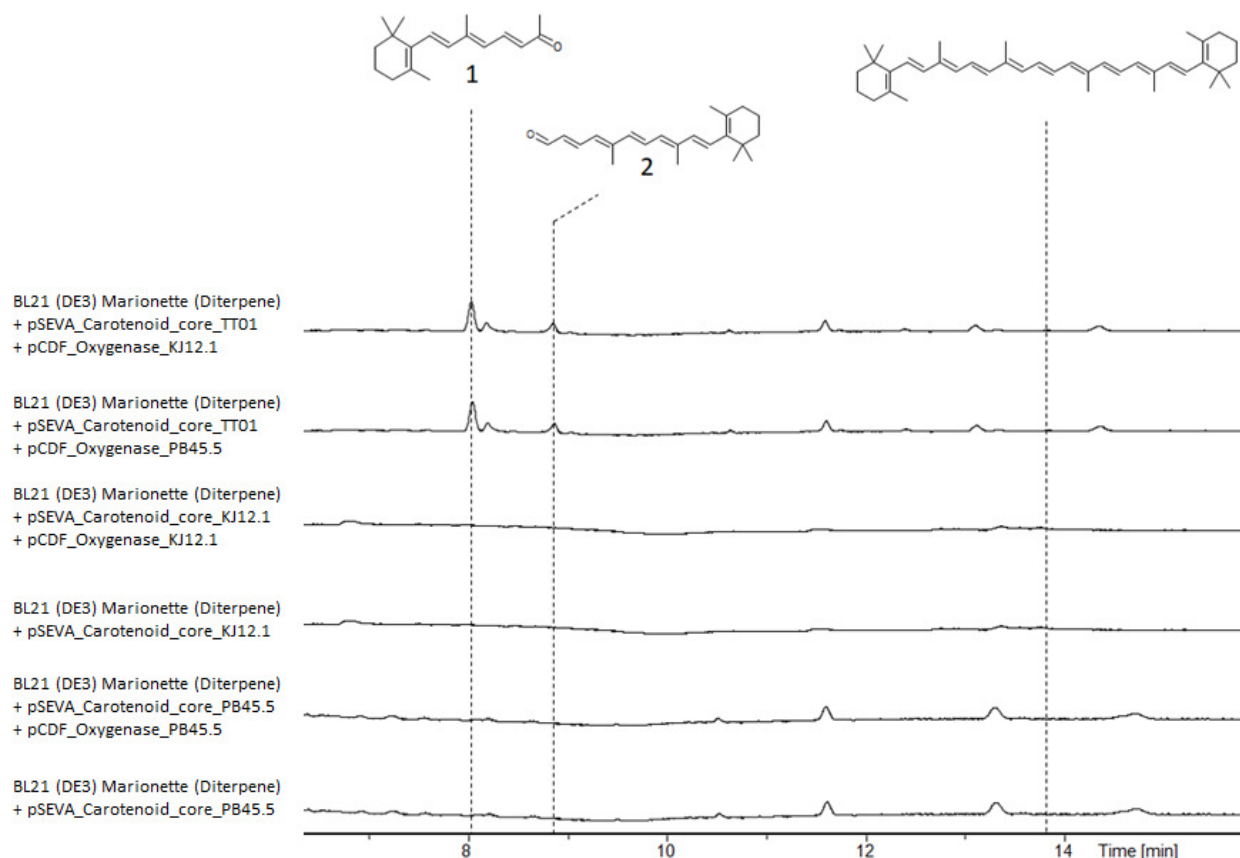


**Fig. 47.** Oxygenase activities of *Photorhabdus luminescens* subs. PB45.5 and *Xenorhabdus* subs. KJ12.1. *Photorhabdus luminescens* TT01 carotenoid genes *crtB*, *crtE*, *crtI*, *crtY*, and *fni* were expressed to produce  $\beta$ -carotene. Production was carried out in *Escherichia coli* BL21 (DE3) Marionette (Diterpene). Shown are HPLC-UV-basepeak-chromatograms ranging from 100-800 nm of MeOH/ $\text{CHCl}_3$  extracts. All chromatograms are scaled equally. Cultures were cultivated for 72 h in LB broth at 30°C while being supplemented with the respective antibiotics and gene expression was induced as described earlier. Culture extracts in presence of the empty vectors were analyzed as control (data not shown). Dashed lines indicate the retention times of the respective compounds.

As already shown before, the expression of the carotenoid cluster from *P. luminescens* subs. PB45.5 did not result in any production of retinoid derivatives or carotenoids. Accordingly, upon induction of constructs generated from the carotenoid cluster of *Xenorhabdus* sp. KJ12.1 no production was detected. Crucially, when substituting  $\beta$ -carotene biosynthetic genes from *P. luminescens* subs. PB45.5 and *Xenorhabdus* sp. KJ12.1 with the genes from *P. luminescens* TT01, the respective oxygenase was able to cleave  $\beta$ -carotene into **1** and **2**. These findings are discussed later on.



### 6.3.8 Carotenoid cluster exhibits in vivo effect in insect killing assays

In the case of *Xenorhabdus* and *Photorhabdus*, NPs play an essential role in cross-kingdom interactions with nematodes, various insects, as well as bacterial and fungal species competing for the same food source<sup>9</sup>. Despite NPs playing a central role in the life cycle of the symbiosis, the exact ecological function for many of these compounds remained unknown. In order to investigate a putative biological function of the compounds produced by the carotenoid cluster, the deletion mutants *P. luminescens*  $\Delta$ oxygenase and *P. luminescens*  $\Delta$ carotenoid were generated as described before. While  $\Delta$ carotenoid harbors deletions of *crtE*, *fni*, *crtY*, *crtI* and *crtB* and is thus unable to produce  $\beta$ -carotene,  $\Delta$ oxygenase still has the functional genes for  $\beta$ -carotene production but is missing the oxygenase. Subsequently, the strains were tested in insect killing assays as described in Material and Methods chapter 5.4 (Fig. 48). In short, *Galleria mellonella* were grown for three weeks and subsequently injected with the respective *Photorhabdus* strains (wildtype,  $\Delta$ carotenoid,  $\Delta$ oxygenase). Death was determined by loss of larvae movement.

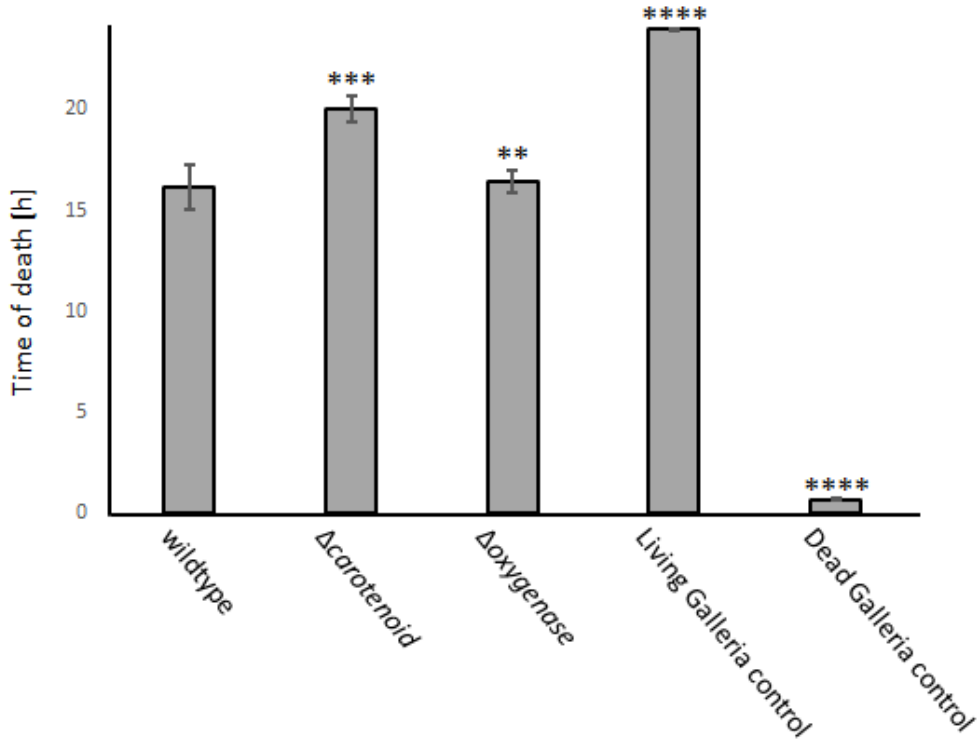


**Fig. 48.** *G. mellonella* killing assay with different *Photorhabdus luminescens* TT01. Assay was conducted for 24h. Insects were grown for 3 weeks and subsequently injected with the respective *Photorhabdus* strains (wildtype,  $\Delta$ carotenoid,  $\Delta$ oxygenase). Death was determined by missing movement of the larvae. All bars represent the absolute timespan of movement. Error bars represent the standard error of the mean. Asterisks indicate statistical significance (\*  $p < 0.05$ , \*\*  $p < 0.005$ , \*\*\*  $p < 0.0005$ , \*\*\*\*  $p < 0.00005$ ). Living *Galleria mellonella* and dead *Galleria mellonella* were used as controls.

*G. mellonella* infected with *P. luminescens*  $\Delta$ oxygenase died after 16.4 h on average, which is comparable to wildtype mortality levels, while infection with *P. luminescens*  $\Delta$ carotenoid killed the insects after 20.1 h on average. As  $\beta$ -carotene is not known to exhibit an insecticidal activity, these findings indicate that it might have a protective function against the insect's immune system. This topic will be discussed below.

### 6.3.9 Retinoid production in insect infection assays

Once the insect is infected by *P. luminescens* subsp. TT01 and its associated nematode *Heterorhabditis bacteriophora*, both need to overcome the insect's immune system. Generally, retinoid derivatives regulate various physiological outputs in several classes of organisms by binding to nuclear hormone receptors (NHRs), retinoic acid receptors (RARs) or

retinoid X receptors (RXRs)<sup>161</sup>. In case of *P. luminescens subsp.* TT01, none of the compounds produced by the carotenoid cluster were detected under laboratory conditions. However, it was shown that deletion of the carotenoid cluster led to a decreased mortality of *Galleria mellonella* infected by *P. luminescens subs.* TT01. Consequently, it was investigated whether retinoid production was induced in an insect environment. For this purpose, *Galleria mellonella* were cultivated as described before. In the following step, insects were infected with either *Heterorhabditis bacteriophora* carrying *P. luminescens subs.* TT01 wildtype or solely *P. luminescens subs.* TT01. Samples were taken as described in Material and Methods chapter 5.4. Extracts were generated by Dr. Yi-Ming Shi and kindly provided for analysis. Results are displayed in Fig. 49 and Fig. 50.

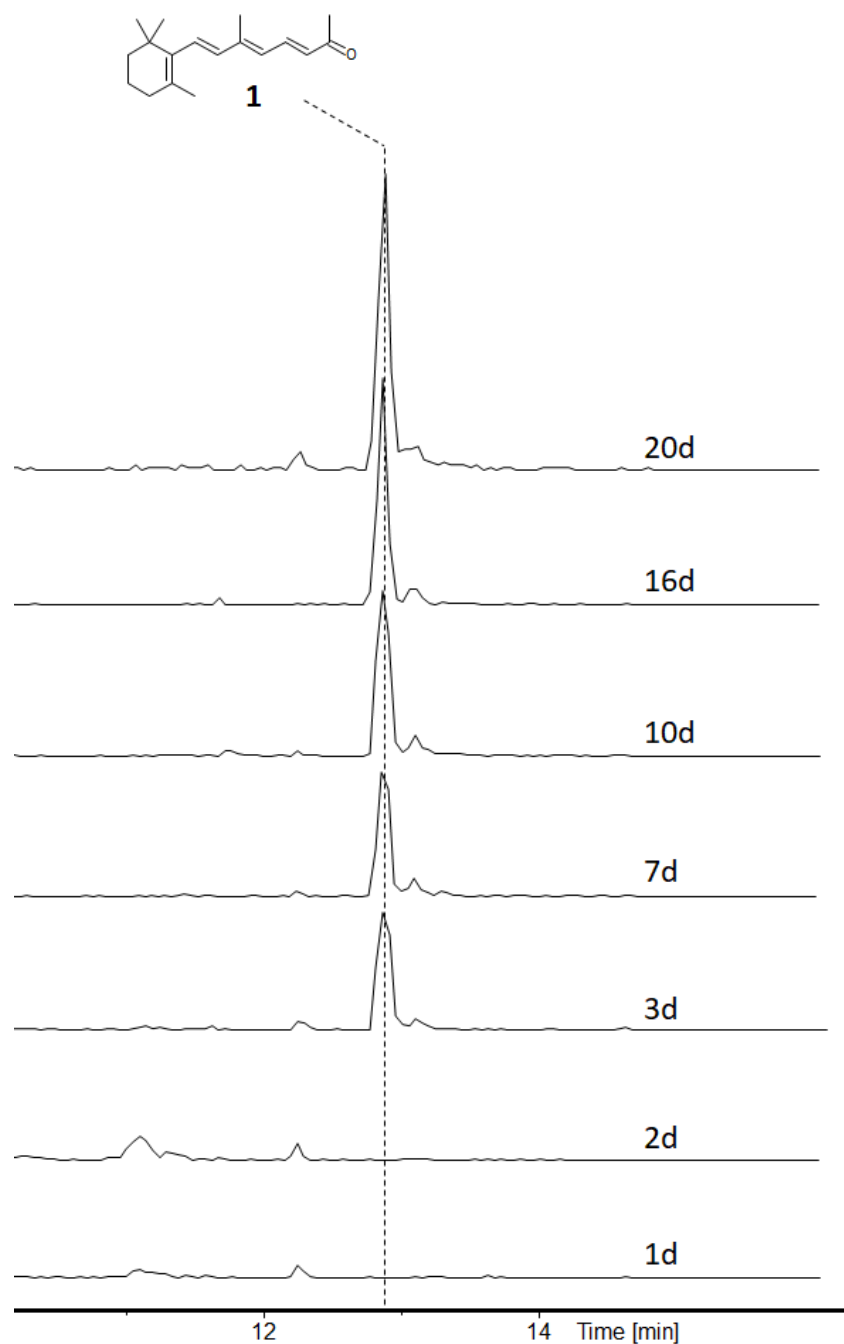


**Fig. 49.** Production of **1** in *Galleria mellonella* infected with *Photorhabdus luminescens* TT01. Shown are EICs of 259.205  $m/z$   $[M+H]^+$  of ACN extracts. All chromatograms are scaled equally. Samples were taken at the indicated time points. Extracts were kindly provided by Dr. Yi-Ming Shi, Bode group.

When infecting *Galleria mellonella* with *Photorhabdus luminescens* TT01, production of **1** is indeed detectable after 3 days. Furthermore, the concentration of **1** increases over time, reaching its maximum after 20 days (last time point).

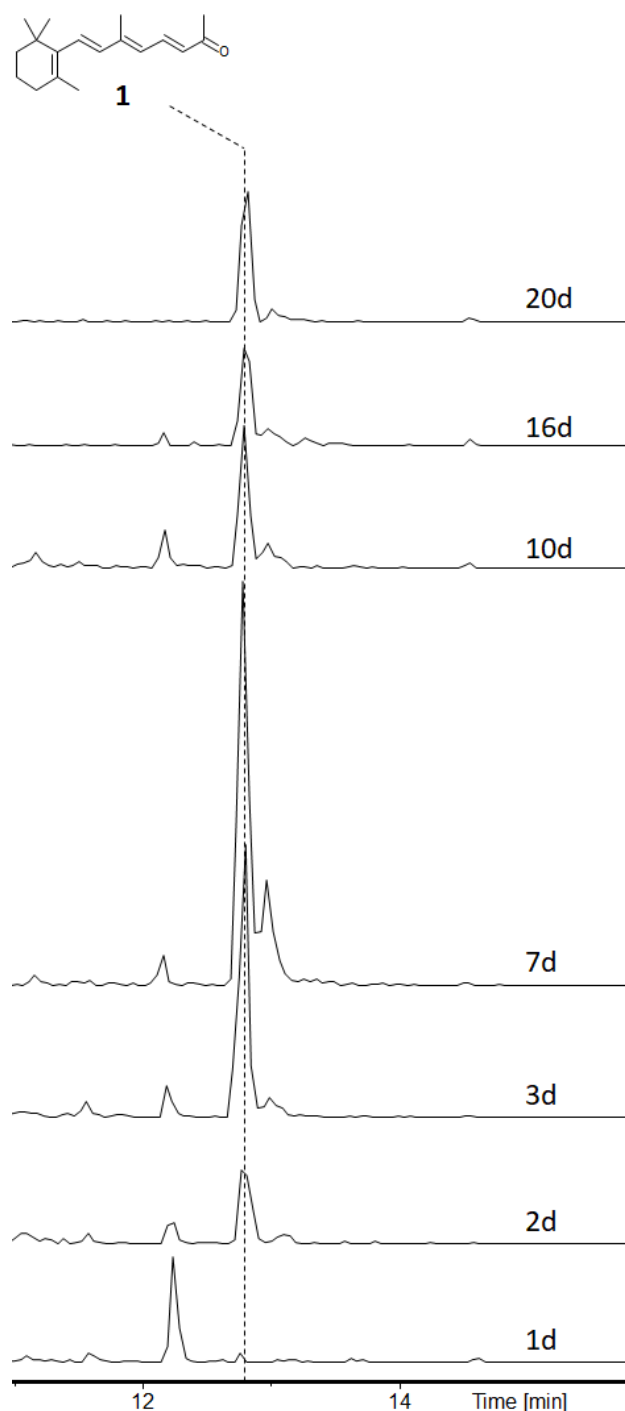


**Fig. 50.** Production of **1** in *Galleria mellonella* infected with *Heterorhabditis bacteriophora* carrying *Photorhabdus luminescens* TT01. Shown are EICs of 259.205  $m/z$   $[M+H]^+$  of ACN extracts. All chromatograms are scaled equally. Samples were taken at the indicated time points. Extracts were kindly provided by Dr. Yi-Ming Shi, Bode group.

Interestingly, upon infection of *Galleria mellonella* with *Heterorhabditis bacteriophora* carrying *Photorhabdus luminescens* TT01, production of **1** is already detectable after 1 day whereas the maximum production level is reached after 7 days. Subsequently, the concentration decreases again. Additionally, in both cases, it was not possible to detect signals for **2**. However, this was most likely due to the vast amount of compounds present in

the insect extract. In addition, as aldehydes are generally rather reactive compounds, it was assumed that **2** was already modified by various side reactions. In the next step, NP production levels of selected NPs of *Photorhabdus luminescens* TT01 infecting *Galleria mellonella* with and without the associated host nematode *Heterorhabditis bacteriophora* were compared (Fig. 51).

- Galleria infected by TT01 without nematode
- Galleria infected by TT01 with nematode

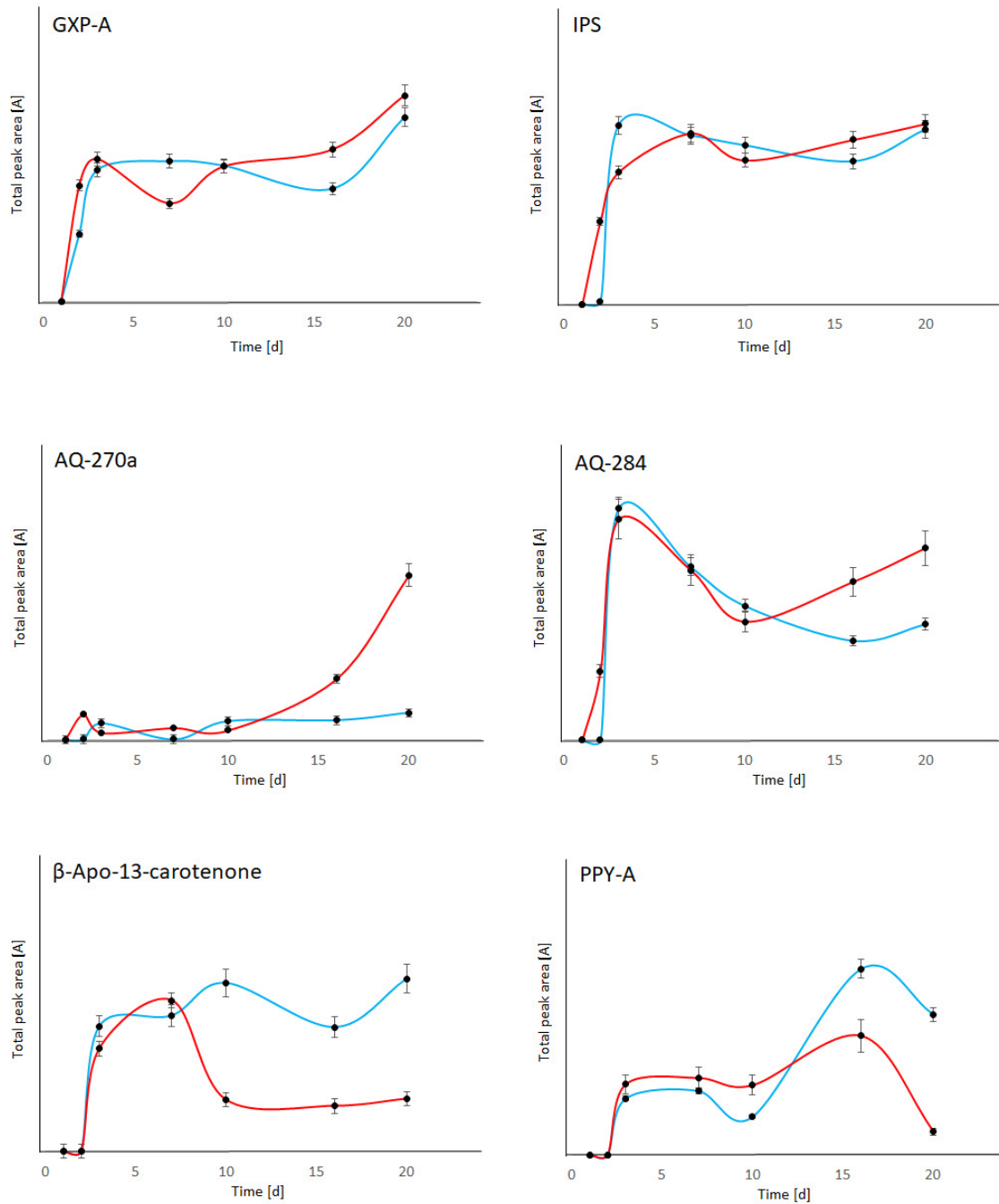


**Fig. 51.** Comparison of NP production levels of *Photorhabdus luminescens* TT01 infecting *Galleria mellonella* with and without the associated host nematode *Heterorhabditis bacteriophora*. Relative NP production was compared by absolute peak area [A] comparison of the respective compounds. Error bars represent SD of three independent biological replicates. Extracts were kindly provided by Dr. Yi-Ming Shi, Bode group.

For GXPA and IPS, the relative production increased rapidly for 3 days and remained at approximately equal levels until day 20 in both cases. In case of photopyrone A (PPY-A) and **1** the NP levels continuously increased when *G. mellonella* was only infected with *P. luminescens subs. TT01* over 20 days. In contrast, production titers increased over a certain period (7 days for **1**, 16 days for PPY-A) when *G. mellonella* was infected with *P. luminescens subs. TT01* and its associated nematode until the levels decreased again. For AQ-270a, production levels remained roughly equal after 3 days throughout the remaining time of the assay when *G. mellonella* was only infected with *P. luminescens subs. TT01*. Contrary, AQ-270a titers increased continuously over 20 days when *G. mellonella* was infected with *P. luminescens subs. TT01* and its associated nematode. Finally, AQ-284 levels increased rapidly for 3 days in both cases, decreased again for 7 days (*Photorhabdus* with associated nematode) and 13 days (*Photorhabdus* only), respectively, until approximately 50% of the maximum titer was reached and increased again until day 20.

### **6.3.10 Putative targets of retinoid derivatives produced by *P. luminescens***

As already described before, retinoid derivatives regulate various physiological outputs in several kingdoms of life by binding to nuclear hormone receptors (NHRs), retinoic acid receptors (RARs) or retinoid X receptors (RXRs)<sup>161</sup>. The findings presented in chapter 6.3.9 clearly display that the retinoid derivatives produced by *P. luminescens subs. TT01* are induced after infection of insect prey. Additionally, the differences in NP levels of **1** when infecting *G. mellonella* with *P. luminescens subs. TT01* and its associated nematode *H. bacteriophora* indicate that **1** is either presumably bound to a target entity or converted. Consequently, the next step was to identify putative binding partners of **1** and **2**. Hitherto, signaling pathways in parasitic nematodes are yet to be fully elucidated. In a literature research, different classes of fatty acid- and retinol-binding proteins (FARs) and NHRs were identified in the well-studied nematode *Caenorhabditis elegans*<sup>162</sup>. Subsequently, the amino acid sequences of the respective proteins were subjected to bioinformatics analysis in order to identify homologues in other organisms. Database blast was performed in cooperation with Prof. Dr. Ingo Ebersberger, Goethe University, Frankfurt. Results are shown in Fig 52.



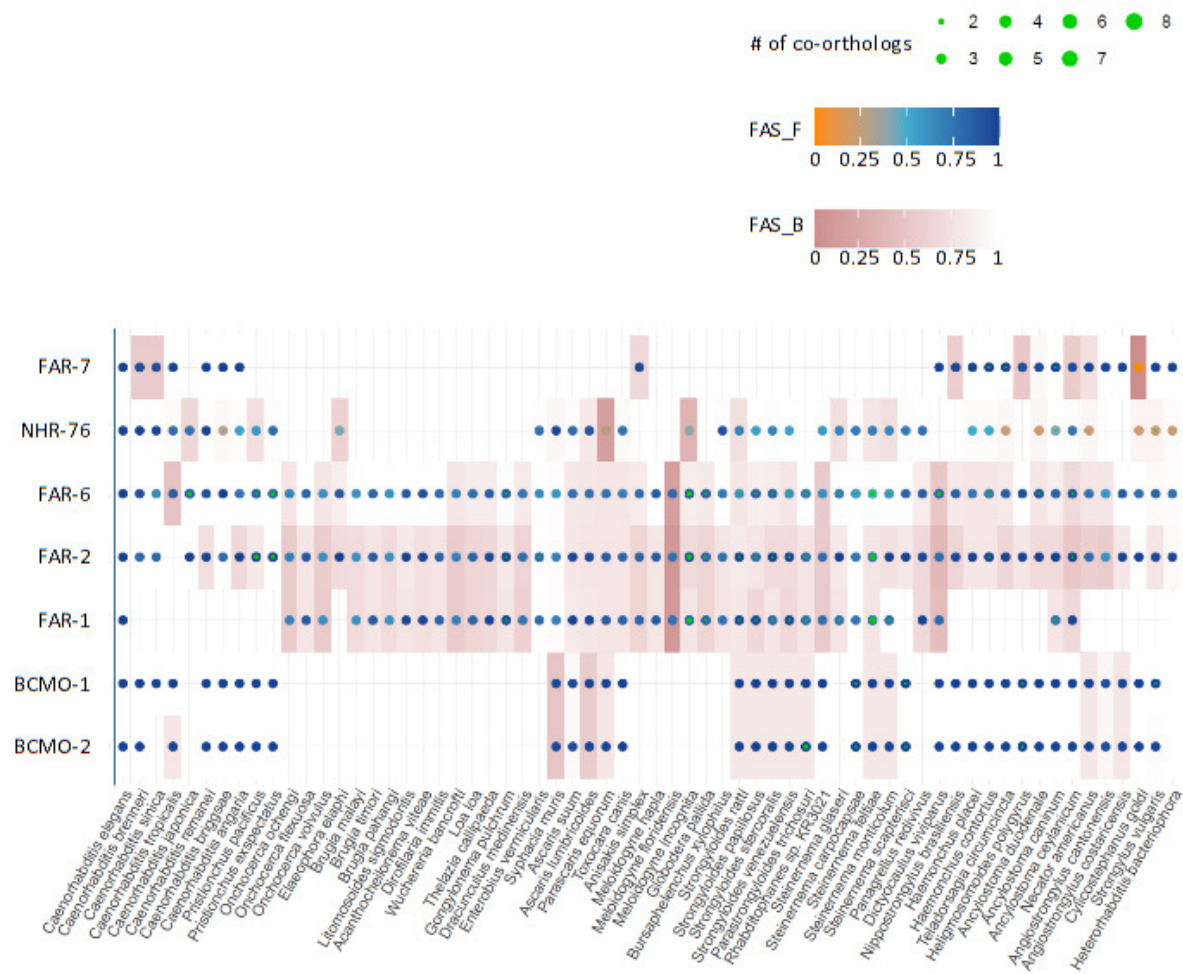


**Fig. 52** Excerpt of protein blast analysis. Amino acid sequences for different classes of fatty acid- and retinoid-binding proteins (FARs), nuclear hormone receptors (NHRs) and two carotenoid dioxygenases BCMO-1 and BCMO-2 from *C. elegans* were used as inputs. Score of protein domain presence is represented by FAS\_F, score of domain architecture is depicted by FAS\_B. In both cases the score ranges from 0.00 – 1.00 whereas a higher score accounts for higher similarities. Full blast analysis is shown in supplemental Figures (Fig. S28).

Crucially, the identified FARs and NHRs are widely nematode specific features (see also Fig. S28). *C. elegans* is known to utilize retinoid derivatives as signaling molecules for processes such as sex determination, molting, developmental timing, diapause, and life span<sup>160</sup>. In case of *H. bacteriophora*, several FARs and NHRs except FAR-1 are encoded as homologues in its genomes indicating related underlying regulatory networks. Importantly, *C. elegans* encodes two carotenoid dioxygenases BCMO-1 and BCMO-2 in its genome. Therefore, it is assumed that the required carotenoids are scavenged from its surrounding and subsequently cleaved into the desired retinoid derivatives. In case of *H. bacteriophora*, no homologues of BCMO-1 and BCMO-2 are encoded on its genome. Here, presumably the association with *P. luminescens* strains provides the retinoid substrate necessary for pathway activation. This hypothesis is further supported by the fact that *S. carpocapsae*, which is mutualistically associated with *Xenorhabdus nematophila*, harbors homologues of BCMO-1 and BCMO-2 on its genome. Crucially, *X. nematophila* does not encode any terpenoid producing clusters in its genome.

### **6.3.11 Retinoid activity on channelrhodopsin ChR2 in *C. elegans***

Generally, attributing functions of specific NPs in higher organisms is difficult as they are often part of a complex machinery of regulatory elements. However, expressing known interaction partners of respective NPs can yield an insight in their putative function. Channelrhodopsins are a subfamily of retinylidene proteins that function as light-gated ion channels.<sup>163</sup> Upon binding of different retinoid-derived compounds, ion influx is mediated that enables electrical excitability, intracellular acidity and other cellular processes.<sup>164–168</sup> In cooperation with Prof. Dr. Alexander Gottschalk (Goethe University, Frankfurt), an assay was conducted in order to investigate whether **1** or **2** can act as putative binding partner the channelrhodopsin ChR2 from *Chlamydomonas reinhardtii*. For this, ChR2 was produced in muscle cells of *C. elegans*. Subsequently, the nematodes were fed with *E. coli* strains that were producing **1**, **2** and all-*trans*-retinal. In the following, *C. elegans* was irradiated with blue light at 470 nm and the contraction was measured (Fig. 53).

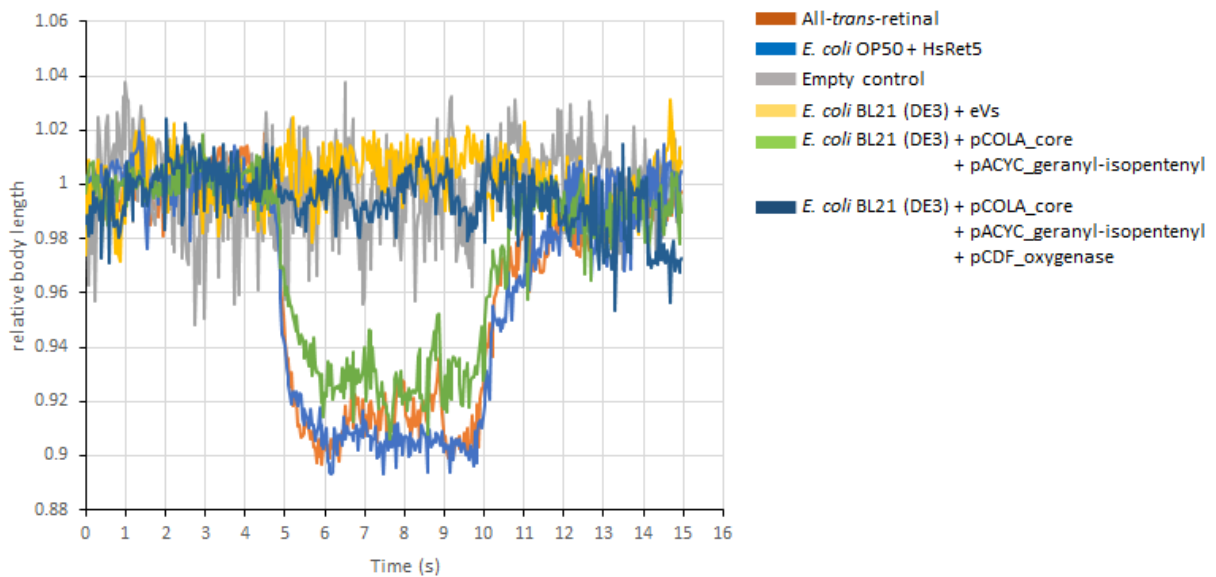


**Fig. 53** Light irradiation assay of *C. elegans* expressing *ChR2*. Nematodes were fed with the indicated strains and irradiated with blue light at 470 nm for 15 seconds. Contraction of *C. elegans* was measured as relative body length. Upon successful binding of the interaction partner to *ChR2*, nematodes contract at 470 nm and their body length is reduced. N=6 worms were used for each individual sample. Depicted are: All-*trans*-retinal (orange), *E. coli* OP50 + HsRet5 (blue), empty control (grey), *E. coli* BL21 (DE3) + eVs (yellow), *E. coli* BL21 (DE3) producing  $\beta$ -carotene (green) and *E. coli* BL21 (DE3) producing **1** and **2** (olive). Experiments were conducted in cooperation with Prof. Dr. Gottschalk, Goethe University, Frankfurt.

As expected, the native binding partner of *ChR2* all-*trans*-retinal led to a significant reduction in body length through contraction. Congruently, feeding of *C. elegans* with *E. coli* OP50 expressing human genes responsible for retinol production led to activation of *ChR2* and subsequent contraction. In contrast, the production of **1** and **2** in *E. coli* BL21 (DE3) did not result in a reduction of relative body length, thus it did not act as a specific interaction partner of *ChR2*. However, these findings do not account for a global mechanism as they are limited on *ChR2* as a unique binding partner. Interestingly, *C. elegans* exhibited contraction when fed with *E. coli* BL21 (DE3) producing  $\beta$ -carotene. Here, it is assumed that  $\beta$ -carotene is cleaved through the activity of BCMO-1 or BCMO-2 into retinal that subsequently acts as a ligand for *ChR2*.

## 7 Discussion

### 7.1 Topic A: Anthraquinone derivative formation in *Photorhabdus*

The BGC responsible for AQ biosynthesis was already described in 2007<sup>74</sup> and encodes the biosynthetic genes involved in AQ-256 production. However, the MTs involved in converting AQ-256 into its methylated derivatives remained unknown until bioinformatic analysis of the *P. luminescens* genome identified a set of SAM-dependent MTs (*plu4895-plu4890*) that are putatively involved in AQ derivative formation.<sup>37</sup> As query for a MT search in the genome of *P. luminescens* the O-methyltransferase DnrK from *Streptomyces peucetius* was chosen, which is involved in the biosynthesis of the aromatic polyketide daunorubicin showing some similarity to AQ-256<sup>169</sup>. Interestingly, the locus of *AntA-I* is situated approximately 1 mbp apart from *plu4890-plu4895*. Based on their high sequence identity, the MTs are supposed to originate from several gene duplication events and to have similar function<sup>47</sup>. Upon deletion of *plu4895-plu4890* only the non-methylated precursor AQ-256 was detectable after cultivation (Fig. 11). Generally, all investigated *Photorhabdus* strains carry the genes encoding for *plu4895-plu4890* in their genomes with the only exception being *P. temperata* that misses *plu4895*. This data supports the idea that the AQs exhibit a highly conserved function in all *Photorhabdus* strains.

A major aspect of this topic addressed the question whether the five highly homologous MTs differ in their specificity for the position of methylation. For this, *in vivo* and *in vitro* approaches were chosen in order to identify the respective mono-methylation patterns. Additionally, it was not clear yet if multi-methylated derivatives were formed sequentially where single-methylated derivatives are accepted and converted by additional MTs or whether a single MT catalyzes the formation of multi-methylated derivatives.

#### 7.1.1 AQ diversification in *P. luminescens*

Consequently, in order to investigate the putative involvement of *plu4895-plu4890*, several *P. luminescens* deletion mutants were generated. Upon deletion of the whole MT cluster, the production of methylated AQ derivatives vanished, confirming the involvement of *plu4895-4890* in AQ derivative formation. Subsequently, *P. luminescens* strains were generated that

express only one of the respective MT-encoding genes and harbor deletions in the remaining four. Crucially, expression of *plu4895* resulted in the formation of AQ-270a as the major product. Furthermore, AQ-256 was also converted into minor amounts of AQ-270b by *plu4895*. These findings suggest a rather unspecific substrate conversion *in vivo* with the C2-position for AQ-270a being the preferential one over C14 of AQ-270b. Typically, MTs show a distinctly specific product composition, still, multi-product formation has been described before.<sup>170</sup> In case of *plu4891*, single expression led to the formation of AQ-270b as the sole product. Interestingly, *plu4891* was not able to fully convert AQ-256 into the methylated derivative indicating that *plu4891* either exhibits less enzymatic activity or has a lower turnover rate in general in comparison to *plu4895*. Here, the question arises whether the lower conversion rate occurs as a result of lower enzymatic activity or if putatively less intracellular enzyme copies are part of the reason. Unpublished data showed that the promoters located in front of the respective MTs account for similar transcription rates, which suggests that the different conversion rates result out of different enzymatic activities. Furthermore, the single expression of *plu4890* led to the production of a single methylated AQ derivative AQ-270c that has not been observed to be produced in the wildtype. Exactly like the single expression of *plu4891*, the strain was not able to fully convert AQ-256 into the single-methylated derivative after 72h. The absence of AQ-270c in wildtype extracts after 72h of cultivation can be explained by one of the following postulations: Either, AQ-270c undergoes conversion by *plu4895* subsequent to its formation or *plu4890* is only responsible for the second-step tailoring of AQ-270a into AQ-284a *in vivo*. In addition, the attempt to activate the *in vivo* inactive MTs *plu4892* and *plu4894* *in vitro* through active site mutagenesis failed. These findings indicate that *plu4892* and *plu4894* are indeed not active on any AQ-substrate in *P. luminescens subs. TT01*. Interestingly, both encoding genes are still expressed under laboratory conditions which may point towards different targets for methylation other than AQs. Since the expression of single MTs did not result in any double-methylated derivatives, deletion mutants were generated that harbored combinations of the active MTs on their genome. Here, both  $\Delta$ *plu4894-4892* and  $\Delta$ *plu4894-4891* yielded two AQ-284 derivatives that were subsequently elucidated as AQ-284a/b. Thus, this confirms the involvement of *plu4890* and *plu4895* as the MTs responsible for the formation of AQ-284 derivatives. In contrast, *plu4891* is not necessary for the generation of the latter *in vivo*. In summary, it was shown that the active MTs *plu4890*, *plu4891* and *plu4895* are responsible

for generation of single methylated AQ-270 species, while combinatorial activity of plu4890 and plu4895 yielded double methylated AQ versions. These findings were congruent with the observations made *in vitro* with purified MTs and AQ-256 as the substrate. Importantly, *in vitro* assays with purified MTs and AQ-270 derivatives allowed clarification of the exact methylation patterns regarding double-methylated derivatives. As expected, plu4895 was active on the purified AQ-270c (produced by plu4890) derivative resulting in AQ-284b which also showed to be the main AQ-284 derivative produced *in vivo*. In addition, plu4890 converted AQ-270a (produced by plu4895) into AQ-284a as second AQ-284 derivative observed *in vivo*. Interestingly, plu4890 was also active on AQ-270b (produced by plu4891) which stands in contrast to the findings made in section 6.1.3. Additionally, when using AQ-270c as a substrate for its own responsible MT plu4890, a small UV-signal corresponding to the mixture of AQ-284a/b was observed. Finally, when combining plu4895 with AQ-270b a small UV-signal corresponding to AQ-284b was detectable. These findings fortify the assumptions made for the rather unspecific methylation patterns of plu4895 and plu4890. While both are clearly responsible for the formation of double-methylated derivatives, their positions of methylation are not distinct. It has been reported before, that MTs can form heterodimeric structures to yield substrate-specific enzyme complexes.<sup>170</sup> In case of the MT variants found in *P. luminescens* this does not seem to hold true as single versions of MTs were solely active on single-methylated AQ-derivatives. Whether they do form homodimeric structures remains unclear. For this, co-crystallization experiments could uncover the underlying protein organization. In essence, the *in vitro* approach confirmed the findings of the *in vivo* experiments and additionally unraveled underlying mechanisms for the formation of multi-methylated AQs. Ultimately, a comprehensive scheme of MT methylation patterns is displayed in Fig. 54.

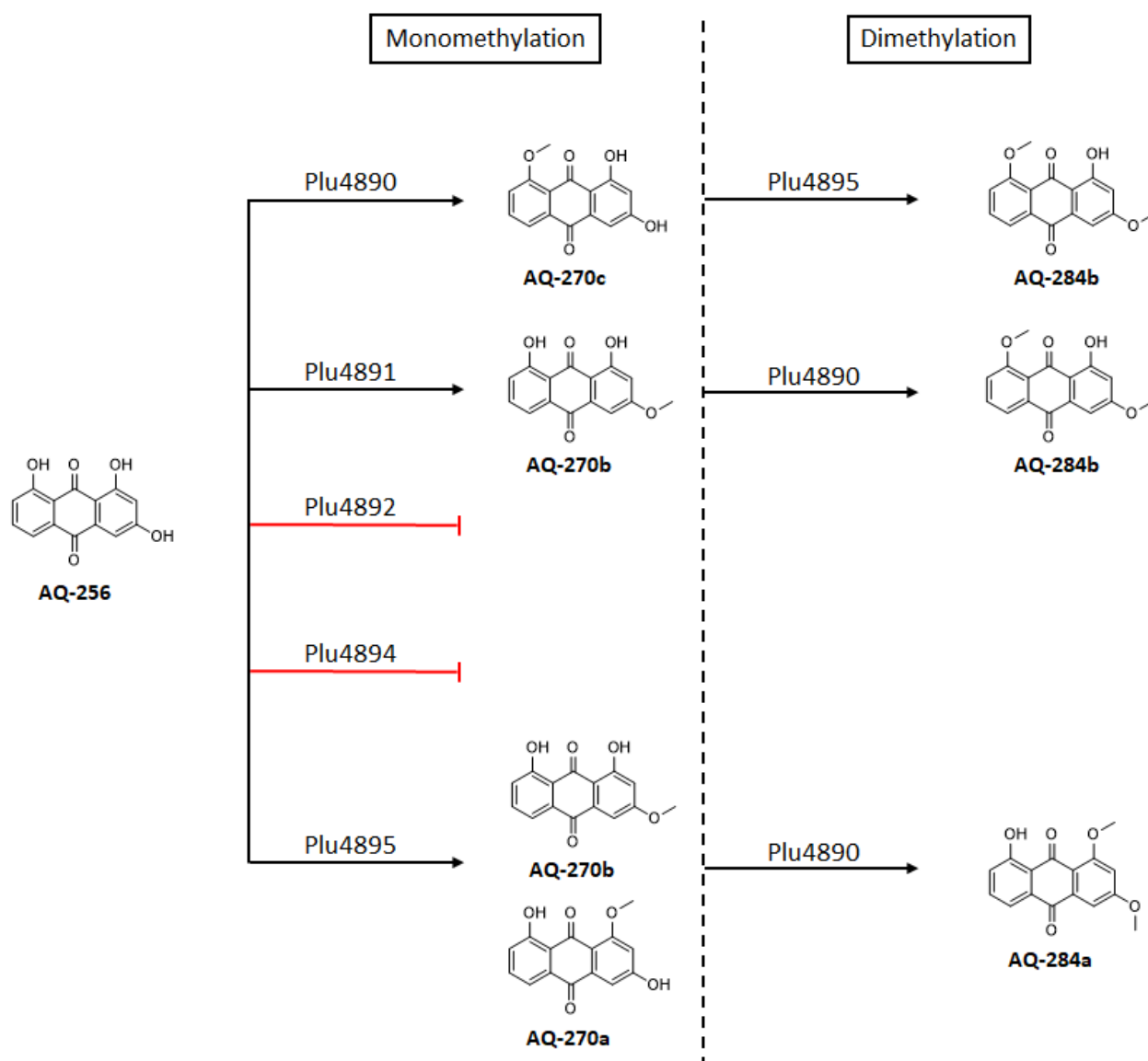


**Fig. 54** Overview of AQ-256 methylation patterns and corresponding enzymes. Plu4890, Plu4891 and Plu4895 catalyze the formation of monomethylated AQ derivatives at distinct positions, but can also synergistically produce two dimethylated versions of AQ-256, AQ-284a/b. Sequential involvement of Plu4895 and Plu4890 leads to formation of AQ-284a, while sequential action of Plu4890 and Plu4895 results in AQ-284b. Additionally, low levels of AQ-284b are formed through sequential action of Plu4891 and Plu4890 *in vitro*.

### 7.1.2 Monooxygenase plu0947 has an effect on AQ formation

In section 6.2.4, it was shown that the MO plu0947 is involved in AQ formation as deletion resulted in significantly decreased AQ production titers. Interestingly, the impact on formation of AQ-284a/b was higher in comparison to AQ-270a/b. These observations indicate that plu0947 not only is involved in AQ biosynthesis in general, but also potentially has an effect on the activity of plu4890. Whether this effect occurs on protein -or transcript level is unclear. Unpublished results showed that deletion of the gene cluster *rdpA-C* responsible for

production of rhabdopeptides in *Xenorhabdus nematophila* shut down production of unrelated xenortides. Crucially, xenortide production was restored upon reintegration of the first 500 bp of *rdpA*, despite still no rhabdopeptides being produced (Alexander Rill, unpublished results). This interaction could point towards synergistic mRNA stabilization. In order to investigate the presence of such an effect, transcriptomic analysis would have to be conducted in a  $\Delta plu0947$  background with respects to the transcript levels of the respective MTs. On the same note, *plu0947* could have an effect on protein stability, although unlikely, as the purified MTs exhibited activity in conversion assays in absence of *plu0947*. Finally, *P. luminescens*  $\Delta MT \Delta plu0947$  needs to be generated to investigate the impact of the MO on AQ-256 production in general.

### 7.1.3 Different *Photorhabdus* species show different AQ product spectra

Bioinformatic analysis revealed that all investigated *Photorhabdus* species (Fig. 21) carry the genes encoding for *plu4895-plu4890* in their genomes with the only exception being *P. temperata* that is missing *plu4895*. Interestingly, the respective MTs thoroughly show a high amino acid sequence similarity to the ones identified in *P. luminescens* TT01 (>90%). Again, the exception being *P. temperata*. Here, *plu4891* and *plu4894* only show amino acid sequence similarity <80%, while *plu4892* is 81.1% similar. Additionally, *plu4890* is located 2000 kb apart from the other MTs. Typically, with the MTs being highly conserved features in all investigated *Photorhabdus* species, the assumption that the respective AQ product spectra would exhibit the same compounds seemed obvious. Contradictory, the AQ product compositions differed significantly between the respective strains. *P. luminescens subs. akhurstii* features the highest similarity among all MTs in comparison to the other *Photorhabdus* strains to *P. luminescens subs. TT01*. Similarly, the strain shares the AQ product spectrum with *P. luminescens subs. TT01*. Interestingly, the overall amounts of produced AQ in *P. luminescens subs. akhurstii* were significantly reduced in comparison to *P. luminescens subs. TT01*, especially regarding AQ-270a, which is the main compound produced by *P. luminescens subs. TT01*. Additionally, unlike *P. luminescens subs. TT01*, *P. luminescens subs. akhurstii* does not fully convert the entire precursor AQ-256 into methylated derivatives. Here, lower levels of methylated Aqs stands in agreement with an overall reduced AQ production. Furthermore, *P. temperata* shows a different AQ product spectrum. In this case,



no single-methylated AQ derivative is detectable, while both double-methylated AQ-284a/b are still present. Crucially, the strain is the only investigated *Photorhabdus* species that is capable of producing a triple methylated AQ-314 derivative. The absence of AQ-270a is congruent with the missing *plu4895*. However, it is not clear, how AQ-284a/b are formed without the presence of *plu4895* as the combination of *plu4891* and *plu4890* did not yield any multi-methylated AQs in *P. luminescens* *in vitro* assays. Pivotaly, the amino acid similarity between the respective MTs of *P. temperata* and *P. luminescens* differs vastly, explaining possible shifts in AQ derivative compositions. In the following, the involvement of the different MTs found in *P. luminescens subs. akhurstii* and *P. temperata* is postulated (Fig. 55).

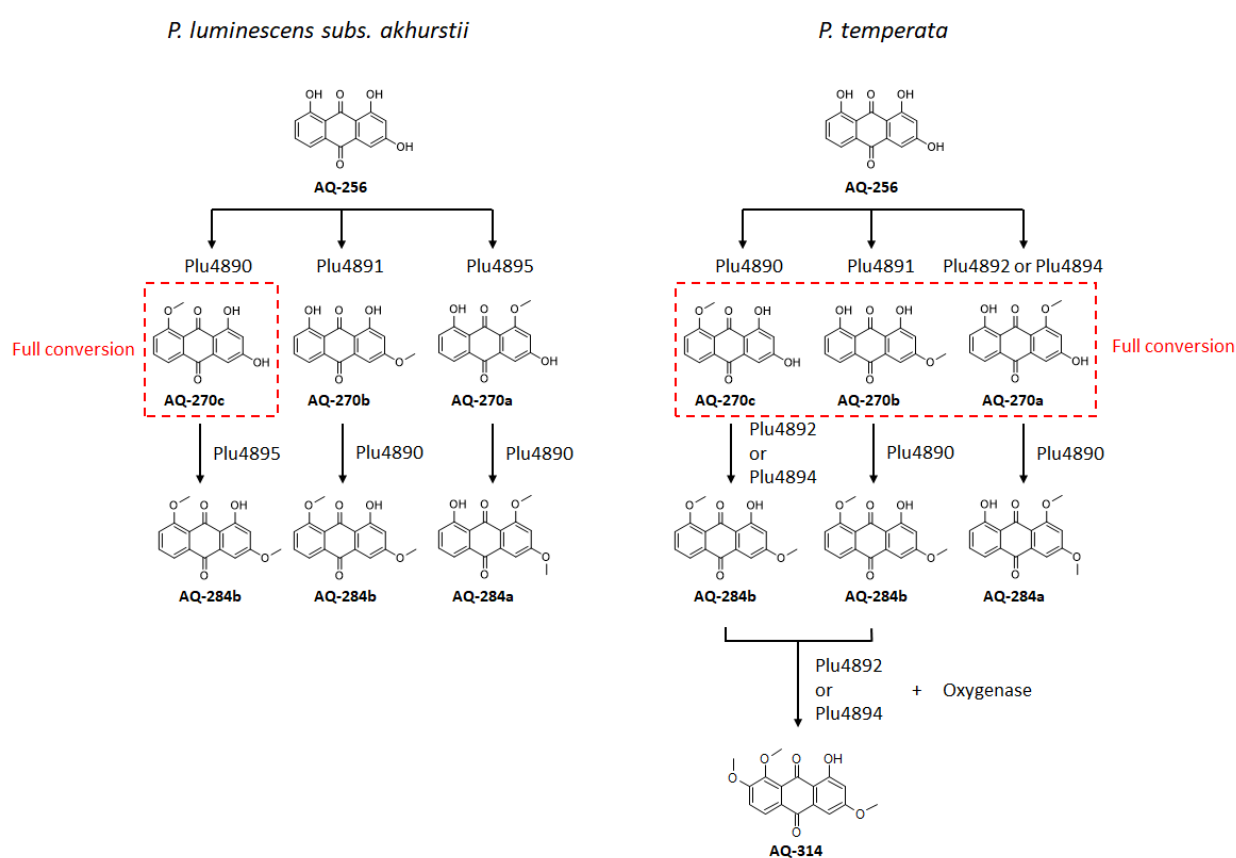


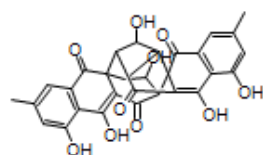
**Fig. 55.** Involvement of the different MTs in *P. luminescens subs. akhurstii* and *P. temperata*. *P. luminescens subs. akhurstii* shows the same product spectrum as *P. luminescens subs. TT01* and thus the MTs involved in product formation are assumed the same. In case of *P. temperata*, either Plu4892 or Plu4894 presumably complements the missing Plu4895. Additionally, it is postulated that Plu4892 or Plu4894 are involved in AQ-314 formation.

In case of *P. luminescens subs. akhurstii*, it is predicted that the same MTs (Plu4890, Plu4891 and Plu4895) are active and involved in AQ diversification as in *P. luminescens subs. TT01*. AQ-270c presumably is not detectable in culture extracts because it is immediately converted to AQ-284b as in *P. luminescens subs. TT01*. For *P. temperata*, the missing Plu4895 is presumably

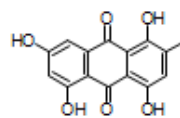
complemented by either Plu4892 or Plu4894. The high differences in AA similarities of the respective MTs in *P. temperata* in comparison to *P. luminescens subs. TT01* may also explain why it is the only strain capable of producing AQ-314. Crucially, the formation of AQ-314 demands a hydroxylation of AQ-284b prior to methylation. While the involved hydroxylase remains unknown, the methylation is presumably catalyzed by either plu4892 or plu4894. Additionally, all mono-methylated AQ species are probably fully converted to double-methylated variants. In contrast, *P. luminescens subs. namnaonensis* PB45.5, *P. luminescens subs. hainanensis* and *P. bodei* do not exhibit any AQ production at all under laboratory conditions despite harboring homologues of *antA-I*. Crucially, these strains do not harbor *antJ* in their respective genomes. Potentially, AQ biosynthesis is regulated by a regulatory system that is different than the one found in *P. luminescens subs. TT01*. The question whether these strains exhibit AQ production in a natural environment could be tested in insect infection assays in combinations with nematodes, as it was shown in 6.3.9. Additionally, putative transcriptional activators could be identified in a pulldown assay as it was described for *antJ*<sup>77</sup>. In all of the above cases, a similar *in vitro* approach as presented for MTs from *P. luminescens* could elucidate the possibly underlying methylation patterns. Purifying the MTs of the respective strains and subsequent *in vitro* conversion assays with AQ-256 and mono-methylated AQ species could possibly elucidate the respective enzyme specificities and their activity. Additionally, *in vivo* experiments with deletion mutant strains expressing only one MT-encoding gene would verify which MT is active *in vivo*.

#### **7.1.4 Putative functions of AQs**

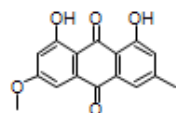
While the function of AQs produced by *Photorhabdus* remained unknown in an ecological context, AQs in general are among the most investigated groups of NPs regarding their mechanism of action.<sup>171</sup> Critically, AQs produced by plants, fungi and other microorganisms exhibit a plethora of biological activities.<sup>172</sup> In the following, different AQ derivatives with an assigned biological role from various organisms are depicted (Fig. 56).



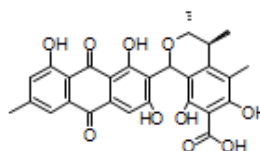
Rugulosin



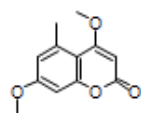
Catenarin



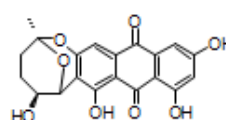
Physcion



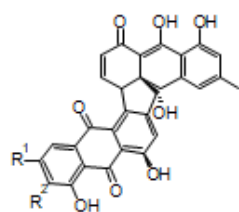
Penicillanthranin A



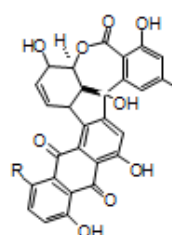
Siderin



Nidurufin



Torrubiellin A    R1=R2=H  
B                    R1=R2=OH



Rubellin A    R=H  
B                    R=OH

**Fig. 56.** Bioactive AQs and analogues produced by various organisms. Rugulosin from *Hormonema dematioides*, Physcion from *Microsporium* sp, Siderin from *Halimeda opuntia*, Torrubiellin A and B from *Torrubiella* sp., Catenarin from *Drechslera teres*, Penicillanthranins from *Penicillium citrinum*, Nidurufin from *Aspergillus versicolor*, Rubellin A and B from *Ramularia colloocygni*.

Rugulosin was isolated from the fungus *Hormonema dematioides* and showed insecticidal activity against budworm larvae.<sup>173</sup> Additionally, physcion produced by the fungus *Microsporium* sp. exhibited cytotoxic effects on human cervical carcinoma HeLa cells as it caused the formation of reactive oxygen species (ROS).<sup>174</sup> Furthermore, siderin found in extracts of the seaweed *Halimeda opuntia* showed moderate antibacterial activity against *B. subtilis*, *B. cereus*, and *S. aureus*. The two dimeric AQs torrubiellin A and B were isolated from the insect-scavenging fungus *Torrubiella* sp. and exhibited a broad range of biological activities such as insecticidal, antifungal, and antibacterial effects.<sup>175</sup> In addition, while

catenarin from the fungus *Drechslera teres* was biological active against Gram-positive bacteria and fungi<sup>176</sup>, penicillanthranins A and B synthesized by *Penicillium citrinum* showed a general antibacterial activity.<sup>177</sup> Importantly, nidurufin from *Aspergillus versicolor* had antibacterial activity against several clinical isolates of Gram-positive strains.<sup>178</sup> Finally, the fungus *Ramularia colloocygni* produced rubellin A, which increased photodynamic oxygen activation<sup>179</sup> and rubellin B, which exhibited antibacterial activity.<sup>180</sup>

Generally, production of NPs has been observed to be crucial to maintain the symbiosis of *Photorhabdus* with their respective host, and especially for insecticidal activity.<sup>42,181,182</sup> Interestingly, Crawford and colleagues could show that the production of various NPs such as AQs is stimulated when supplementing cultures with insect hemolymph.<sup>56</sup> As described above, various AQ derivatives from different classes of organisms exhibit a plethora of biological activities, which include insecticidal and antibacterial effects. Although it has been shown that the loss of AQ production in *Photorhabdus* does impair neither the mutualistic interaction with the nematodes, nor pathogenicity towards insects<sup>74</sup>, it is still feasible that they contribute to either thereof. Insect killing assays were only performed in a  $\Delta antH$  background where still an array of NPs are produced that exhibit insecticidal effects such as rhabduscin.<sup>40</sup> Consequently, AQs could potentially not be mandatory for insect killing but add to the overall arsenal of tools that *Photorhabdus* utilizes. Furthermore, the examples of torrubellin A/B and rubellin A/B, respectively, showed that even minor modifications of a NP are sufficient to result in vastly different activities. In case of *Photorhabdus*, the different produced AQ variants could play specialized roles in their respective subspecies. As it was shown in chapter 6.1.10, the AQ compositions between the different *Photorhabdus* strains differs vastly. Importantly, the respective strains were isolated from diverse habitats with different environmental conditions such as Cuba, Russia, the Netherlands, USA, Trinidad, Dominican Republic or Israel.<sup>183</sup> Here, different AQ derivatives could be utilized to overcome challenges like varying food competitors or modified immune responses of the respective prey. In order to investigate possible ecological functions of the respective AQ derivatives produced by various *Photorhabdus* strains, multiple experiments could be conducted. Firstly, pathogenicity assays and nematode development assays with different MT deletion mutants of certain *Photorhabdus* species could mediate a better understanding of a possible biological or ecological activity of certain derivatives. In this case, it would also be crucial to use insects

that populate the same habitats as the respective strains. Furthermore, isolated AQ variants could be tested on a vast amount of different organisms with respects to their biological activity. In essence, it has been shown that Aqs produced by different classes of organisms exhibit various functions. However, the role of Aqs produced by *Photorhabdus* remains speculative and needs further investigations.

### **7.1.5 Conclusion and Outlook**

The five MTs plu4895-4890 were identified on the genetic level and were found to be putatively involved in AQ-256 modification. *In vivo* and *in vitro* studies confirmed activity for three of them (plu4895, plu4891, plu4890) towards AQ-256 and revealed certain specificities. While each enzyme produces a mono-methylated AQ variant, sequential action of two of them (plu4895, plu4890) is sufficient to yield double-methylated derivatives. While the generation of methylated AQ species has been studied extensively in this work, the identification and description of the MO plu0947 emerges new questions with respects to the regulatory machinery behind the AQ biosynthesis. In order to address these questions, both transcriptomic and proteomic analysis could provide crucial information for a better understanding thereof. Although the biological activity of the respective AQ derivatives remains to be tested, Aqs are known pigments and their weak antibiotic activity might contribute to the insecticidal symbiosis of *P. luminescens* and *H. bacteriophora*. Considering that the scaffold of AQ-256 is also shared by other NPs which are applied in several clinical studies, the here presented results might offer new routes for engineering PKS II-based biosynthetic pathways and expanding the chemical diversity of biologically active compounds in the future.

## **7.2 Topic B: AQ overproduction in *Photorhabdus* for redox flow batteries**

Greenhouse gas neutrality represents one of the key challenges that the modern world is facing in order to counteract human caused climate change and is concomitant with the invocation for innovative technologies regarding a turnaround in energy policy.<sup>79</sup> The German government developed a five-point approach in order to establish greenhouse gas neutrality until 2050.<sup>79</sup> Here, one of the key aspects is represented by the utilization of residual waste

streams for energy generation and storage. Consequently, with increasing demand for energy from renewables, reliability of power supply is crucial and requires expansion of the power grid and establishment of decentral energy storage.<sup>80</sup> Currently, while the power generation in Germany lies within the range of TWh, the energy storage capacity of battery-based systems is limited to kWh.<sup>81</sup> Thus, in order to overcome these limitations, researchers heavily focus on advancement of lithium-ion batteries and development of novel redox-flow batteries. In 2014, a quinone-based redox-flow battery was developed by scientists in Harvard.<sup>85</sup> However, the harvest of the respective electrolytes is connected to high operating expenses.<sup>86</sup> Consequently, this work described an alternative biotechnological approach to produce the quinone-derived AQ-256 that can be utilized as an electrolyte in redox-flow batteries.

### **7.2.1 Manipulation of AQ biosynthesis in *P. luminescens***

Specific regulation of NP production is of major importance during the life cycle of *P. luminescens* as they fulfill various critical tasks.<sup>60,64,184</sup> In case of the AQ BGC, the pathway-specific regulation is mediated by AntJ, a transcriptional activator that exclusively activates AQ biosynthesis. Interestingly, AntJ is only the second described example of a pathway-specific transcriptional activator in *P. luminescens*, which is encoded in the same locus as the regulated BGC.<sup>77</sup> Generally, pathway-specific regulators harbor tremendous potential as tools for pathway engineering and manipulation of product yields. It has been previously shown that overexpression of pathway-specific regulators can result in higher productivity.<sup>185,186</sup> When comparing relative AQ-256 production in  $\Delta MT$  background, plasmid-based overexpression of *antJ* led to increase of 3.2-fold. Additionally, in a second approach, deletion of the Sfp-type PPTase NgrA was introduced in order to shut down NP production other than AQ biosynthesis. For NRPS –and PKS-derived NPs, the production is strongly dependent on activity of phosphopantetheinyltransferases (PPTase).<sup>66</sup> The PPTase converts inactive *apo*-acyl-carrier-proteins (ACPs) (part of PKS) or *apo*-peptidyl-carrier-proteins (PCPs) (part of NRPS) to their respective *holo* forms by posttranslational transfer of the 4'-phosphopantetheinyl (P-pant) moiety of coenzyme A to the side chain of a conserved serine residue in each carrier protein domain. The underlying idea was to increase the availability of malonate building blocks for AQ biosynthesis by preventing the production of other NPs.

Indeed, upon deletion of *ngrA* the AQ-256 production was elevated by 2.5-fold in  $\Delta MT \Delta ngrA$ . Logically consistent, the two approaches were combined and resulted in an increase in production by 7.2-fold, which accounted for a production titer of 253 mg/l in LB medium. Interestingly, production was elevated above the sum of the separate approaches when combined, which could indicate, that the PKS II system is limited in its native state by the availability of building blocks. Possibly, AQ production could be increased further through disruption of malonyl-dependent pathways such as parts of the fatty acid biosynthesis as already performed in *E. coli*, *S. cerevisiae* and *C. glutamicum*.<sup>187</sup> Crucially, the research of Yang *et al.* utilized the usage of CRIPR/Cas9-based RNAi-constructs in order to mediate inhibition of genes like *fabH* and *fabF*. Here, in order to employ such an approach in *Photorhabdus* strains, the CRISPR/Cas12 system (developed by Alexander Rill, unpublished results) needs to be refined further as, hitherto, only generation of deletion and promoter exchange constructs is possible while RNAi-mediated manipulation of gene expression has not been employed, yet. Finally, in a third approach, the involvement of *plu0947* in AQ biosynthesis was investigated. In preliminary work, it was shown that the mRNA levels of *plu0947* and *plu0948* were strongly downregulated in a  $\Delta antJ$  background.<sup>37</sup> While BlastP analysis identified *plu0947* as a MO, *plu0948* was predicated as a transcriptional regulator. Previous work already considered *plu0947* to be putatively involved in AQ formation through introduction of the quinone-oxygen but its role has not been investigated, yet. Crucially, while the deletion of *plu0948* had no effect in AQ production, the deletion of *plu0947* decreased AQ levels significantly, yet AQ formation did not disappear completely. These findings suggested that, while not being essential for AQ biosynthesis in general, *plu0947* supports the product formation. However, as the subsequent *in trans* overexpression of *plu0947* did not increase AQ yields, it was not further pursued as a vital target for metabolic engineering. In essence, it was shown that generally, strain engineering harbors great potential for applications in pharmaceutical, chemical or cosmetic industries as the production titers of desired compounds can be elevated significantly.

### 7.2.2 Utilizing the ecological background of *Photorhabdus* to develop a NP production medium from waste residues

The German government developed a five-point approach in order to establish greenhouse gas neutrality until 2050.<sup>79</sup> Here, one of the key aspects is represented by the utilization of residual waste streams for energy generation and storage. Crucially, we wanted to establish a cost efficient AQ production medium and moreover being compatible and consistent with environment conservation guidelines. For this reason, major parts of the media contents were taken from recyclable waste products. Additionally, the ecological background of *Photorhabdus* was utilized to significantly increase AQ titers in the respective production medium. Preliminary data<sup>153</sup> suggested that XPP medium allows compound extraction with considerably low background in comparison to LB and additionally, production titers of certain NPs are elevated. Thus, XPP medium was used as the basis for medium generation. An amino acid screening of the respective medium contents revealed that presence of arginine, histidine, cysteine, isoleucine, phenylalanine, methionine and valine exhibited significant positive effects on AQ production. While cysteine, isoleucine and phenylalanine can be converted to acetyl-CoA<sup>188</sup> which is used for PKS-related building blocks, arginine, histidine, methionine and valine are converted to  $\alpha$ -ketoglutarate or succinyl-CoA and funneled into the TCA cycle.<sup>189</sup> Additionally, in a vitamin screening, only thiamine and pantothenic acid had a positive effect on AQ-256 biosynthesis. Recent research revealed that certain class B vitamins can modulate the human gut microbiome in terms of metabolic activity.<sup>190</sup> Subsequently, the improved XPP medium was used as the basis for residual waste stream media testing. In preliminary work, the influence of simulating the insect host environment was assayed for alterations on NP production<sup>154</sup>. It was shown, that supplementing insect homogenate from *Galleria mellonella* larvae to LB cultures altered the NP profile of *P. luminescens*. Crucially, NPs like AQs and isopropylstilbene (IPS) were overproduced. Unfortunately, *Galleria mellonella* larvae are not recyclable waste products, costly and thus not suited for generating an inexpensive NP production medium. In an extensive literature research, two insect candidates were identified that are cost efficient to obtain and part of industrially recyclable waste products. Firstly, the black soldier fly (*Hermetia illucens*) is an insect that can be grown and harvested without dedicated facilities and is not pestiferous<sup>88</sup>. Importantly, their biggest advantage over other insects is their ability to convert waste into food, generating value and closing nutrient loops as they reduce



pollution and costs. Secondly, the silkworm (*Bombyx mori*) is industrially used for silk production. However, after entering pupal phase, the silk cocoons are harvested while the silkworms remain as leftovers. Both XPP insect media resulted in a higher production of the selected NPs in comparison to XPP medium. In case of the XPP medium supplemented with powder from *Hermetia illucens*, the AQ production was elevated by 1.5-fold. Furthermore, using insect powder from *Bombyx mori* resulted in an increase in AQ levels by 2.4-fold. Finally, continues extraction of secreted AQ with XAD-16 doubled the production titers ultimately leading to a productivity of >1 g/l. Majorly, similar approaches in different organisms yielded only 100-250 mg/l of comparable PKS-derived compounds in different organisms.<sup>191</sup>

### 7.2.3 Conclusion and Outlook

Based on the results obtained through manipulation of AQ biosynthesis on a genomic and ecological level, a schematic illustration is presented that shows the fundamental process behind biotechnological redox flow batteries (Fig. 56). In the depicted approach, the electrolytes are fermentatively overproduced by *P. luminescens*, harvested and subsequently inducted into the reactor. In order to further induce AQ overproduction, insect powder from residual waste products of the silk industry in the form of *Bombyx mori* is used. Generally, it was shown, that understanding the ecological context of *Photorhabdus* was crucial for elevation of AQ production. Majorly, this work showed the tremendous potential that is held by the combination of medium optimization and genetic manipulation to increase NP production while additionally making use of ecological friendly resources. Reaching AQ production titers of over 1 g/l shows, that *P. luminescens* is capable of producing NPs in industrial scales, which makes it a competitive model organism for industrial NP production in general. Crucial for this work, a prototype battery was already employed by CMBlu Energy AG (unpublished results). Here, AQ-256 exhibited a redox activity thus making it a suitable electrolyte for energy storage in redox flow systems (shown in supplementary Figure S32). In future work, as already discussed, genomic manipulation with RNAi-based techniques could potentially increase the AQ yields even further<sup>187</sup> and allow for an easier extraction, as the production of undesired metabolites could be inhibited. In essence, this work showed that *P. luminescens* harbors great potential for industrial NP production in general. Additionally, efficient microbe-facilitated electrolyte production for redox-flow systems opens the gates

for ecological friendly energy storage which is crucial to combat human-caused climate change.

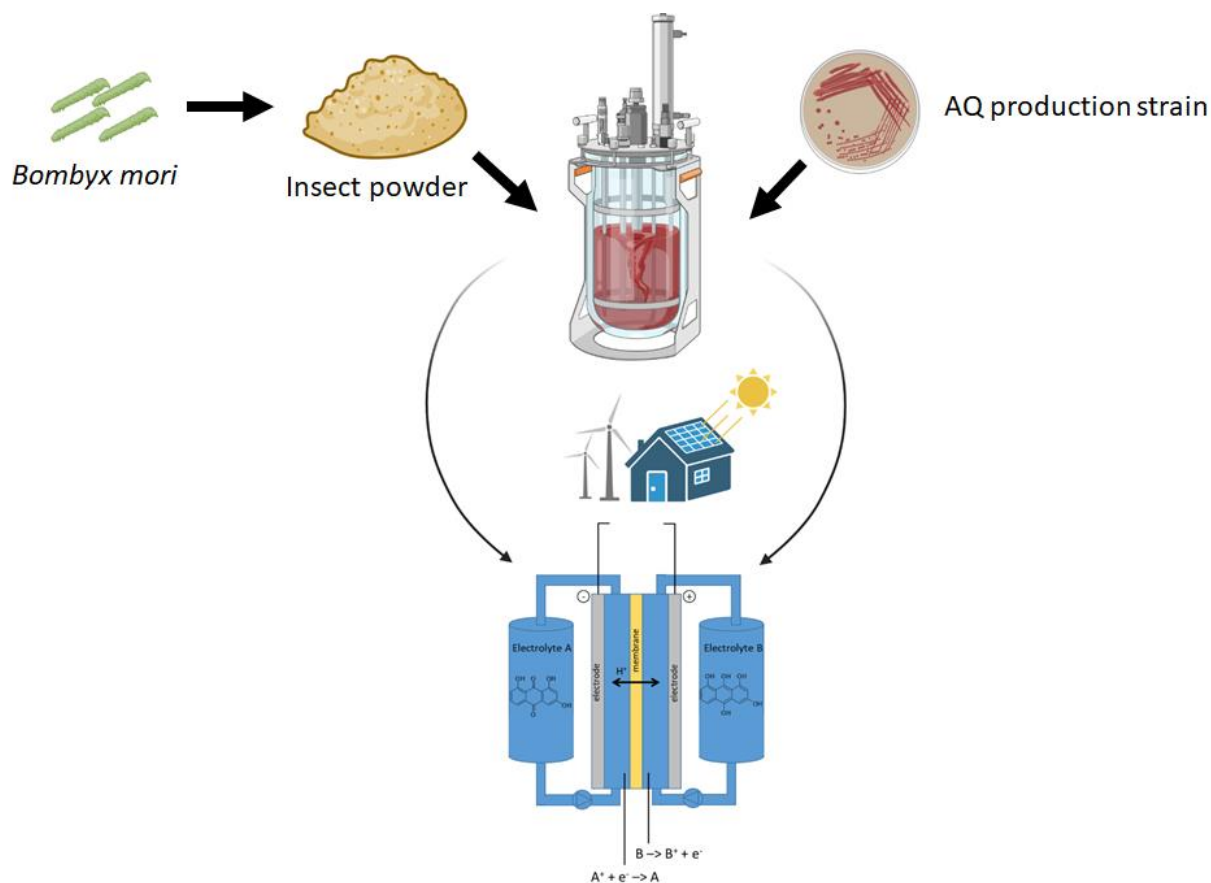


**Fig. 56.** Schematic illustration of a redox flow battery that facilitates quinone-derived electrolytes to store energy produced by renewable energy sources. In the depicted approach, the electrolytes are fermentatively overproduced by *P. luminescens*, harvested and subsequently induced into the reactor. To further induce AQ overproduction, insect powder from residual waste products of the silk industry in the form of *Bombyx mori* is used. Figure was partially generated with biorender.com.

### 7.3 Topic C: Elucidation of a putative terpenoid cluster in *Photorhabdus*

Within its complex life cycle, *Photorhabdus* produces an array of NPs, which exhibit various functions such as nematode development, protection against the prey's defensive immune response or mediate cell-cell communication.<sup>58-61</sup> These NPs are produced by activation of a specific set of BGCs in distinct stages of their life cycle. A combination of antiSMASH and blastP analysis revealed the presence of a highly conserved BGC in several *Photorhabdus* species predicted to be responsible for terpenoid biosynthesis. Interestingly, upstream of the BGC, a

gene putatively encoding a carotenoid oxygenase protein is located. Transcriptome analysis revealed that the BGC remains silent under laboratory conditions. Carotenoids are one of the most widely spread and ubiquitous compounds, which are found in plants, algae, bacteria and fungi.<sup>106</sup> In terms of application, carotenoids play a versatile biological role that crucially contribute to therapeutic effects.<sup>107–117</sup> Thus, carotenoid-derived compounds represent an attractive research field for pharmaceutical applications. This topic focused on characterization of the cluster. Here, the generated products were elucidated and their putative ecological function was investigated.

### **7.3.1 $\beta$ -carotene as the product of core gene expression**

In a recent publication<sup>149</sup>, it was shown that an engineered *E. coli* BL21 strain is able to produce lycopene through a combination of plasmid-based and genomic expression of different pathways. Firstly, the strain harbors the genes encoding the MEV pathway for overproduction of isoprenoid building blocks on its genome. Secondly, the genes for lycopene biosynthesis were introduced in a plasmid-based approach. Hence, it was employed in order to elucidate the products of the carotenoid BGC from *P. luminescens*. Upon expression of the carotenoid core genes,  $\beta$ -carotene production was detected. Blastp analysis revealed that the core genes are homologues of bacteria-derived *crtB*, *crtE*, *crtI*, *crtY*, and *fni* genes. It has been shown before that *crtB*, *crtE* and *crtI* are responsible for converting isopentenyl diphosphate yielded by the MEV pathway into lycopene in multiple steps.<sup>192</sup> While *crtE* catalyzed the formation of geranylgeranyl diphosphate (GGPP) from farnesyl diphosphate (FPP), *crtB* converts GGPP into phytoene. Finally, phytoene is converted into lycopene by *crtI*.<sup>192</sup> Ultimately, *crtY* is responsible for the formation of  $\beta$ -carotene. A pathway is postulated based on the findings in Fig. 57. In essence, these findings harmonize well with the literature.

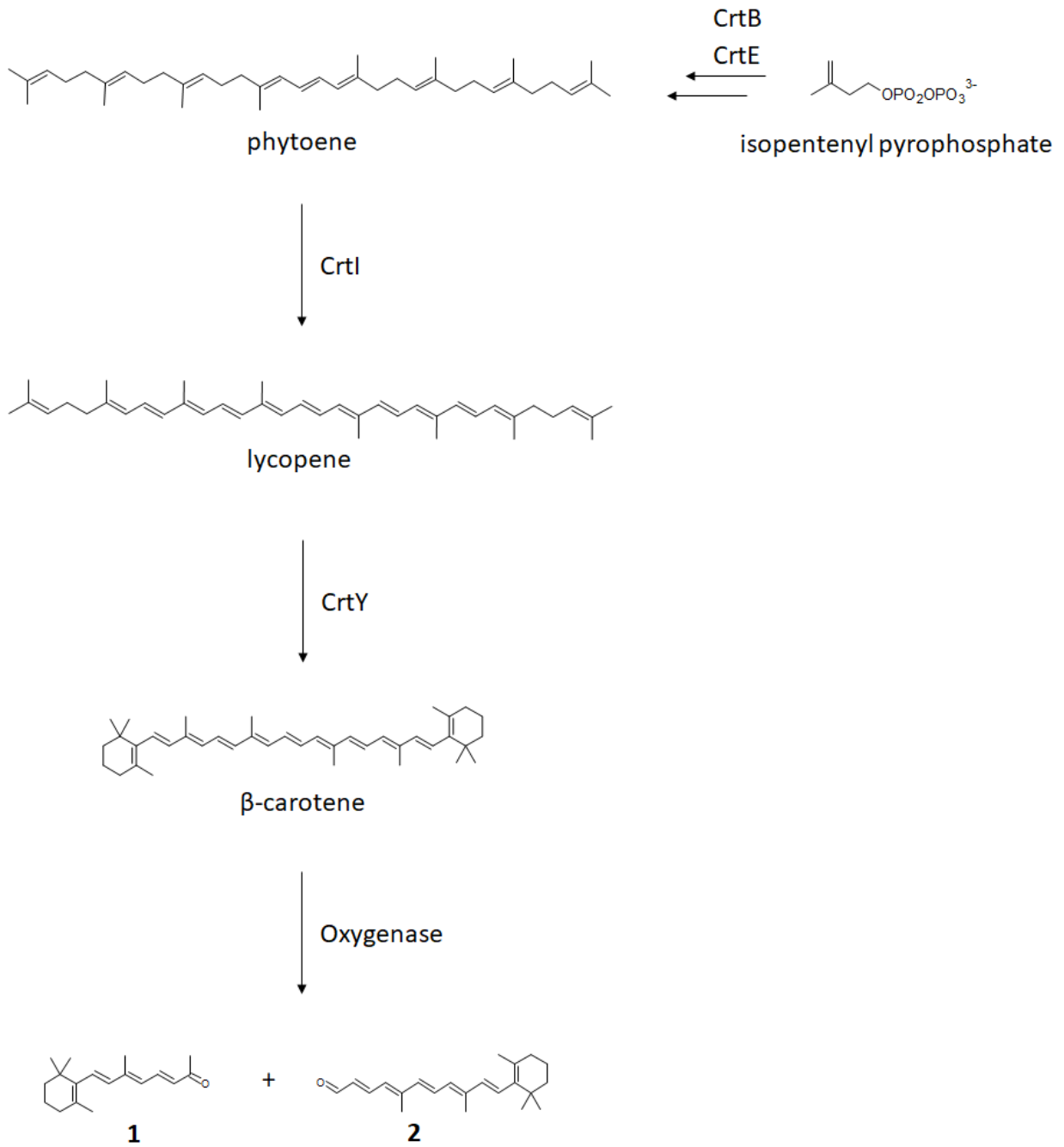


**Fig. 57.** Postulated carotenogenesis pathway in *P. luminescens*. CrtB and CrtE catalyze the formation of phytoene in multiple steps. Subsequently, CrtI converts phytoene into lycopene, which is further processed to result in the formation of  $\beta$ -carotene. Finally, the oxygenase cleaves  $\beta$ -carotene in 1 and 2.

### 7.3.2 Cleavage of $\beta$ -carotene through BGC-associated CCD

In the next step, the role of the predicted CCD was investigated. Expression of the latter in a  $\beta$ -carotene producing *E. coli* led to the appearance of two new UV signals (**1** and **2**) at 8.1 with  $m/z$  259.205  $[M+H]^+$  and 8.9 min with  $m/z$  311.236  $[M+H]^+$ , respectively. Furthermore, the signal corresponding to  $\beta$ -carotene was only detectable in very low amounts, indicating a modification of the latter. Congruently, a phenotypical shift was observed as the deep orange color exhibited by  $\beta$ -carotene changed back to the original yellow color. Structural elucidation identified **1** as  $\beta$ -Apo-13-carotenone and **2** as  $\beta$ -Apo-14'-carotenal, respectively. Thus, it was confirmed that the CCD performs an asymmetrical cleavage reaction on  $\beta$ -carotene. Several carotenoid cleavage enzymes have been identified in plants, animals and microorganisms and grouped into different classes based on their substrate specificity.<sup>123–125</sup> In general, CCDs can be grouped by their ability to cleave carotenoids either symmetrically or asymmetrically.<sup>126</sup> In the following, the cleavage mechanism of the CCD from *P. luminescens* is proposed (Fig. 58). Presumably, dioxygen activation occurs via single electron transfer from Fe (II) generating a stabilized substrate radical intermediate. Next, single electron transfer to Fe (III) would generate a stabilized carbocation intermediate. The fact that the carotenoid harbors a conjugated polyene backbone, stabilizing the carbocation, supports this hypothesis. Finally, dioxetane formation results in a four-membered cyclo-dioxygen intermediate, which is subsequently cleaved into **1** and **2**. Crucially, a comparable mechanism has already been investigated for extradiol catechol dioxygenases or 2-oxoglutarate-dependent dioxygenases.<sup>193,194</sup> In vertebrates, BCO1 and BCO2 mechanistically are  $\beta$ -carotene 15,15'-oxygenase and  $\beta$ -carotene 9',10'-oxygenases that cleave  $\beta$ -carotene in either two all *trans* retinal molecules or  $\beta$ -ionone and  $\beta$ -Apo-10'-carotenal, respectively. In case of the CCD originating from *P. luminescens* the cleavage occurs eccentrically at the 13',14'-double bond, resulting in **1** and **2**. Generally, the biological roles of CCDs in bacteria are not well established. Studies on bacterial CCDs usually focused the attention on the purification of different enzymes and the determination of their specificity through their incubation with diverse carotenoid substrates. While often symmetrical cleavage of the target substrate was observed<sup>195–197</sup>, asymmetrical cleavage was also shown.<sup>198</sup>

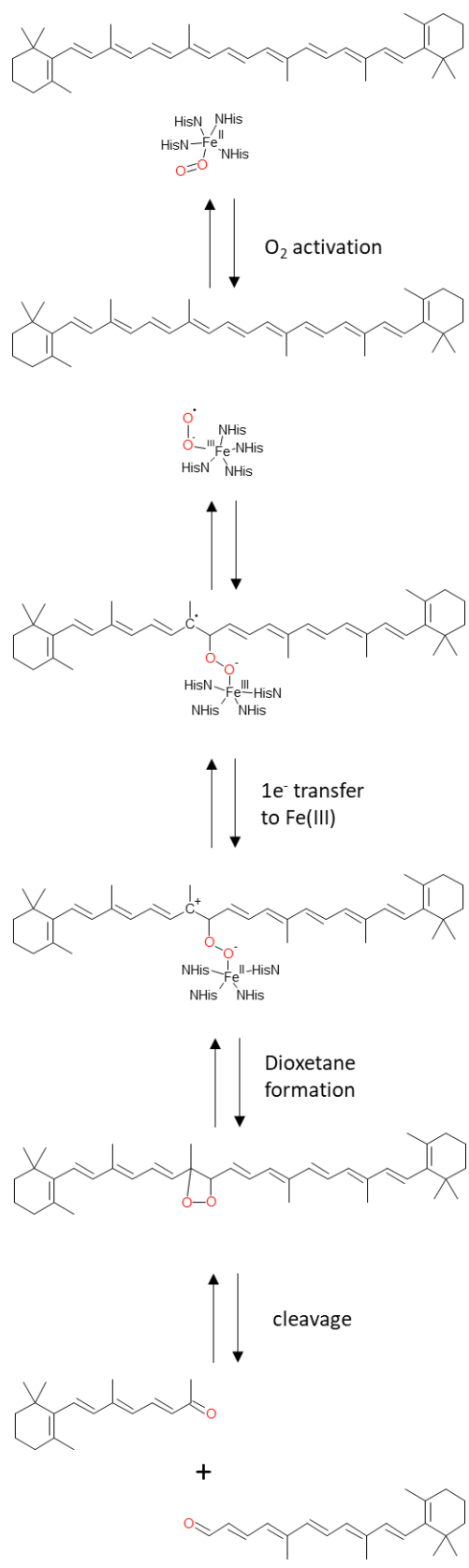


**Fig. 58.** Possible 13',14'-CCD mechanism for the cleavage reaction of  $\beta$ -carotene.

### 7.3.3 Carotenoid BGC is activated in insect environment

Once the insect prey is infected by *P. luminescens subs. TT01* and its associated nematode *Heterorhabditis bacteriophora*, both need to overcome the insect's immune system. Generally, retinoid derivatives regulate various physiological outputs in several classes of organisms by binding to nuclear hormone receptors (NHRs), retinoic acid receptors (RARs) or retinoid X receptors (RXRs)<sup>161</sup>. In case of *P. luminescens subs. TT01*, none of the compounds produced by the carotenoid cluster were detected under laboratory conditions. However, it was shown that upon infection of *G. mellonella* with only *P. luminescens subs. TT01*, **1** was detectable in crude extracts. Here concentration increased gradually over a period of 20 d. In contrast, production titers of **1** increased over 7 d when *G. mellonella* was infected with *P. luminescens subs. TT01* and its associated nematode until the levels decreased again. Firstly, these findings show that the BGC is activated in an insect environment and secondly that the cleavage products are either controlled by an additional underlying regulatory mechanisms or utilized by the nematode in a way.

### 7.3.4 Chimeric role of carotenoid BGC in *Photorhabdus* species

As it was shown in section 6.1.3, the carotenoid cluster is conserved in several *Photorhabdus* species. Consequently, it was shown that the production of **1** and **2** is universally featured in all of the analyzed strains that harbor fully functional versions of the BGC. Interestingly, the expression of the carotenoid cluster from *P. luminescens subs. PB45.5* did not result in any retinoid or carotenoid production possibly due to the absence of *fni* and truncation of *crtE*. However, expression of the CCD from *P. luminescens subs. PB45.5* in combination with *crtB*, *crtE*, *crtI*, *crtY*, and *fni* from *P. luminescens subs. TT01* resulted in the cleavage of  $\beta$ -carotene in **1** and **2**. On the same note, *Xenorhabdus sp. KJ12.1* is the only *Xenorhabdus* species that encodes a carotenoid oxygenase in its genome but without a fully functional BGC for carotenoid core production. Here, the CCD was also able to yield **1** and **2** from  $\beta$ -carotene. Consequently, as the production of **1** and **2** was a shared feature among all other *Photorhabdus* carotenoid clusters, the compounds presumably exhibit a certain function *in vivo*. Additionally, the respective CCDs never fully converted  $\beta$ -carotene into **1** and **2** suggesting that it also plays an ecological role in the bacteria's life cycle. In the case of *Xenorhabdus* and *Photorhabdus*, NPs play an essential role in cross-kingdom interactions with

nematodes, various insects, as well as bacterial and fungal species competing for the same food source<sup>9</sup>. Despite NPs playing a central role in the life cycle of the symbiosis, the exact ecological function for many of these compounds remains unknown.

### 7.3.5 Putative ecological role of $\beta$ -carotene in *Photorhabdus* species

In order to investigate a putative biological function of the compounds produced by the carotenoid cluster, the mutant strains *P. luminescens*  $\Delta$ oxygenase and *P. luminescens*  $\Delta$ carotenoid were tested in insect killing assays. *Galleria mellonella* infected with *P. luminescens*  $\Delta$ oxygenase died after 16.4 h on average, which was comparable to wildtype mortality levels, while infection with *P. luminescens*  $\Delta$ carotenoid killed the insects after 20.1 h on average and significantly later than the latter. As  $\beta$ -carotene is not known to exhibit an insecticidal activity, these findings indicate that it might have a protective function against the insect's immune system. Comprehensive analysis of the silkworm midgut responses to bacterial infection by transcriptome sequencing revealed that reactive oxygen species play a critical role in eliminating invading bacteria during early stage infections, while antimicrobial peptides work mainly during late stage infections<sup>199</sup>. Evidently, as  $\beta$ -carotene is known as a potent reagent against oxidative stress in different organisms, it is proposed that it also exhibits such a function in *Photorhabdus* during the infection cycle.<sup>200,201</sup> Thus, it is presumed that the bacteria exhibit an increased survivability rate against the insect's immune response when producing  $\beta$ -carotene, which results in a higher density of alive bacterial cells inside the insect subsequently killing it more efficiently.

Crucially, both, *Xenorhabdus* sp. KJ12.1 and *P. luminescens* subs. PB45.5 harbor the genes responsible for arylpolyene (APE) biosynthesis in their genomes, which are assumed to exhibit protection against oxidative stress<sup>202</sup>. In this case, it is postulated that the APE BGC complements the missing biosynthesis of  $\beta$ -carotene. This theory could be verified in a similar insect killing assay with a *Xenorhabdus* sp. KJ12.1 and *P. luminescens* subs. PB45.5  $\Delta$ APE mutants as shown in 6.3.9. Presumably, only the CCDs of both strains exhibit an ecological function whereas  $\beta$ -carotene as the substrate is scavenged by their associated nematode.



### 7.3.6 Putative ecological role of **1** and **2**

The findings presented in chapter 6.3.9 clearly display that the production of retinoid derivatives produced by *P. luminescens subs.* TT01 is induced after infection of insect prey. Additionally, the differences in NP levels of **1** when infecting *G. mellonella* with *P. luminescens subs.* TT01 and its associated nematode *H. bacteriophora* indicate that **1** is either presumably bound to a target entity or converted. Crucially, the identified FARs and NHRs are widely nematode specific features. *C. elegans* is known to utilize retinoid derivatives as signaling molecules for processes such as sex determination, molting, developmental timing, diapause, and life span<sup>160</sup>. In case of *H. bacteriophora*, several FARs and NHRs except FAR-1 are encoded as homologues in its genomes indicating related underlying regulatory networks. Importantly, *C. elegans* encodes two carotenoid dioxygenases BCMO-1 and BCMO-2 on its genome. Therefore, it is assumed that the required carotenoids are scavenged from its surrounding and subsequently cleaved into the desired retinoid derivatives. In case of *H. bacteriophora*, no homologues of BCMO-1 and BCMO-2 are encoded in its genome. Here, presumably the association with *P. luminescens* strains provides the retinoid substrate necessary for pathway activation. This hypothesis is further substantiated by the fact that *Steinernema carpocapsae*, which is mutualistically associated with *Xenorhabdus nematophila*, harbors homologues of BCMO-1 and BCMO-2 on its genome. Crucially, *Xenorhabdus nematophila* does not encode any terpenoid producing clusters on its genome nor does the strain harbor any putative CCDs. In order to elucidate the ecological role of **1** and **2**, developmental assays of axenic *H. bacteriophora* together with *P. luminescens* are necessary. Involvement in nematode development could be confirmed by monitoring physiological attributes such as size, lifespan or morphology of the respective nematodes when carrying either *P. luminescens* WT or *P. luminescens*  $\Delta$ oxygenase strains. Unfortunately, the generation of axenic *H. bacteriophora* renders difficult and needs an established protocol. Ultimately, an ecological function for the whole carotenoid BGC is proposed based on all findings described above (Fig. 57).

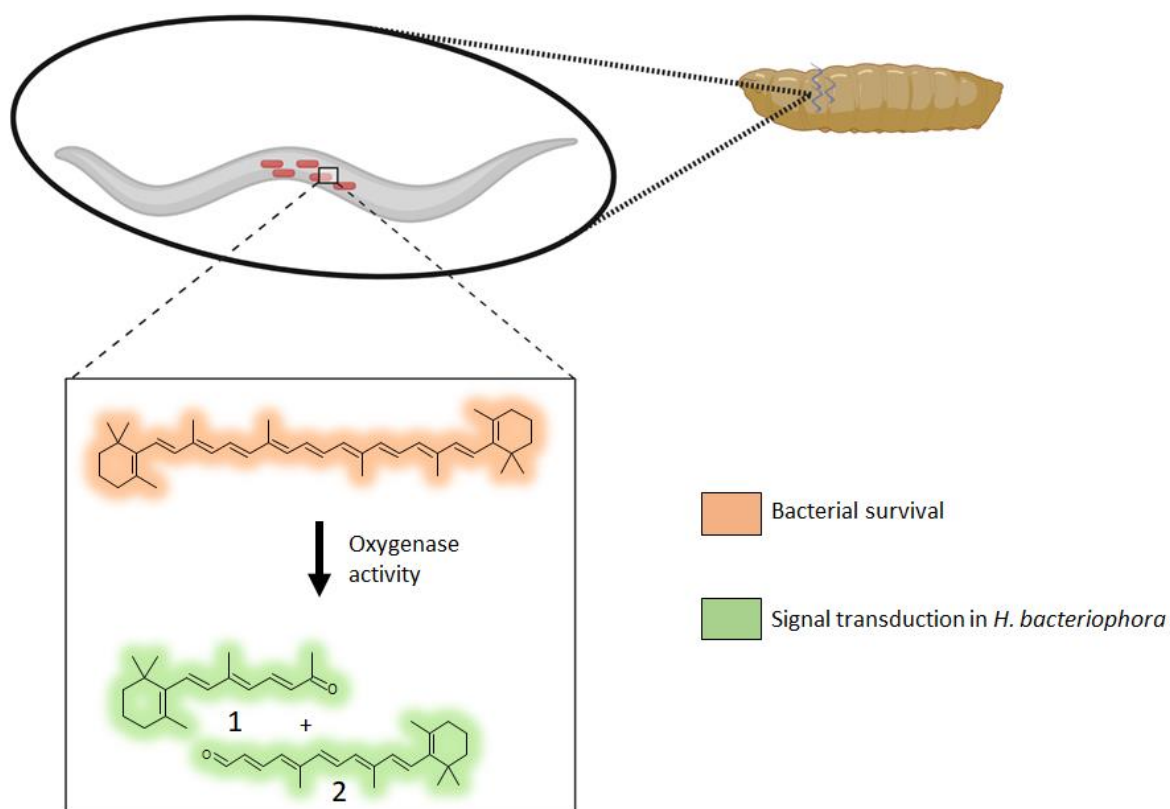


**Fig. 59** Proposed roles of β-carotene, **1** and **2**. Upon infection, the BGC is induced and β-carotene is produced protecting *P. luminescens* against reactive oxygen species during early stage infections. Cleavage of β-carotene resulting in **1** and **2** activates signaling pathways in *H. bacteriophora* putatively involved in processes such development or life span. Figure was partially generated with Biorender.com.

Based on the findings of chapter 6.3 it is postulated that the carotenoid BGC in *Photorhabdus* exhibits a chimeric function. Firstly, the produced β-carotene acts a defense mechanism against the insect's immune system in early stages of infection (<48 h) as it promotes the bacteria's survival rate. Secondly, the cleavage products **1** and **2** possibly fulfill various roles in signal transduction in *H. bacteriophora* as ligands for certain retinoid-binding receptors. Importantly, the latter function presumably occurs in later stages of infection as processes like development of new IJs typically take place after the insect's death (>48 h).

### 7.3.7 Conclusion and Outlook

This work deals with the elucidation of a terpenoid BGC in *P. luminescens*. The resulting NPs and the corresponding biosynthesis have been studied extensively leading to a full characterization thereof. Additionally, a combination of bioinformatic approaches and *in vivo* insect killing assays provided crucial information in order to understand the ecological function of the BGC and its products. It was shown, that  $\beta$ -carotene effectively protects *P. luminescens* against the insect's immune response. Furthermore, characterization of the inherent CCD and identification of putative binding partners of its products **1** and **2** gave insights in a novel host-symbiont interaction. Still, to identify the exact binding partner of **1** and **2** in *H. bacteriophora*, there are several assays that could be conducted, which would allow for identification e.g. isothermal titration calorimetry (ITC) with the putative receptors, pulldown-assays, co-crystallization of the putative receptor with **1** and **2** or *in silico* protein-ligand modelling. In addition, the ecological role of **1** and **2** in the host-symbiont relationship could be addressed in developmental assays of axenic *H. bacteriophora* with *P. luminescens*  $\Delta$ oxygenase and *P. luminescens*  $\Delta$ carotenoid while monitoring physiological attributes such as size, lifespan or morphology of the respective nematodes.

In essence, this work provides important findings for a better understanding of the complex host-symbiont interaction between *P. luminescens* and *H. bacteriophora*. Critically, getting an in depth understanding of this mutualistic relationship is of great importance for a vast amount of biotechnological and pharmaceutical applications. On the one hand, *Xenorhabdus* and *Photorhabdus* are already used as an effective tool to efficiently deal with agricultural pests and provide many advantages over commonly used chemical insecticides, as they do not have detrimental effects on animals and plants<sup>203</sup>. Additionally, they are safe in handling and have no pathogenic effects on humans. Here, uncovering the regulatory machinery and factors behind the symbiotic relationship provides crucial information to increase their benefits for agricultural applications even further. On the other hand, as this work showed, some of the BGCs are silent under laboratory conditions and only active during certain stages of the life cycle. As it has already been demonstrated, certain NPs produced by the bacteria can be utilized for pharmaceutical applications as antibiotics, anti-tumor agents or enzyme inhibitors<sup>203</sup>. Majorly, getting a better understanding of the host-symbiont interaction can open the door to uncover new, potent NPs for clinical utilization.

## 8 References

- 1 D. J. Newman and G. M. Cragg, Natural products as sources of new drugs over the last 25 years, *Journal of natural products*, 2007, **70**, 461–477.
- 2 D. J. Newman and G. M. Cragg, Natural products as sources of new drugs over the 30 years from 1981 to 2010, *Journal of natural products*, 2012, **75**, 311–335.
- 3 D. J. Newman and G. M. Cragg, Natural Products as Sources of New Drugs from 1981 to 2014, *Journal of natural products*, 2016, **79**, 629–661.
- 4 D. J. Newman, G. M. Cragg and K. M. Snader, Natural products as sources of new drugs over the period 1981-2002, *Journal of natural products*, 2003, **66**, 1022–1037.
- 5 J. R. Porter, Antony van Leeuwenhoek: tercentenary of his discovery of bacteria, *Bacteriological reviews*, 1976, **40**, 260–269.
- 6 M. A. Fischbach and J. A. Segre, Signaling in Host-Associated Microbial Communities, *Cell*, 2016, **164**, 1288–1300.
- 7 G. Sharon, N. Garg, J. Debelius, R. Knight, P. C. Dorrestein and S. K. Mazmanian, Specialized metabolites from the microbiome in health and disease, *Cell metabolism*, 2014, **20**, 719–730.
- 8 N. M. Dheilly, R. Poulin and F. Thomas, Biological warfare: Microorganisms as drivers of host-parasite interactions, *Infection, genetics and evolution : journal of molecular epidemiology and evolutionary genetics in infectious diseases*, 2015, **34**, 251–259.
- 9 Y.-M. Shi and H. B. Bode, Chemical language and warfare of bacterial natural products in bacteria-nematode-insect interactions, *Natural product reports*, 2018, **35**, 309–335.
- 10 N. J. Tobias, J. Brehm, D. Kresovic, S. Brameyer, H. B. Bode and R. Heermann, New Vocabulary for Bacterial Communication, *Chembiochem : a European journal of chemical biology*, 2020, **21**, 759–768.
- 11 S. W. Fuchs, F. Grundmann, M. Kurz, M. Kaiser and H. B. Bode, Fabclavines: bioactive peptide-polyketide-polyamino hybrids from *Xenorhabdus*, *Chembiochem : a European journal of chemical biology*, 2014, **15**, 512–516.
- 12 T. A. Ciche, M. Blackburn, J. R. Carney and J. C. Ensign, Photobactin: a catechol siderophore produced by *Photobacterium luminescens*, an entomopathogen mutually associated with *Heterorhabditis bacteriophora* NC1 nematodes, *Applied and environmental microbiology*, 2003, **69**, 4706–4713.
- 13 J. Li, G. Chen and J. M. Webster, Nematophin, a novel antimicrobial substance produced by *Xenorhabdus nematophilus* (Enterobacteriaceae), *Canadian journal of microbiology*, 1997, **43**, 770–773.
- 14 Y. S. Polikanov, I. A. Osterman, T. Szal, V. N. Tashlitsky, M. V. Serebryakova, P. Kusochek, D. Bulkley, I. A. Malanicheva, T. A. Efimenko, O. V. Efremenkova, A. L. Konevega, K. J. Shaw, A. A. Bogdanov, M. V. Rodnina, O. A. Dontsova, A. S. Mankin, T. A. Steitz and P. V. Sergiev, Amicoumacin inhibits translation by stabilizing mRNA interaction with the ribosome, *Molecular cell*, 2014, **56**, 531–540.
- 15 M. Groll, B. Schellenberg, A. S. Bachmann, C. R. Archer, R. Huber, T. K. Powell, S. Lindow, M. Kaiser and R. Dudler, A plant pathogen virulence factor inhibits the eukaryotic proteasome by a novel mechanism, *Nature*, 2008, **452**, 755–758.

- 16 G. Lang, T. Kalvelage, A. Peters, J. Wiese and J. F. Imhoff, Linear and cyclic peptides from the entomopathogenic bacterium *Xenorhabdus nematophilus*, *Journal of natural products*, 2008, **71**, 1074–1077.
- 17 A. F. Kisselev, Joining the army of proteasome inhibitors, *Chemistry & biology*, 2008, **15**, 419–421.
- 18 A. Proschak, Q. Zhou, T. Schöner, A. Thanwisai, D. Kresovic, A. Dowling, R. ffrench-Constant, E. Proschak and H. B. Bode, Biosynthesis of the insecticidal xenocycloins in *Xenorhabdus bovienii*, *Chembiochem : a European journal of chemical biology*, 2014, **15**, 369–372.
- 19 Y. Tang, *Natural product biosynthesis - chemical logic and enzymatic machinery. Chemical logic and enzymatic machinery*, Royal Society of Chemistry, London, UK, 2017.
- 20 C. T. Walsh and M. A. Fischbach, Natural Products Version 2.0: Connecting Genes to Molecules, *Journal of the American Chemical Society*, 2010, **132**, 2469–2493.
- 21 E. L. Miller, THE PENICILLINS: A REVIEW AND UPDATE, *Journal of Midwifery & Women's Health*, 2002, **47**, 426–434.
- 22 R. I. Aminov, A brief history of the antibiotic era: lessons learned and challenges for the future, *Frontiers in microbiology*, 2010, **1**, 134.
- 23 J. Clardy, M. A. Fischbach and C. T. Walsh, New antibiotics from bacterial natural products, *Nature biotechnology*, 2006, **24**, 1541–1550.
- 24 B. Da Ribeiro Cunha, L. P. Fonseca and C. R. C. Calado, Antibiotic Discovery: Where Have We Come from, Where Do We Go?, *Antibiotics (Basel, Switzerland)*, 2019, **8**. DOI: 10.3390/antibiotics8020045.
- 25 F. von Nussbaum, M. Brands, B. Hinzen, S. Weigand and D. Häbich, Antibacterial natural products in medicinal chemistry--exodus or revival?, *Angewandte Chemie (International ed. in English)*, 2006, **45**, 5072–5129.
- 26 C. L. Ventola, The antibiotic resistance crisis: part 1: causes and threats, *Pharmacy and Therapeutics*, 2015, **40**, 277–283.
- 27 A. F. Read and R. J. Woods, Antibiotic resistance management, *Evolution, medicine, and public health*, 2014, **2014**, 147.
- 28 U.S. Centers for Disease Control and Prevention, *Antibiotic resistance threats in the United States*, 2019, 2019.
- 29 M. J. Bibb, Regulation of secondary metabolism in streptomycetes, *Current opinion in microbiology*, 2005, **8**, 208–215.
- 30 A. A. Brakhage, Regulation of fungal secondary metabolism, *Nature reviews. Microbiology*, 2013, **11**, 21–32.
- 31 G. M. Thomas and G. O. Poinar, *Xenorhabdus* gen. nov., a Genus of Entomopathogenic, Nematophilic Bacteria of the Family Enterobacteriaceae, *International Journal of Systematic and Evolutionary Microbiology*, 1979, **29**, 352–360.
- 32 M. Fischer-Le Saux, H. Mauléon, P. Constant, B. Brunel and N. Boemare, PCR-ribotyping of *Xenorhabdus* and *Photorhabdus* isolates from the Caribbean region in relation to the taxonomy and geographic distribution of their nematode hosts, *Applied and environmental microbiology*, 1998, **64**, 4246–4254.
- 33 N. R. Waterfield, T. Ciche and D. Clarke, *Photorhabdus* and a host of hosts, *Annual review of microbiology*, 2009, **63**, 557–574.

- 34 T. A. Ciche, C. Darby, R.-U. Ehlers, S. Forst and H. Goodrich-Blair, Dangerous liaisons: The symbiosis of entomopathogenic nematodes and bacteria, *Biological Control*, 2006, **38**, 22–46.
- 35 T. Ciche, The biology and genome of *Heterorhabditis bacteriophora*, *WormBook : the online review of C. elegans biology*, 2007, 1–9.
- 36 G. O. Poinar, G. Thomas, M. Haygood and K. H. Neilson, Growth and luminescence of the symbiotic bacteria associated with the terrestrial nematode, *Heterorhabditis bacteriophora*, *Soil Biology and Biochemistry*, 1980, **12**, 5–10.
- 37 Antje Heinrich, Regulation of natural product production of *Photorhabdus luminescens* via both pathway-specific and global regulators., Goethe University, 2017.
- 38 H. K. Kaya and R. Gaugler, Entomopathogenic Nematodes, *Annu. Rev. Entomol.*, 1993, **38**, 181–206.
- 39 T. A. Ciche and J. C. Ensign, For the insect pathogen *Photorhabdus luminescens*, which end of a nematode is out?, *Applied and environmental microbiology*, 2003, **69**, 1890–1897.
- 40 J. M. Crawford, C. Portmann, X. Zhang, M. B. J. Roeffaers and J. Clardy, Small molecule perimeter defense in entomopathogenic bacteria, *Proceedings of the National Academy of Sciences of the United States of America*, 2012, **109**, 10821–10826.
- 41 D. Reimer, K. N. Cowles, A. Proschak, F. I. Nollmann, A. J. Dowling, M. Kaiser, R. French-Constant, H. Goodrich-Blair and H. B. Bode, Rhabdopeptides as insect-specific virulence factors from entomopathogenic bacteria, *Chembiochem : a European journal of chemical biology*, 2013, **14**, 1991–1997.
- 42 R. Han and R. U. Ehlers, Pathogenicity, development, and reproduction of *Heterorhabditis bacteriophora* and *Steinernema carpocapsae* under axenic in vivo conditions, *Journal of invertebrate pathology*, 2000, **75**, 55–58.
- 43 Ri-Chou Han, Wim M. Wouts and Li-ying Li, in 1990.
- 44 H. Goodrich-Blair and D. J. Clarke, Mutualism and pathogenesis in *Xenorhabdus* and *Photorhabdus*: two roads to the same destination, *Molecular microbiology*, 2007, **64**, 260–268.
- 45 J. E. Milstead, *Heterorhabditis bacteriophora* as a vector for introducing its associated bacterium into the hemocoel of *Galleria mellonella* larvae, *Journal of invertebrate pathology*, 1979, **33**, 324–327.
- 46 G. O. Poinar, JR and P. S. Grewal, History of entomopathogenic nematology, *Journal of nematology*, 2012, **44**, 153–161.
- 47 E. Duchaud, C. Rusniok, L. Frangeul, C. Buchrieser, A. Givaudan, S. Taourit, S. Bocs, C. Boursaux-Eude, M. Chandler, J.-F. Charles, E. Dassa, R. Derose, S. Derzelle, G. Freyssinet, S. Gaudriault, C. Médigue, A. Lanois, K. Powell, P. Siguier, R. Vincent, V. Wingate, M. Zouine, P. Glaser, N. Boemare, A. Danchin and F. Kunst, The genome sequence of the entomopathogenic bacterium *Photorhabdus luminescens*, *Nature biotechnology*, 2003, **21**, 1307–1313.
- 48 All natural, *Nature Chemical Biology*, 2007, **3**, 351.
- 49 P. M. Dewick, *Medicinal natural products. A biosynthetic approach*, Wiley, Chichester, U.K., 3rd edn., 2010.

- 50 B. P. Singh, M. E. Rateb, S. Rodriguez-Couto, Polizeli, Maria de Lourdes Teixeira de Moraes and W.-J. Li, Editorial: Microbial Secondary Metabolites: Recent Developments and Technological Challenges, *Frontiers in microbiology*, 2019, **10**, 914.
- 51 B. Ruiz, A. Chávez, A. Forero, Y. García-Huante, A. Romero, M. Sánchez, D. Rocha, B. Sánchez, R. Rodríguez-Sanoja, S. Sánchez and E. Langley, Production of microbial secondary metabolites: regulation by the carbon source, *Critical reviews in microbiology*, 2010, **36**, 146–167.
- 52 Q. Yan, L. D. Lopes, B. T. Shaffer, T. A. Kidarsa, O. Vining, B. Philmus, C. Song, V. O. Stockwell, J. M. Raaijmakers, K. L. McPhail, F. D. Andreote, J. H. Chang and J. E. Loper, Secondary Metabolism and Interspecific Competition Affect Accumulation of Spontaneous Mutants in the GacS-GacA Regulatory System in *Pseudomonas protegens*, *mBio*, 2018, **9**. DOI: 10.1128/mBio.01845-17.
- 53 F. I. Nollmann, C. Dauth, G. Mulley, C. Kegler, M. Kaiser, N. R. Waterfield and H. B. Bode, Insect-specific production of new GameXPeptides in *photorhabdus luminescens* TTO1, widespread natural products in entomopathogenic bacteria, *Chembiochem : a European journal of chemical biology*, 2015, **16**, 205–208.
- 54 N. J. Tobias, H. Wolff, B. Djahanschiri, F. Grundmann, M. Kronenwerth, Y.-M. Shi, S. Simonyi, P. Grün, D. Shapiro-Ilan, S. J. Pidot, T. P. Stinear, I. Ebersberger and H. B. Bode, Natural product diversity associated with the nematode symbionts *Photorhabdus* and *Xenorhabdus*, *Nature microbiology*, 2017, **2**, 1676–1685.
- 55 A. Dudnik, L. Bigler and R. Dudler, Heterologous expression of a *Photorhabdus luminescens* syrbactin-like gene cluster results in production of the potent proteasome inhibitor glidobactin A, *Microbiological Research*, 2013, **168**, 73–76.
- 56 J. Crawford, R. Kontnik and J. Clardy, Regulating Alternative Lifestyles in Entomopathogenic Bacteria, *Current biology : CB*, 2009, **20**, 69–74.
- 57 R. Kontnik, J. M. Crawford and J. Clardy, Exploiting a global regulator for small molecule discovery in *Photorhabdus luminescens*, *ACS chemical biology*, 2010, **5**, 659–665.
- 58 R. J. Akhurst, Antibiotic activity of *Xenorhabdus* spp., bacteria symbiotically associated with insect pathogenic nematodes of the families Heterorhabditidae and Steinernematidae, *Journal of general microbiology*, 1982, **128**, 3061–3065.
- 59 X. Zhou, H. K. Kaya, K. Heungens and H. Goodrich-Blair, Response of ants to a deterrent factor(s) produced by the symbiotic bacteria of entomopathogenic nematodes, *Applied and environmental microbiology*, 2002, **68**, 6202–6209.
- 60 D. J. Clarke, The Regulation of Secondary Metabolism in *Photorhabdus*, *Current topics in microbiology and immunology*, 2017, **402**, 81–102.
- 61 Ciche Todd A., Bintrim Scott B., Horswill Alexander R. and Ensign Jerald C., A Phosphopantetheinyl Transferase Homolog Is Essential for *Photorhabdus luminescens* To Support Growth and Reproduction of the Entomopathogenic Nematode *Heterorhabditis bacteriophora*, *Journal of Bacteriology*, 2001, **183**, 3117–3126.
- 62 S. Brameyer, D. Kresovic, H. B. Bode and R. Heermann, Dialkylresorcinols as bacterial signaling molecules, *Proceedings of the National Academy of Sciences of the United States of America*, 2015, **112**, 572–577.
- 63 L. Lango-Scholey, A. O. Brachmann, H. B. Bode and D. J. Clarke, The expression of *stIA* in *Photorhabdus luminescens* is controlled by nutrient limitation, *PloS one*, 2013, **8**, e82152.

- 64 K. A. J. Bozhüyük, Q. Zhou, Y. Engel, A. Heinrich, A. Pérez and H. B. Bode, Natural Products from *Photobacterium* and Other Entomopathogenic Bacteria, *Current topics in microbiology and immunology*, 2017, **402**, 55–79.
- 65 M. A. Fischbach and C. T. Walsh, Assembly-line enzymology for polyketide and nonribosomal Peptide antibiotics: logic, machinery, and mechanisms, *Chemical reviews*, 2006, **106**, 3468–3496.
- 66 R. H. Lambalot, A. M. Gehring, R. S. Flugel, P. Zuber, M. LaCelle, M. A. Marahiel, R. Reid, C. Khosla and C. T. Walsh, A new enzyme superfamily - the phosphopantetheinyl transferases, *Chemistry & biology*, 1996, **3**, 923–936.
- 67 C. Hertweck, The biosynthetic logic of polyketide diversity, *Angewandte Chemie (International ed. in English)*, 2009, **48**, 4688–4716.
- 68 B. Shen, Polyketide biosynthesis beyond the type I, II and III polyketide synthase paradigms, *Current opinion in chemical biology*, 2003, **7**, 285–295.
- 69 C. Hertweck, A. Luzhetskyy, Y. Rebets and A. Bechthold, Type II polyketide synthases: gaining a deeper insight into enzymatic teamwork, *Nat. Prod. Rep.*, 2007, **24**, 162–190.
- 70 W. Zhang and Y. Tang, In vitro analysis of type II polyketide synthase, *Methods in enzymology*, 2009, **459**, 367–393.
- 71 P. Kumar, A. T. Koppisch, D. E. Cane and C. Khosla, Enhancing the modularity of the modular polyketide synthases: transacylation in modular polyketide synthases catalyzed by malonyl-CoA:ACP transacylase, *Journal of the American Chemical Society*, 2003, **125**, 14307–14312.
- 72 Y. Tang, S.-C. Tsai and C. Khosla, Polyketide Chain Length Control by Chain Length Factor, *Journal of the American Chemical Society*, 2003, **125**, 12708–12709.
- 73 U. Rix, C. Fischer, L. L. Remsing and J. Rohr, Modification of post-PKS tailoring steps through combinatorial biosynthesis, *Natural product reports*, 2002, **19**, 542–580.
- 74 A. O. Brachmann, S. A. Joyce, H. Jenke-Kodama, G. Schwär, D. J. Clarke and H. B. Bode, A type II polyketide synthase is responsible for anthraquinone biosynthesis in *Photobacterium luminescens*, *Chembiochem : a European journal of chemical biology*, 2007, **8**, 1721–1728.
- 75 B. Kunze, G. Höfle and H. Reichenbach, The aurachins, new quinoline antibiotics from myxobacteria: production, physico-chemical and biological properties, *The Journal of antibiotics*, 1987, **40**, 258–265.
- 76 Antje Heinrich, PhD Thesis, Goethe University, 2017.
- 77 A. K. Heinrich, A. Glaeser, N. J. Tobias, R. Heermann and H. B. Bode, Heterogeneous regulation of bacterial natural product biosynthesis via a novel transcription factor, *Heliyon*, 2016, **2**, e00197.
- 78 Nicholas J. Tobias, Antje K. Heinrich, Helena Eresmann, Patrick R. Wright, Nick Neubacher, Rolf Backofen and Helge B. Bode, *Photobacterium*-nematode symbiosis is dependent on hfq-mediated regulation of secondary metabolites, *Environmental Microbiology*, 2017, **19**, 119–129.
- 79 Bundesministerium für Umwelt, Naturschutz, Bau und Reaktorsicherheit, Paper, Bundesamt für Naturschutz, 2021.
- 80 Agora\_Studie\_Kostenoptimaler\_Ausbau\_der\_EE\_Web\_optimiert.
- 81 Winfried Hoffmann, 2014.



- 82 S. P. S. Badwal, S. S. Giddey, C. Munnings, A. I. Bhatt and A. F. Hollenkamp, Emerging electrochemical energy conversion and storage technologies, *Frontiers in chemistry*, 2014, **2**, 79.
- 83 P. Alotto, M. Guarnieri and F. Moro, Redox flow batteries for the storage of renewable energy: A review, *Renewable and Sustainable Energy Reviews*, 2014, **29**, 325–335.
- 84 Q. Xu, Y. N. Ji, L. Y. Qin, P. K. Leung, F. Qiao, Y. S. Li and H. N. Su, Evaluation of redox flow batteries goes beyond round-trip efficiency: A technical review, *Journal of Energy Storage*, 2018, **16**, 108–115.
- 85 Michael J. Aziz, Organic mega flow battery promises breakthrough for renewable energy, 2014.
- 86 K. Lin, Q. Chen, M. R. Gerhardt, L. Tong, S. B. Kim, L. Eisenach, A. W. Valle, D. Hardee, R. G. Gordon, M. J. Aziz and M. P. Marshak, Alkaline quinone flow battery, *Science (New York, N.Y.)*, 2015, **349**, 1529–1532.
- 87 Nick Neubacher, PhD, Goethe University, 2020.
- 88 Y.-S. Wang and M. Shelomi, Review of Black Soldier Fly (*Hermetia illucens*) as Animal Feed and Human Food, *Foods (Basel, Switzerland)*, 2017, **6**. DOI: 10.3390/foods6100091.
- 89 K. M. Babu, *Silk. Processing, properties and applications*, Elsevier Science, Philadelphia, PA, 2013.
- 90 A. G. Atanasov, S. B. Zotchev, V. M. Dirsch and C. T. Supuran, Natural products in drug discovery: advances and opportunities, *Nature reviews. Drug discovery*, 2021, **20**, 200–216.
- 91 K. Scherlach and C. Hertweck, Triggering cryptic natural product biosynthesis in microorganisms, *Organic & biomolecular chemistry*, 2009, **7**, 1753–1760.
- 92 H. B. Bode, B. Bethe, R. Höfs and A. Zeeck, Big effects from small changes: possible ways to explore nature's chemical diversity, *Chembiochem : a European journal of chemical biology*, 2002, **3**, 619–627.
- 93 J. H. Kim, N. Lee, S. Hwang, W. Kim, Y. Lee, S. Cho, B. O. Palsson and B.-K. Cho, Discovery of novel secondary metabolites encoded in actinomycete genomes through coculture, *Journal of Industrial Microbiology and Biotechnology*, 2021, **48**. DOI: 10.1093/jimb/kuaa001.
- 94 A. Marmann, A. H. Aly, W. Lin, B. Wang and P. Proksch, Co-Cultivation—A Powerful Emerging Tool for Enhancing the Chemical Diversity of Microorganisms, *Marine Drugs*, 2014, **12**, 1043–1065.
- 95 M. H. Medema, R. Kottmann, P. Yilmaz, M. Cummings, J. B. Biggins, K. Blin, I. de Bruijn, Y. H. Chooi, J. Claesen, R. C. Coates, P. Cruz-Morales, S. Duddela, S. Düsterhus, D. J. Edwards, D. P. Fewer, N. Garg, C. Geiger, J. P. Gomez-Escribano, A. Greule, M. Hadjithomas, A. S. Haines, E. J. N. Helfrich, M. L. Hillwig, K. Ishida, A. C. Jones, C. S. Jones, K. Jungmann, C. Kegler, H. U. Kim, P. Kötter, D. Krug, J. Masschelein, A. V. Melnik, S. M. Mantovani, E. A. Monroe, M. Moore, N. Moss, H.-W. Nützmann, G. Pan, A. Pati, D. Petras, F. J. Reen, F. Rosconi, Z. Rui, Z. Tian, N. J. Tobias, Y. Tsunematsu, P. Wiemann, E. Wyckoff, X. Yan, G. Yim, F. Yu, Y. Xie, B. Aigle, A. K. Apel, C. J. Balibar, E. P. Balskus, F. Barona-Gómez, A. Bechthold, H. B. Bode, R. Borriss, S. F. Brady, A. A. Brakhage, P. Caffrey, Y.-Q. Cheng, J. Clardy, R. J. Cox, R. de Mot, S. Donadio, M. S. Donia, van der Donk, Wilfred A, P. C. Dorrestein, S. Doyle, A. J. M. Driessen, M. Ehling-Schulz, K.-D. Entian, M. A. Fischbach, L.

- Gerwick, W. H. Gerwick, H. Gross, B. Gust, C. Hertweck, M. Höfte, S. E. Jensen, J. Ju, L. Katz, L. Kaysser, J. L. Klassen, N. P. Keller, J. Kormanec, O. P. Kuipers, T. Kuzuyama, N. C. Kyrpides, H.-J. Kwon, S. Lautru, R. Lavigne, C. Y. Lee, B. Linqun, X. Liu, W. Liu, A. Luzhetskyy, T. Mahmud, Y. Mast, C. Méndez, M. Metsä-Ketelä, J. Micklefield, D. A. Mitchell, B. S. Moore, L. M. Moreira, R. Müller, B. A. Neilan, M. Nett, J. Nielsen, F. O'Gara, H. Oikawa, A. Osbourn, M. S. Osburne, B. Ostash, S. M. Payne, J.-L. Pernodet, M. Petricek, J. Piel, O. Ploux, J. M. Raaijmakers, J. A. Salas, E. K. Schmitt, B. Scott, R. F. Seipke, B. Shen, D. H. Sherman, K. Sivonen, M. J. Smanski, M. Sosio, E. Stegmann, R. D. Süßmuth, K. Tahlan, C. M. Thomas, Y. Tang, A. W. Truman, M. Viaud, J. D. Walton, C. T. Walsh, T. Weber, G. P. van Wezel, B. Wilkinson, J. M. Willey, W. Wohlleben, G. D. Wright, N. Ziemert, C. Zhang, S. B. Zotchev, R. Breitling, E. Takano and F. O. Glöckner, Minimum Information about a Biosynthetic Gene cluster, *Nature Chemical Biology*, 2015, **11**, 625–631.
- 96 P. J. Rutledge and G. L. Challis, Discovery of microbial natural products by activation of silent biosynthetic gene clusters, *Nature reviews. Microbiology*, 2015, **13**, 509–523.
- 97 K. Blin, H. U. Kim, M. H. Medema and T. Weber, Recent development of antiSMASH and other computational approaches to mine secondary metabolite biosynthetic gene clusters, *Brief Bioinform*, 2019, **20**, 1103–1113.
- 98 Y. Engel, C. Windhorst, X. Lu, H. Goodrich-Blair and H. B. Bode, The Global Regulators Lrp, LeuO, and HexA Control Secondary Metabolism in Entomopathogenic Bacteria, *Frontiers in microbiology*, 2017, **8**. DOI: 10.3389/fmicb.2017.00209.
- 99 A. Klamrak, J. Nabnueangsap, P. Puthongking and N. Nualkaew, Synthesis of Ferulenol by Engineered Escherichia coli: Structural Elucidation by Using the In Silico Tools, *Molecules (Basel, Switzerland)*, 2021, **26**. DOI: 10.3390/molecules26206264.
- 100 A. D. Kinghorn, H. Falk, S. Gibbons, J. Kobayashi, Y. Asakawa and J.-K. Liu, *Progress in the Chemistry of Organic Natural Products 107*, Springer International Publishing, Cham, 2018.
- 101 N. Stoll, E. Schmidt and K. Thurow, Isotope pattern evaluation for the reduction of elemental compositions assigned to high-resolution mass spectral data from electrospray ionization fourier transform ion cyclotron resonance mass spectrometry, *Journal of The American Society for Mass Spectrometry*, 2006, **17**, 1692–1699.
- 102 H. B. Bode, D. Reimer, S. W. Fuchs, F. Kirchner, C. Dauth, C. Kegler, W. Lorenzen, A. O. Brachmann and P. Grün, Determination of the absolute configuration of peptide natural products by using stable isotope labeling and mass spectrometry, *Chemistry (Weinheim an der Bergstrasse, Germany)*, 2012, **18**, 2342–2348.
- 103 D. Reimer, F. I. Nollmann, K. Schultz, M. Kaiser and H. B. Bode, Xenortide Biosynthesis by Entomopathogenic Xenorhabdus nematophila, *Journal of natural products*, 2014, **77**, 1976–1980.
- 104 Y. Tsunematsu, Genomics-directed activation of cryptic natural product pathways deciphers codes for biosynthesis and molecular function, *Journal of natural medicines*, 2021, **75**, 261–274.
- 105 M. Tosin, L. Betancor, E. Stephens, W. M. A. Li, J. B. Spencer and P. F. Leadlay, Synthetic chain terminators off-load intermediates from a type I polyketide synthase, *ChemBiochem : a European journal of chemical biology*, 2010, **11**, 539–546.

- 106 F. Nabi, M. A. Arain, N. Rajput, M. Alagawany, J. Soomro, M. Umer, F. Soomro, Z. Wang, R. Ye and J. Liu, Health benefits of carotenoids and potential application in poultry industry: A review, *Journal of animal physiology and animal nutrition*, 2020, **104**, 1809–1818.
- 107 Carotenoids in Cardiovascular Disease Prevention.
- 108 T. P. Almeida, A. A. Ramos, J. Ferreira, A. Azqueta and E. Rocha, Bioactive Compounds from Seaweed with Anti-Leukemic Activity: A Mini-Review on Carotenoids and Phlorotannins, *Mini reviews in medicinal chemistry*, 2020, **20**, 39–53.
- 109 E. Aziz, R. Batool, W. Akhtar, S. Rehman, T. Shahzad, A. Malik, M. A. Shariati, A. Laishevtcev, S. Plygun, M. Heydari, A. Rauf and S. Ahmed Arif, Xanthophyll: Health benefits and therapeutic insights, *Life sciences*, 2020, **240**, 117104.
- 110 J. Fiedor and K. Burda, Potential role of carotenoids as antioxidants in human health and disease, *Nutrients*, 2014, **6**, 466–488.
- 111 I. Jaswir and A. Hammed, Anti-inflammatory compounds of macro algae origin: A review, *J. Med. Plants Res*, 2011, **5**, 7146–7154.
- 112 J. Y. Lim and X.-D. Wang, Mechanistic understanding of  $\beta$ -cryptoxanthin and lycopene in cancer prevention in animal models, *Biochimica et biophysica acta. Molecular and cell biology of lipids*, 2020, **1865**, 158652.
- 113 D. Mohana, S. Thippeswamy and R. Abhishek, Antioxidant, antibacterial, and ultraviolet-protective properties of carotenoids isolated from *Micrococcus* spp, *Radiat Prot Environ*, 2013, **36**, 168.
- 114 K. Pal, I. Banerjee, P. Sarkar, D. Kim, W.-P. Deng, N. K. Dubey and K. Majumder, eds., *Biopolymer-Based Formulations*, Elsevier, 2020.
- 115 J. Rzaiew, T. Radzik and E. Rebas, Calcium-Involved Action of Phytochemicals: Carotenoids and Monoterpenes in the Brain, *International journal of molecular sciences*, 2020, **21**. DOI: 10.3390/ijms21041428.
- 116 T. Bhatt and K. Patel, Carotenoids: Potent to Prevent Diseases Review, *Natural products and bioprospecting*, 2020, **10**, 109–117.
- 117 R. G. Bodade and A. G. Bodade, in *Biopolymer-Based Formulations*, ed. K. Pal, I. Banerjee, P. Sarkar, D. Kim, W.-P. Deng, N. K. Dubey and K. Majumder, Elsevier, 2020, pp. 381–404.
- 118 P. M. Dey, J. B. Harborne and J. Bonner, *Plant biochemistry*, Academic Press, San Diego, 1997.
- 119 F. Bouvier, J.-C. Isner, O. Dogbo and B. Camara, Oxidative tailoring of carotenoids: a prospect towards novel functions in plants, *Trends in plant science*, 2005, **10**, 187–194.
- 120 S. H. Schwartz, X. Qin and J. A. Zeevaart, Characterization of a novel carotenoid cleavage dioxygenase from plants, *The Journal of biological chemistry*, 2001, **276**, 25208–25211.
- 121 B. Camara and F. Bouvier, Oxidative remodeling of plastid carotenoids, *Archives of Biochemistry and Biophysics*, 2004, **430**, 16–21.
- 122 O. Ahrazem, L. Gómez-Gómez, M. J. Rodrigo, J. Avalos and M. C. Limón, Carotenoid Cleavage Oxygenases from Microbes and Photosynthetic Organisms: Features and Functions, *International journal of molecular sciences*, 2016, **17**. DOI: 10.3390/ijms17111781.

- 123 B. Camara and F. Bouvier, Oxidative remodeling of plastid carotenoids, *Archives of Biochemistry and Biophysics*, 2004, **430**, 16–21.
- 124 S. H. Schwartz, X. Qin and J. A. D. Zeevaart, Elucidation of the indirect pathway of abscisic acid biosynthesis by mutants, genes, and enzymes, *Plant Physiol*, 2003, **131**, 1591–1601.
- 125 G. Giuliano, S. Al-Babili and J. von Lintig, Carotenoid oxygenases: cleave it or leave it, *Trends in plant science*, 2003, **8**, 145–149.
- 126 E. H. Harrison, C. dela Sena, A. Eroglu and M. K. Fleshman, The formation, occurrence, and function of  $\beta$ -apocarotenoids:  $\beta$ -carotene metabolites that may modulate nuclear receptor signaling, *The American journal of clinical nutrition*, 2012, **96**, 1189S-92S.
- 127 C. A. Llewellyn, R. L. Airs, G. Farnham and C. Greig, Synthesis, Regulation and Degradation of Carotenoids Under Low Level UV-B Radiation in the Filamentous Cyanobacterium *Chlorogloeopsis fritschii* PCC 6912, *Frontiers in microbiology*, 2020, **11**, 163.
- 128 S. P. Balashov and J. K. Lanyi, Xanthorhodopsin: Proton pump with a carotenoid antenna, *Cellular and Molecular Life Sciences*, 2007, **64**, 2323–2328.
- 129 J. Pinhassi, E. F. DeLong, O. Béjà, J. M. González and C. Pedrós-Alió, Marine Bacterial and Archaeal Ion-Pumping Rhodopsins: Genetic Diversity, Physiology, and Ecology, *Microbiology and molecular biology reviews : MMBR*, 2016, **80**, 929–954.
- 130 K.-H. Jung, V. D. Trivedi and J. L. Spudich, Demonstration of a sensory rhodopsin in eubacteria, *Molecular microbiology*, 2003, **47**, 1513–1522.
- 131 N. B. Ghyselinck and G. Duyster, Retinoic acid signaling pathways, *Development (Cambridge, England)*, 2019, **146**. DOI: 10.1242/dev.167502.
- 132 X. Sui, P. D. Kiser, J. von Lintig and K. Palczewski, Structural basis of carotenoid cleavage: from bacteria to mammals, *Archives of Biochemistry and Biophysics*, 2013, **539**, 203–213.
- 133 E. H. Harrison, C. dela Sena, A. Eroglu and M. K. Fleshman, The formation, occurrence, and function of  $\beta$ -apocarotenoids:  $\beta$ -carotene metabolites that may modulate nuclear receptor signaling, *The American journal of clinical nutrition*, 2012, **96**, 1189S-92S.
- 134 P. J. Harrison and T. D. H. Bugg, Enzymology of the carotenoid cleavage dioxygenases: reaction mechanisms, inhibition and biochemical roles, *Archives of Biochemistry and Biophysics*, 2014, **544**, 105–111.
- 135 R. M. Evans and D. J. Mangelsdorf, Nuclear Receptors, RXR, and the Big Bang, *Cell*, 2014, **157**, 255–266.
- 136 R. P. Koldamova, I. M. Lefterov, M. Staufenbiel, D. Wolfe, S. Huang, J. C. Glorioso, M. Walter, M. G. Roth and J. S. Lazo, The Liver X Receptor Ligand T0901317 Decreases Amyloid  $\beta$  Production in Vitro and in a Mouse Model of Alzheimer's Disease\*, *The Journal of biological chemistry*, 2005, **280**, 4079–4088.
- 137 K.-P. Jia, L. Baz and S. Al-Babili, From carotenoids to strigolactones, *Journal of experimental botany*, 2018, **69**, 2189–2204.
- 138 S. K. Reddy, S. V. Holalu, J. J. Casal and S. A. Finlayson, Abscisic acid regulates axillary bud outgrowth responses to the ratio of red to far-red light, *Plant Physiol*, 2013, **163**, 1047–1058.

- 139 K.-P. Jia, C. Li, H. J. Bouwmeester and S. Al-Babili, in *Strigolactones -- biology and applications*, ed. H. Koltai and C. Prandi, Springer, Cham, Switzerland, 2019, pp. 1–45.
- 140 M. J. Rodrigo, B. Alquézar, E. Alós, V. Medina, L. Carmona, M. Bruno, S. Al-Babili and L. Zacarías, A novel carotenoid cleavage activity involved in the biosynthesis of Citrus fruit-specific apocarotenoid pigments, *Journal of experimental botany*, 2013, **64**, 4461–4478.
- 141 A. Rubio-Moraga, J. L. Rambla, A. Fernández-de-Carmen, A. Trapero-Mozos, O. Ahrazem, D. Orzáez, A. Granell and L. Gómez-Gómez, New target carotenoids for CCD4 enzymes are revealed with the characterization of a novel stress-induced carotenoid cleavage dioxygenase gene from *Crocus sativus*, *Plant molecular biology*, 2014, **86**, 555–569.
- 142 C. Fu, W. P. Donovan, O. Shikapwashya-Hasser, X. Ye and R. H. Cole, Hot Fusion: an efficient method to clone multiple DNA fragments as well as inverted repeats without ligase, *PLoS one*, 2014, **9**, e115318.
- 143 M. R. Green and J. Sambrook, *Molecular cloning. A laboratory manual*, Cold Spring Harbor Laboratory Press, Cold Spring Harbor N.Y., 4th edn., 2012.
- 144 T. Durfee, R. Nelson, S. Baldwin, G. Plunkett, V. Burland, B. Mau, J. F. Petrosino, X. Qin, D. M. Muzny, M. Ayele, R. A. Gibbs, B. Csörgo, G. Pósfai, G. M. Weinstock and F. R. Blattner, The complete genome sequence of *Escherichia coli* DH10B: Insights into the biology of a laboratory workhorse, *Journal of Bacteriology*, 2008, **190**, 2597–2606.
- 145 S. G. Grant, J. Jessee, F. R. Bloom and D. Hanahan, Differential plasmid rescue from transgenic mouse DNAs into *Escherichia coli* methylation-restriction mutants, *Pnas*, 1990, **87**, 4645–4649.
- 146 R. Simon, U. Priefer and A. Pühler, A Broad Host Range Mobilization System for In Vivo Genetic Engineering: Transposon Mutagenesis in Gram Negative Bacteria, *Bio/Technology*, 1983, **1**, 784–791.
- 147 M. Fischer-Le Saux, V. Viallard, B. Brunel, P. Normand and N. E. Boemare, Polyphasic classification of the genus *Photobacterium* and proposal of new taxa: *P. luminescens* subsp. *luminescens* subsp. nov., *P. luminescens* subsp. *akhurstii* subsp. nov., *P. luminescens* subsp. *laumondii* subsp. nov., *P. temperata* sp. nov., *P. temperata* subs, *International Journal of Systematic Bacteriology*, 2009, **49**, 1645–1656.
- 148 W. Lorenzen, T. Ahrendt, K. A. J. Bozhüyük and H. B. Bode, A multifunctional enzyme is involved in bacterial ether lipid biosynthesis, *Nature Chemical Biology*, 2014, **10**, 425–427.
- 149 A. J. Meyer, T. H. Segall-Shapiro, E. Glassey, J. Zhang and C. A. Voigt, *Escherichia coli* "Marionette" strains with 12 highly optimized small-molecule sensors, *Nature Chemical Biology*, 2019, **15**, 196–204.
- 150 Bundesministerium für Umwelt, Naturschutz, Bau und Reaktorsicherheit, Paper, Bundesamt für Naturschutz, 2021.
- 151 Y. Zhang, L. Zheng, B. Liu, H. Wang and H. Shi, Sulfonated polysulfone proton exchange membrane influenced by a varied sulfonation degree for vanadium redox flow battery, *Journal of Membrane Science*, 2019, **584**, 173–180.
- 152 Lukas Kreling, Goethe University Frankfurt, 2019.
- 153 E. Bode, A. K. Heinrich, M. Hirschmann, D. Abebew, Y.-N. Shi, T. D. Vo, F. Wesche, Y.-M. Shi, P. Grün, S. Simonyi, N. Keller, Y. Engel, S. Wenski, R. Bennet, S. Beyer, I. Bischoff,

- A. Buaya, S. Brandt, I. Cakmak, H. Çimen, S. Eckstein, D. Frank, R. Fürst, M. Gand, G. Geisslinger, S. Hazir, M. Henke, R. Heermann, V. Lecaudey, W. Schäfer, S. Schiffmann, A. Schöffler, R. Schwenk, M. Skaljic, E. Thines, M. Thines, T. Ulshöfer, A. Vilcinskis, T. A. Wichelhaus and H. B. Bode, Promoter Activation in  $\Delta$ hfq Mutants as an Efficient Tool for Specialized Metabolite Production Enabling Direct Bioactivity Testing, *Angewandte Chemie (International ed. in English)*, 2019, **58**, 18957–18963.
- 154 Nick Neubacher, PhD, Goethe University, 2020.
- 155 W. Eisenreich, A. Bacher, D. Arigoni and F. Rohdich, Biosynthesis of isoprenoids via the non-mevalonate pathway, *Cellular and molecular life sciences : CMLS*, 2004, **61**, 1401–1426.
- 156 Z. Al Tanoury, A. Piskunov and C. Rochette-Egly, Vitamin A and retinoid signaling: genomic and nongenomic effects, *Journal of lipid research*, 2013, **54**, 1761–1775.
- 157 V. Dhokia and S. Macip, A master of all trades - linking retinoids to different signalling pathways through the multi-purpose receptor STRA6, *Cell death discovery*, 2021, **7**, 358.
- 158 S. Ding, C. Xu, C. Chen, J. Li, J. Wang and H. Xie, Novel Functions of the Fatty Acid and Retinol Binding Protein (FAR) Gene Family Revealed by Fungus-Mediated RNAi in the Parasitic Nematode, *Aphelenchoides besseyi*, *International journal of molecular sciences*, 2021, **22**. DOI: 10.3390/ijms221810057.
- 159 Y.-K. Kim, L. Wassef, S. Chung, H. Jiang, A. Wyss, W. S. Blaner and L. Quadro,  $\beta$ -Carotene and its cleavage enzyme  $\beta$ -carotene-15,15'-oxygenase (CMOI) affect retinoid metabolism in developing tissues, *FASEB journal : official publication of the Federation of American Societies for Experimental Biology*, 2011, **25**, 1641–1652.
- 160 A. Antebi, Nuclear hormone receptors in *C. elegans*, *WormBook : the online review of C. elegans biology*, 2006, 1–13.
- 161 B. C. Das, P. Thapa, R. Karki, S. Das, S. Mahapatra, T.-C. Liu, I. Torregroza, D. P. Wallace, S. Kambhampati, P. van Veldhuizen, A. Verma, S. K. Ray and T. Evans, Retinoic acid signaling pathways in development and diseases, *Bioorganic & medicinal chemistry*, 2014, **22**, 673–683.
- 162 W. Pan, Y.-L. Zhou, J. Wang, H.-E. Dai, X. Wang and L. Liu, Structural and Functional Analysis of Nonheme Iron Enzymes BCMO-1 and BCMO-2 from *Caenorhabditis elegans*, *Frontiers in molecular biosciences*, 2022, **9**, 844453.
- 163 G. Nagel, D. Ollig, M. Fuhrmann, S. Kateriya, A. M. Musti, E. Bamberg and P. Hegemann, Channelrhodopsin-1: a light-gated proton channel in green algae, *Science (New York, N.Y.)*, 2002, **296**, 2395–2398.
- 164 Y.-P. Zhang, N. Holbro and T. G. Oertner, Optical induction of plasticity at single synapses reveals input-specific accumulation of  $\alpha$ CaMKII, *Proceedings of the National Academy of Sciences of the United States of America*, 2008, **105**, 12039–12044.
- 165 Y.-P. Zhang and T. G. Oertner, Optical induction of synaptic plasticity using a light-sensitive channel, *Nature methods*, 2007, **4**, 139–141.
- 166 L. Petreanu, D. Huber, A. Sobczyk and K. Svoboda, Channelrhodopsin-2-assisted circuit mapping of long-range callosal projections, *Nature neuroscience*, 2007, **10**, 663–668.
- 167 D. Huber, L. Petreanu, N. Ghitani, S. Ranade, T. Hromádka, Z. Mainen and K. Svoboda, Sparse optical microstimulation in barrel cortex drives learned behaviour in freely moving mice, *Nature*, 2008, **451**, 61–64.

- 168 A. D. Douglass, S. Kraves, K. Deisseroth, A. F. Schier and F. Engert, Escape behavior elicited by single, channelrhodopsin-2-evoked spikes in zebrafish somatosensory neurons, *Current biology : CB*, 2008, **18**, 1133–1137.
- 169 K. Madduri, F. Torti, A. L. Colombo and C. R. Hutchinson, Cloning and sequencing of a gene encoding carminomycin 4-O-methyltransferase from *Streptomyces peucetius* and its expression in *Escherichia coli*, *Journal of Bacteriology*, 1993, **175**, 3900–3904.
- 170 M. R. Park, X. Chen, D. E. Lang, K. K. Ng and P. J. Facchini, Heterodimeric O-methyltransferases involved in the biosynthesis of noscapine in opium poppy, *The Plant Journal*, 2018, **95**, 252–267.
- 171 M. Locatelli, Anthraquinones: analytical techniques as a novel tool to investigate on the triggering of biological targets, *Current drug targets*, 2011, **12**, 366–380.
- 172 M. Masi and A. Evidente, Fungal Bioactive Anthraquinones and Analogues, *Toxins*, 2020, **12**. DOI: 10.3390/toxins12110714.
- 173 L. A. Calhoun, J. A. Findlay, J. David Miller and N. J. Whitney, Metabolites toxic to spruce budworm from balsam fir needle endophytes, *Mycological Research*, 1992, **96**, 281–286.
- 174 I. Wijesekara, C. Zhang, Q. van Ta, T.-S. Vo, Y.-X. Li and S.-K. Kim, Physcion from marine-derived fungus *Microsporum* sp. induces apoptosis in human cervical carcinoma HeLa cells, *Microbiological Research*, 2014, **169**, 255–261.
- 175 M. Isaka, S. Palasarn, P. Tobwor, T. Boonruangprapa and K. Tasanathai, Bioactive anthraquinone dimers from the leafhopper pathogenic fungus *Torrubiella* sp. BCC 28517, *The Journal of antibiotics*, 2012, **65**, 571–574.
- 176 K. Engström, S. Brishammar, C. Svensson, M. Bengtsson and R. Andersson, Anthraquinones from some *Drechslera* species and *Bipolaris sorokiniana*, *Mycological Research*, 1993, **97**, 381–384.
- 177 N. Khamthong, V. Rukachaisirikul, S. Phongpaichit, S. Preedanon and J. Sakayaroj, Bioactive polyketides from the sea fan-derived fungus *Penicillium citrinum* PSU-F51, *Tetrahedron*, 2012, **68**, 8245–8250.
- 178 Y. M. Lee, H. Li, J. Hong, H. Y. Cho, K. S. Bae, M. A. Kim, D.-K. Kim and J. H. Jung, Bioactive metabolites from the sponge-derived fungus *Aspergillus versicolor*, *Archives of pharmacal research*, 2010, **33**, 231–235.
- 179 S. Miethbauer, S. Haase, K.-U. Schmidtke, W. Günther, I. Heiser and B. Liebermann, Biosynthesis of photodynamically active rubellins and structure elucidation of new anthraquinone derivatives produced by *Ramularia collo-cygni*, *Phytochemistry*, 2006, **67**, 1206–1213.
- 180 S. Miethbauer, F. Gaube, U. Möllmann, H.-M. Dahse, M. Schmidtke, M. Gareis, M. Pickhardt and B. Liebermann, Antimicrobial, antiproliferative, cytotoxic, and tau inhibitory activity of rubellins and caeruleoramularin produced by the phytopathogenic fungus *Ramularia collo-cygni*, *Planta medica*, 2009, **75**, 1523–1525.
- 181 Ri-Chou Han, Wim M. Wouts and Li-ying Li, in 1990.
- 182 D. J. Bowen and J. C. Ensign, Purification and characterization of a high-molecular-weight insecticidal protein complex produced by the entomopathogenic bacterium *Photobacterium luminescens*, *Applied and environmental microbiology*, 1998, **64**, 3029–3035.

- 183 M. Fischer-Le Saux, V. Viallard, B. Brunel, P. Normand and N. E. Boemare, Polyphasic classification of the genus *Photobacterium* and proposal of new taxa: *P. luminescens* subsp. *luminescens* subsp. nov., *P. luminescens* subsp. *akhurstii* subsp. nov., *P. luminescens* subsp. *laumondii* subsp. nov., *P. temperata* sp. nov., *P. temperata* subsp. *temperata* subsp. nov. and *P. asymbiotica* sp. nov., *International Journal of Systematic Bacteriology*, 1999, **49 Pt 4**, 1645–1656.
- 184 S. A. Joyce, L. Lango and D. J. Clarke, The Regulation of Secondary Metabolism and Mutualism in the Insect Pathogenic Bacterium *Photobacterium luminescens*, *Advances in applied microbiology*, 2011, **76**, 1–25.
- 185 S. Li, C. Lu, J. Ou, J. Deng and Y. Shen, Overexpression of *hgc1* increases the production and diversity of hygrocins in *Streptomyces* sp. LZ35, *RSC Adv.*, 2015, **5**, 83843–83846.
- 186 Y. Mao, G. Li, Z. Chang, R. Tao, Z. Cui, Z. Wang, Y.-J. Tang, T. Chen and X. Zhao, Metabolic engineering of *Corynebacterium glutamicum* for efficient production of succinate from lignocellulosic hydrolysate, *Biotechnology for biofuels*, 2018, **11**, 95.
- 187 D. Yang, W. J. Kim, S. M. Yoo, J. H. Choi, S. H. Ha, M. H. Lee and S. Y. Lee, Repurposing type III polyketide synthase as a malonyl-CoA biosensor for metabolic engineering in bacteria, *Proceedings of the National Academy of Sciences of the United States of America*, 2018, **115**, 9835–9844.
- 188 R. Rezaei, W. Wang, Z. Wu, Z. Dai, J. Wang and G. Wu, Biochemical and physiological bases for utilization of dietary amino acids by young Pigs, *Journal of animal science and biotechnology*, 2013, **4**, 7.
- 189 L. Stryer, R. Tasker and C. Rhodes, *Biochemistry*, W.H. Freeman, New York, 4th edn., 2000, 1995.
- 190 T. van Pham, S. Fehlbaum, N. Seifert, N. Richard, M. J. Bruins, W. Sybesma, A. Rehman and R. E. Steinert, Effects of colon-targeted vitamins on the composition and metabolic activity of the human gut microbiome- a pilot study, *Gut microbes*, 2021, **13**, 1–20.
- 191 J.-H. Nah, H.-J. Kim, H.-N. Lee, M.-J. Lee, S.-S. Choi and E.-S. Kim, Identification and biotechnological application of novel regulatory genes involved in *Streptomyces* polyketide overproduction through reverse engineering strategy, *BioMed research international*, 2013, **2013**, 549737.
- 192 J. Yang and L. Guo, Biosynthesis of  $\beta$ -carotene in engineered *E. coli* using the MEP and MVA pathways, *Microbial cell factories*, 2014, **13**, 160.
- 193 J. D. Lipscomb, Mechanism of extradiol aromatic ring-cleaving dioxygenases, *Current opinion in structural biology*, 2008, **18**, 644–649.
- 194 C. R. Schlachter, L. Daneshian, J. Amaya, V. Klapper, N. Wybouw, T. Borowski, T. van Leeuwen, V. Grbic, M. Grbic, T. M. Makris and M. Chruszcz, Structural and functional characterization of an intradiol ring-cleavage dioxygenase from the polyphagous spider mite herbivore *Tetranychus urticae* Koch, *Insect biochemistry and molecular biology*, 2019, **107**, 19–30.
- 195 E. Rodríguez-Bustamante and S. Sánchez, Microbial production of C13-norisoprenoids and other aroma compounds via carotenoid cleavage, *Critical reviews in microbiology*, 2007, **33**, 211–230.



- 196 C. Höckelmann and F. Jüttner, Off-flavours in water: hydroxyketones and  $\beta$ -ionone derivatives as new odour compounds of freshwater cyanobacteria, *Flavour Fragr. J.*, 2005, **20**, 387–394.
- 197 F. Jüttner and B. Höflacher, Evidence of  $\beta$ -carotene 7,8(7',8') oxygenase ( $\beta$ -cyclocitral, crocetindial generating) in *Microcystis*, *Arch. Microbiol.*, 1985, **141**, 337–343.
- 198 D. Scherzinger, E. Scheffer, C. Bär, H. Ernst and S. Al-Babili, The *Mycobacterium tuberculosis* ORF Rv0654 encodes a carotenoid oxygenase mediating central and excentric cleavage of conventional and aromatic carotenoids, *The FEBS journal*, 2010, **277**, 4662–4673.
- 199 R.-J. Wang, K. Chen, L.-S. Xing, Z. Lin, Z. Zou and Z. Lu, Reactive oxygen species and antimicrobial peptides are sequentially produced in silkworm midgut in response to bacterial infection, *Developmental and comparative immunology*, 2020, **110**, 103720.
- 200 L. Zhou, L. Ouyang, S. Lin, S. Chen, Y. Liu, W. Zhou and X. Wang, Protective role of  $\beta$ -carotene against oxidative stress and neuroinflammation in a rat model of spinal cord injury, *International immunopharmacology*, 2018, **61**, 92–99.
- 201 M. A. Gammone, G. Riccioni and N. D'Orazio, Marine Carotenoids against Oxidative Stress: Effects on Human Health, *Marine Drugs*, 2015, **13**, 6226–6246.
- 202 G. L. C. Grammbitter, M. Schmalhofer, K. Karimi, Y.-M. Shi, T. A. Schöner, N. J. Tobias, N. Morgner, M. Groll and H. B. Bode, An Uncommon Type II PKS Catalyzes Biosynthesis of Aryl Polyene Pigments, *Journal of the American Chemical Society*, 2019, **141**, 16615–16623.
- 203 R. D. Parihar, U. Dhiman, A. Bhushan, P. K. Gupta and P. Gupta, Heterorhabdus and Photorhabdus Symbiosis: A Natural Mine of Bioactive Compounds, *Frontiers in microbiology*, 2022, **13**, 790339.

## 9 Appendix

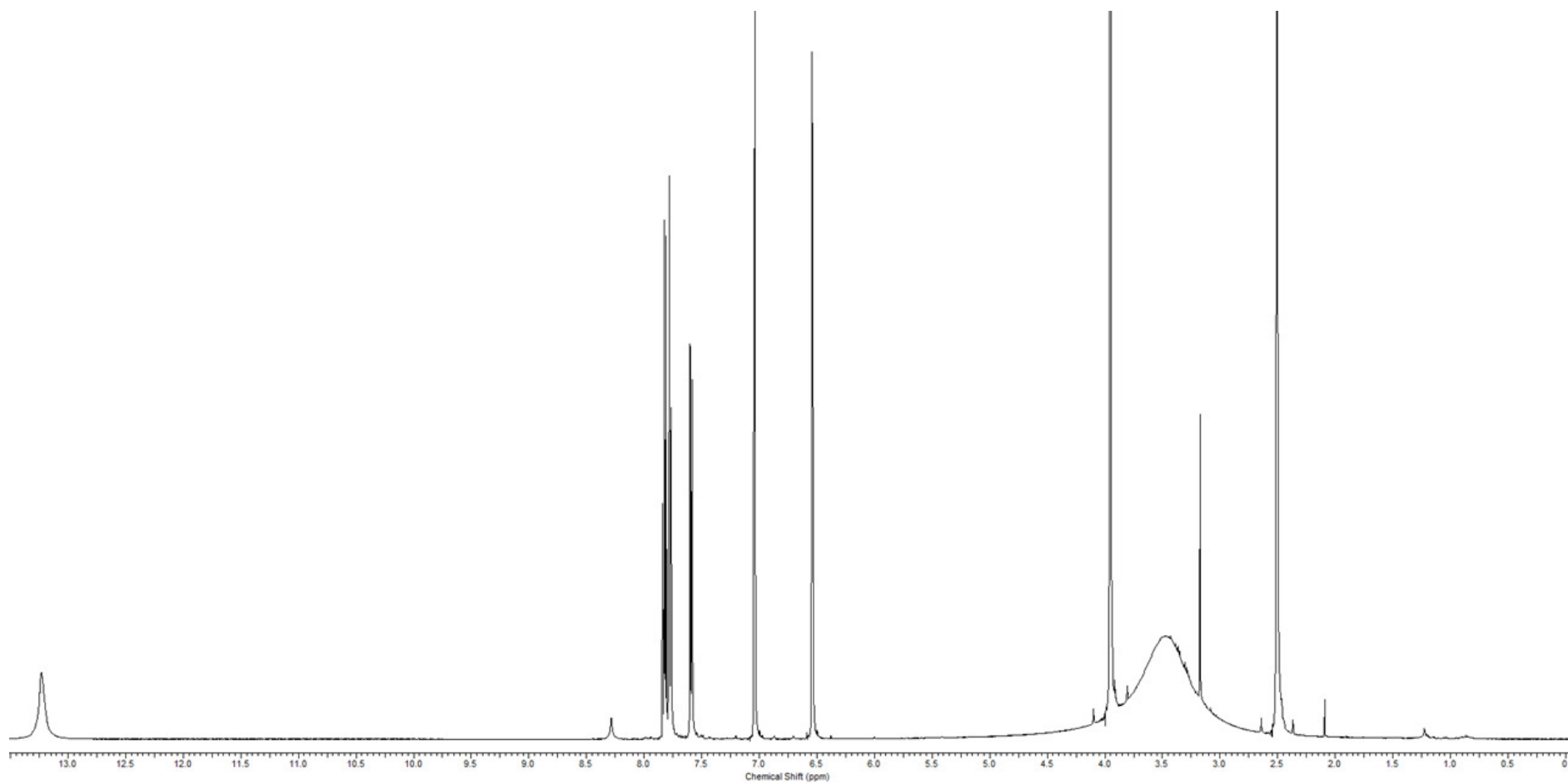


**Figure S1.**  $^1\text{H}$ -NMR spectrum [500 MHz] of AQ-270a in  $\text{D}_6$ -DMSO.

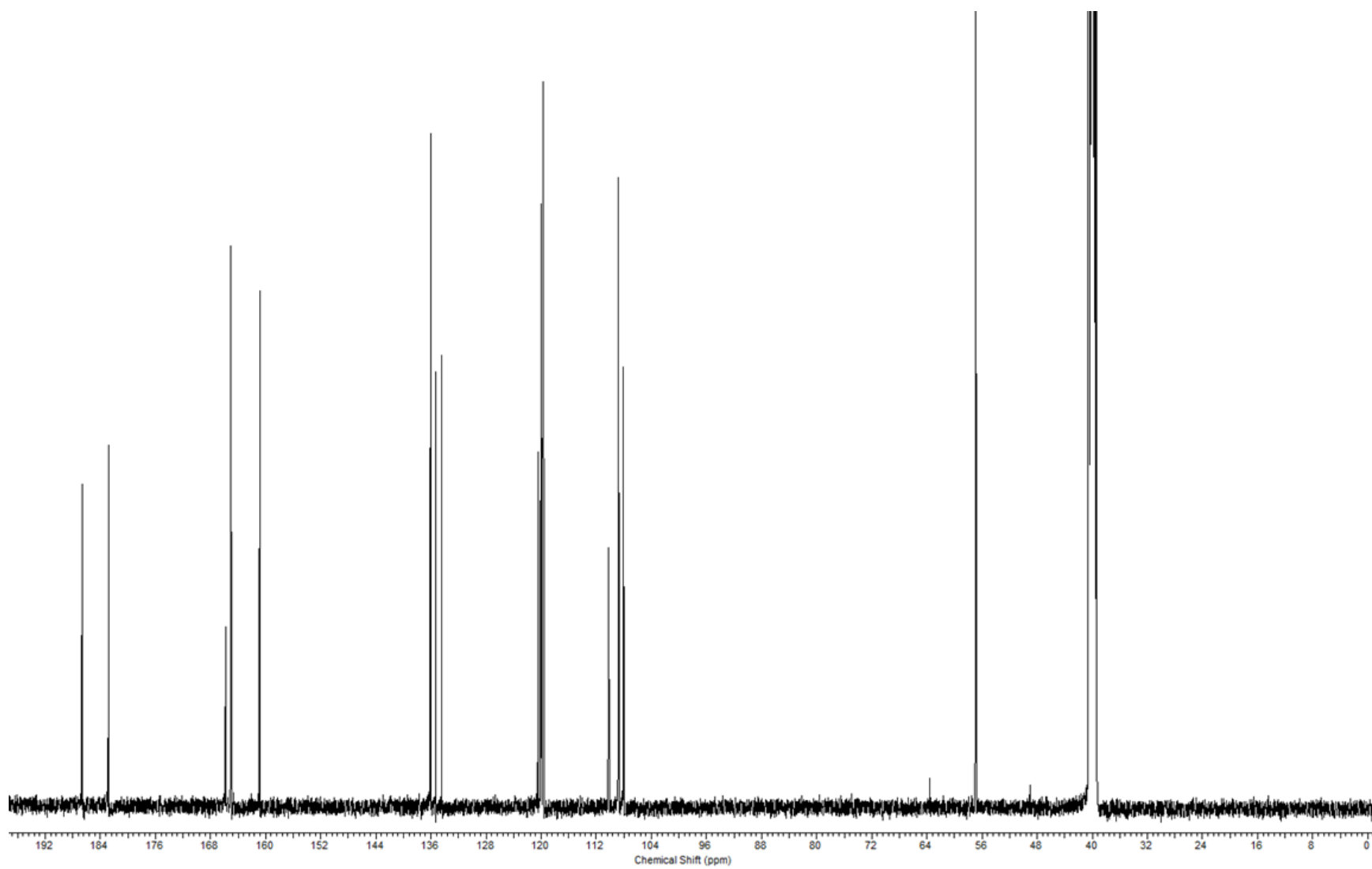


**Figure S2.**  $^{13}\text{C}$ -NMR spectrum [125 MHz] of AQ-270a in  $\text{D}_6$ -DMSO.

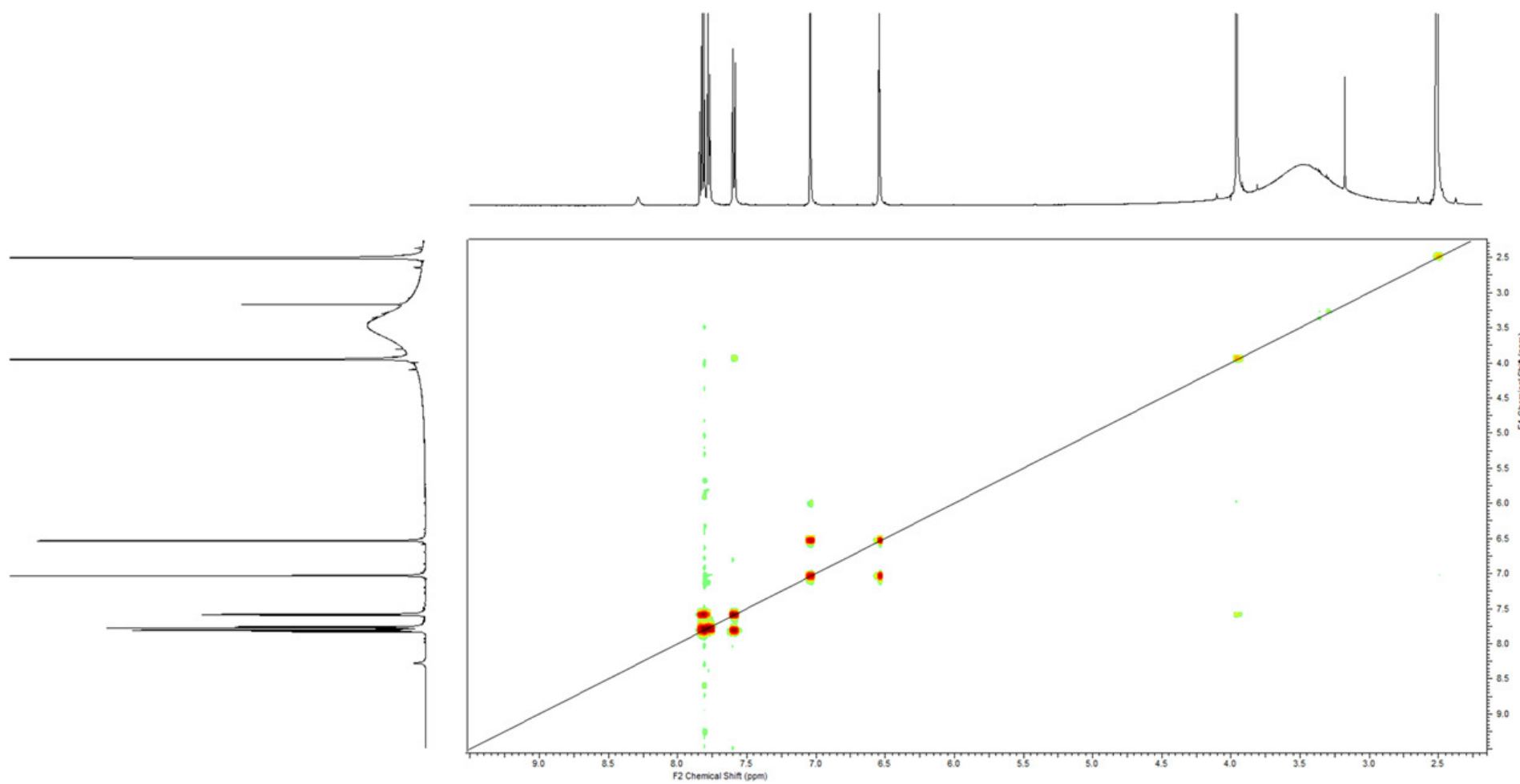


**Figure S3.**  $^1\text{H}$ - $^1\text{H}$  COSY-NMR spectrum of AQ-270a in  $\text{D}_6$ -DMSO.

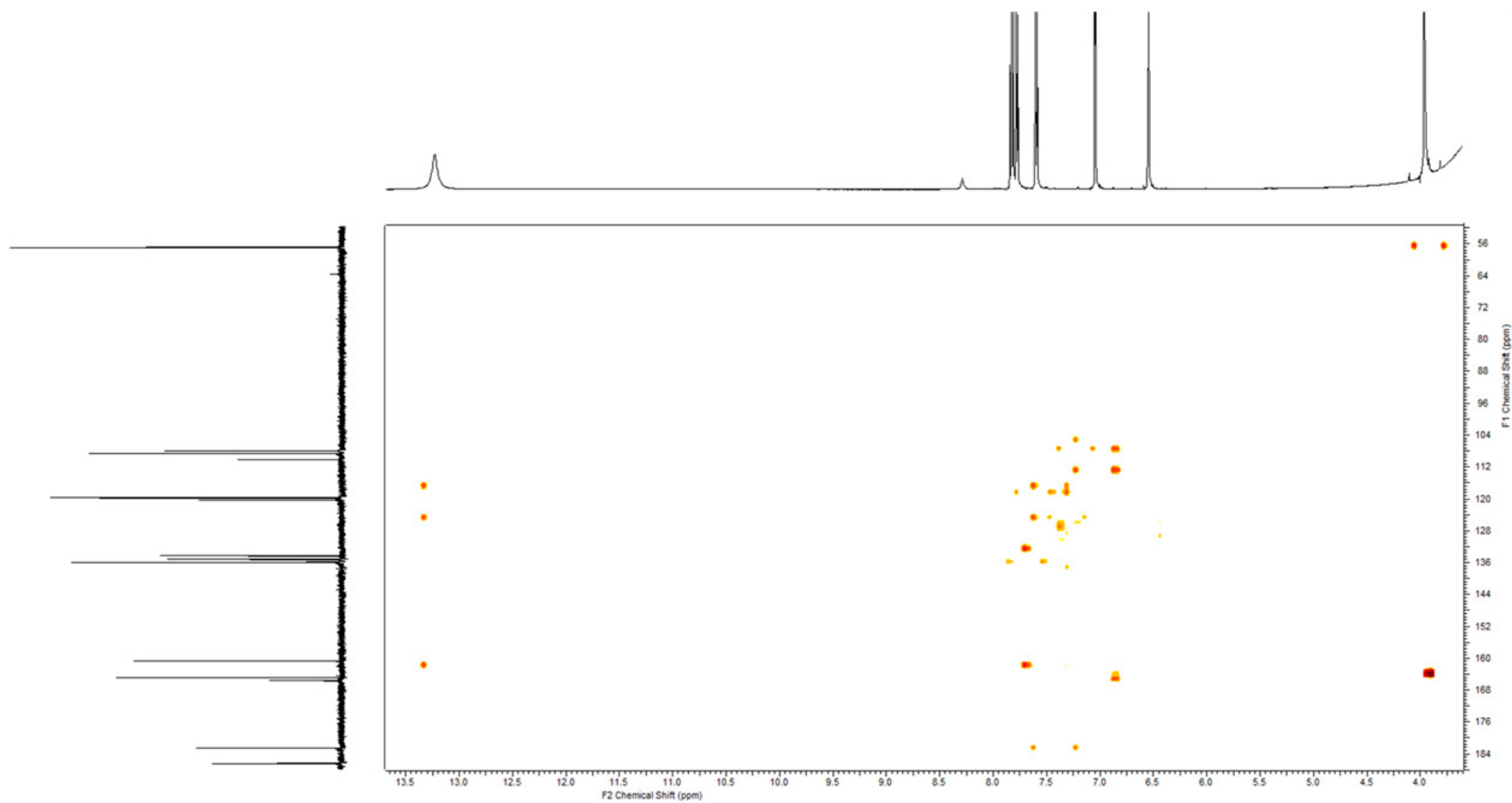


**Figure S4.** HMBC-NMR spectrum of AQ-270a in D<sub>6</sub>-DMSO.

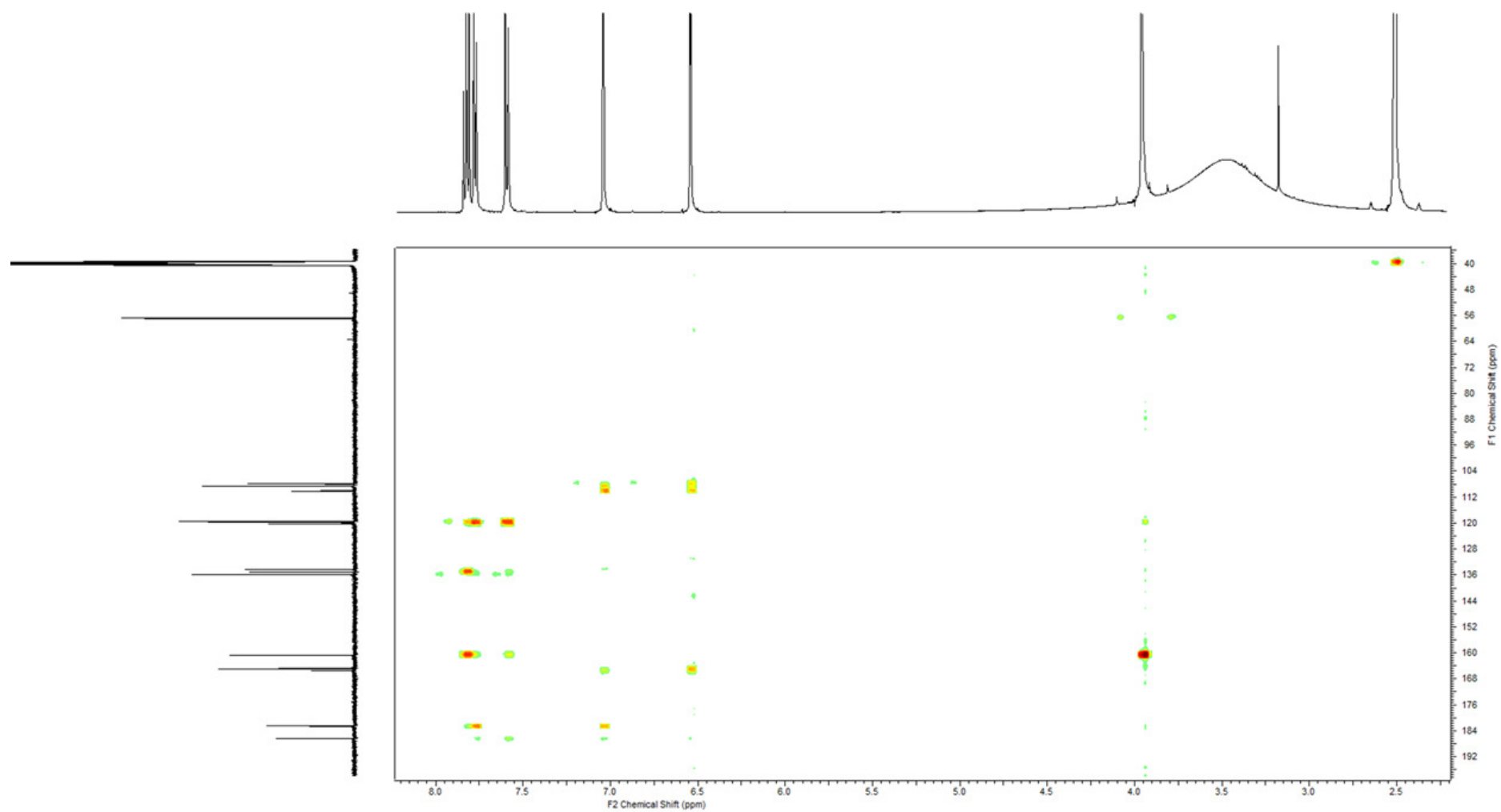


**Figure S5.** HSQC-NMR spectrum of AQ-270a in D<sub>6</sub>-DMSO.

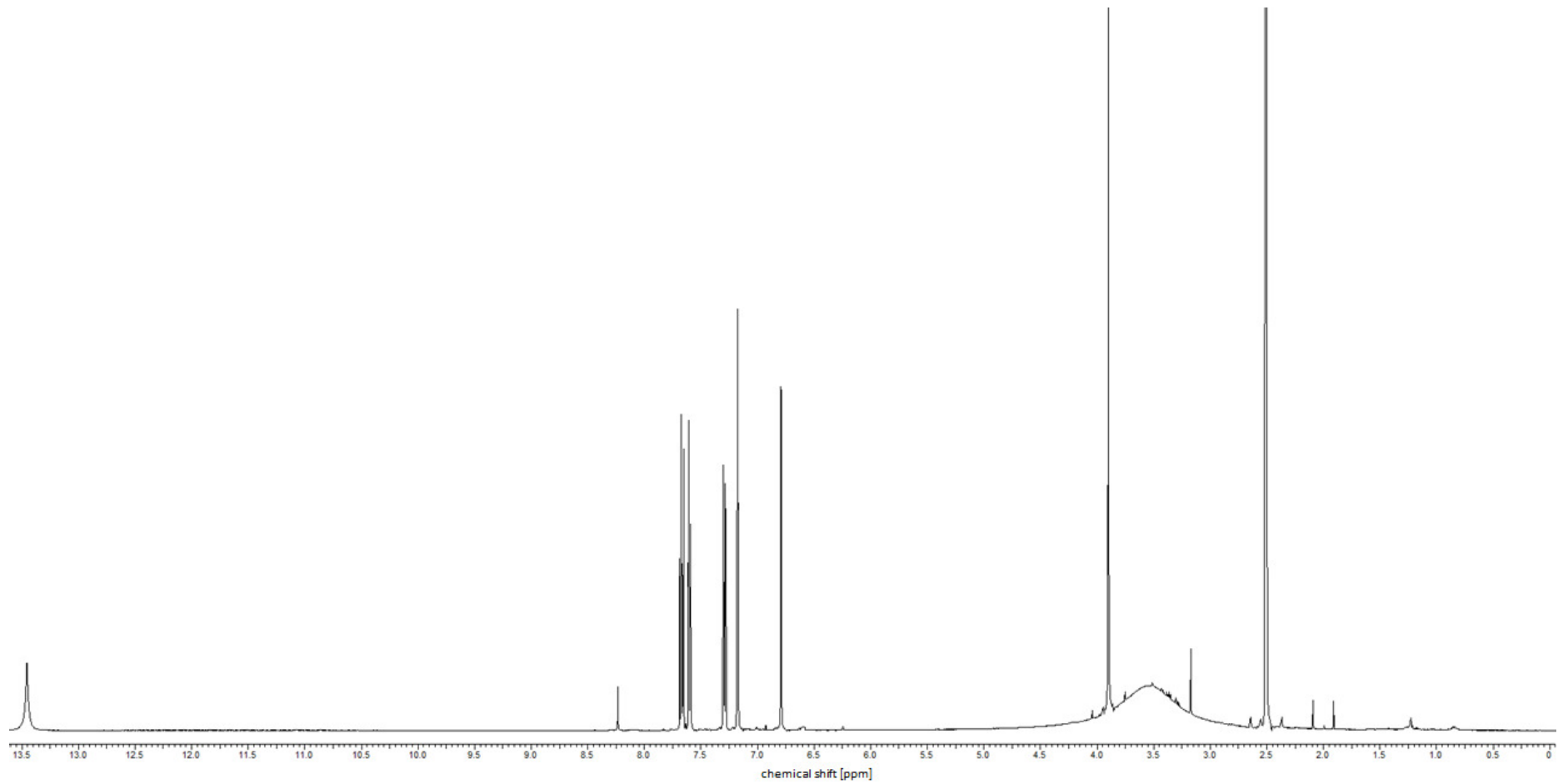


**Figure S6.**  $^1\text{H-NMR}$  spectrum [500 MHz] of AQ-270b in  $\text{D}_6\text{-DMSO}$ .



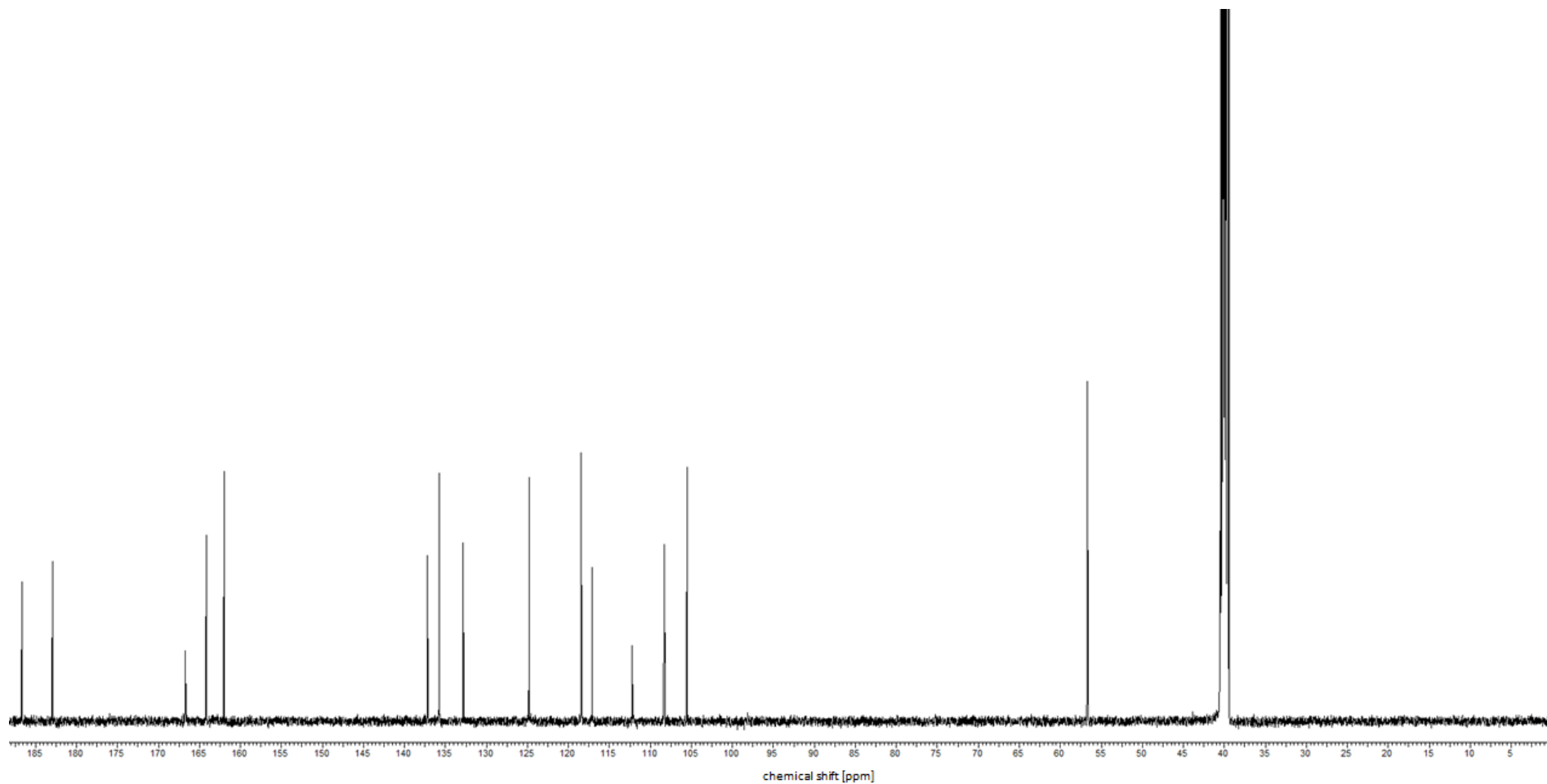


**Figure S7.**  $^{13}\text{C}$ -NMR spectrum [125 MHz] of AQ-270b in  $\text{D}_6$ -DMSO.

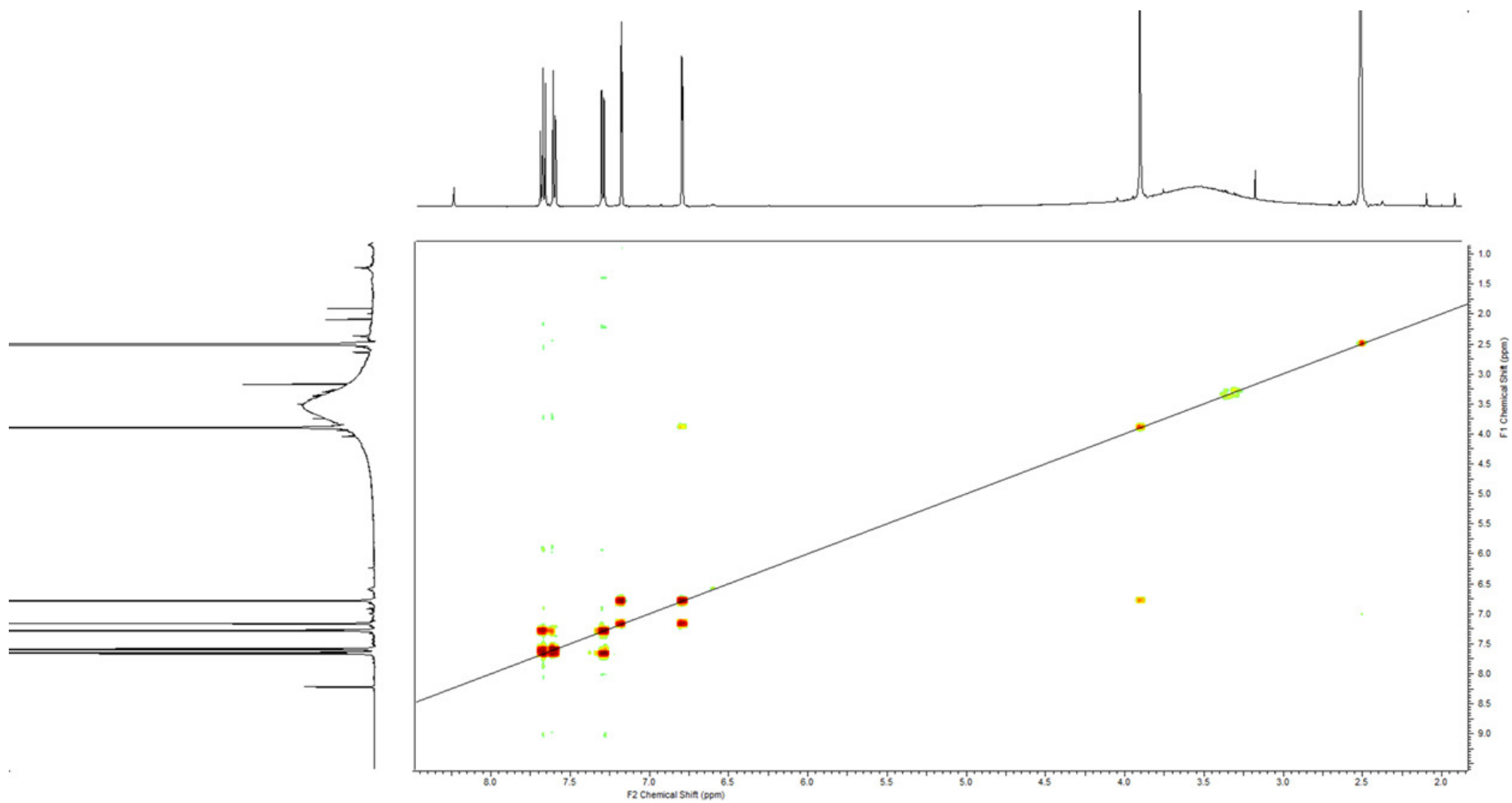


**Figure S8.**  $^1\text{H}$ - $^1\text{H}$  COSY-NMR spectrum of AQ-270b in  $\text{D}_6$ -DMSO.

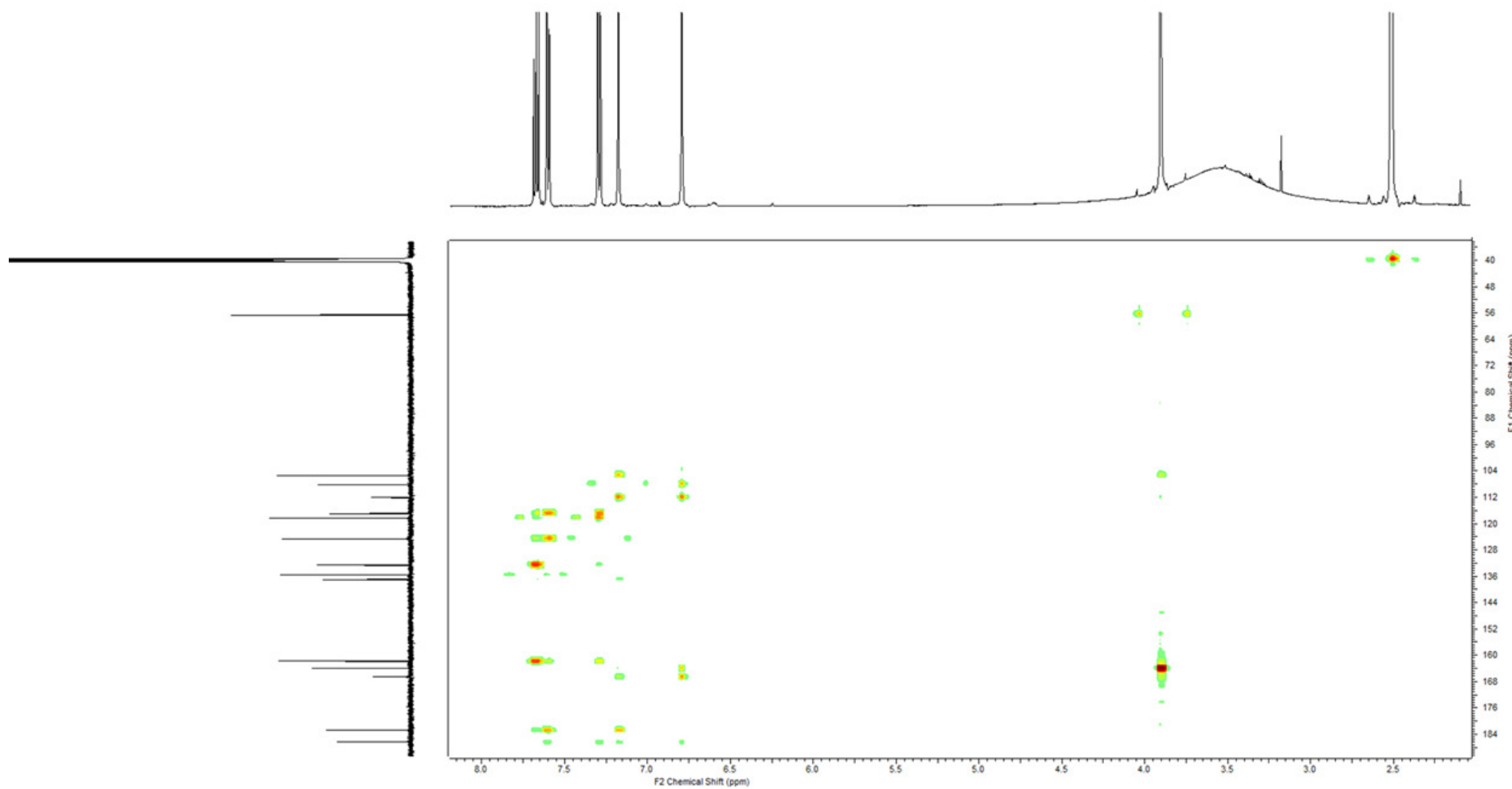


**Figure S9.** HMBC-NMR spectrum of AQ-270b in D<sub>6</sub>-DMSO.

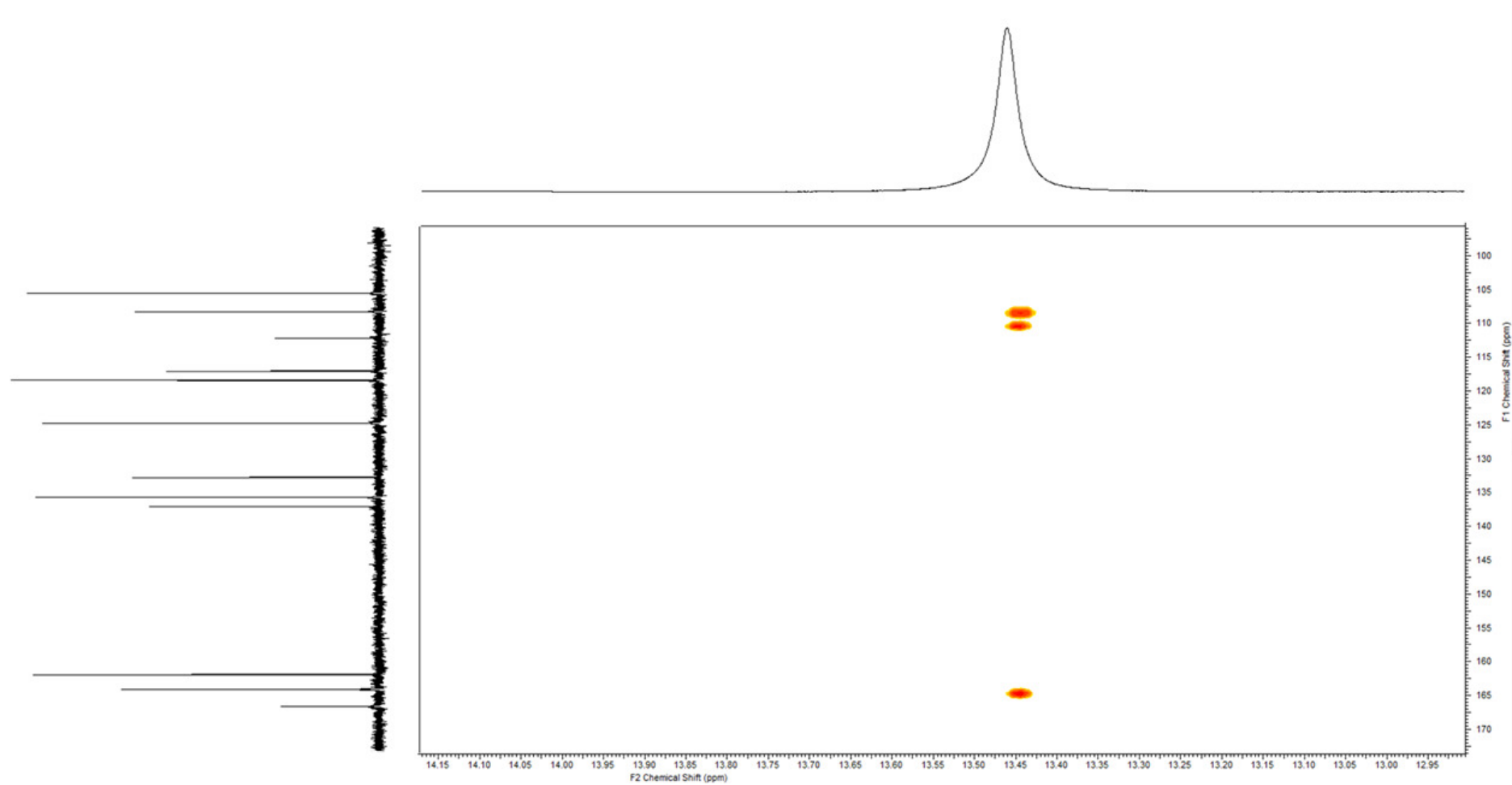


**Figure S10.** HMBC-NMR spectrum of AQ-270b in D<sub>6</sub>-DMSO.

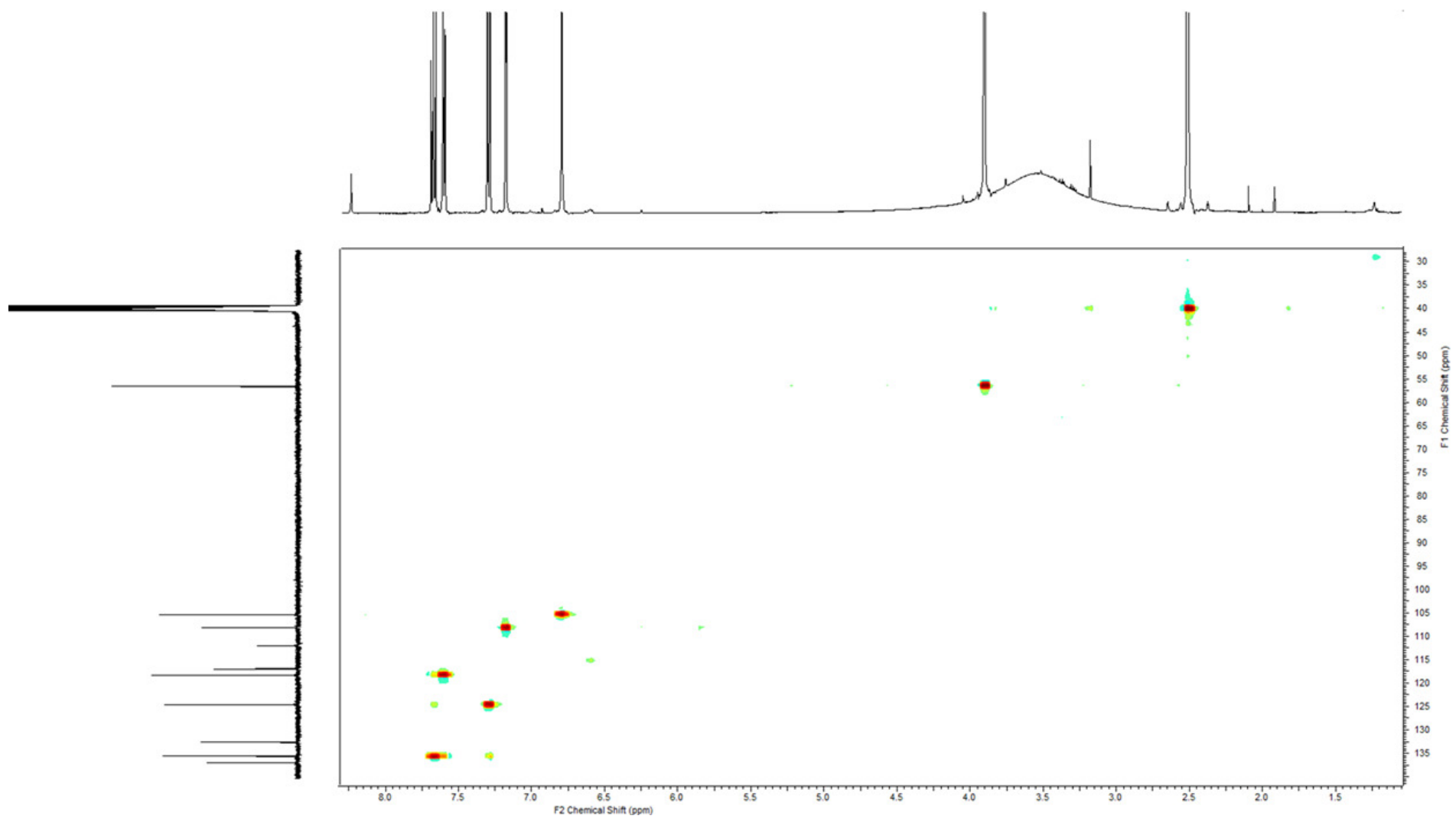


**Figure S11.** HSQC-NMR spectrum of AQ-270b in D<sub>6</sub>-DMSO.

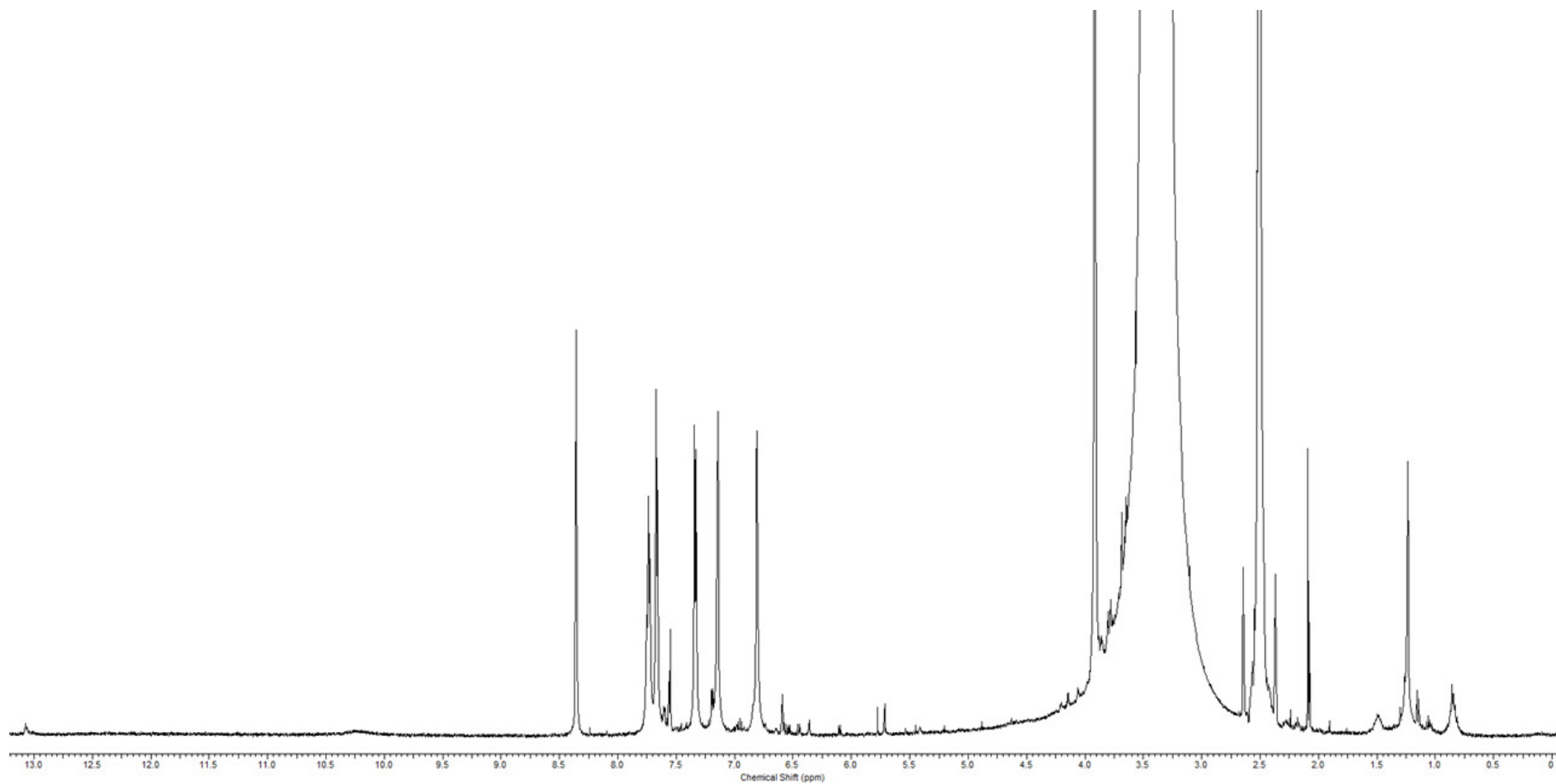


**Figure S12.** <sup>1</sup>H-NMR spectrum [500 MHz] of AQ-270c in D<sub>6</sub>-DMSO.

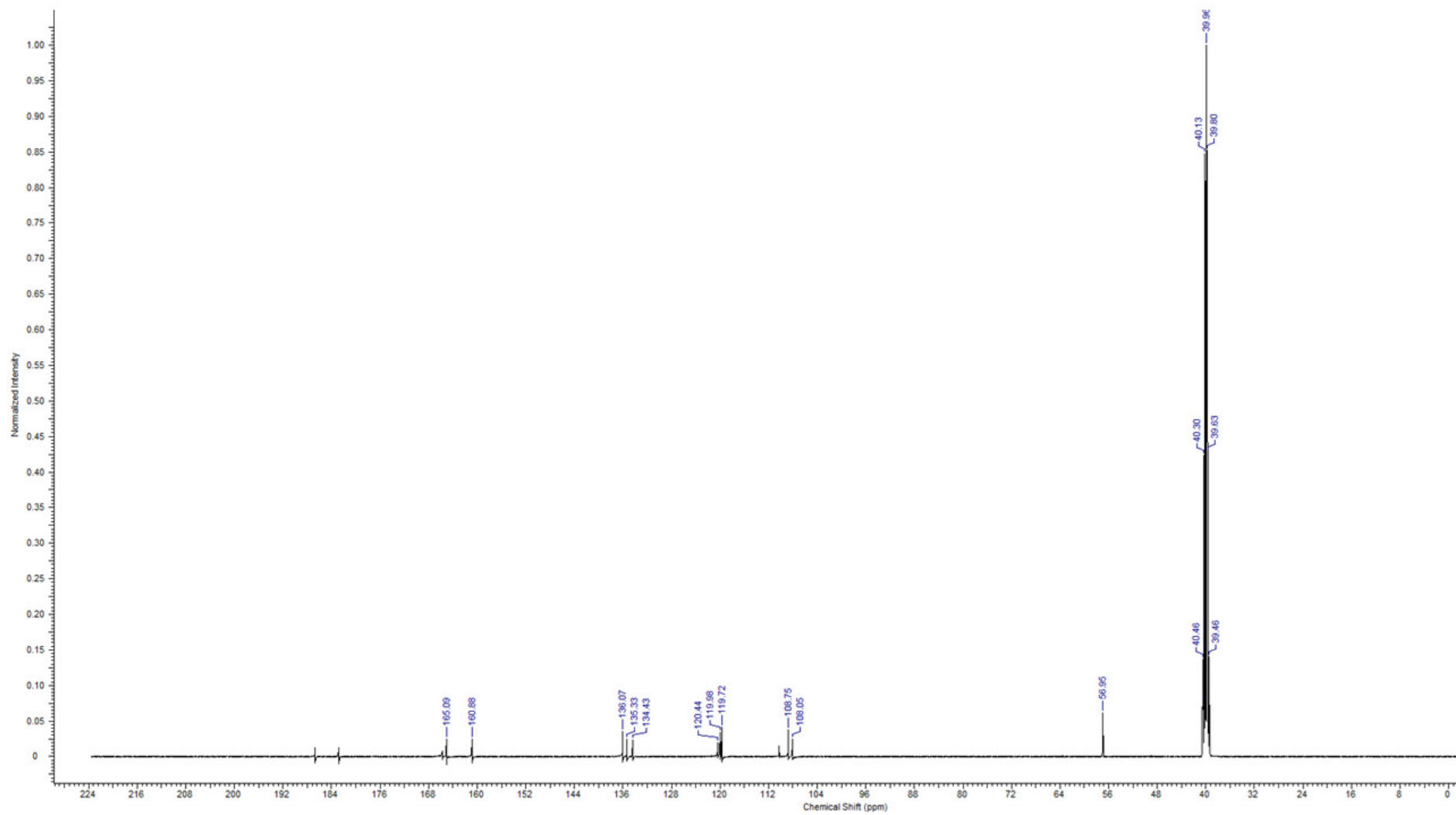


**Figure S13.**  $^{13}\text{C}$ -NMR spectrum [125 MHz] of AQ-270c in  $\text{D}_6$ -DMSO.

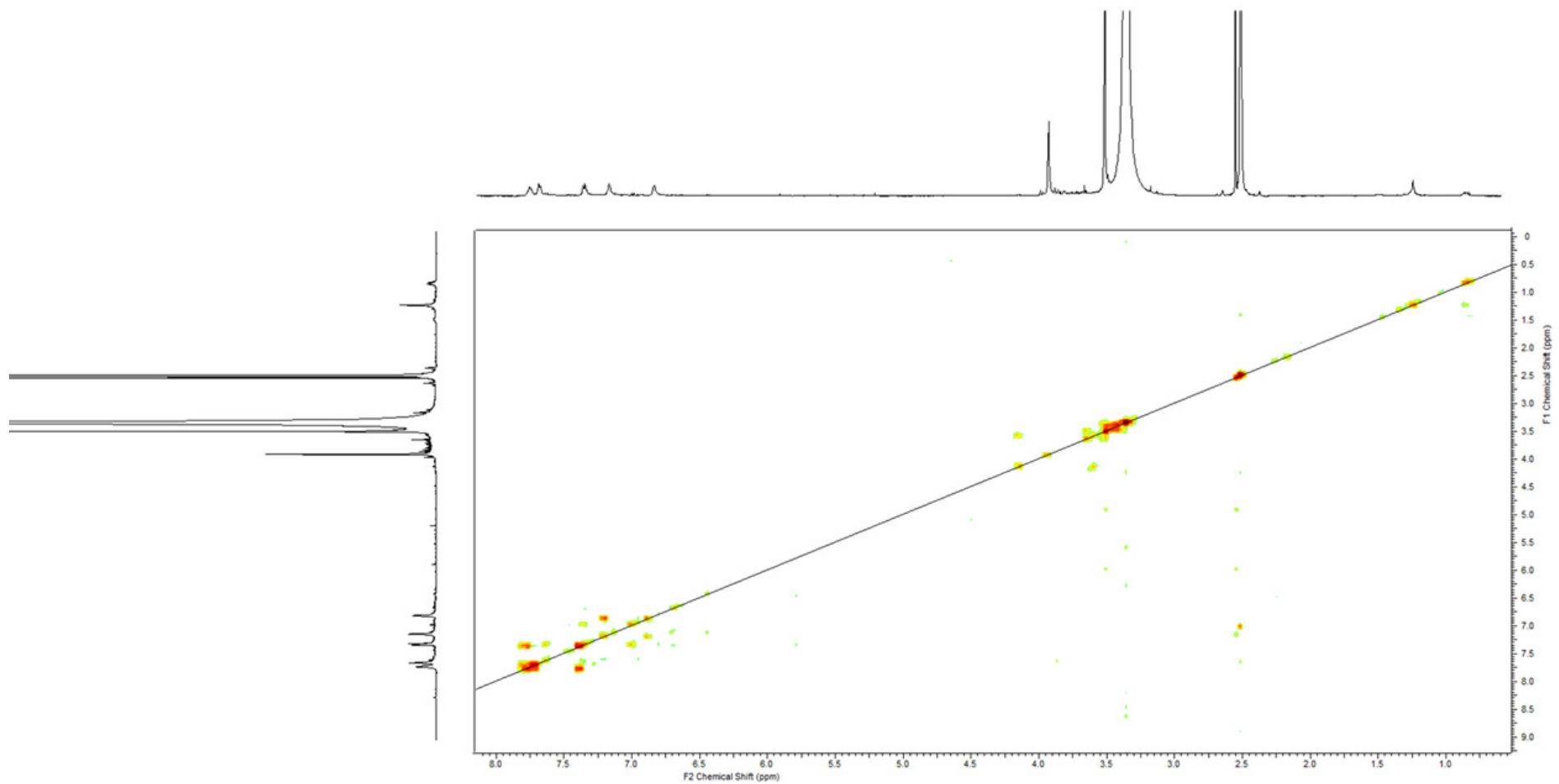


**Figure S14.**  $^1\text{H}$ - $^1\text{H}$  COSY-NMR spectrum of AQ-270c in  $\text{D}_6$ -DMSO.



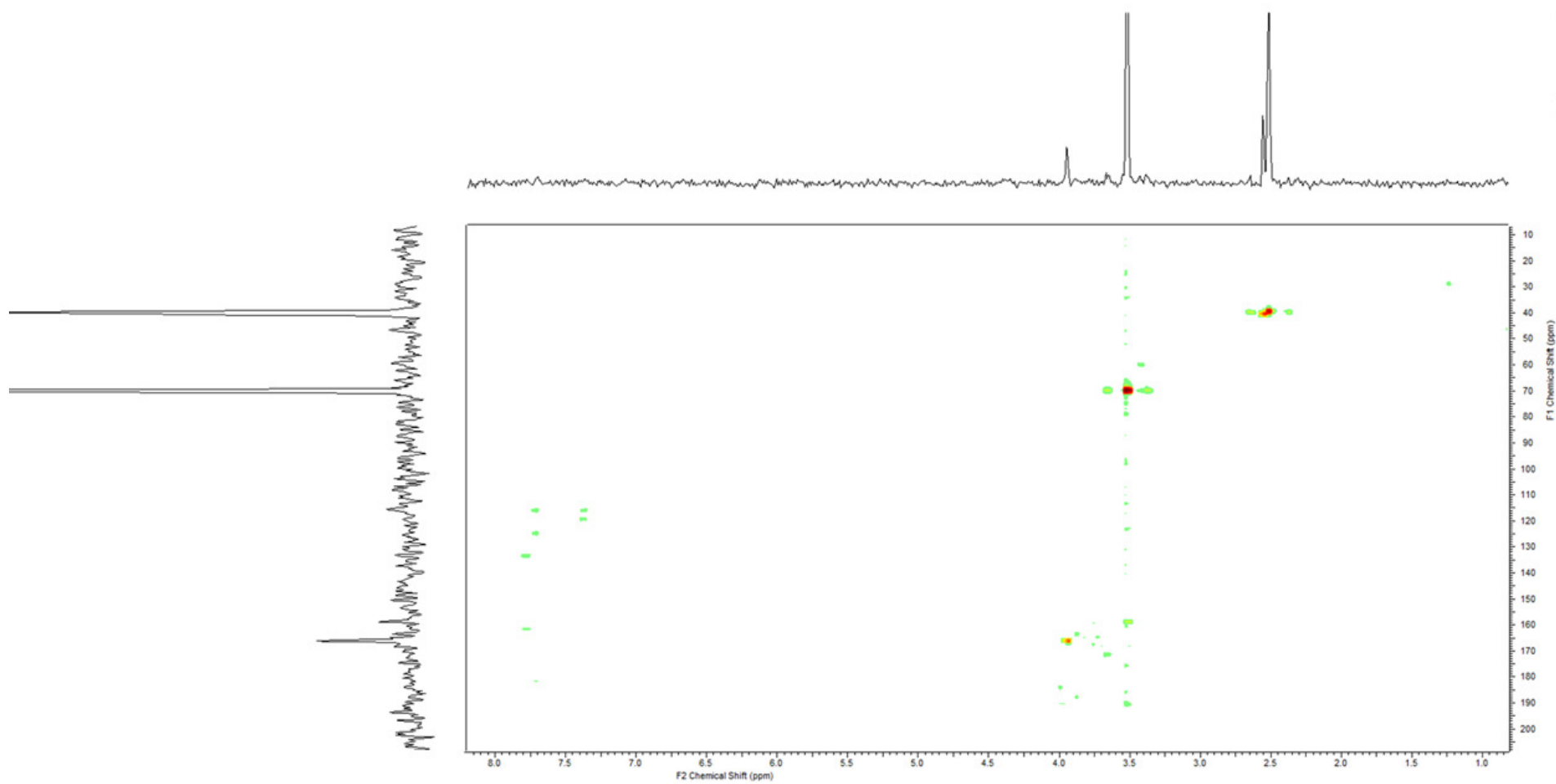


**Figure S15.** HMBC-NMR spectrum of AQ-270c in D<sub>6</sub>-DMSO.

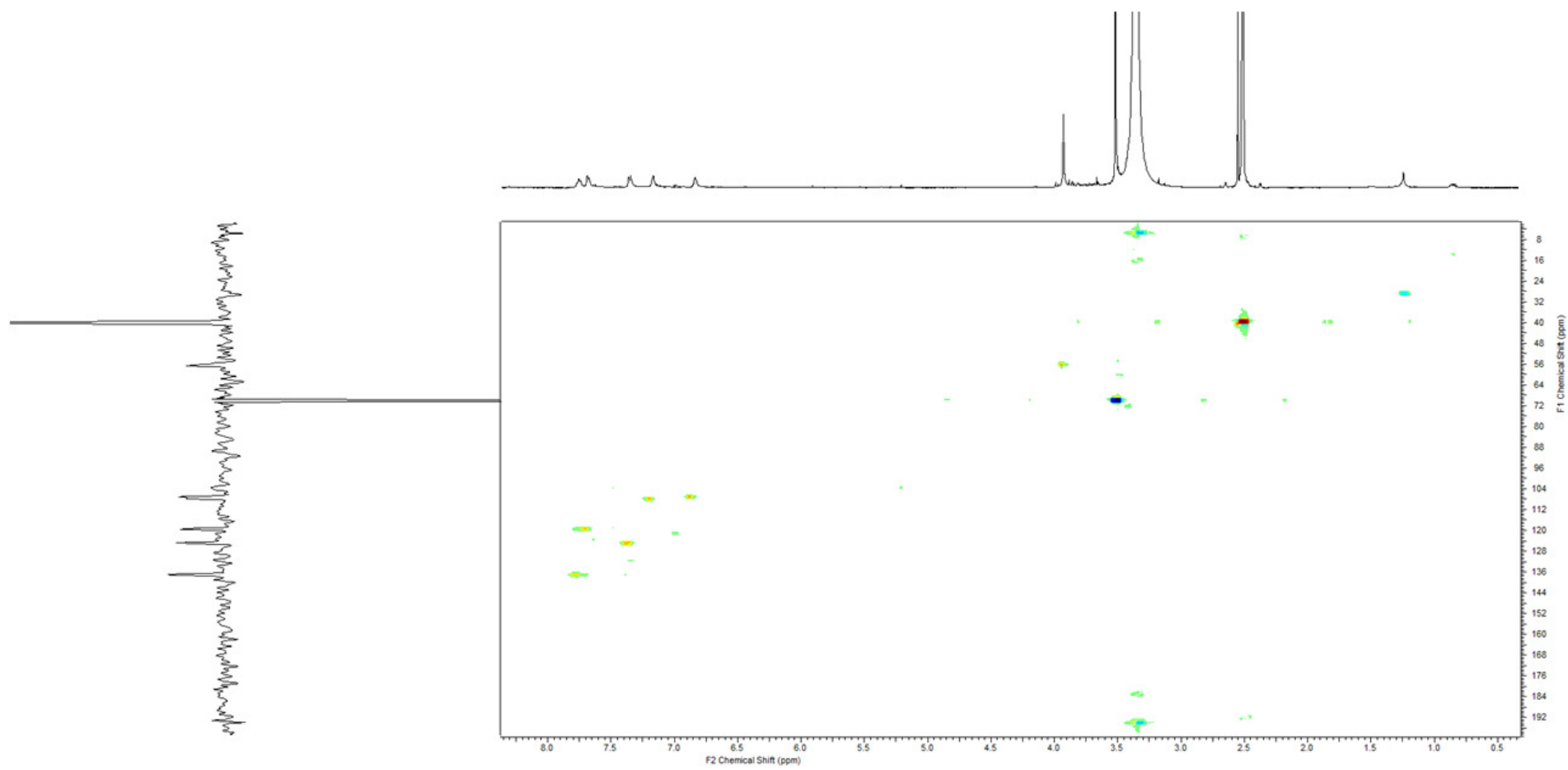


**Figure S16.** HSQC-NMR spectrum of AQ-270c in D<sub>6</sub>-DMSO.

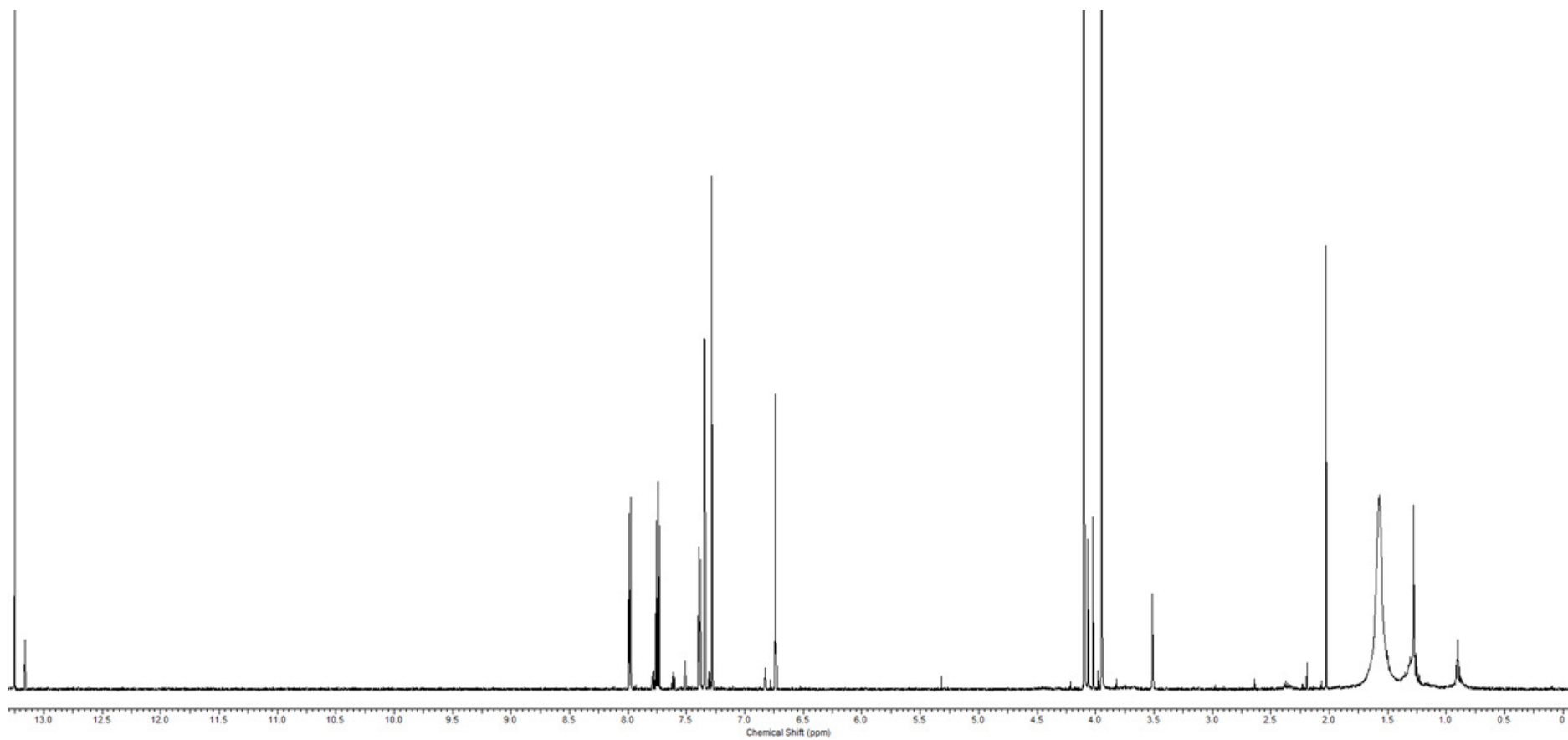


**Figure S17.** <sup>1</sup>H-NMR spectrum [500 MHz] of AQ-284a in D<sub>6</sub>-DMSO.

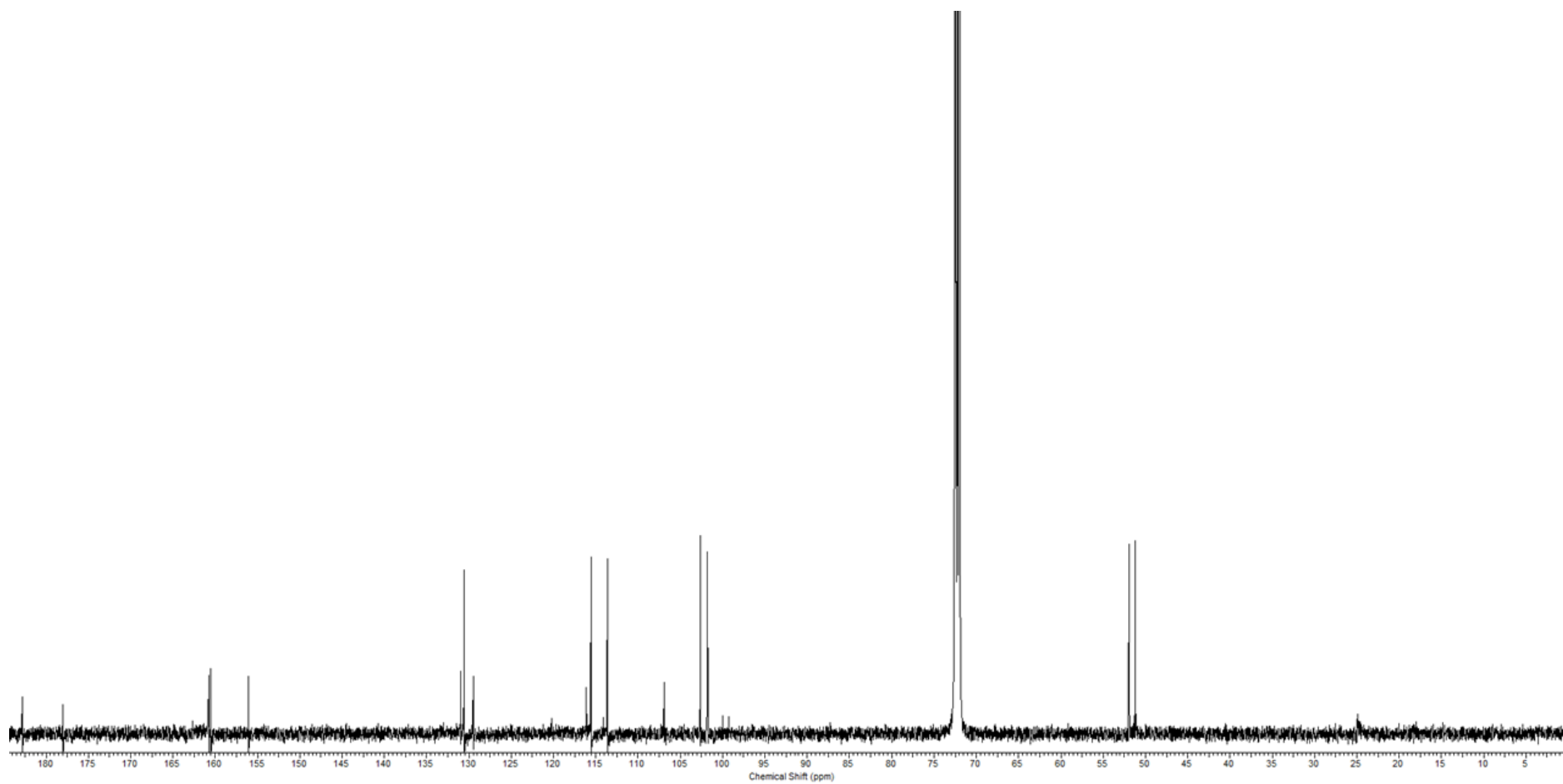


**Figure S18.**  $^{13}\text{C}$ -NMR spectrum [125 MHz] of AQ-284a in  $\text{D}_6$ -DMSO.

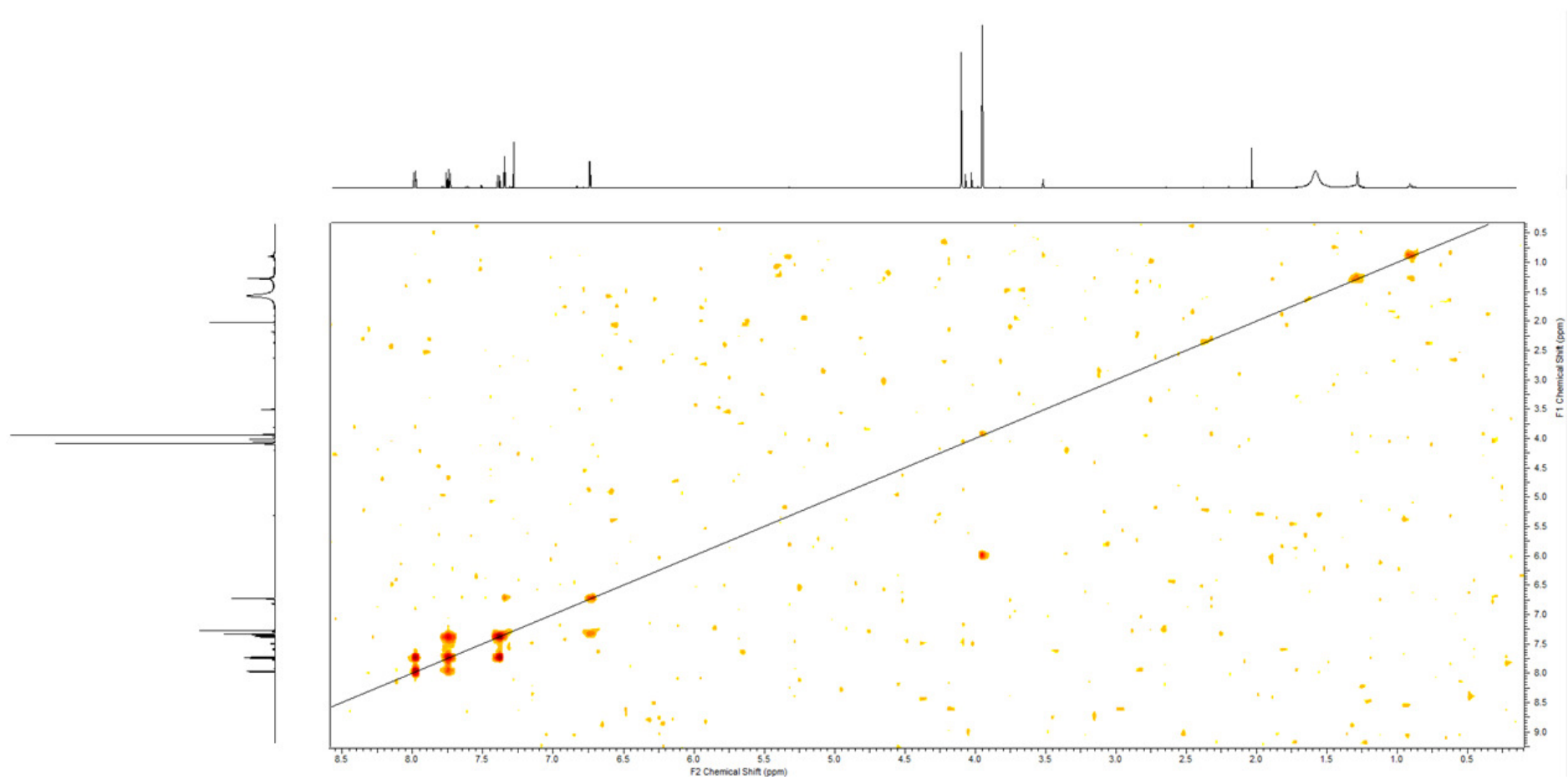


**Figure S19.**  $^1\text{H}$ - $^1\text{H}$  COSY-NMR spectrum of AQ-284a in  $\text{D}_6$ -DMSO.

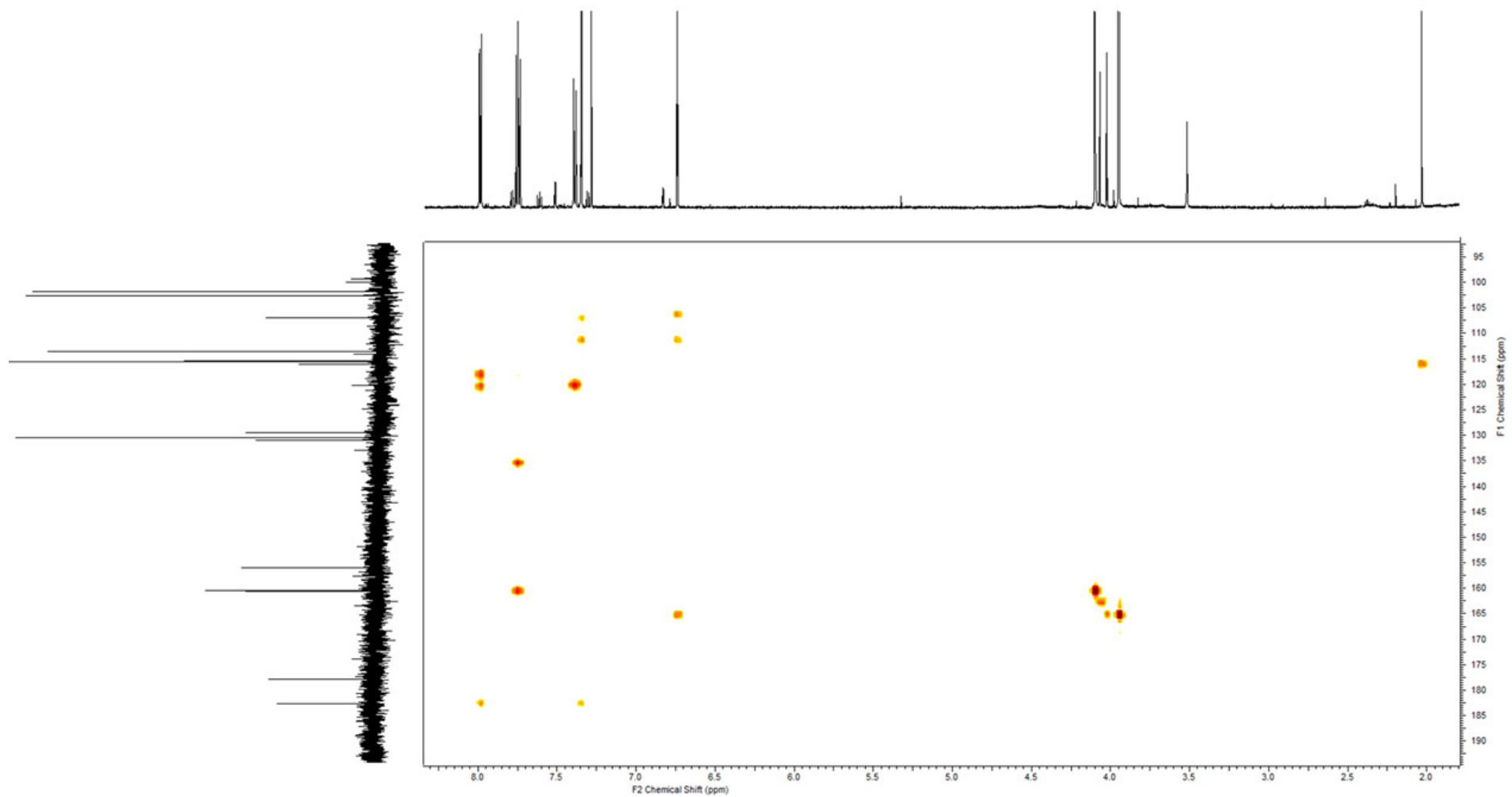


**Figure S20.** HMBC-NMR spectrum of AQ-284a in D<sub>6</sub>-DMSO.

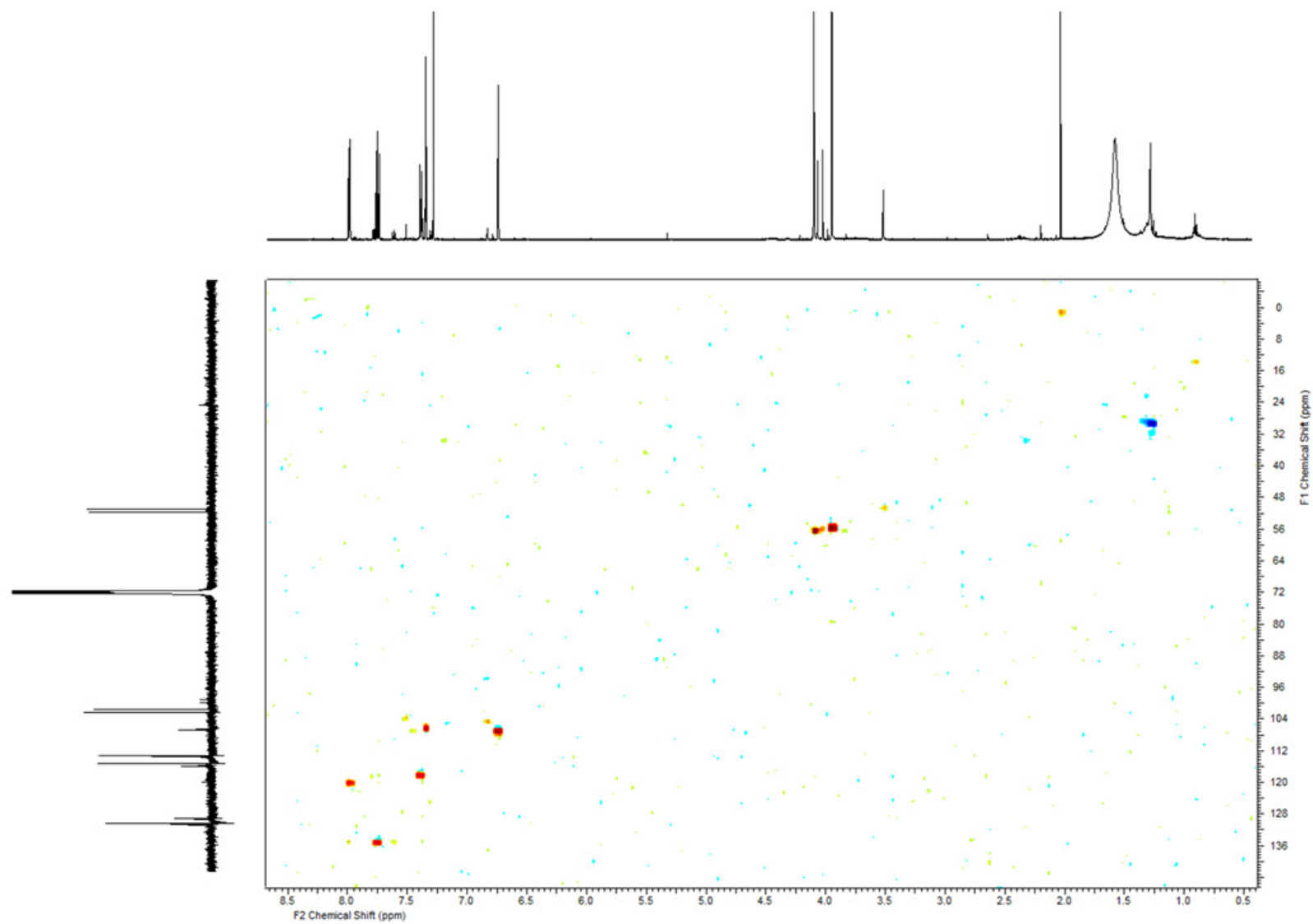


**Figure S21.** HSQC-NMR spectrum of AQ-284a in D<sub>6</sub>-DMSO.

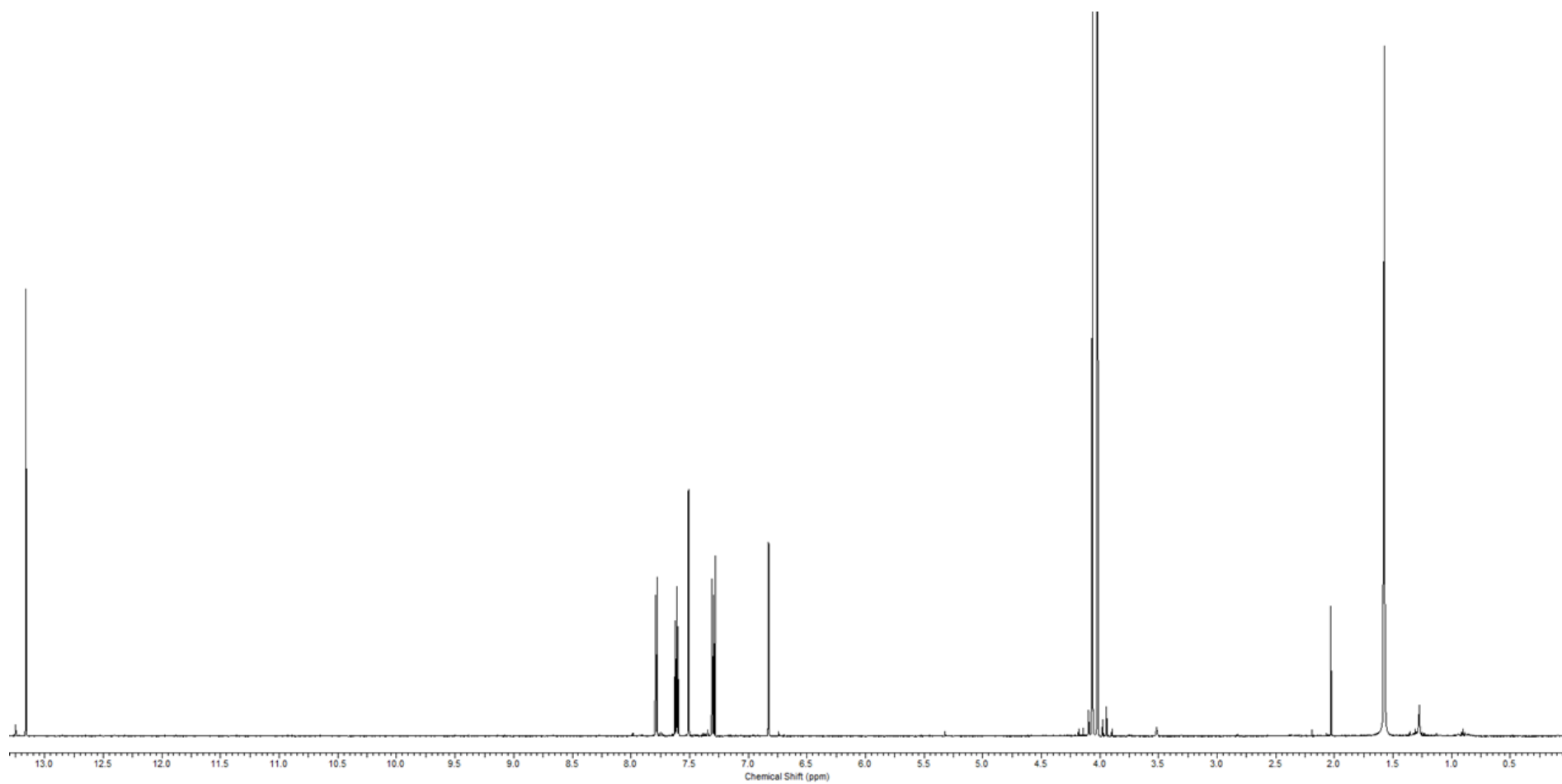


**Figure S22.**  $^1\text{H}$ -NMR spectrum [500 MHz] of AQ-284b in  $\text{D}_6$ -DMSO.



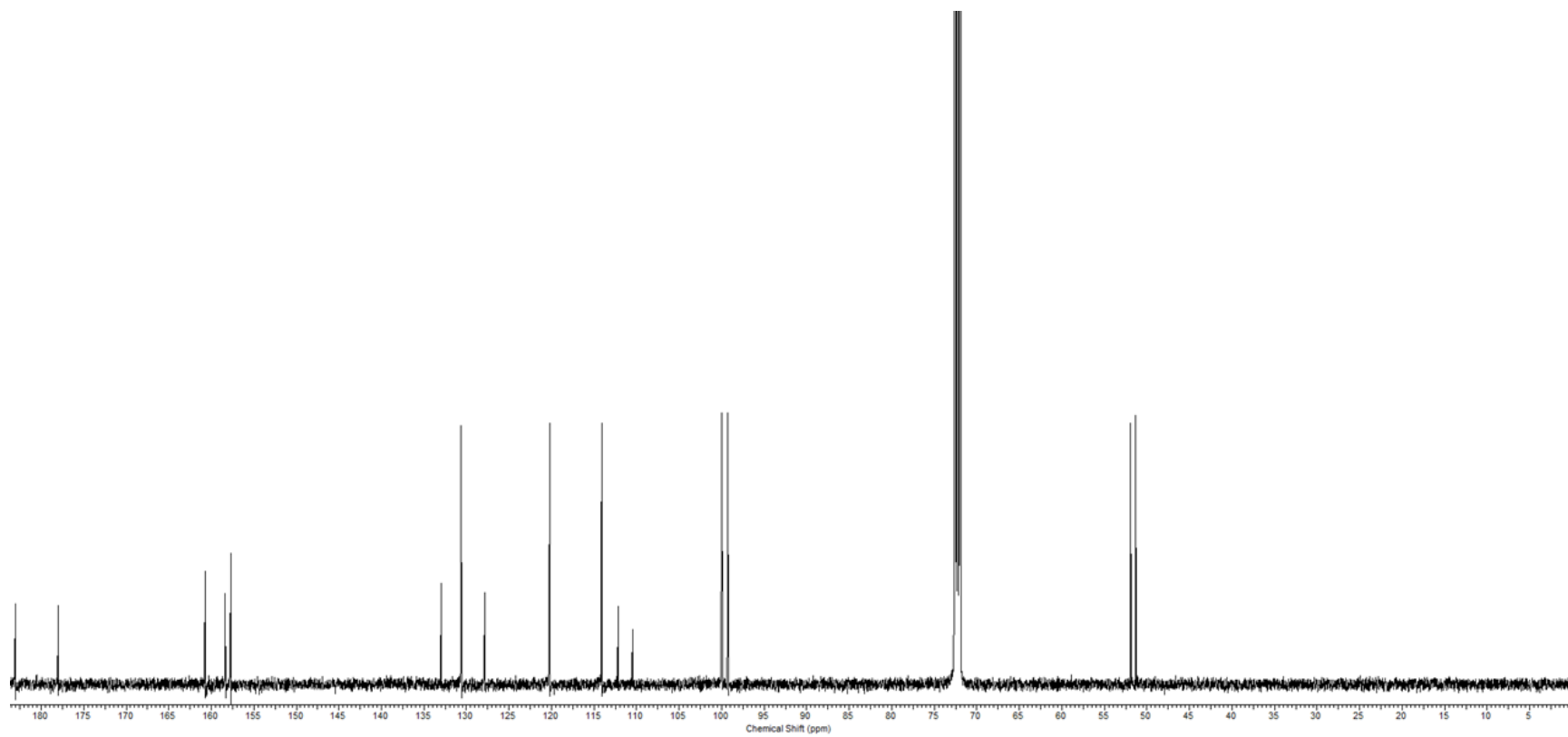


**Figure S23.**  $^{13}\text{C}$ -NMR spectrum [125 MHz] of AQ-284b in  $\text{D}_6$ -DMSO.

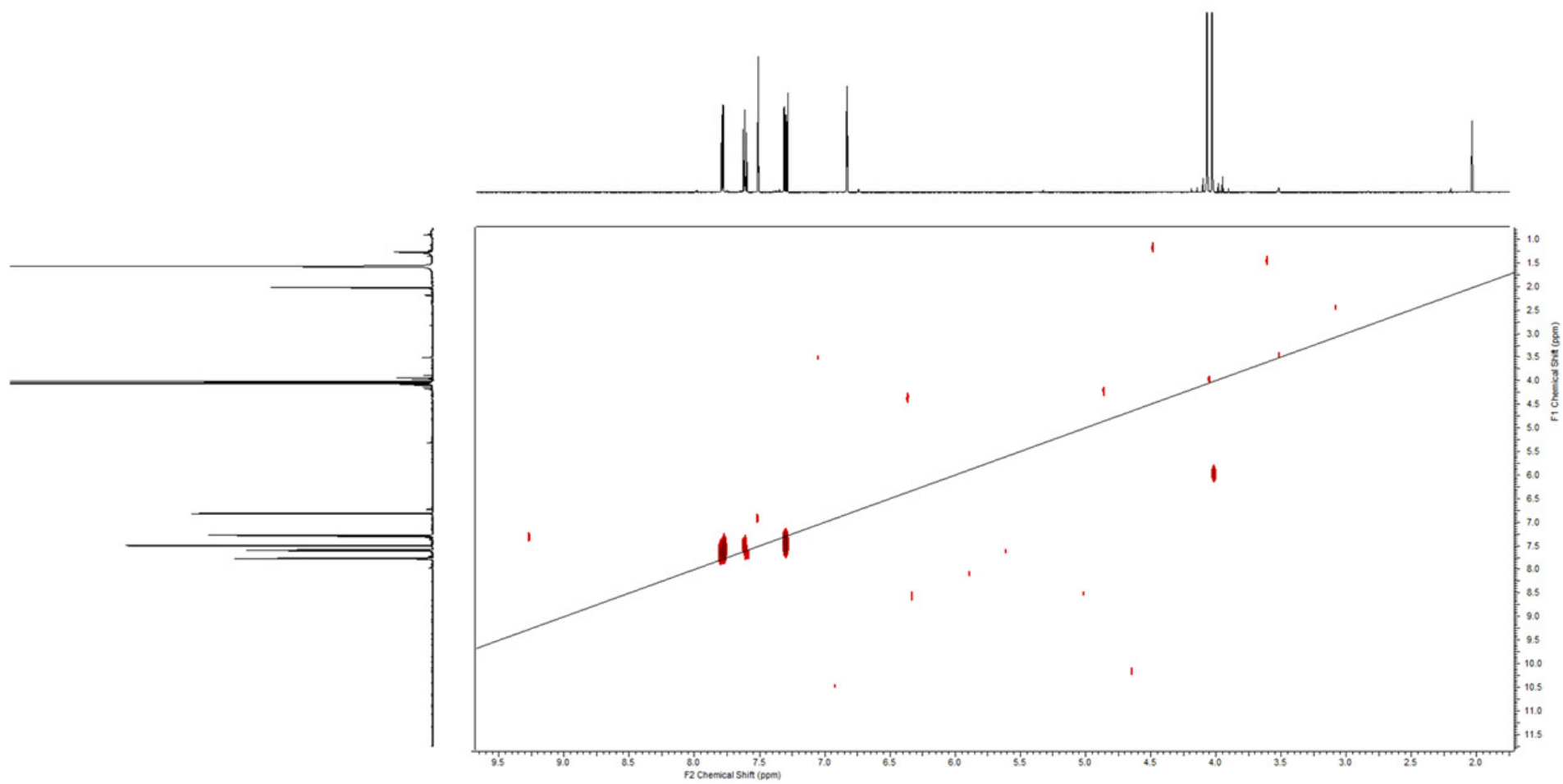


**Figure S24.**  $^1\text{H}$ - $^1\text{H}$  COSY-NMR spectrum of AQ-284b in  $\text{D}_6$ -DMSO.

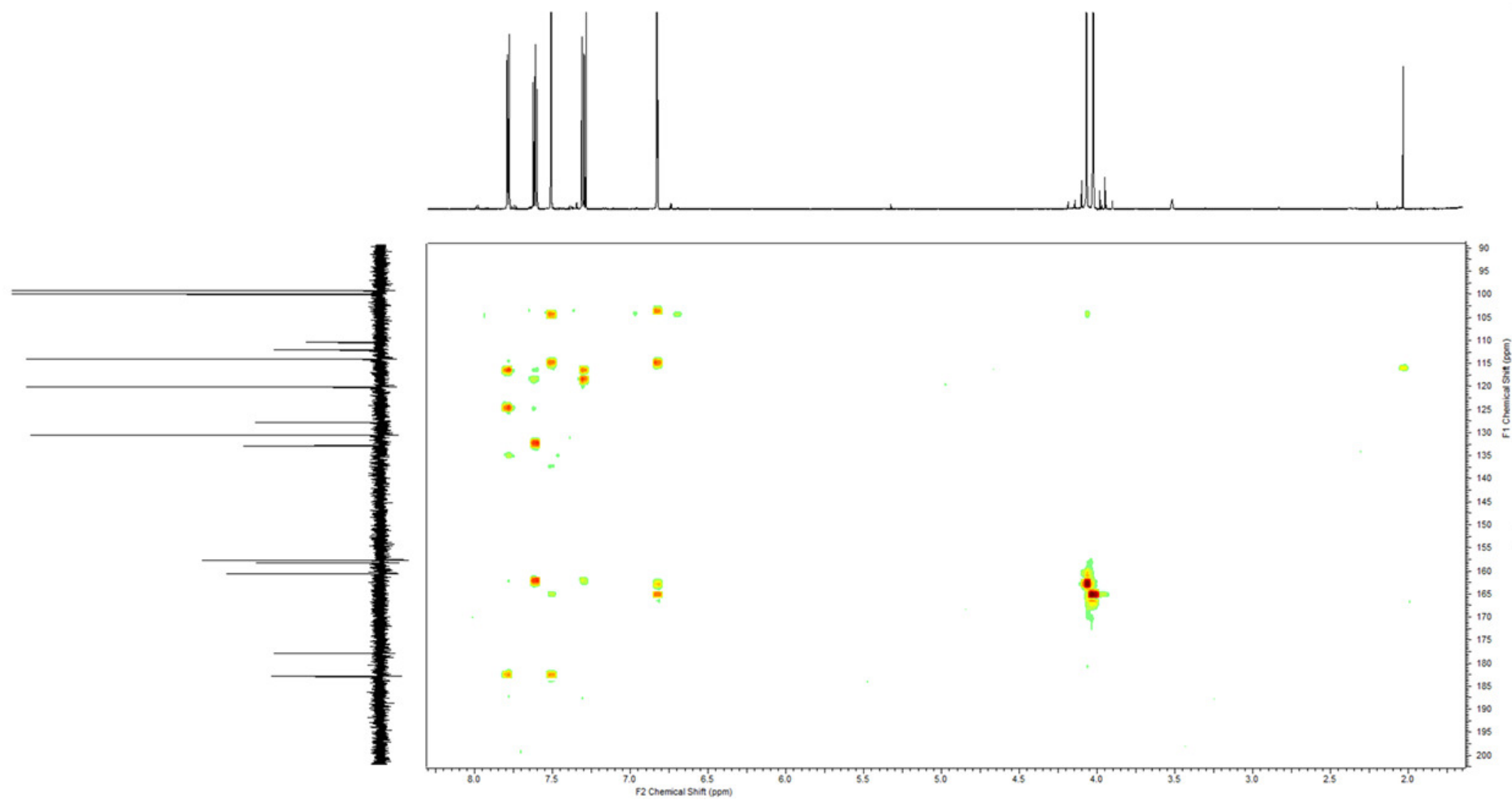


**Figure S25.** HMBC-NMR spectrum of AQ-284b in D<sub>6</sub>-DMSO.

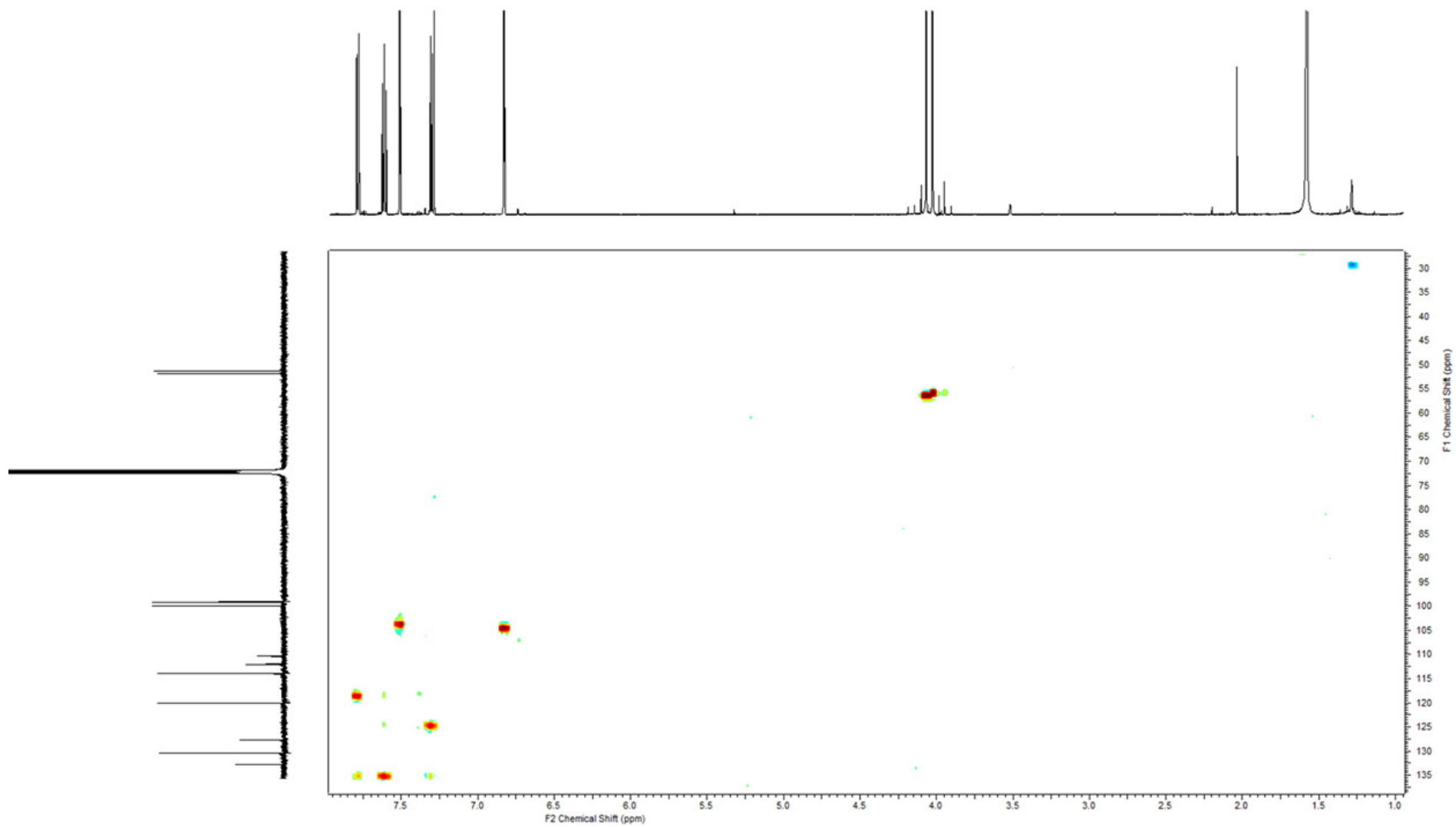


**Figure S26.** HSQC-NMR spectrum of AQ-284b in D<sub>6</sub>-DMSO.

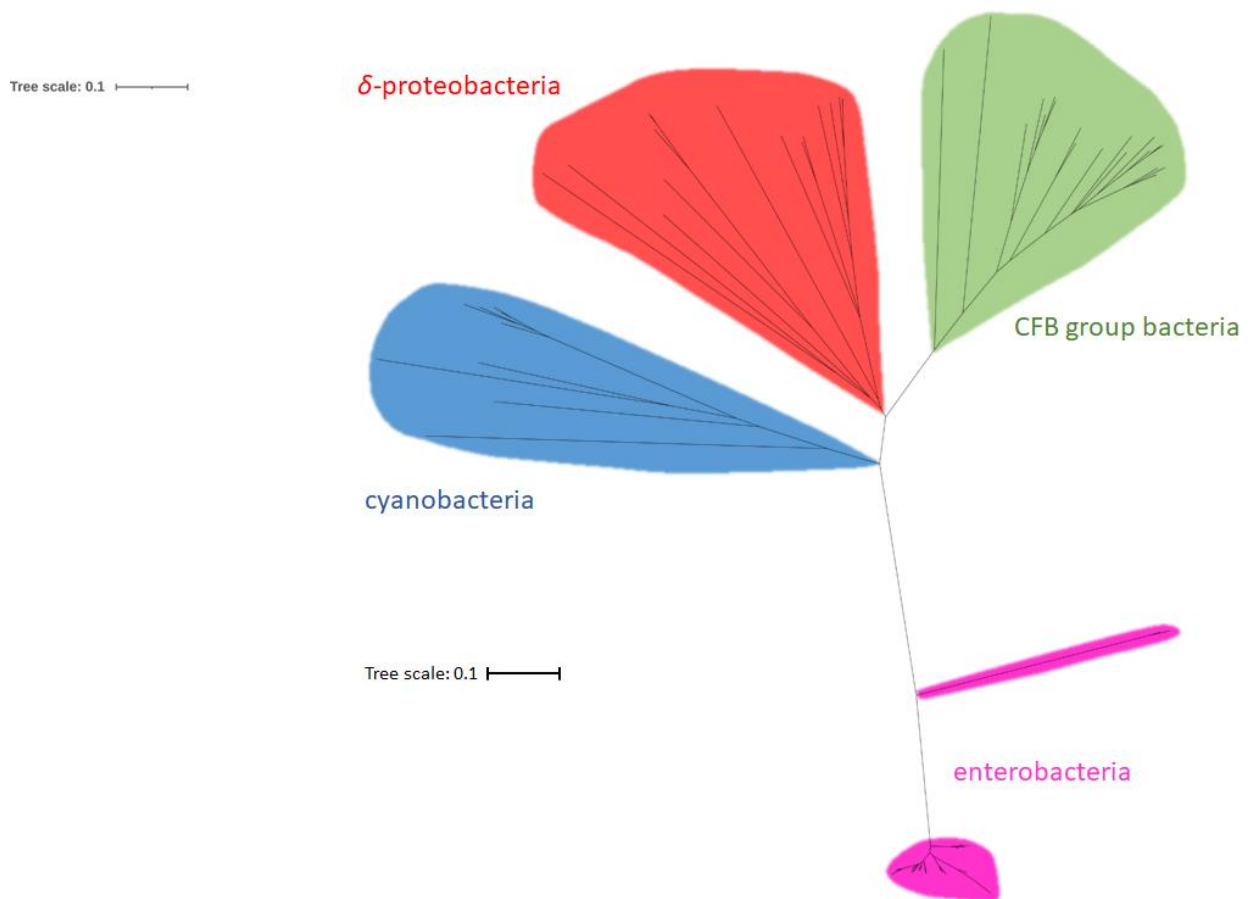


**Figure S27.** Carotenoid dioxygenases are distributed among different groups of bacteria. Sequences were aligned using clustalW and the tree was generated using Geneious 6.1.8. Scale bar represents amino acid substitutions per amino acid position. Carotenoid dioxygenase from *P. luminescens* TT01 was used as query.

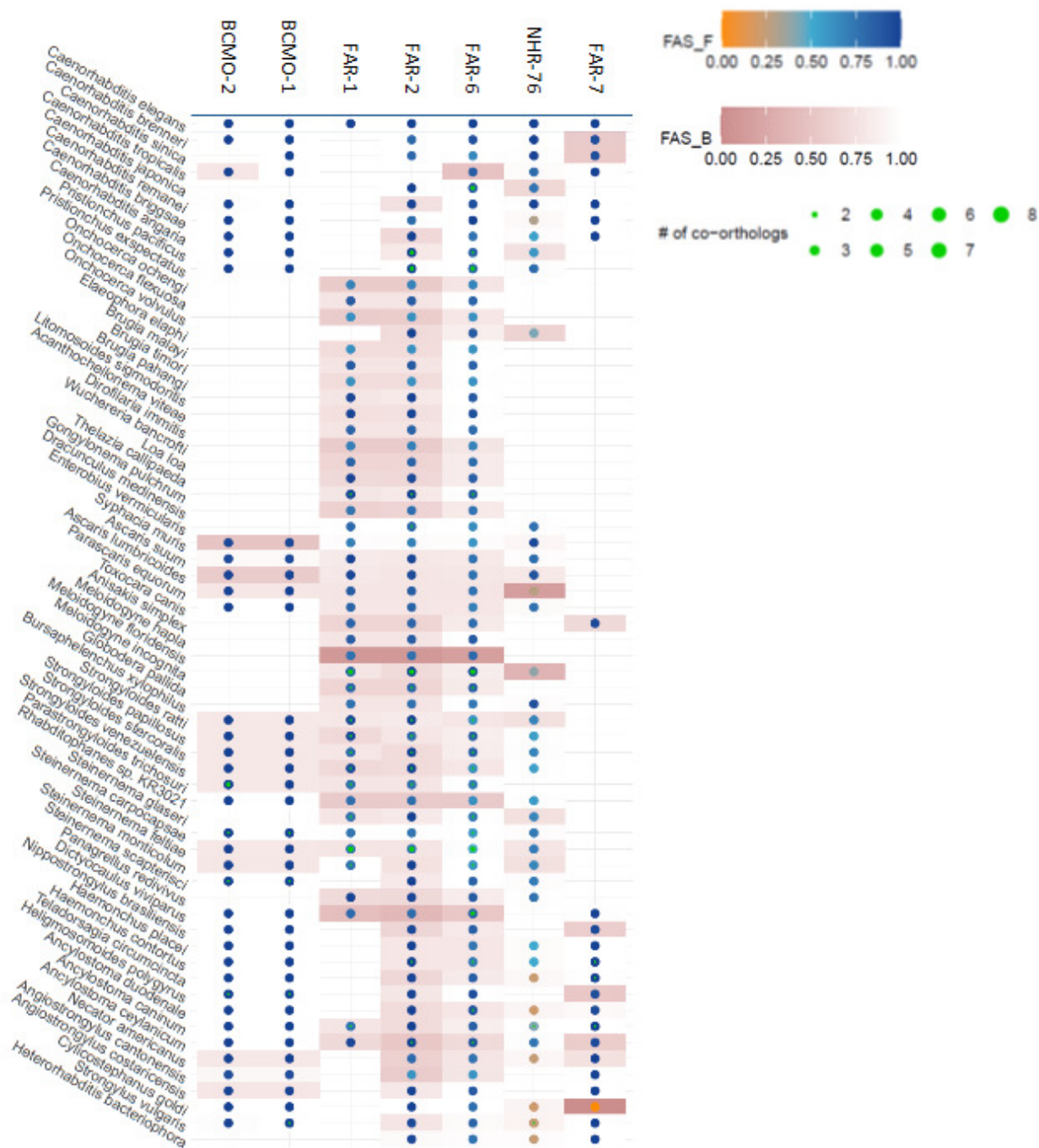


**Figure S28.** Protein blast analysis. Amino acid sequences for different classes of fatty acid- and retinoid-binding proteins (FARs), nuclear hormone receptors (NHRs) and two carotenoid dioxygenases BCMO-1 and BCMO-2 from *C. elegans* were used as inputs. Score of protein domain presence is represented by FAS\_F, score of domain architecture is depicted by FAS\_B.

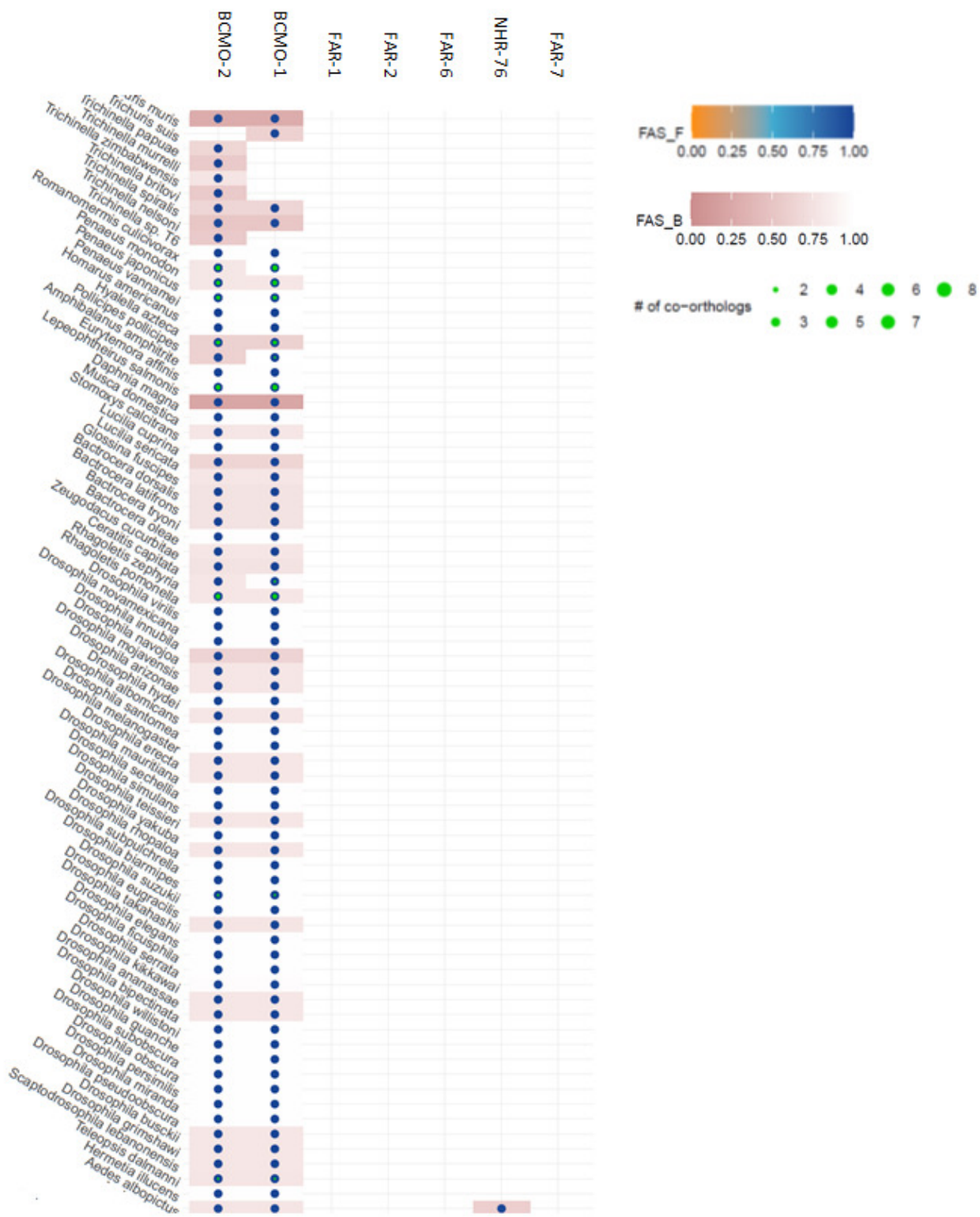


Figure S28. Continued.

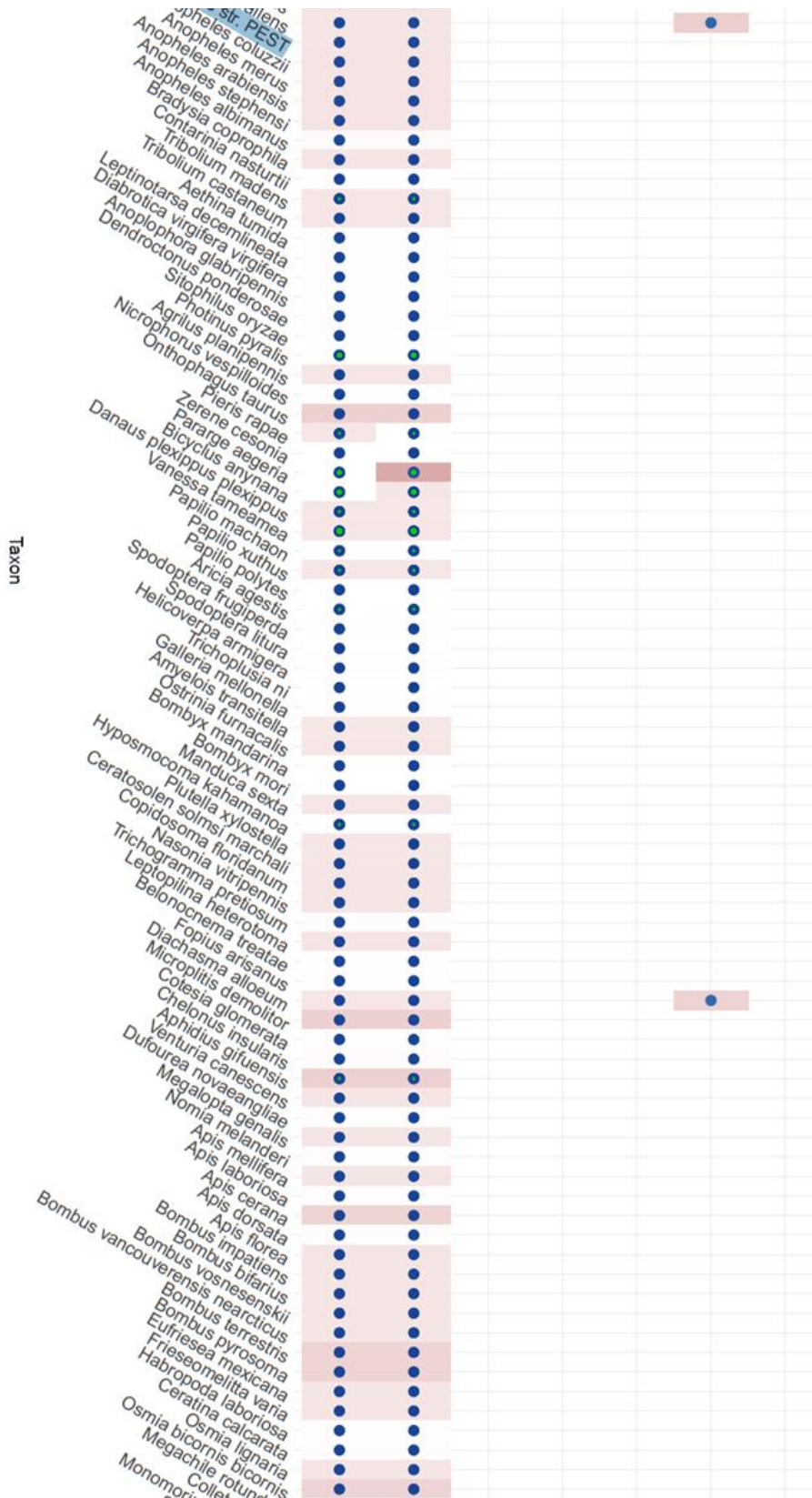


Figure S28. Continued.



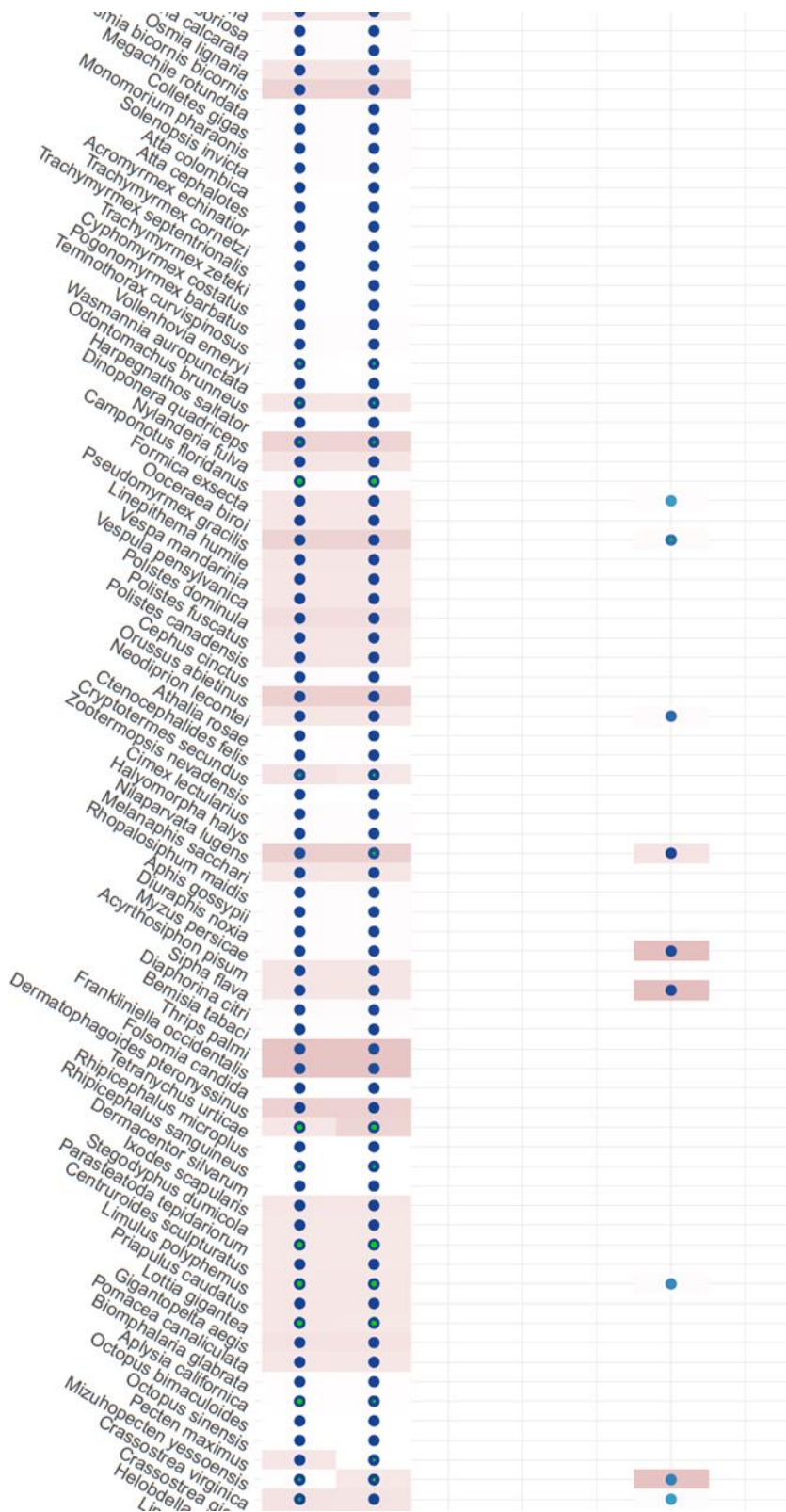


Figure S28. Continued.

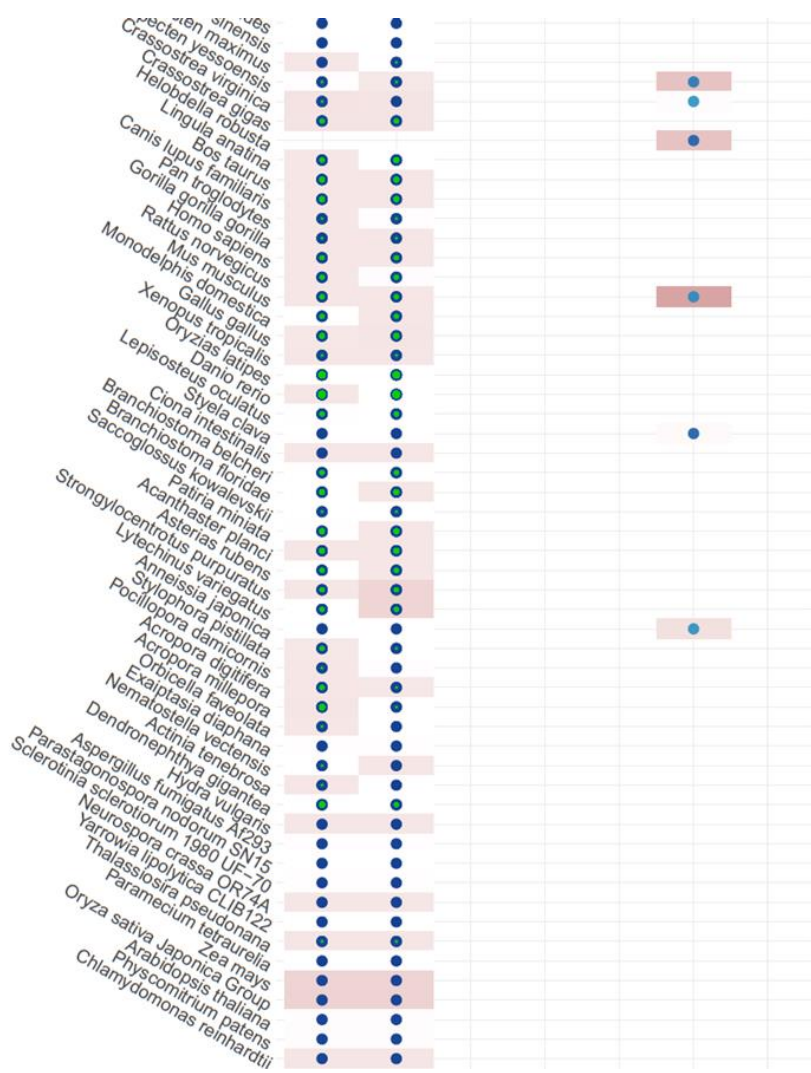


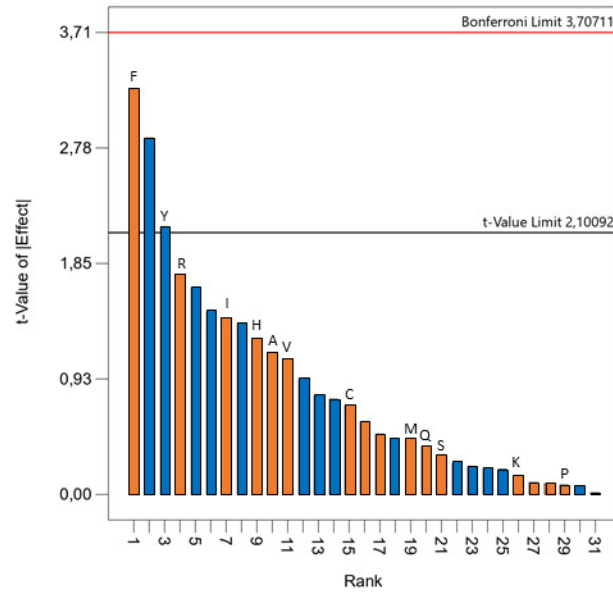


Figure S28. Continued.

A: alanine  
 R: arginine  
 N: asparagine  
 D: aspartic acid  
 C: cysteine  
 Q: glutamine  
 E: glutamic acid  
 G: glycine  
 H: histidine  
 I: isoleucine  
 L: leucine  
 K: lysine  
 M: methionine  
 F: phenylalanine  
 P: proline  
 S: serine  
 T: threonine  
 W: tryptophane  
 Y: tyrosine  
 V: valine

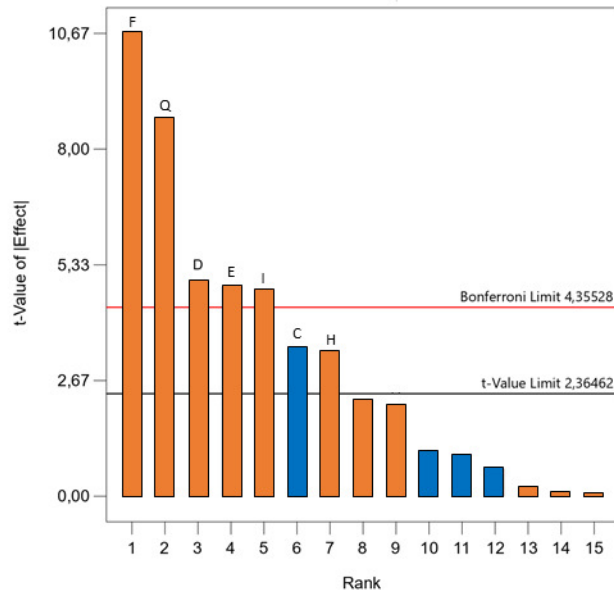
 Positive effect  
 Negative effect



**Figure S29.** Pareto-chart of the amino acid screening. Depicted is a significance model ( $p < 0.05$ ). 430 nm UV absorption of the crude extract was taken as the model input. Plot was generated and analyzed with Design-Expert 12 (Stat-Ease, Minneapolis, USA). Cultivation was conducted in 30 mL cultures at 30°C for 72h. Analysis was performed by Jan Burkhardt, AG Czermak, THM.



A: alanine  
 R: arginine  
 N: asparagine  
 D: aspartic acid  
 C: cysteine  
 Q: glutamine  
 E: glutamic acid  
 G: glycine  
 H: histidine  
 I: isoleucine  
 L: leucine  
 K: lysine  
 M: methionine  
 F: phenylalanine  
 P: proline  
 S: serine  
 T: threonine  
 W: tryptophane  
 Y: tyrosine  
 V: valine

Positive effect  
 Negative effect



**Figure S30.** Pareto-chart of the amino acid screening. Depicted is a significance model ( $p < 0.05$ ). 430 nm UV absorption of the crude extract was taken as the model input. Plot was generated and analyzed with Design-Expert 12 (Stat-Ease, Minneapolis, USA). Cultivation was conducted in 30 mL cultures at 30°C for 72h. Analysis was performed by Jan Burkhardt, AG Czermak, THM.

A: biotin  
 B: riboflavin  
 C: folic acid  
 D: PABA  
 E: thiamine  
 F: pantothenic acid  
 G: nicotinic acid  
 H: pyridoxine  
 I: VB12

 Positive effect  
 Negative effect

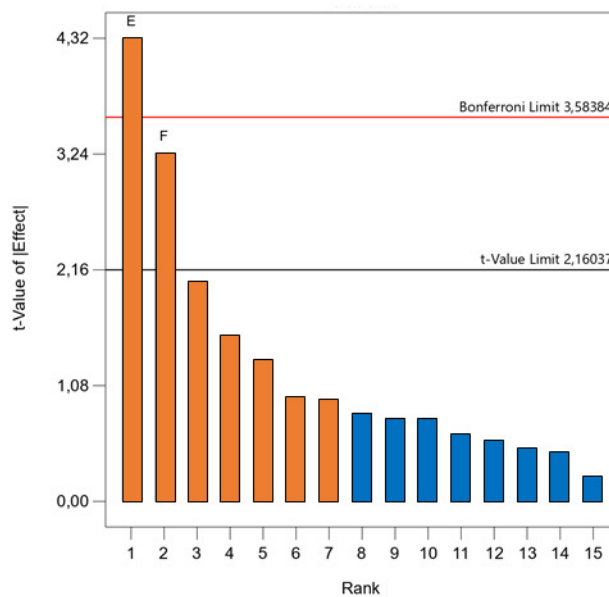


**Figure S31.** Pareto-chart of the amino acid screening. Depicted is a significance model ( $p < 0.05$ ). 430 nm UV absorption of the crude extract was taken as the model input. Plot was generated and analyzed with Design-Expert 12 (Stat-Ease, Minneapolis, USA). Cultivation was conducted in 30 mL cultures at 30°C for 72h. Analysis was performed by Jan Burkhardt, AG Czermak, THM.

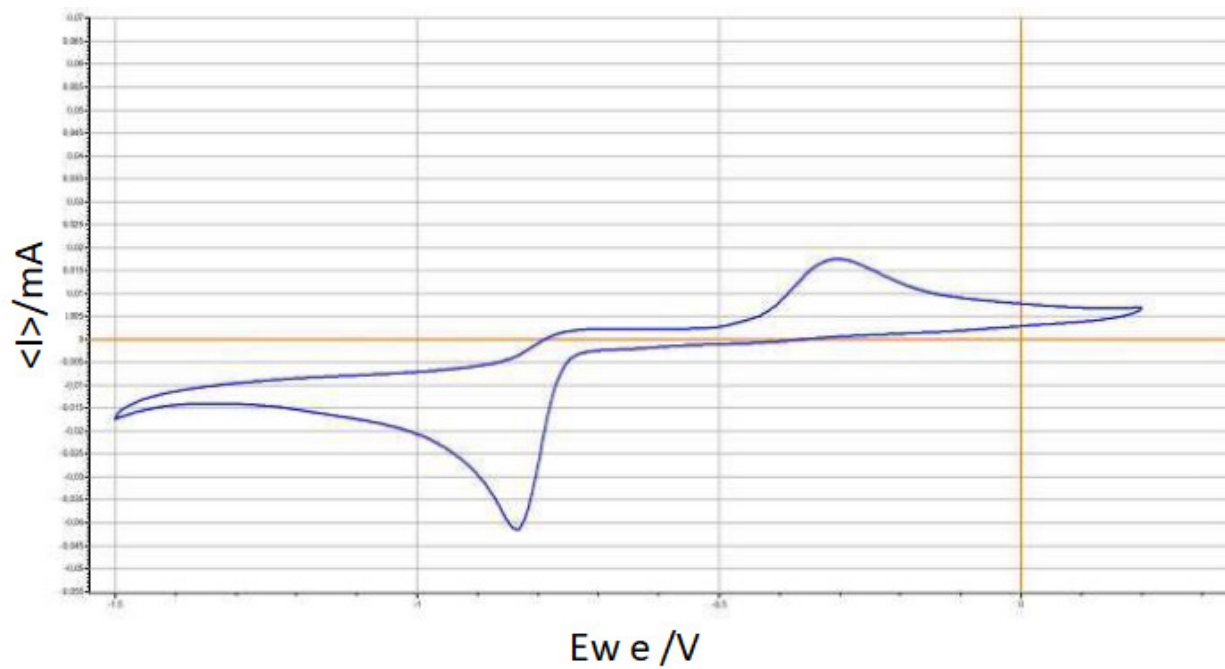


**Figure S32.** CV of 30mM solution of AQ256. CM-A-1575 (0.1M, 2M NaOH/KOH). Experiment and figure done by CMBlu Energy AG.

```

Consensus      MLINLITSYRKTAAIYTFVEAGLSIHFKNGTYVDINKLADQYGIDYSRLNRLCDFLTEIG 60
plu4895_TT01  ...D.....D.....D.....S.....I... 60
plu4895_PB45.5 ..... 60
plu4895_hainanensis ..... 60
plu4895_bodei  ...D.....D.....D.....S.....I... 60
plu4895_akhurstii ..... 60

Consensus      VLVSGNXGVALSEECALADPDSXEFLTIKYEINXEHWDSWLMYPKSLLENNGKSAFEMV120
plu4895_TT01  ...SD.....N.....V..... 120
plu4895_PB45.5 ...G...F...D.....G...A..... 120
plu4895_hainanensis .....P..D.A120
plu4895_bodei  ...S.....D.....N.....V..... 120
plu4895_akhurstii .....P..D.A120

Consensus      HGKSFEXWDSKXLKSNFDALMSKYTNKIKELLVIYDFNKYNRILDGGGDGELLIRI180
plu4895_TT01  .....L..N.....D.....D.H..... 180
plu4895_PB45.5 Y..P.....R..E.....V180
plu4895_hainanensis .....Y...N.....VH..... 180
plu4895_bodei  .....L..N.....D.....H..... 180
plu4895_akhurstii .....Y...N.....V..... 180

Consensus      SEKFKGKDYAVLDRYNEIPIYEGIDFINGDFEPIPSGYDLYILKNVLHNWPDND AISLL240
plu4895_TT01  ..QV.....T.....V..S...N..K...K...T.....I.240
plu4895_PB45.5 .....D.....E.....240
plu4895_hainanensis .....S.....240
plu4895_bodei  ..QV.....V..S..VN..S...K...T.....I.240
plu4895_akhurstii .....R.....S.....240

Consensus      KNCREVMDDNANLLIITLMKKTSPMVKSVDLLMDMLYLGKERYLSEFEHLANQAGLVVR300
plu4895_TT01  .....A..N..T.....PQ.LV.....I.....FSA.Q.....DI.....I.300
plu4895_PB45.5 .....K.....V.....D.....300
plu4895_hainanensis .....I.....Q.....I..300
plu4895_bodei  .....A..N..TT.....PQ.LV.....I.....F.A.Q.....DI.SH...I.300
plu4895_akhurstii .....I.....Q.....I..300

Consensus      YSKDIDGMFSLIELGVK 317
plu4895_TT01  HY..L.EI.....K.. 317
plu4895_PB45.5 ..... 317
plu4895_hainanensis ..... 317
plu4895_bodei  SY..L.EI..F..... 317
plu4895_akhurstii ..... 317

```

**Figure S33.** Amino acid alignment of plu4895 in different *Photorhabdus* strains.

Consensus	MLAELITSYRKSAAIYAFVDTGLSIHFKNGAYVDIDELSRQCGIDYSRLDRLCDFLIEIG	60
plu4894_TT01	.....R.....	60
plu4894_PB45.5	.....A.....I.....D.....E.....	60
plu4894_haina	.....	60
plu4894_bodei	.....A.....R.....	60
plu4894_akhurstii	.....	60
plu4894_temperata	..IN.....VY..D...I..S...HKSD..H...S.....	60
Consensus	ILVNHGKVTLSEECALADPESMESLIVKWELSPDCWNAWSMYSXSLLENDGKPAFEIM	120
plu4894_TT01	.....P.....T	120
plu4894_PB45.5	..I...D.....P.....	120
plu4894_haina	.....R.....R.....P.....	120
plu4894_bodei	V.....D.....P.....T	120
plu4894_akhurstii	.....R.....I.....G...ST...	120
plu4894_temperata	...SNND.IA..D.....N.....MT.C.I..EF.L..L.....N.....V	120
Consensus	HGKSFFEHLASNKXLKSNFDSMSKXSDKIIIXKLLDIYDFSQYNRILDVGGGEGNLLVKI	180
plu4894_TT01	.....G.....I.....S...M	180
plu4894_PB45.5	.....V.....D.....L..	180
plu4894_haina	.....V.....D.....L..	180
plu4894_bodei	.....G.....I.....M	180
plu4894_akhurstii	.....DY.....A.....N.....R.	180
plu4894_temperata	...P..DY.EN.Q.....HF.....V.E.....L.....R.	180
Consensus	SEKVKGKHAYVLDRYXEIPVLENIDFINGDFXKSIKPSGYDLYILKNXJHDWXDBKAILIL	240
plu4894_TT01	.....Y.....V.....D.....N....	240
plu4894_PB45.5	.....L.....V...	240
plu4894_haina	.....L.....V...	240
plu4894_bodei	.....N....	240
plu4894_akhurstii	.....Y.M.	240
plu4894_temperata	..A.....M...V..SGDME...N.....N...DS...	240
Consensus	ENCRKAMDNGAKXLLIXYMKKPKQSKAVIYLDXLMVLFSGKERXLTEFERLANQAGLVIQ	300
plu4894_TT01	.....SA.....M.....	300
plu4894_PB45.5	.....S.....I...Y.....A.....	300
plu4894_haina	.....Y.....A.....	300
plu4894_bodei	.....SA.....M.....	300
plu4894_akhurstii	.....S.....V.C.....L.....	300
plu4894_temperata	K.....DS.T....LI..SP.ERIKST..A...L.....Y..D...I.K	300
Consensus	DVKDIDEXFSIIQLGIK	317
plu4894_TT01	.....S.....	317
plu4894_PB45.5	....V.....	317
plu4894_haina	....V.....	317
plu4894_bodei	.....S.....	317
plu4894_akhurstii	.....	317
plu4894_temperata	NT.N.N..Y...E..V.	317

**Figure S34.** Amino acid alignment of plu4894 in different *Photorhabdus* strains.



```

Consensus      MLVELIASYRKSIAIYAFVDTGLSVHFKDGAYMDINELASQYGIDYSRLNRLCDLLIEIG 60
plu4892_TT01  .....A...N..RV...I.I..... 60
plu4892_PB45.5 .....T.....C.....C..... 60
plu4892_hainanensis .....Y.....C.....C..... 60
plu4892_bodei ..A...T.....T.....N.T.....F..... 60
plu4892_akhurstii .....Y.....D..... 60
plu4892_temperata .....T....A.....I..S..SDKF...H...S...F.... 60

Consensus      VLVSSNDXVALSDECXALADPESIESLMIKWEFDSDFWNAWLMYPKSLLENNGKSAFEIA120
plu4892_TT01  ...G.....R.....120
plu4892_PB45.5 .....D.....G.....S.....120
plu4892_hainanensis I.....S.....L.....120
plu4892_bodei ...C.....E..V.....M..IA...N..L.....120
plu4892_akhurstii .....G.....R.....120
plu4892_temperata ...NN.....M...F...LSP.C..V.S.....D.....T120

Consensus      HGKPIFEYLDSELLRAKFNLSMKNKSDKMIEKLFDIYDFSQHDKILDVGGGRGNLLIKI180
plu4892_TT01  .....E.....G.....180
plu4892_PB45.5 .....180
plu4892_hainanensis .....P.....V.....180
plu4892_bodei N...F..H...K..KS..D...D.....Y.....E....RM180
plu4892_akhurstii .....N.....180
plu4892_temperata ....F...FYN.K.V.SI.D.A...T..RI...L.....YNR.....E.....180

Consensus      SEXVK--GKHYAVLDRYNKSPXYENIDFIDGDFFKSIPSGYDLYILKNIHHDWSDNESIL238
plu4892_TT01  .....Y.....I.....---238
plu4892_PB45.5 .....VK.....240
plu4892_hainanensis ...T--.....238
plu4892_bodei .....--E.....AL.....A.....V....P..DA..238
plu4892_akhurstii .....--.....L.....238
plu4892_temperata R....--V.....EI..S...E..N..L..V.....L.....DA..238

Consensus      ILENCRKAMBNNATILLITLMKKPQSKFVKYLDILMDMTSLGQERNLTFEXLANQAGLI298
plu4892_TT01  -----298
plu4892_PB45.5 .....R....300
plu4892_hainanensis .....D.....298
plu4892_bodei .....G.....VI..F....VS...K..D.....V298
plu4892_akhurstii .....KR....298
plu4892_temperata .....I..G..V...NYT..S..SM..IF.....VLFS.K..F.N.....V298

Consensus      IQDVKDIDESYSIIQLGVK 317
plu4892_TT01  ----- 235
plu4892_PB45.5 ..... 319
plu4892_hainanensis ..... 317
plu4892_bodei ..... 317
plu4892_akhurstii ..... 317
plu4892_temperata ...T.....S.....IE 317

```

**Figure S35.** Amino acid alignment of plu4892 in different *Photorhabdus* strains.

Consensus	MLIELITSCRKSTAIYAFVDMGLSVHFKDGACVNISEISRQYGLDHARFSRLCEYLIKIG	60
plu4891_TT01	.....T.....L.....S.....	60
plu4891_PB45.5	.....I.....	60
plu4891_haina	.....G.....	60
plu4891_bodei	-----	
plu4891_akhurstii	.....	60
plu4891_temperata	...D...H..TAT.....T...D...N...D.D.L.HKS.V.KS.LNQ..D..E..	60
Consensus	VLVNSGEGVALSEECALADPESMESLMIRCEVSPEFWNAWSMYSKSLSENNSKTAFEIA	120
plu4891_TT01	...S.N.....V.....Y.....Y...N.....	120
plu4891_PB45.5	.....I.....	120
plu4891_haina	.....	120
plu4891_bodei	-----.....Y...N.....	18
plu4891_akhurstii	.....R.....S.....	120
plu4891_temperata	...SNNH.IT..D.....T....L.....KY.TNQ.H..S.V.....R...G.S...MV	120
Consensus	HGKPFPEYLDNHELFRSNFDSFMSKNSDKIIDKILDIDYDFSQYNRILDVGGGEGKLLIRM	180
plu4891_TT01	.....N..K.....	180
plu4891_PB45.5	.....	180
plu4891_haina	.....	180
plu4891_bodei	.....E.....H.....V.I	78
plu4891_akhurstii	.....	180
plu4891_temperata	Y..TI..H.ADNKSL.AD..AL.T...NTL.KNL..V...N...M....AR.H..KSI	180
Consensus	NEKVKGKHYAVLDRYNETPVLIEDIEFINGDFFKSVPSGYDLYILKNI IHNWSDNNAVLIL	240
plu4891_TT01	...I.....I.....V.....D.....	240
plu4891_PB45.5	.....	240
plu4891_haina	.....L.....	240
plu4891_bodei	...I.....I.....I...	138
plu4891_akhurstii	.....	240
plu4891_temperata	.....L..S...D.....M..I.....M.....DVIS..	240
Consensus	QSCRKAMDDNATVLLISTVKKPRLEIIDSTDILMDVLLLGKERYLNELEDLAHQAGFVVK	300
plu4891_TT01	.....L.....N.....	300
plu4891_PB45.5	.....	300
plu4891_haina	.....I..	300
plu4891_bodei	EN.....G...LK.....V.....	198
plu4891_akhurstii	.....S...E..C.....	300
plu4891_temperata	NN.....G..I...MM...QSP.AN.MS...M.F.S....D.V.Y..N...LTI.	300
Consensus	GIKXINEKYSIIELGVKS	318
plu4891_TT01	R.....A.....-	317
plu4891_PB45.5	.....-	317
plu4891_haina	.....-	317
plu4891_bodei	D.....NKI.	216
plu4891_akhurstii	.....-	317
plu4891_temperata	DS...D.TF.T...K..-	317

**Figure S36.** Amino acid alignment of plu4891 in different *Photorhabdus* strains.

```

Consensus      MLTELIASNRSSAAIHAFVDTGLSTHFKDGIYVDISELSRKSGVNYARFSRLCDFLVEMG 60
plu4890_temperata  ....I.TGY.K...LN...KSKAPIFIGKMGAMTLD.IACYTKTSAE..G..L.VMIDCE 60
plu4890_PB45.5    .....V.....A... 60
plu4890_hainanensis ..... 60
plu4890_akhurstii ..... 60
plu4890_TT01     ..... 60
plu4890_bodei    .....V..... 60

Consensus      VLVSKDKNFRLSDECQVFADPESFETFMIKLEICSYYXNAWLMYGKSLFEDDGKSAFEMA120
plu4890_temperata  I..ILSEG.YS.TKNAVAL.SED..I..LW.NC.LGEH..EI.PD.FG..GSGATR....KK120
plu4890_PB45.5    .....D.....120
plu4890_hainanensis .....K.....D.....120
plu4890_akhurstii .....SN.....120
plu4890_TT01     ...N.....H...N...S.....H.....120
plu4890_bodei    ...N.....N..H.....S.....120

Consensus      HGKPFPEYLDGNKFLKSNFDALMTRVSNLIVEXLLGIYDFNQHNRIILDVGGGEGELLARI180
plu4890_temperata  ...K..DFITDVPS..TT..S..AAITDE.SD..IK.F.IHPNH.VV.I...K.I.AKKL180
plu4890_PB45.5    .....D.....K...K.180
plu4890_hainanensis .....180
plu4890_akhurstii .....180
plu4890_TT01     ..R.....V..180
plu4890_bodei    .....L.....K....180

Consensus      SEKVKGKHYAVLDRYN-ELPVSNDIDFINGNFLXSIPSGYDLYILKNXLHNWSDSDSILI239
plu4890_temperata  KQTF SF.DCT.I...AK..EF..G.TYL.CD.F.Q.K..ANV.....D.D.DKAGK.240
plu4890_PB45.5    .....Y.....-.....S.....239
plu4890_hainanensis .....-.....E.....239
plu4890_akhurstii .....-...I...E.....239
plu4890_TT01     .....S-.....239
plu4890_bodei    .....-.....239

Consensus      LENFRKAMDKNSSLLLINMVKEPE--FSRSFDILMDMLFLGKERSXAEFEYLANQAGLVV297
plu4890_temperata  .A.CAH..S...I.YIVEII..HGSKVKGKTL.L...A..V...Y.D.Y.R..FKND..I300
plu4890_PB45.5    .....A...V...S...--.....V..A.....D.....297
plu4890_hainanensis .....--.....297
plu4890_akhurstii .....--.....K.....297
plu4890_TT01     .....--.....V.....T.....297
plu4890_bodei    .....--.....297

Consensus      QEXKIVDQSYSPYSFIKLRKHG 320
plu4890_temperata  DS.IQTSH.Q.V---LL..KA.. 320
plu4890_PB45.5    K.....E.....E....-- 318
plu4890_hainanensis .....-- 318
plu4890_akhurstii .D.....E....-- 318
plu4890_TT01     ...VI.....Q...-- 318
plu4890_bodei    ...VI.....-- 318

```

**Figure S37.** Amino acid alignment of plu4890 in different *Photorhabdus* strains.

## 10 Record of Conferences

International VAAM Workshop on Biology of Bacteria Producing Natural Products

Poster presentation: Late stage biosynthesis of Anthraquinones in *P. luminescens*

Frankfurt am Main, Germany, 31.08 - 02.09.2018

International VAAM Workshop on Biology of Microorganisms Producing Natural Products

Poster presentation: Regulation of Anthraquinone biosynthesis in *P. luminescens*

Jena, Germany, 15.09 - 17.09.2019

Sino-German MegaSyn Symposium

Poster presentation: Anthraquinone diversification in *P. luminescens*

Frankfurt am Main, Germany, 10.10 – 12.10.2022

## 11 Erklärung

Ich erkläre hiermit, dass ich mich bisher keiner Doktorprüfung im Mathematisch-Naturwissenschaftlichen Bereich unterzogen habe.

---

Ort/Datum

---

Lukas Kreling

# 12 Eidesstattliche Versicherung

Ich erkläre hiermit, dass ich die vorgelegte Dissertation mit dem Titel

**Biotechnological production of natural products in entomopathogenic bacteria**

selbstständig angefertigt und mich anderer Hilfsmittel als der in ihr angegebenen nicht bedient habe, insbesondere, dass alle Entlehnungen aus anderen Schriften mit Angabe der betreffenden Schrift gekennzeichnet sind.

Ich versichere, die Grundsätze der guten wissenschaftlichen Praxis beachtet, und nicht die Hilfe einer kommerziellen Promotionsvermittlung in Anspruch genommen zu haben.

---

Ort/Datum

---

Lukas Kreling